Synthesis of Amphiphilic Copolymwers by Atom Transfer Radical Polymerization

Hansen, Natanya Majbritt Louie

Publication date:
2007

Document Version
Publisher's PDF, also known as Version of record

Synthesis of Amphiphilic Copolymers by Atom Transfer Radical Polymerization

Natanya Majbritt Louie Hansen

2007

Ph.D. Thesis

DTU

TECHNICAL UNIVERSITY OF DENMARK
DEPARTMENT OF CHEMICAL ENGINEERING

Synthesis of Amphiphilic Copolymers by Atom Transfer Radical Polymerization

Natanya Majbritt Louie Hansen

March, 2007

Danish Polymer Centre
Department of Chemical Engineering
Technical University of Denmark
DK-2800 Kongens Lyngby, Denmark

ISBN 978-87-91435-61-7
Printed by Frydenberg a/s, Copenhagen, Denmark

Preface

This thesis is the result of the work on my Ph.D. project carried out at the Danish Polymer Centre (DPC), Department of Chemical Engineering starting in January, 2004 and completed in March, 2007. The project was cofinanced by the Technical University of Denmark (DTU), the Graduate School of Polymer Science and the Danish corporation Novo Nordisk A/S. Professor Søren Hvilsted was my supervisor, while Michael Gerstenberg from Novo Nordisk cosupervised me.

I am sincerely grateful to Søren for giving me the opportunity to work on this project and making me feel that this was indeed *my* project by giving me a great degree of freedom. You have let me make my own decisions and have always been supportive of these, which I greatly appreciate. I would like thank Michael for initially voicing the idea of writing a review article and for giving me helpful guidelines to survive the three years as a Ph.D. student.

Six months of my thesis work was performed at the University of Warwick under the supervision of Professor David M. Haddleton, who is warmly thanked for supporting and encouraging me. I would like to thank everyone in the group at Warwick for making me feel welcome and teaching me the subtle yet very important difference between American and English. In turn I am sure they have all learned the importance of *lunch* from me. Thanks to Daniel for teaching me everything about honeycomb structures and to Patricia for demonstration to me the therapeutical effects of shopping during my stay in the UK.

I would sincerely like to thank Jens Glastrup, National Museum of Denmark for being supportive throughout the work on SPME and for never giving up although the experimental results were infuriating. His comments on my thesis are also greatly appreciated.

DSC and TGA analysis were performed by Kim Chi Szabo, whom I wish to thank for her kind help and promt sample handling at *all* times. Thanks to Maria Juhl for synthesizing the PEG-macroinitiators. I would also like to thank all my colleagues at DPC for these last three years - it has been fun and I am glad, I came back! To Katja and Anne Kathrine, thank you for your support and encouragement, which you have both shown in your own unique way. I appreciate it.

The warmest thanks to all my friends and my family, who have listened to my obsessions over linear fits in reaction kinetics and similarly exciting topics, while cheering me up and helping me through the inevitable rough periods. My critical proof readers Dorte, Katja and Morten are thanked

for their comments and corrections. Last, but not least I would like to thank Thomas for his support and understanding, especially through the last months of my work.

Lyngby, March 28^{th} 2007

Natanya M.L. Hansen

Synopsis

Fluorinated polymers are highly hydrophobic and have a number of unique properties including high biocompatibility and low surface energy, as well as good chemical and thermal resistance. In this thesis fluorinated polymers and copolymers were targeted as potentially biocompatible materials. The following approaches were undertaken during the work on this Ph.D.: 1) Two difunctional poly(ethylene glycol) macroinitiators were used for the polymerization of a fluorinated methacrylate to form triblock copolymers. 2) Three different fluorinated methacrylates were copolymerized with non-fluorinated monomers yielding diblock copolymers. 3) A fluorinated surfactant was functionalized to form a macroinitiator species, which was utilized for the polymerization of non-fluorinated monomers. Atom transfer radical polymerization (ATRP) a technique of controlled/"living" radical polymerization was used for all polymerizations.

Three different fluorinated methacrylates: 2,2,2-trifluoroethyl methacrylate (3FM), 2,2,3,3,4,4,5,5-octafluoropentyl methacrylate (8FM) and 1,1,-2,2-tetrahydroperfluorodecyl methacrylate (17FM) were utilized as monomers in ATRP. Triblock copolymers were synthesized using two different terminally functionalized poly(ethylene glycol)s (PEGs) (M_n = 2000 and 4600 g/mol) as macroinitiators. These were utilized to polymerize 3FM to obtain amphiphilic triblock copolymers with molecular weights between 6000 and 32,000 g/mol and PDIs of 1.2 to 1.9.

A certain lack of control over polymerization was observed in preliminary homopolymerizations of 3FM and 17FM, which lead to the study of reaction kinetics to optimize reaction conditions. It was attempted to develop an analysis method for monitoring monomer conversion during polymerization of 3FM using gas chromatography for analysis of samples extracted during polymerization. Volatiles (solvent, monomer & internal standard) were extracted from the samples by solid-phase microextraction (SPME) and analyzed. However, this method regrettably did not yield reproducible results presumably due to the inhomogeneity of the extracted samples. ^{1}H NMR analysis was subsequently used in a kinetic study of 3FM, which indicated that polymerization follows first-order kinetics and that the reaction is controlled giving molecular weights close to target and relatively low PDIs. The use of ^{1}H NMR analysis for 8FM gave less conclusive results due to the limited solubility of the polymeric product.

Diblock copolymers of methyl methacrylate (MMA) and each of the three fluorinated methacrylates were polymerized by ATRP. Sequential addition was used in most instances to form gradient copolymers and it was possible to synthesize block copolymers of MMA and 3FM starting with either monomer. The polymerization starting from MMA yielded

better results exhibiting low polydispersity and a linear evolution of molecular weights with conversion. Well-defined diblock copolymers of MMA and 8FM and 17FM, respectively were synthesized by sequential addition, however, only with MMA as the first monomer. Comparison of the first-order kinetics of the copolymerizations indicated that the length of the fluorinated pendant chain does not influence the reactivity of these monomers in ATRP.

Novel diblock copolymers of 3FM and hydrophilic monomer poly(ethylene glycol) methyl ether methacrylate (PEGMA) were synthesized by ATRP using different reaction temperatures for the two monomers (90 and 50 °C, respectively). Polymerization starting with PEGMA was successful, while the initiation of PEGMA from P3FM was more problematic, due to lack of initiation at the low polymerization temperature for PEGMA. Copolymerization of 3FM and the blood compatible 2-methoxyethyl acrylate (MEA) was possible, but polymerizations were not entirely controlled, presumably due to the incompatibility of the two monomers.

A fluorinated macroinitiator (FMI) based on a commercially available 2-perfluoroalkyl ethyl-copoly(ethylene glycol) surfactant was utilized in controlled polymerizations of MMA, MEA and PEGMA. Excellent results were achieved with MMA and MEA, which exhibited first-order kinetics, linear evolution of molecular weights and low polydispersities (PDI < 1.25).

Polymerization of PEGMA from FMI did not proceed in an entirely first-order manner, however, polydispersities were low throughout reaction (PDI < 1.2) and the evolution of molecular weight was relatively linear. The block copolymer FMI-PMMA-*b*-PPEGMA was furthermore synthesized by sequential addition.

The glass transition temperatures (T_gs) of the diblock copolymers of 3FM and MEA and PEGMA, respectively, were increased compared to the non-fluorinated homopolymers, which was also the case for the triblock copolymers. The opposite was seen for polymers initiated from FMI, where the macroinitiator behaved as a plasticizer in most of the polymers.

The introduction of the fluorinated monomers lead to a reduction in the thermal stability of all the synthesized copolymers. The same tendency was seen for the polymers initiated by FMI, where the non-fluorinated analogues exhibited higher thermal stability.

Flat films cast from the fluorinated copolymers and polymers exhibited increased hydrophobicity compared to the non-fluorinated homopolymers. The most hydrophobic behavior was seen for the diblock copolymers with advancing contact angles above 90° in all cases with a maximum of 118°, which was measured for a film of PMMA-*b*-P17FM. Honeycomb structured films were cast under humid conditions from copolymers of 3FM and MMA to yield highly hydrophobic surfaces with static contact angles of water up to 144°.

Resumé

Fluorerede polymerer besidder en række enestående egenskaber såsom god biokompatibilitet og lav overfladeenergi såvel som god kemisk og termisk stabilitet. Målsætningen for denne afhandling var at fremstille fluorerede polymerer og copolymerer, der potentielt kunne finde anvendelse som biokompatible materialer. Følgende strategier blev fulgt i løbet af dette ph.d.-projekt: 1) To difunktionelle poly(ethylenglykol) makroinitiatorer blev anvendt til polymerisation af en fluoreret methakrylat, hvorved triblok copolymerer blev dannet. 2) Diblok copolymerer blev fremstillet ved kombination af tre forskellige fluorerede methakrylater og en række ikke-fluorerede monomerer. 3) Et fluoreret overfladeaktivt makromolekyle blev omdannet til en makroinitiator ved funktionalisering og herefter anvendt til polymerisation af ikke-fluorerede monomerer. Den kontrollerede/"levende" radikal polymerisationsmetode atom transfer radikal polymerisation (ATRP) blev anvendt til alle polymerisationerne.

Tre forskellige fluorerede methakrylater blev anvendt som monomerer i ATRP: 2,2,2-trifluorethyl methakrylat (3FM), 2,2,3,3,4,4,5,5-octafluorpentyl methakrylat (8FM) og 1,1,2,2-tetrahydroperfluordecyl methakrylat (17-FM). Triblok copolymerer blev syntetiseret vha. to forskellige terminalt funktionaliserede poly(ethylenglykol) (PEG) makroinitiatorer ($M_n = 2000$ og 4600 g/mol). Disse blev anvendt til polymerisation af 3FM til fremstilling af amfifile triblok copolymerer med molekylvægte på mellem 6000 og 32.000 g/mol samt PDI'er fra 1,2 til 1,9.

Ved homopolymerisation af 3FM og 17FM var kontrollen over reaktionen utilstrækkelig, hvilket førte til et studie af reaktionskinetikken som led i en optimeringsproces. Det blev forsøgt at udvikle en analysemetode til at følge omsætningen af monomer under polymerisationen, hvor gas kromatografi blev anvendt til analyse af prøver udtaget i løbet af reaktionen. De flygtige komponenter (monomer, solvent & intern standard) blev ekstraheret fra prøverne ved "solid-phase microextraction" (SPME) og efterfølgende analyseret. Der kunne beklageligvis ikke opnås reproducerbare resultater ved denne metode antageligvis pga. de udtagne prøvers inhomogenitet. Efterfølgende blev ^{1}H NMR analyse anvendt til at studere kinetikken for 3FM. Resultaterne her indikerede, at polymerisationen er en 1.ordens reaktion, som er kontrolleret ved det, at de opnåede molekylvægte er tæt på de teoretisk opnåelige og at PDI'erne var relativt lave. En tilsvarende analyse af 8FM gav mere uklare resultater som følge af den lave opløselighed af det polymere produkt.

Diblok copolymerer of methyl methakrylat (MMA) og hver af de tre fluorerede methakrylater blev fremstillet ved ATRP. Sekventiel tilsætning blev anvendt i de fleste tilfælde, hvorved "gradient" (gradueret) copoly-

merer blev dannet. Det var muligt at opnå copolymerer af MMA og 3FM fra hver af de to monomerer, dog gav polymerisation startende med MMA de bedste resultater med lav polydispersitet og lineært voksende molekylvægte som funktion af omsætning. Veldefinerede diblok copolymerer af MMA og 8FM hhv. 17FM er blevet fremstillet ved sekventiel tilsætning, dog er disse kun polymeriseret med MMA som første blok. Kinetikresultaterne viste, at størrelsen af den fluorerede sidekæde ikke har betydning for reaktiviteten af monomererne i ATRP.

Diblok copolymerer af 3FM og den hydrofile monomer poly(ethylenglykol)-methyl-ether-methacrylate (PEGMA) blev syntetiseret ved ATRP, hvor forskellige temperaturer anvendtes for de to monomerer (hhv. 90 og 50 °C). Polymerisation lykkedes med PEGMA som første monomer, mens initiering af PEGMA fra P3FM var mere problematisk grundet den lave reaktionstemperatur for PEGMA. Copolymerisation af 3FM og den blodkompatible 2-methoxyethyl akrylat (MEA) var mulig, men polymerisationerne var ikke fuldstændigt kontrollerede sandsynligvis pga. monomererernes forskellighed.

En fluoreret makroinitiator (FMI) fremstillet fra en kommercielt tilgængelig 2-perfluoralkylethyl-copoly(ethylenglykol) blev anvendt i polymerisationer af MMA, MEA og PEGMA. Udemærkede resultater blev opnået med MMA og MEA, som begge udviste 1.ordens kinetik, lineært voksende molekylvægte som funktion af omsætning samt lave polydispersiteter (PDI $<$ 1,25).

Polymerisationen af PEGMA fra FMI fulgte ikke et 1.ordens forløb, men polydispersiteten var lav gennem hele reaktionen (PDI $<$ 1,2) og molekylvægten øgedes lineært med omsætningen. Det var desuden muligt at syntetisere blok copolymeren FMI-PMMA-*b*-PPEGMA ved sekventiel tilsætning af anden monomer.

Glasovergangstemperaturen (T_g) for diblok copolymererne af 3FM og MEA hhv. PEGMA blev øget i sammenligning med de ikke-fluorerede homopolymerer, hvilket også var tilfældet for triblok copolymererne. Det omvendte var tilfældet for polymererne initieret af FMI, hvor makroinitiatoren virkede som en blødgører i de fleste af polymererne.

Tilstedeværelsen af de fluorerede monomerer medførte et fald i den termiske stabilitet for alle de syntetiserede copolymerer. Den samme tendens gjorde sig gældende for polymererne fremstillet fra FMI, hvor de tilsvarende ikke-fluorerede polymerer udviste bedre termisk stabilitet.

Film fremstillet af de fluorerede copolymerer og polymerer udviste øget hydrofobicitet i sammenligning med de ikke-fluorerede homopolymerer. De mest hydrofobe egenskaber blev målt for diblok copolymererne, hvor kontaktvinkler på over 90° blev fundet i alle tilfælde med et maximum på 118° målt for en film bestående af PMMA-*b*-P17FM. Film med "Honeycomb" struktur blev fremstillet ved høj luftfugtighed fra copolymerer af 3FM og MMA, hvilket resulterede i meget hydrofobe overflader med statiske kontaktvinkler for vand på op til 144°.

Contents

List of Abbreviations

17FM	1,1,2,2-tetrahydroperfluorodecyl methacrylate
3FM	2,2,2-trifluoroethyl methacrylate
8FM	2,2,3,3,4,4,5,5-octafluoropentyl methacrylate
AIBN	2,2'-azo-bis-isobutyronitrile
AN	Acrylonitrile
ATRP	Atom transfer radical polymerization
BA	*n*-butyl acrylate
Bipy	2,2'-bipyridine
BMA	*n*-butyl methacrylate
CA	Contact angle
CL	ϵ-caprolactone
DCM	Dichlormethane
DMAEMA	2-(dimethylamino)ethyl methacrylate
DMAP	4-dimethylaminopyridine
dNbipy	4,4'-di(5-nonyl)-2,2'-bipyridine
dR_{f6}bipy	4,4'-di(tridecafluoro-1,1,2,2,3,3-hexahydrononyl)-2,2'-bipyridine
DSC	Differential scanning calorimetry
EBB	Ethyl-2-bromoisobutyrate
EGMAFO	Ethylene glycol monomethacrylate monoperfluorooctanoate
FAEM	Perfluoroalkyl acylate
FDA	1,1,2,2-tetrahydroperfluorodecyl acrylate
FEMA	Perfluoroalkyl ethyl methacrylate, *equivalent to 17FM*
FMA	1H,1H,2H,2H-tridecafluorooctyl methacrylate
FNEMA	2-[(perfluorononenyl)oxy] ethyl methacrylate
FOA	1,1-dihydroperfluorooctyl acrylate
FOMA	1,1-dihydroperfluorooctyl methacrylate
HEA	2-hydroxyethyl acrylate
HEMA	2-hydroxyethyl methacrylate
HMTETA	1,1,4,7,10,10-hexamethyltriethylene tetramine
IR	Infrared spectroscopy
MA	Methyl acrylate
MEA	2-methoxyethyl acrylate
MI	Macroinitiator
MMA	Methyl methacrylate
M_n	Number average molecular weight
M_w	Weight average molecular weight
NMP	Nitroxide mediated polymerization
NMR	Nuclear magnetic resonance spectroscopy
n-Pen-1	*N*-(*n*-pentyl)-2-pyridyl-methanimine

n-Pr-1	*N*-(*n*-propyl)-2-pyridyl-methanimine
PDI	Polydispersity index
PEGMA	Poly(ethylene glycol) methyl ether methacrylate
PEG	Poly(ethylene glycol)
PEO	Poly(ethylene oxide)
PFA	2,2,3,3,3-pentafluoropropyl acrylate
PHEA	Poly(2-hydroxyethyl acrylate)
PHEMA	Poly(2-hydroxyethyl methacrylate)
PMDETA	N,N,N',N',N"-pentamethyldiethylenetriamine
PPGM	Poly(propylene glycol) methacrylate
PS	Polystyrene
P*t*BA	Poly(*tert*-butyl acrylate)
PVDF	Poly(vinylidene fluoride)
RAFT	Reversible addition-fragmentation transfer polymerization
$scCO_2$	Supercritical carbon dioxide
SANS	Small-angle neutron scattering
SAXS	Small-angle X-ray scattering
SEC	Size exclusion chromatography
SPME	Solid-phase microextraction
St	Styrene
*t*BA	*t*-butyl acrylate
TEA	Triethylamine
TEMPO	2,2,6,6-tetramethyl-1-piperidinyloxy
TFEMA	2,2,2-trifluoroethyl methacrylate, *equivalent to 3FM*
TFT	α,α,α-trifluorotoluene
TGA	Thermogravimetric analysis
THF	Tetrahydrofuran
THFOMA	1H,1H,2H,2H-perfluorooctyl methacrylate
XPS	X-ray photoelectron spectroscopy

1

Background

1.1 Biocompatible Polymers

The use of tailored polymers for medico purposes has become increasingly important. Polymers that are compatible with human tissue can be used for purposes such as components in drug delivery and coatings for implants. The aim of this work was originally to synthesize amphiphilic copolymers capable of forming membranes meant for incorporation in a glucose microsensor for *in vivo* use. The membranes have several prospective functions such as control of diffusion (reduction of the glucose concentration relative to oxygen concentration, retain interfering components), ensuring biocompatibility and encapsulating non-biocompatible materials (needed for analysis of glucose).

Numerous patents and articles have been published on materials suitable for membranes in biosensors [1–3]. The use of block copolymers has often been a sought route, since these structures can be tailored to have the desired properties. In order to meet the requirements it is especially important that the copolymer can be cast into thin films i.e. form membranes. Biosensors intended for *in vivo* use are subject to the harsh working conditions resulting from the immune response, and the demands on the materials are therefore high. This leads to criteria of good chemical and mechanical stability of the membranes.

1.2 Fluorinated Polymers

Fluorinated polymers are highly hydrophobic and have lately received increased interest due to a number of unique properties including high biocompatibility and low surface energy, as well as good chemical and thermal resistance. The potential applications of fluorinated polymers are many and controlled radical polymerization methods have been used to synthesize tailored architectures for specific uses. Fluorinated block copolymers have been used to prepare low energy surfaces including water- and oil-repellent materials [4, 5]. Biomimicking and potentially biocompatible copolymers have been introduced by combining inert fluoropolymers with biopolymers or polymers known to circumvent immunological rejection [6–10]. The chemical inertness of fluorine has been exploited for synthesizing fluorinated copolymers for coatings on metals that form

a corrosion-protective layer on the surface [11]. Surface-initiated polymerizations of (co)polymer brushes on various surfaces have produced hydrophobic surfaces [12, 13] as well as materials that are tunable in hydrophobicity and permeability dependent on treatment in terms of change in pH, temperature, or solvent [14–17]. A range of porous membranes with three-dimensionally ordered structures have been prepared and some have shown great potential as proton-conducting materials for applications such as solid-state electrolytes in batteries [18, 19]. Fluorinated compounds including commercially available polymers have additionally been used as macroinitiators for non-fluorinated monomers to incorporate a fluorinated species in this way [20–22].

1.3 Scope of Thesis

The aim of the thesis work was to synthesize fluorinated copolymers for a glucose microsensor. In order to design the copolymers to fulfill their purpose, it was essential to understand the relationship between the polymer structure and the membrane behavior in use. Control over structure as well as chemical and physical properties was therefore vital, which lead to the choice of utilizing controlled radical polymerization for the synthesis of the fluorinated copolymers. Studies of filmforming and membrane properties would be conducted, when the targeted copolymers were synthesized. Membrane parameters such as the permeability of glucose and other penetrants could then be determined, if free films were produced.

During the period of this project the object of developing a membrane for a glucose sensor ceased to exist due to structural changes in Novo Nordisk A/S, which resulted in the discontinuation of the research on glucose sensors. The aim of the thesis was therefore changed to be the development of fluorinated copolymers with potential use as biocompatible materials.

In this work fluorinated polymers and copolymers were targeted as potential film forming components for uses in drug delivery. Three general routes were undertaken during the work on this Ph.D.:

- A difunctional macroinitiator based on a commercially available polymer was used for the polymerization of fluorinated monomers to form triblock copolymers.
- Fluorinated monomers were copolymerized with non-fluorinated monomers yielding block copolymers.
- A commercially available fluorinated surfactant was utilized as a macroinitiator for the polymerization of non-fluorinated monomers.

In all cases atom transfer radical polymerization (ATRP)[23, 24] was chosen as the polymerization method. ATRP is a technique of con-

trolled/living radical polymerization whereby polymer products with well-defined structures and narrow molecular weight distributions can be obtained.

1.4 Thesis Outline

1.4.1 Chapters

The experimental work performed as part of this thesis is reported chronologically to the extent it has been possible.

Chapter 2 gives an introduction to controlled radical polymerization methods and a thorough description of ATRP.

Initially the literature was studied before the polymerization of several fluorinated monomers, which we had at our disposal. In *Chapter 3* a short review on ATRP of fluorinated monomers from the literature is given followed by results of the preliminary polymerizations. These include polymerizations of non-fluorinated monomer methyl methacrylate (MMA) as a model compound for the fluorinated monomers as well as homopolymerizations of two of the fluorinated methacrylates. Finally the synthesis of triblock copolymers using poly(ethylene glycol) (PEG) macroinitiators for the polymerization of 2,2,2-trifluoroethyl methacrylate (3FM) is recounted.

The preliminary experiments with two of the fluorinated monomers indicated a lack of control over kinetics evidenced by relatively high polydispersities in several cases. An optimization process seemed necessary, which lead to the study of reaction kinetics (*Chapter 4*). The use of ^{1}H NMR analysis was initially attempted, but there were practical problems connected with this approach, as NMR apparatus is not part of the facilities at the Danish Polymer Centre, DTU. It is possible to analyze by NMR at Risø National Laboratory, Roskilde which is situated at a considerable distance from DTU, Kgs. Lyngby. It would therefore not have been possible to withdraw samples and analyze them during polymerization, which gave rise to the idea of an alternative method for monitoring conversions. We attempted to develop an analysis method for assessing monomer consumption by gas chromatography of samples extracted during polymerization. The polymerizations were performed at DTU, Lyngby while the analysis by gas chromatography took place at the nearby Danish National Museum, Brede in collaboration with Jens Glastrup. It was, however, not possible to obtain reproducible results by the chosen analysis method. In conclusion the results of a successful kinetic study utilizing ^{1}H NMR are reported.

I spent the first six months of 2006 in the group of professor David M. Haddleton at the University of Warwick, where the most recent kinetic study by ^{1}H NMR was carried out. Furthermore, the synthesis of fluorinated block copolymers were undertaken using the fluorinated methacry-

lates in combination with MMA (*Chapter 5*). Amphiphilic copolymers of 3FM and 2-methoxyethyl acrylate (MEA) and poly(ethylene glycol) methyl ether methacrylate (PEGMA), respectively were also synthesized. An alternative means of incorporating fluorine in a polymer was also chosen, namely polymerization of non-fluorinated monomers MMA, MEA and PEGMA utilizing a fluorinated macroinitiator (*Chapter 6*). The properties of all the synthesized polymers are recounted in *Chapter 7* and comparisons between the different synthetic approaches are made. During my stay at Warwick I collaborated with Daniel Nyström from the Royal Institute of Technology (KTH), Stockholm. The results of this work are also described in Chapter 7. Here we used the synthesized diblock copolymers to form structured films, which could be manipulated to yield highly hydrophobic surfaces.

Chapters 5 through 7 are meant to be complimentary to the papers found in the appendices. In the thesis I have thus tried to present the data in a different manner in order to draw some larger perspectives on the obtained results. Therefore the synthesis of the different polymers are treated in individual chapters e.g. only the synthesis of diblock copolymers is treated in Chapter 5. The discussion of properties is in a separate chapter, where all the fluorinated polymers and copolymers are included. Data that have been omitted in the publications have also been included in the thesis, when they illustrate the reasoning behind the decisions made during the work.

The experimental details are not given in the respective chapters, but can be found in *Chapter 10*, where the analysis methods are also described. This chapter mainly includes descriptions of the experimental work that has not been submitted for publication. The information given in this chapter may therefore in some cases seem to be contradictory to the appendices.

1.4.2 Appendices

In the appendices there are 4 papers, which are supplementary to the topics in the chapters.

Appendix 1. Natanya M.L. Hansen, Katja Jankova and Søren Hvilsted: *Fluoropolymer Materials and Architectures Prepared by Controlled Radical Polymerizations*, European Polymer Journal, *43 (2)*, 255-293, **2007**.

This review article gives an overview of fluorinated polymers synthesized by controlled radical polymerization methods, including ATRP. It is a more extensive introduction than the short review in Chapter 3 on the subject of synthesis of fluorinated polymers by ATRP. In addition to synthesis by ATRP, this article covers polymerization of fluorinated monomers by NMP and RAFT. The polymerization of fluorinated styrenic monomers is treated, while the use of fluorinated macroinitiators is also included.

Appendix 2. Natanya M.L. Hansen, Søren Hvilsted, Michael Gerstenberg, Daniel Nyström, David M. Haddleton: *Synthesis of Fluorinated Block Copolymers by Living Radical Polymerization*, Polymer Preprints, **2006**, *47(2)*, 689-690.

This short paper is both an early version of Appendix 4 and a publication treating the work on the polymers films having honeycomb structures, which are described in Chapter 7.

Appendix 3. Natanya M.L. Hansen, David M. Haddleton, Søren Hvilsted: *Fluorinated Bio-acceptable Polymers via an ATRP Macroinitiator Approach.*

The paper has been submitted to Journal of Polymer Science Part A: Polymer Chemistry. Chapter 6 recounts the most important polymerization results of this paper, while properties are covered in Chapter 7.

Appendix 4. Natanya M.L. Hansen, Michael Gerstenberg, David M. Haddleton, Søren Hvilsted: *Synthesis of Fluorinated Copolymers by Controlled Radical Polymerization*

This paper is a finished manuscript that has not yet been submitted. The material in this article is partly covered in Chapter 5 and partly in Chapter 7. The successful kinetic study of 3FM monitored by ^{1}H NMR analysis is also included in this paper (Chapter 4.4).

2

Methods of Controlled Polymerization

2.1 Living Polymerization

The definition of living polymerization is a polymerization reaction, where no unwanted side reactions such as transfer or termination take place, and where all polymer chains are initiated simultaneously. Thus, the growing ends of the polymer chains are active indefinitely and an ideally living system should yield polymers with polydispersities of 1.0. In reality no such reactions have been found, but some systems are not far from achieving this goal. For these reaction systems a number of terms have been used including "living", pseudo-living, quasi-living and living/controlled, which has led to confusion and frustration among researchers in the field [25].

As stated by Szwarc [26] no reaction can be truly living, therefore in this thesis the terms living polymerization and controlled polymerization will be used interchangeably and be applied to reactions, where termination and chain transfer are negligible, i.e. significantly slower than propagation, and where molecular weight distributions are narrow.

A living reaction defined as stated above fulfills the following criteria:

- Kinetics are first order with respect to the monomer
- Degree of polymerization is directly proportional to the initial monomer to initiator ratio
- Narrow molecular weight distributions are obtained
- After consumption of monomer the reaction can continue by addition of new monomer

Living polymerizations are interesting from both a scientific and an industrial viewpoint, as the discovery of these reactions opened up a whole new world of possibilities regarding design of novel polymeric architectures and compositions. The main types of living polymerization will be presented in the following.

2.2 Ionic Polymerization

2.2.1 Anionic Polymerization

Living anionic polymerization, the oldest living polymerization method known, was discovered in 1956 by M. Szwarc, who used sodium naphthalene to polymerize polystyrene in THF [27]. The "livingness", i.e. lack of termination, of the reaction was proved by continued reaction, when more monomer was added after consumption of the initial monomer amount. The simultaneous increase of the viscosity indicated that chain transfer was not taking place, but that the polymers instead were increasing in size. In the reaction a difunctional growing polymer chain is formed (Figure 2.1 (3)) through dimerization of the styrene radical anions created by transfer from the initially formed naphthalene radical anions (fig. 2.1 (1) & (2)). The sodium naphthalene initiator and equivalent species can be used to synthesize triblock copolymers, whereas e.g. the monofunctional n-butyl lithium can be used for the formation of homopolymers and diblock copolymers.

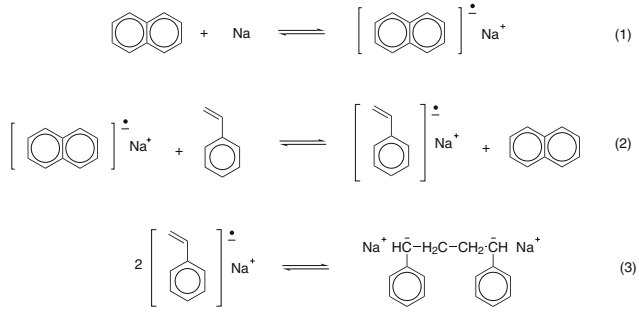

Figure 2.1. Mechanism of living anionic polymerization using sodium naphthalene as initiator. (1) Generation of radical anions of naphthalene with sodium (2) Transfer of charge to styrenic monomer (3) Dimerization yields dianion [28].

Anionic polymerization can in theory be used for any monomer that has a functional group next to the double bond, which is capable of stabilizing the anion formed by nucleophilic attack from the propagating species. It is, however, primarily used for styrenes and dienes, as a number of functional groups (amino, carboxyl, hydroxyl etc.) interfere with the propagation reaction [28]. Living anionic polymerization yields polymers with narrow polydispersities (< 1.1) and can be utilized for preparing a number of advanced polymer structures such as star shaped polymers with different (mikto) arms. The technique is currently used in the industry mainly for the production of thermoplastic elastomers and block copolymers of poly(ethylene oxide) and poly(propylene oxide), Pluronics ®.

2.2.2 Cationic Polymerization

Following the discovery of anionic polymerization the idea of cationic polymerization was obvious. Systems maintaining a certain control over reaction (termed quasiliving) were discovered in the 1970s, but it was not until 1984 that T. Higashimura and coworkers [29] succeeded in polymerizing isobutyl vinyl ether by living cationic polymerization (Figure 2.2).

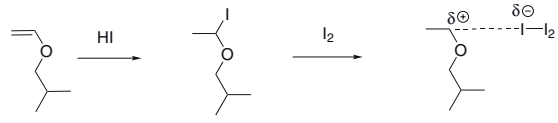

Figure 2.2. Living cationic polymerization of isobutyl vinyl ether using HI as initiator and I_2 as coinitiator [29].

In cationic polymerization an initiator (proton or cation donor) and a Lewis acid (coinitiator) are used to introduce an electrophile that can generate the cationic site on the growing chain. Cationic polymerization can be used for monomers that stabilize the cationic reactive site i.e. a tertiary or styrenic carbocation. Isobutene has therefore been studied extensively as is also the case for styrene and derivatives thereof (*para*-substituted mainly) [30].

2.3 Radical Polymerization

Controlled ionic polymerization is a powerful tool for designing polymers with specific structures and functionalities, but there are obvious limitations to these techniques in terms of choice of monomers and reaction conditions. After the triumphs in the area of ionic polymerization including commercial use of these techniques, there was a certain drive to develop methods for obtaining controlled reactions employing radical mechanisms. The main problem in controlling radical polymerization is that unlike ionic polymerization, the active chain ends can react with one another either by radical combination or by disproportionation. The strategy for eliminating aforementioned termination reactions has been to ensure that only a fraction of the polymer in question is activated at a given time, i.e. present as an active radical, while the majority of polymer chains are in a dormant/inactivated state. There must exist a dynamic equilibrium between the two states in order for the growth of the polymer chains to be equal. When the polymer is only in the activated state for short time periods, another unwanted side reaction, namely transfer of a free radical from an active to a dormant chain, can be suppressed. This is required to obtain control over the polymerization, as transfer reactions will in most cases lead to broad molecular weight distributions.

2.3.1 Nitroxide Mediated Polymerization

The first step toward a controlled polymerization reaction involving radicals was nitroxide mediated polymerization, which was undertaken in 1993 by M. Georges and coworkers [31], inspired by the work done by G. Moad and E. Rizzardo [32] on using nitroxides as radical trapping agents. The nitroxide 2,2,6,6-tetramethyl-1-piperidinyloxy (TEMPO) was used by Georges *et al.* to control the polymerization of styrene, where the reaction was initiated by a free radical initiator, benzoyl peroxide. During reaction the nitroxide efficiently end-capped the growing polymer chains by a reversible termination reaction ensuring equal growth of all chains, while suppressing termination. Alkoxyamines have proved more efficient than TEMPO by being able to function as both initiator and end-capping group as outlined in Figure 2.3, giving full control over the concentration of initiating radicals. The TEMPO-type nitroxides (piperidine structure) have mainly been used for styrenic monomers, but improved types have made the polymerization of acrylates, acrylamides, 1,3-dienes and acrylonitrile monomers by nitroxide mediated polymerization possible. Different functional groups are tolerated in NMP such as amino, carboxylic acid and glycidyl. NMP has furthermore been used for design of complex architectures such as star, graft and dendritic polymers [33].

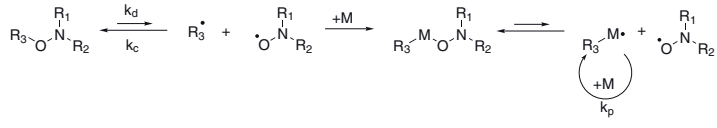

Figure 2.3. Mechanism of Nitroxide Mediated Polymerization with alkoxyamine functioning as both initiator and end-capping group [34]. The alkoxyamine is homolytically cleaved to the initiating radical $\bullet R_3$ and the stabilized, persistent radical $\bullet ONR_1R_2$. The monomer (M) reacts with the initiating radical before recombination takes place. k_d and k_c are the rate constants of dissociation and combination, respectively.

2.3.2 Atom Transfer Radical Polymerization

Reactions, where metal catalysts were utilized in combination with aromatic ligands yielding well-controlled structures and narrow molecular weight distributions, were concurrently carried out in 1995 by research groups headed by K. Matyjaszewski [24] and M. Sawamoto [23]. The term Atom Transfer Radical Polymerization was coined by Matyjaszewski, whereas Sawamoto's groups termed this type of reaction Metal Catalyzed Living Radical Polymerization. The mechanism involves the transfer of a halogen atom from the polymer to a metal catalyst yielding an active chain end (a radical), hence the term Atom Transfer Radical Polymerization (ATRP). Reaction is outlined in Figure 2.4 and takes place through

a reversible redox reaction involving the transition metal catalyst (Mt), which is oxidized as the polymer is converted from the dormant state (P-X) to the active species (P•) through the transfer of the halogen (X). The metal catalyst is bound in a complex with a multidentate ligand (L), which assists in binding the halogen. The deactivation reaction is kinetically favored in the equilibrium ($k_d \gg k_a$) thus rendering only a small concentration of active radical species present at a given time. Ideally, this eliminates the possibility of two activated polymer chain ends encountering to give termination, while in practice termination does occur.

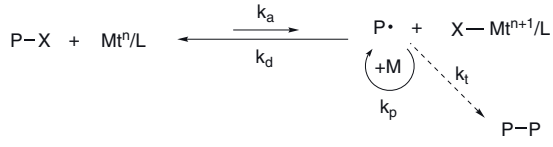

Figure 2.4. Mechanism of Atom Transfer Radical Polymerization [35]. The halogen-bound polymer chain (P-X) is converted to an activated form (P•), which can propagate the monomer (M). Activation is facilitated by the transfer of the halogen (X) to the metal-ligand complex (Mt/L). k_a, k_d, k_p and k_t are the rate constants of activation, deactivation, propagation and termination, respectively.

2.3.3 Reversible Addition-Fragmentation Transfer Polymerization

One of the newest methods of controlling molecular structure when employing radical mechanisms is Reversible Addition-Fragmentation Transfer Polymerization, RAFT, which was introduced by E. Rizzardo and G. Moad in 1998 [36]. Reaction is controlled via a dithio compound, the RAFT agent, which is transferred between the active and dormant chains by a reversible addition-fragmentation reaction. During reaction the active polymer formed by initiation adds to the RAFT agent to form a radical species (see Figure 2.5), which fragments into a new active radical and a dormant polymer-RAFT adduct. The formed radical is either the species R•, which can start a new polymer chain (Figure 2.5 (1)), or the polymer chain P_n•, that can continue growing (Figure 2.5 (2)). Rapid transfer between the different radical species ensures that the formed polymers grow to equal lengths. X is normally a sulfur atom, while Z is a group that influences addition and fragmentation rates (this can be a phenyl, pyrrole or other group). The correct choice of RAFT agent ensures that the exchange reaction is significantly faster than the propagation reaction, so in combination with a higher concentration of RAFT agent than initiator, a polymer product with a narrow molecular weight distribution is obtained.

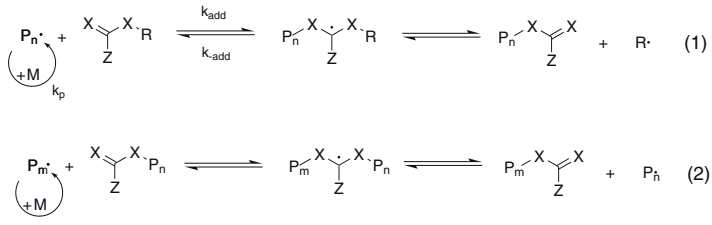

Figure 2.5. Mechanism of Reversible Addition-Fragmentation Transfer Polymerization [37]. (1) The active polymer ($P_n\bullet$) adds to the RAFT agent (ZC(X)XR) to form a radical species, which fragments into a new active radical (R$\bullet$) and a dormant polymer-RAFT adduct (ZC(X)XP_n). (2) A dormant polymer-RAFT adduct reacts with an active polymer chain ($P_m\bullet$) resulting in a new active polymer ($P_n\bullet$). k_{add} and k_{-add} are the rate constants of addition and the reverse reaction, respectively.

The advantage of the RAFT method is that virtually the same reaction conditions as for free radical polymerization can be used including initiators such as 2,2'-azo-bis-isobutyronitrile (AIBN) and dibenzoyl peroxide. RAFT is tolerant of a number of functional groups in the monomer including carboxylic acids, amides and tertiary amines and has been used in design of di- and triblock copolymers as well as star structures [37].

2.4 Ionic versus Radical Polymerization

While there are limitations in the ionic polymerization methods regarding possible monomer structures, there are also advantages compared to radical polymerization. The foremost advantage of ionic polymerization compared to radical polymerization is that the active ionic species do not react with one another. There are very stringent demands on purity when using ionic polymerization techniques, more than in controlled radical polymerization, but nevertheless controlled ionic polymerization is used in large scale industrial production as opposed to controlled radical polymerization, which is presently only exploited for very specific uses by a limited number of companies. This is probably in part due to the fact that controlled ionic polymerization has a head start over controlled radical polymerization of more than 20 years!

The current work is focused on the use of ATRP as a tool for synthesizing amphiphilic block copolymers with well-defined structures. ATRP is a convenient method for synthesizing polymers with various side-groups, as the reaction conditions are mild and therefore tolerant of a number of different functionalities in both monomer and initiator. In the following a more detailed account of ATRP is given.

2.5 Polymerization by ATRP

2.5.1 Monomers

ATRP can be carried out with monomers that have a functional group, which can stabilize the propagating radical. The most common monomers include styrene, (meth)acrylates, (meth)acrylamides and acrylonitrile. Monomers with highly labile or reactive groups that have been polymerized by ATRP are shown in Figure 2.6, but this is only a few examples of the versatility of this technique and must not been seen as an exhaustive recount of the possibilities of the method. For each monomer the rates of activation and deactivation (k_a and k_d, Figure 2.4) are unique, and these in combination with the rate of propagation k_p determine the polymerization rate.

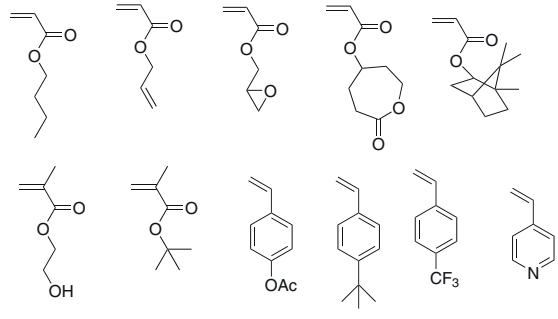

Figure 2.6. Examples of monomers with different functionalities polymerized by ATRP [38].

2.5.2 Initiators

Initiators for ATRP must have a halogen (Br or Cl) and a functional group that can stabilize the formed radical e.g. carbonyl, cyano or phenyl. The initiator is normally chosen so that the structure mimics the structure of the monomer with the aim of making the rate of initiation and propagation equivalent ($k_i = k_p$), e.g. 1-phenylethyl bromide is a natural choice of initiator for polymerization of styrene. The product of an ATRP reaction is a potential initiator for yet another reaction, as it still has the halogen moiety in the growing chain end. This allows reactivation of the chain end using the initially synthesized polymer as a macroinitiator for a second polymerization reaction, making ATRP especially suited for synthesizing tailored block copolymers. Alternatively a macromolecular species can be functionalized and thereby be a potential (macro)initiator for polymerization. Different functionalities can be incorporated in the initiator and a number of functional groups are tolerated, some examples are given in

Figure 2.7 [38]. Multifunctional initiators can be used to synthesize more advanced architectures such as star polymers.

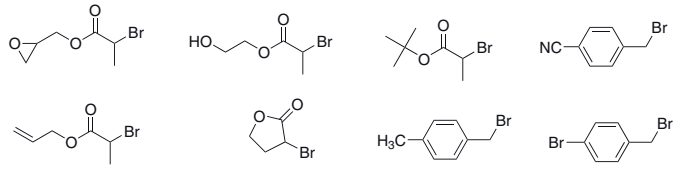

Figure 2.7. Examples of initiators used for ATRP [38].

2.5.3 Catalysts

The catalyst consists of a transition metal and a halogen, with the metal being a transition metal such as copper, nickel, ruthenium, palladium, rhodium or iron. The criteria for the metal are: 1) It has two oxidation steps separated by one electron step 2) It has an affinity for halogen and 3) It can complex strongly with the ligand.

The main criteria for the halogen are that it can migrate rapidly between the growing chain and the catalyst, and that the bonds with both these species are broken homolytically. The halogen is usually bromine or chlorine, but pseudohalogens have also been used. Fluorine is normally too electronegative to allow homolytic cleavage, however, secondary fluorine has been used for ATRP [39], while iodine has been utilized in some cases [40]. The catalyst is susceptible to oxidation to the higher oxidation step during reaction, which can be avoided by operating under inert conditions.

2.5.4 Ligands

The primary function of the ligand is to ensure solubilization of the metal catalyst in the solvent, but the reactivity of the metal catalyst is highly influenced by the steric and electronic properties of the ligand as well. Bulky side groups on the ligand can sterically hinder bond formation with the halogen, while electron withdrawing groups can prevent the homolytic cleavage of the halogen-metal bond. The first ligand used by Matyjaszewski was 2,2'-bipyridine (bipy), which is a bidentate ligand. While still in use bipyridine is being fazed out by other multidentate nitrogen ligands with more complex structures that have proved to be superior in controlling the radical formation, when tailored to fit specific systems. While amino-type ligands are used for copper-based ATRP, phosphorus-based ligands are used for most other transition metals in ATRP [38]. A few examples of used ligands are given in Figure 2.8.

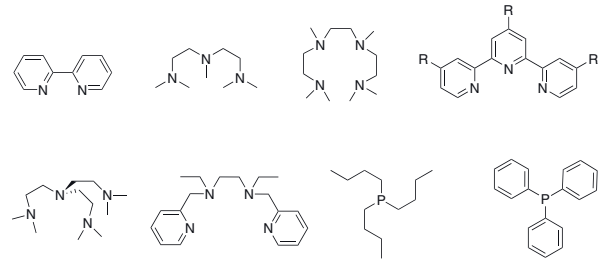

Figure 2.8. Examples of ligands used for ATRP [38]. Bipy is shown top left.

2.5.5 Solvents

ATRP can be run in bulk, but often a solvent is required to ensure dissolution of the catalyst/ligand complex and reduce viscosity at high conversions. Traditionally used solvents such as toluene, acetone, diphenyl ether, dimethyl formamide and various alcohols can be used for ATRP, but more surprisingly polymerization can in some cases also take place in water, which has aroused interest due to the obvious advantages of low solvent price, environmental considerations and eliminated handling precautions. Supercritical carbon dioxide as a solvent has also attracted attention because of environmental friendliness and cost reduction. In general, solvents reduce propagation rate, but polar solvents can increase the rate of reaction, in some cases providing better control over the product [41].

2.5.6 Limitations of ATRP

A number of functional groups in the monomer are not tolerated in ATRP including carboxylic acid and certain ionic groups, which react with the catalyst, thereby impeding the establishment of the equilibrium. Carboxylic acid groups can, however, be introduced by polymerization of the carboxylic acid salt instead. This was first realized by the group of Armes, who polymerized methacrylic acid in aqueous media at pH $\sim$ 9 using a poly(ethylene oxide) macroinitiator [42]. Other monomers such as vinyl acetate and halogenated alkenes can not be polymerized by ATRP, due to insufficient stabilization of the formed radical.

The main concern in using ATRP for synthesis, industrial or otherwise, is removal of the catalyst. The metal catalyst-ligand complex is undesired in the product, as the transition metal induces aging in the polymer, but also for aesthetic (coloration) and toxicological reasons removal is important. Catalyst removal is both difficult and costly, but several methods are presently in use. One procedure is to immobilize the catalyst by having it attached to solid supports during reaction, but this can give loss of control, perhaps due to reduced mobility. Other purification methods

include passing the raw product through an alumina column, precipitation of polymer and use of an absorbant [43].

2.5.7 Copolymers Synthesized by ATRP

A number of different polymer structures have been synthesized by ATRP including star shaped, graft and dendritic polymers. The numerous possibilities for combination of monomers provides the opportunity to obtain products possessing qualities of utterly different nature such as polar/nonpolar, hydrophilic/hydrophobic or rigid/flexible.

There are two different approaches to synthesizing linear di- and triblock copolymers: the macroinitiator method and sequential polymerization. The latter strategy involves synthesizing a polymer of the first monomer, which initiates the second monomer by a continuous reaction. When using the macroinitiator approach, the first polymer is synthesized, analyzed and purified followed by reinitiation of the second monomer. An alternative macroinitiator method is to utilize a macromolecule (considered the first polymer block), which is functionalized to act as an initiator for polymerization of the second polymer block. The macromolecule in question can be a industrially synthesized polymer such as poly(ethylene oxide) or a natural polymer such as chitosan, both of which have hydroxyl groups that can be converted into initiating sites.

3

Polymerization of Fluorinated Methacrylates

3.1 Fluorinated Acrylates and Methacrylates Polymerized by ATRP

One aim of this thesis was to synthesize amphiphilic block copolymers utilizing fluorinated methacrylates and acrylates with a fluorinated pendant alkyl chain. During the study of previous work in the literature a review has been written regarding polymerization of fluorinated monomers by controlled radical polymerization methods and the potential uses of the synthesized products (Appendix 1). Herein descriptions of the polymerization of different fluorinated monomers have been given and the uses of fluorinated (macro)initiators are furthermore described. Figure 3.1 shows the diversity of methacrylates and acrylates containing fluorine employed in ATRP, while more detailed descriptions of the reaction conditions of the polymerizations are given in Table 3.1. In the following a brief recount is given on the experimental complications reported by the researchers in the field regarding this type of monomers. These difficulties must be considered before commencing on polymerization.

Generally, it is possible to polymerize fluorinated methacrylates and acrylates by ATRP, however a number of challenges must be faced upon working with these monomers. Products are generally not soluble in non-fluorinated solvents making characterization difficult, which can be seen from the lack of results for polydispersity index (PDI) in Table 3.1. Due to the low solubility of the fluorine moiety, reaction should preferably take place in a fluorinated solvent, but this can in turn be a poor solvent for the non-fluorinated comonomer(s). One solution to the solubility problem has been to polymerize in supercritical carbon dioxide, which is furthermore considered to be a environmentally friendly solvent. The drawback of this approach is that special equipment is necessary in contrast to when using traditional solvents. Most research groups have polymerized the fluorinated monomer as the second block of the copolymer thereby to a great extent avoiding to solubilize the fluorinated product. Random copolymerization also seems to have been a way of keeping the polymers in solution, as the solubility is higher for the mixed block than for a pure fluorinated polymer block.

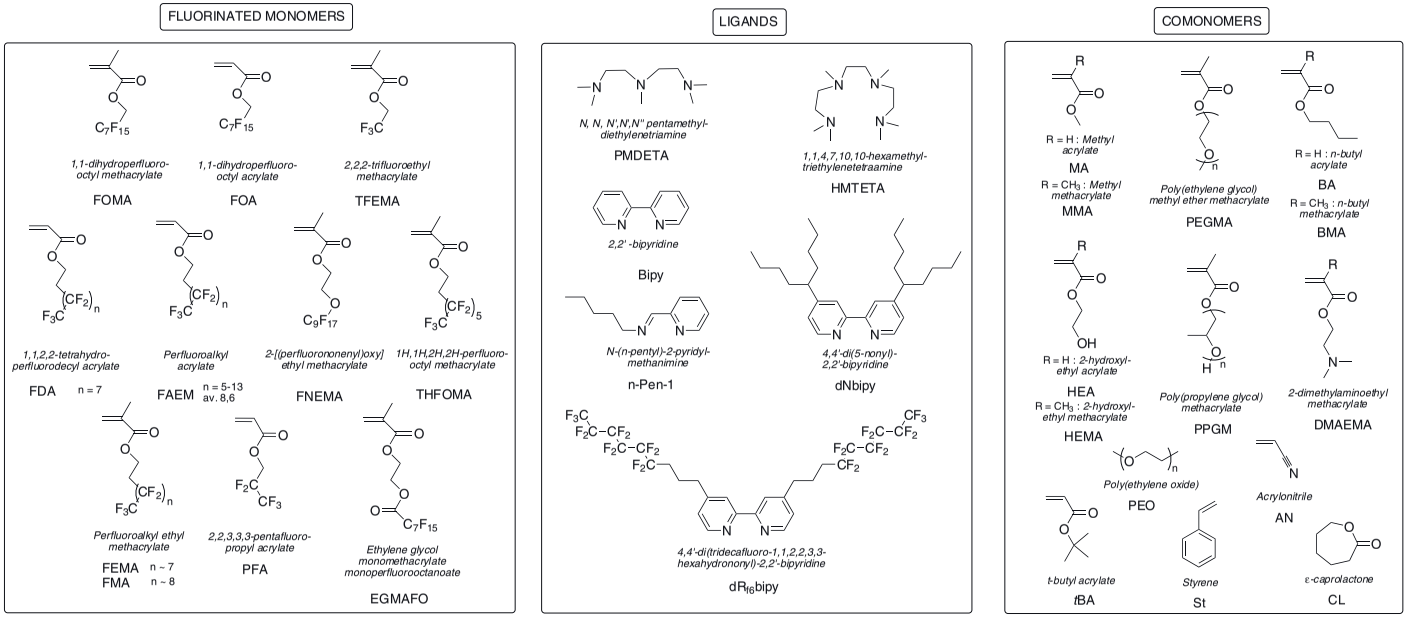

Figure 3.1. Fluorinated methacrylates and acrylates polymerized by ATRP in the literature. Ligands and comonomers used for the reactions according to Table 3.1.

Table 3.1. Overview of ATRP protocols utilized for methacrylates and acrylates having a fluorinated pendant chain.

Source	Monomer	Type	Solvent, temperature	Catalyst, ligand	[I]:[Mt]:[L]	Polydispersities	Molecular weights[a] (g/mol)
[44, 45]	FOMA	AB block from PMMA, P*t*BA & PHEMA	TFT, 110 °C	CuBr, Bipy	1 : 1 : 3	1.3 - 1.6	104,000; 53,000; 40,000
[46]	FOMA, FOA	AB block w. MMA & DMAEMA (FOMA only)	$scCO_2$, 85 °C (4900 psi)	CuCl, Bipy, dNbipy, dR_{f6}bipy	1 : 0.5 : 2 (bipy) 1 : 0.5 : 1	-	6400 & 2800 (NMR) (FOMA copolymers)
[47]	FOMA	AB block from PS-*r*-PAN	TFT/THF (4:1), 100 °C	CuBr, Bipy	1 : 2 : 6	1.13 - 1.18	18,000 - 26,000 (NMR)
[4]	FAEM	AB block from PBMA	cyclohexanone, 100 °C	CuBr, PMDETA	1 : 1 : 2	1.28 - 1.44	8100 - 26,000
[20, 48]	TFEMA, FEMA	Homopolymers, random FEMA w. MMA & St	Toluene, 90 °C	CuBr, n-Pen-1	1 : 1 : 2	1.29 (PTFEMA), 1.12 - 1.2 (co-MMA), 1.19 - 1.48 (co-St)	20,500 (PTFEMA), 8100 - 11,000 (co-MMA) 6500 - 13,000 (co-St)
[21]	FEMA	Homopolymer, random w. PEGMA & PPGM. Star (homopolymer & AB block from PPEGMA)	TFT/benzene, 80 °C (homo & random), 114 °C (star)	CuBr, PMDETA	1 : 1 : 1	1.09 (random w. PEGMA)	7300 (NMR) & 15,000 (random), 8200 (NMR) (homo-star), 17,600 (NMR) (AB-star)
[8]	FOMA, THFOMA	ABA & AB block from PEO-MI (2k & 5k)	TFT/benzene, 120 °C	CuCl, Bipy	1 : 1 : 3	-	20,000; 50,000; 100,000 (monomer conversion)
[9, 49]	THFOMA	ABA & AB block from PEO-MI (2k (diblock), 6k, 10k & 20k)	butyl acrylate, 80 °C	CuBr, Bipy, PMDETA	1 : 1 : 2	1.1 (diblock), 1.1 - 2.1	2,300 (diblock), 6300 - 32,000
[50]	FDA	AB block from PEO-MI (1.7 k)	cyclohexanone, 100 °C	CuBr, HMTETA	1 : 1 : 1	-	31,000 (NMR)
[6]	THFOMA	AB block from PCL	$scCO_2$, 45 °C (1500-1700 psi)	CuBr, Bipy	1.3 : 1 : 2	1.26 - 1.51	13,000 - 33,000
[51, 52]	FNEMA, EGMAFO	ABA & AB block from PMA, PBA & PS	TFT, 100 °C	CuBr, Bipy	1 : 5 : 14	1.27 - 1.49 (FNEMA) 1.38 - 2.41 (EGMAFO)	7200 - 29,000 (FNEMA) 7200 - 45,000 (EGMAFO)
[5, 53]	FNEMA	AB block from PS (SO_3H) & P*t*BA (COOH)	TFT, 100 °C	CuBr, Bipy, PMDETA	1 : 5 : 14 (bipy) 1 : 5 : 5	1.35 & 1.41 (co-*t*BA) 1.21 - 1.60 (co-St)	18,000 (co-*t*BA) 7200 - 32,000 (co-St)
[15]	PFA	AB block from PMA-grafts on silica substrate	TFT, 90-100 °C	CuBr, PMDETA	1 : 1 : 2	-	-
[16]	TFEMA	Homopolymer, Grafted on silica substrate then AB block with MA	TFT, 90 °C	CuCl, dNbipy	1 : 1 : 2	-	-

k: kg/mol, MI: Macroinitiator, NMR: Nuclear magnetic resonance spectrocopy, $scCO_2$: Supercritical carbon dioxide, SEC: Size exclusion chromatography, TFT: α,α,α-trifluorotoluene.

[a] *Molecular weights estimated by SEC unless otherwise stated.*

Apparently it can be problematic to achieve narrow molecular weights, which is probably due to the insolubility of the fluorinated polymers, but also lack of compatibility with the non-fluorinated species could be an explanation. The incompatibility is substantiated in several cases by the presence of microdomains in the final copolymers as seen by DSC.

3.2 Choice of Monomers

Fluorinated styrenes have previously been synthesized in our group [54–57], but there was no specific knowledge of fluorinated methacrylates or acrylates. We were generously provided with three different fluorinated methacrylic monomers (Osaka Chemicals, viscoat®) with perfluorinated pendant alkyl chains of varying length (Figure 3.2). The terminology used for the monomers is connected to the number of fluorine in the pendant alkyl chain (i.e. CF_3 in 3FM etc.), and it has therefore been chosen to operate with these names, although others have used other terms (cf. Figure 3.1, where 3FM is the same as TFEMA, while 17FM is equivalent to FEMA). Before starting polymerization of the fluorinated compounds preliminary experiments were run with the non-fluorinated monomer methyl methacrylate (MMA) as model compound to optimize reaction conditions.

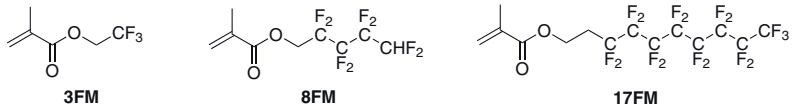

2,2,2-Trifluoroethyl methacrylate

2,2,3,3,4,4,5,5-Octafluoropentyl methacrylate

1,1,2,2-Tetrahydroperfluorodecyl methacrylate

Figure 3.2. Fluorinated methacrylates with potential use as monomers in ATRP for the preparation of amphiphilic copolymers.

3.3 Homopolymerization of MMA

Preliminary syntheses were performed with MMA to test the polymerization method with the existing experimental setup (for further detail see Chapter 10). The polymerizations were performed in xylene using Cu(I)Br catalyst with various ligands. For these and the subsequent homopolymerizations of the fluorinated methacrylates ethyl-2-bromoisobutyrate (EBB) was used as initiator. Four different ligands used in the literature have been studied: Bipy, PMDETA, HMTETA (see Figure 3.1) and tris[2-(dimethylamino)ethyl] amine (Me_6TREN). The latter was synthesized from tris[2-aminoethyl]amine by an Eschweiler-Clarke reductive methylation following the methologies of Matyjaszewski *et al.* [58] and

Ciampolini *et al.* [59] to give a yield of 89 % (Figure 3.3). The successful polymerization of acrylates at ambient temperature using this ligand has previously been reported [60].

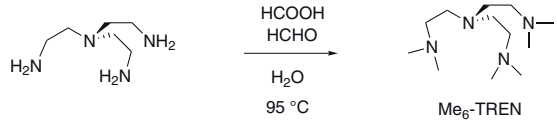

Figure 3.3. The synthesis of ligand Me_6TREN from the equivalent non-methylated amine.

Table 3.2 shows the obtained results for the homopolymerization of MMA. Polydispersities and molecular weights (M_ns) were determined by size exclusion chromatography (SEC), while yields were found gravimetrically. The results of the syntheses of MMA were satisfactory with low PDIs and molecular weights close to the target of 20,000 g/mol, when using PMDETA, HMTETA and bipy. Me_6TREN gave the highest polydispersity (1.39) and a very low molecular weight, indicating that this ligand is not well suited for MMA.

Table 3.2. Polymerization of MMA.

Sample	Ligand	[I]:[L]	Temperature (°C)	Yield (%)	PDI	$M_{n,SEC}$ (g/mol)
1	PMDETA	1:1	90	38	1.07	15,400
2	HMTETA	1:1	90	89	1.21	22,500
3	Bipy	1:2	80	40	1.20	22,600
4	Me_6TREN	1:1	80	11	1.39	5100

Initiator: ethyl 2-bromoisobutyrate, solvent: xylene, monomer concentration: 15 vol%, reaction time: 15 hours, target molecular weight 20,000 g/mol.

3.4 Homopolymerization of 3FM

Based on the preliminary results of the polymerizations of MMA, it was chosen to focus the initial polymerization work on the monomer 3FM, as this compound has been (homo)polymerized previously by several groups. This monomer was also deemed to be the most soluble in the non-fluorinated solvent chosen, xylene. Chen *et al.* reported a PDI as low as 1.15 for a P3FM polymer with M_n = 17,000 g/mol for a preliminary reaction executed before polymerizing this monomer on to a silica surface [16]. Based on the results from the preliminary polymerizations of MMA, PMDETA was chosen as the preferred ligand, although polymerizations with HMTETA and bipy were carried out as well. Finally *N*-(*n*-propyl)-2-pyridylmethanimine (n-Pr-1)(see inset Figure 3.5), was also utilized. The

Haddleton group was the first to synthesize *N*-(*n*-alkyl)-2-pyridylmethanimines and consequently utilize these as ligands for ATRP with good results [61] and therefore this type of ligand has been used for the polymerization of 3FM (*n*-pentyl pendant alkyl chain)[48]. The reaction temperature was kept at 80 °C to maintain control over the polymerization, as the fluorinated monomer was expected to react faster than MMA in accordance with results obtained for fluorosubstituted styrenes [54, 62, 63].

Table 3.3. Polymerization of 3FM.

Sample	Ligand	[I]:[L]	Monomer vol.(%)	Time (h)	Yield (%)	PDI	$M_{n,SEC}$ (g/mol)
1	Bipy	1:2	15	1	18	-	270
2	HMTETA	1:1	15	1	21	1.80	12,900
3	n-Pr-1	1:2	50	4	88	1.41	29,100
4	n-Pr-1	1:2	100	1.7	42	1.32	45,700[a]
5	PMDETA	1:1	15	1	20	1.37	8600
6	PMDETA	1:1	15	5	68	1.58	14,400
7	PMDETA	1:1	15	15	54	1.67	11,000
8	PMDETA	1:1	100	0.5	75	1.64	27,500
9	PMDETA	1:1	100	5	38	2.41	14,600

Initiator: ethyl 2-bromoisobutyrate, reaction temperature: 80 °C, solvent: xylene, target molecular weight: 20,000 g/mol.

[a] *Target molecular weight: 50,000*

The results obtained for the polymerization of 3FM are shown in Table 3.3[1]. The indicated molecular weights are, however, probably lower than the actual values due to the difference in molecular weight and hydrodynamic volume of the 3FM-unit and the PMMA-standards. It was not possible to use ^{1}H NMR (nuclear magnetic resonance spectroscopy) for end-group analysis to estimate molecular weights, as the signals from the initiator and the polymer backbone overlap. The same tendencies are seen as for MMA with the best results in terms of both molecular weight distributions and yields found when using PMDETA ligand (considering only the previously utilized ligands). The n-Pr-1 ligand gave results comparable to PMDETA, in some cases even better, as molecular weights were close to target and yields were fair. PDIs were relatively low and comparable to previously reported results (Table 3.1). Both PMDETA and n-Pr-1 were therefore chosen for the subsequent polymerization of 3FM from poly(ethylene glycol) macroinitiators to yield triblock copolymers (section 3.6).

[1]Reaction time is given in fraction of 100 for all reactions here and in the following

3.5 Homopolymerization of 17FM

Having reached a set of reasonable reaction conditions for the polymerization of 3FM, the polymerization of fluorinated methacrylate 17FM was undertaken, although the system was not considered entirely optimized. The ligands n-Pr-1 and PMDETA were used with longer reaction times than for 3FM. Proceeding in this fashion, we obtained polymeric products that could not be dissolved in THF, the solvent of our SEC system, resulting in lack of PDI determination. The values given in Table 3.4 are only valid for the fraction of low molecular weight product that could be dissolved and analyzed, which accounts for the low M_n and PDI values. ^{1}H NMR analysis indicated the formation of polymer, which could also be confirmed by FT-IR with the disappearance of the double bond at 1640 cm^{-1} (C=C). The latter analysis alone would not have been conclusive, as the C-F bonds at 1199 and 1144 cm^{-1} are very dominant in the spectra as seen in Figure 3.4 reducing the relative intensity of the double bond signal.

Solubility problems during synthesis of this polymer have previously been reported both by Perrier *et al.* [20] and Shemper *et al.* [21]. After these initial results combined with the observations reported in the literature, further reactions of 17FM were abandoned for the time being.

Table 3.4. Polymerization of 17FM.

Sample	Ligand	[I]:[L]	Monomer vol (%)	Time (h)	Yield (%)	PDI[a]	$M_{n,SEC}$[a] (g/mol)
1	n-Pr-1	1:2	50	1.6	69	-	-
2	n-Pr-1	1:2	50	4	20	*1.09*	*3100*
3	n-Pr-1	1:2	100	16	89	-	-
4	PMDETA	1:1	15	1	20	*1.19*	*2500*
5	PMDETA	1:1	15	16	68	*1.18*	*2800*

Initiator: ethyl 2-bromoisobutyrat, solvent: xylene, temperature: 80 °C, target molecular weight: 30,000 g/mol.

[a] *Data for soluble fraction of polymer*

3.6 Synthesis of Triblock Copolymers with Poly(ethylene glycol) Macroinitiators

Poly(ethylene glycol) macroinitiators had previously been synthesized in our lab [64] and by combining these with the fluorinated methacrylates amphiphilic copolymers with two very different blocks would be realized. Amphiphilic triblock copolymers of this type have been synthesized by Lim *et al.* [8] utilizing poly(ethylene oxide) macroinitiators (M_n = 2000

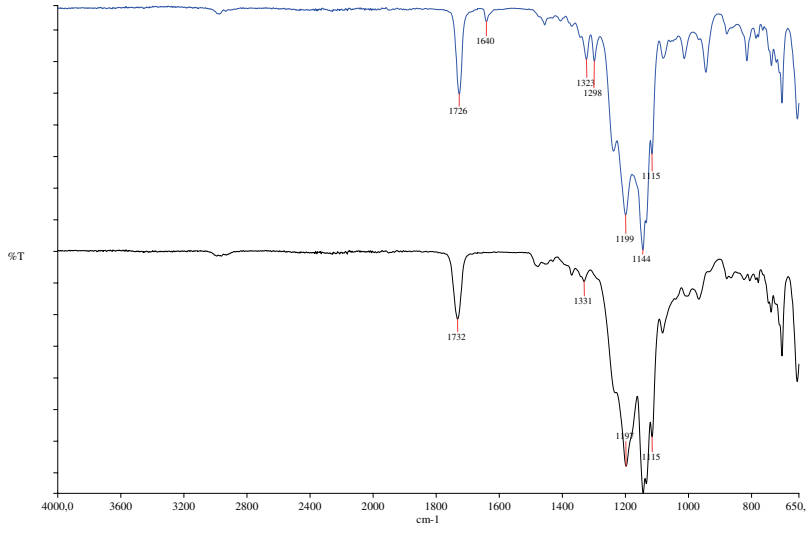

Figure 3.4. FT-IR spectra of 17FM monomer (upper, blue) and P17FM homopolymer (lower, black).

and 5000 g/mol) for the polymerization of the fluormethacrylates 1H,1H-perfluorooctyl methacrylate (FOMA) and 1H,1H,2H,2H-perfluorooctyl methacrylate (THFOMA). Reactions took place in a mixture of trifluorotoluene (TFT) and benzene at 120 °C using Cu(I)Cl/bipy giving high conversions (85 - 95 %) with very high initiator efficiencies (>90 %). It was, however, impossible to analyze the products by SEC, as the amphiphilic polymers aggregated in THF even at low concentrations, consequently the polydispersities were not found. Poly(ethylene oxide) macroinitiators have also been utilized by Hussain *et al.* [9, 49] to synthesize di- and triblock copolymers with perfluorohexylethyl methacrylate, FMA (see Figure 3.1). Poly(ethylene oxide)s (M_n = 2, 6, 10 and 20 kg/mol) were converted to macroinitiators with 2-bromopropionyl bromide and used for polymerization of FMA at 80 °C in butyl acetate using Cu(I)Br as catalyst with bipy or PMDETA as ligand. The authors do not give information on yields or initiator efficiency, but polydispersities as low as 1.1 were found by SEC (THF) and monomodal curves were generated in all cases. A certain degree of aggregation of the block copolymers during SEC analysis was observed, as a lower molecular weight than for the initial macroinitiator was found in some instances.

Using the protocol of the above mentioned studies, 3FM was polymerized using difunctional poly(ethylene glycol)-macroinitiators (PEG) for the formation of amphiphilic triblock copolymers (Figure 3.5). PEG with molecular weights of 2000 and 4600 g/mol, termed PEG2000 and PEG4600, respectively, were used to synthesize the macroinitiators (see 10.3.2 for de-

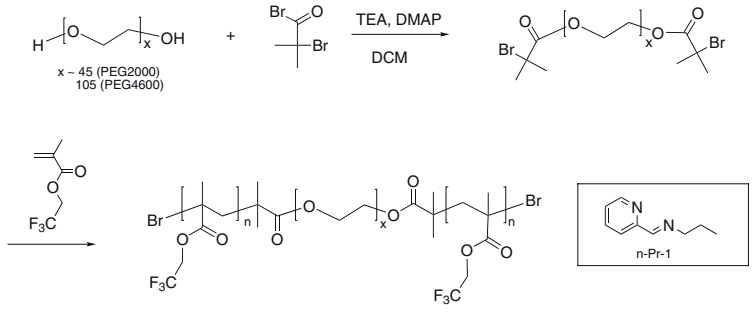

Figure 3.5. Synthesis of triblock copolymers of fluorinated methacrylate 3FM with poly(ethylene glycol) macroinitiators. DCM: dichlormethane, DMAP: 4-dimethylaminopyridine, TEA: triethylamine. Inset: n-Pr-1 ligand.

tails) [65]. Polymerizations were conducted at 80 °C in xylene at different concentrations (15 or 50 %) with Cu(I)Br as catalyst and PMDETA or n-Pr-1 as ligand. Results are shown in Table 3.5.

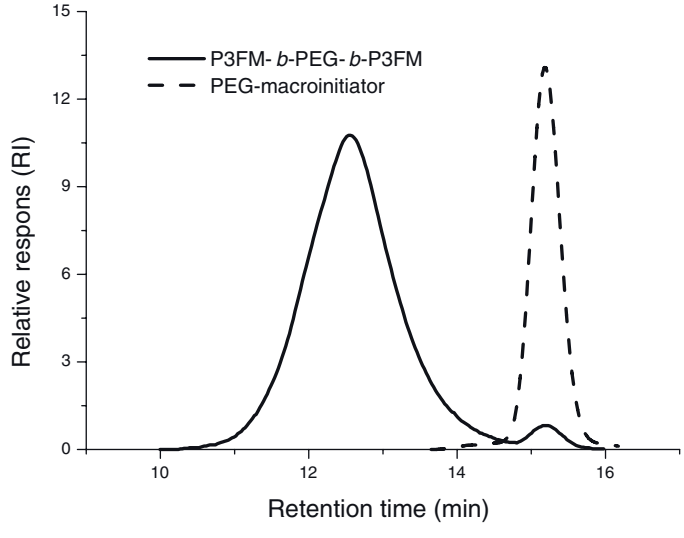

Figure 3.6. SEC-traces for P3FM-*b*-PEG-*b*-P3FM triblock copolymer (entry 5, Table 3.5) and PEG2000-macroinitiator.

Table 3.5. Polymerization of 3FM using PEG-based macroinitiators.

Sample	Ligand	Macroinitiator	Time (h)	Yield (%)	PDI	$M_{n,SEC}$ (g/mol)	$M_{n,NMR}$ (g/mol)	Target (g/mol)
1	PMDETA	PEG2000	1	79	1.60	23,700	20,300	22,000
2	PMDETA	PEG2000	5	79	1.50	19,100	16,800	22,000
3	PMDETA	PEG4600	5	>99	1.88	28,500[a]	30,000	25,000
4	n-Pr-1	PEG2000	1.7	>99	1.39	29,900	26,800	22,000
5	n-Pr-1	PEG2000	4	>99	1.38	30,400	26,300	22,000
6	n-Pr-1	PEG4600	4	97	1.29	31,700	27,600	25,000
7	n-Pr-1	PEG2000	0.5	>99	1.51	6240[a]	5260	4600
8	n-Pr-1	PEG4600	0.5	>99	1.23	12,000[a]	10,000	9800
9[b]	n-Pr-1	PEG2000	1.7	71	1.50	27,600	23,900	22,000

Temperature: 80 °C, solvent: xylene, monomer concentration: 50 vol% (n-Pr-1) or 15 vol% (PMDETA), [I]:[Cu(I)Br]:[ligand] = 1:1:1 (PMDETA) or 1:1:2 (n-Pr-1).

[a] *Complete separation of the peaks from polymer and macroinitiator was not possible.*
[b] *Reaction took place at 100 °C.*

In all cases yields were very good (almost quantitative) and molecular weights close to target were obtained. Molecular weight distributions were quite broad, which was probably due to a combination of low initiator efficiency and differences in solubility between the reacting species. Residual macroinitiator was seen in all SEC-traces (Figure 3.6) and these signals were in some instances overlapping with the polymer signals making separate integration difficult. For entries 7 and 8 in Table 3.5, where polymers with very low molecular weights were targeted, bimodal traces were obtained rather than separate peaks (Figure 3.7).

The molecular weights of the triblock copolymers could be estimated by both SEC and ^{1}H NMR. For the latter method the signals from C$\underline{H}_2$-CF_3 in the fluorinated blocks (4.15 ppm) were compared to the C$\underline{H}_2$-O signals from the macroinitiator (3.6 ppm). Figure 3.8 shows an ^{1}H NMR spectrum of a triblock copolymer synthesized from PEG2000 with a total molecular weight of 16,800 g/mol (entry 2, Table 3.5). There was good correspondence between the molecular weights achieved by SEC and ^{1}H NMR, and these values were also close to the target molecular weights.

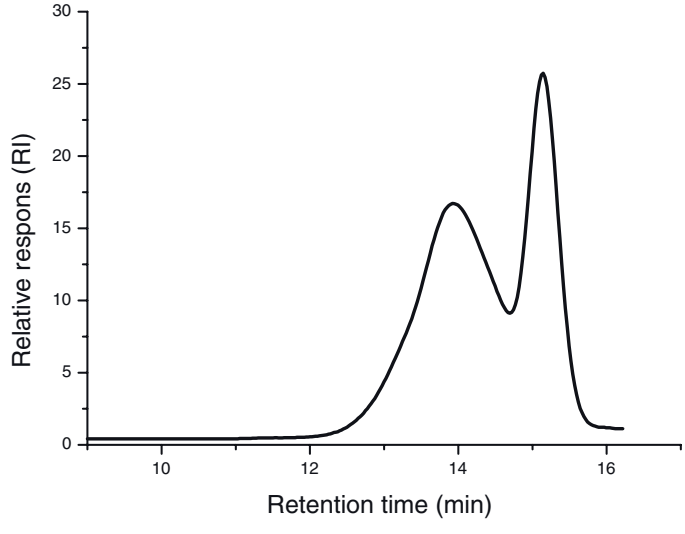

Figure 3.7. SEC-traces for P3FM-*b*-PEG-*b*-P3FM triblock copolymer (entry 7, Table 3.5) and unreacted PEG2000-macroinitiator. The signals overlap due to the low molecular weight of the copolymer.

In conclusion it was possible to synthesize triblock copolymers using the PEG-macroinitiators, although broad molecular weight distributions were obtained in most cases, due to the presence of non-reacted macroinitiator. This is most likely caused by low initiator efficiency, which has also previously been observed by Perrier and Haddleton [66]. The triblock

copolymers could probably have been isolated by fractionation, which was not attempted due to the small amounts of product. Overall the polymerization results were satisfying, as the synthesis of the targeted triblock copolymers, which in principle are novel, was possible.

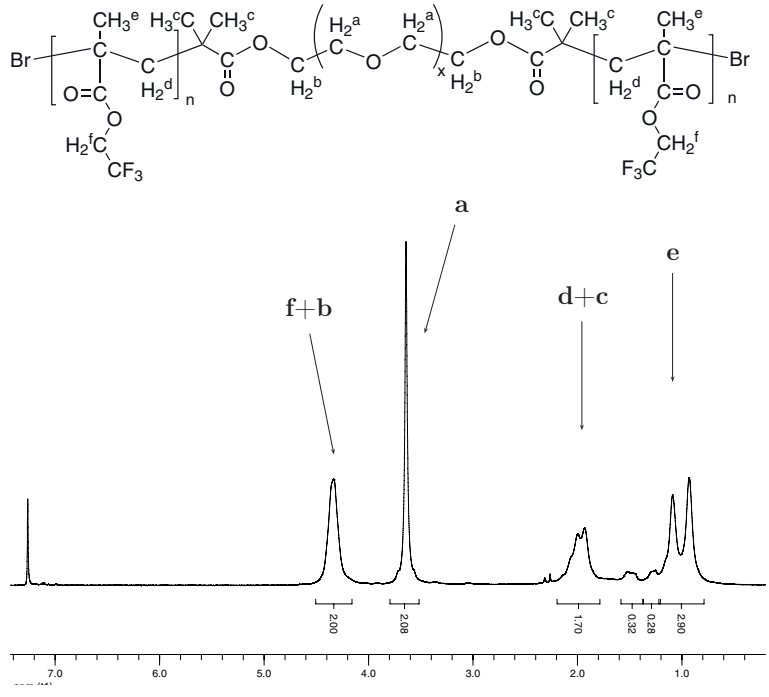

Figure 3.8. ^{1}H NMR spectrum of P3FM-*b*-PEG-*b*-P3FM copolymer. Assignments according to the the structure above are indicated by the arrows.

4

Kinetic Studies

4.1 Kinetics in ATRP

The criteria for a polymerization reaction to be considered living were reflected upon in Chapter 2, and a discussion of the reasoning behind these is given in the following.

In order for an ATRP reaction to be controlled, the kinetics must be first order with respect to the monomer, and the rate of propagation is described by equation (4.1) [35].

$$R_p = \frac{k_p[M][PX]_0 k_a[Mt^n]}{k_d[XMt^{n+1}]} \tag{4.1}$$

The notation refers to the reaction shown in Figure 2.4, where k_a, k_d and k_p are the rate constants of activation, deactivation and propagation, respectively, [M] is the concentration of monomer, [Mt^n] is the concentration of catalyst in the original (reduced) state, [XMt^{n+1}] is the concentration of the halogen bound catalyst (oxidized state), and $[PX]_0$ is initial initiator concentration (equivalent to [I]).

Assuming that [Mt^n] and [XMt^{n+1}] are constant, as these species exist in a dynamic equilibrium, equation (4.1) can be simplified to (4.2), where k_p^{app} is the apparent rate coefficient of reaction.

$$R_p = k_p^{app}[M] \tag{4.2}$$

For a first-order polymerization reaction equation (4.3) applies, where t is reaction time. The combination of (4.3) and (4.2) gives equation (4.4).

$$R_p = \frac{-d[M]}{dt} \tag{4.3}$$

$$\frac{-d[M]}{dt} = k_p^{app}[M]$$

$$\Downarrow$$

$$\int_{[M]_0}^{[M]} \frac{-d[M]}{[M]} = \int_0^t k_p^{app} dt$$

$$\Downarrow$$

$$ln\frac{[M]_0}{[M]} = k_p^{app} t \tag{4.4}$$

A linear relationship between $\ln([M]_0/[M])$ and reaction time, t must therefore exist in order for a polymerization reaction to follow the kinetics of ATRP. The same can however also be found for a non-controlled radical polymerization reaction, which proceeds as a first-order reaction. Hence, other criteria must be fulfilled for a polymerization to be considered controlled.

The second requirement for a controlled polymerization mechanism is that the degree of polymerization (DP) should be proportional to the initial ratio between monomer and initiator by a factor, p, which is equivalent to the degree of conversion cf. equation (4.5). Thus, all the initiator present must react instantaneously in order for equivalent chain lengths to be obtained. Hence, the evolution of molecular weight should be linear with conversion and proceed from origin.

$$DP = \frac{[M]_0}{[PX]_0} p \tag{4.5}$$

After consumption of the monomer the polymerization should be able to continue by addition of new monomer, as this proves the lack of termination, provided the polydispersity does not increase. Polydispersities in ATRP are defined according to equation (4.6). From this it can be seen that an increase in conversion (and molecular weight) reduces the last factor of the equation, whereby the ratio of M_w to M_n decreases.

$$\frac{M_w}{M_n} = 1 + \frac{k_p[PX]_0}{k_d[XMt^{n+1}]}(\frac{2}{p} - 1) \tag{4.6}$$

In order to define a polymerization reaction as controlled, the following must therefore be observed:

- Linear first-order kinetics
- Decrease in polydispersity during reaction or low polydispersity throughout reaction
- Linear evolution of molecular weights with conversion

Several studies of the kinetics of the fluorinated methacrylate 3FM were undertaken as part of this Ph.D. study and will be recounted in the following. In these studies the results were evaluated according to the requirements stated above.

4.2 Monitoring Kinetics by ^{1}H NMR - I

The key to controlling a polymerization is determining the kinetics of the reaction. Often the conversion is found by ^{1}H NMR spectroscopy by monitoring the disappearance of monomer and the formation of polymer in samples extracted during reaction. This approach is, however, only possible when running reaction in bulk or concentrated solution, as a solvent would obliterate the signals from both monomer and polymer.

Kinetics of 3FM were initially studied by ^{1}H NMR on a reaction in bulk, where samples were extracted at regular intervals. Conversions were estimated from the peaks for C$\underline{H}_2$-CF_3 at δ_H 4.49 (2H, q) (monomer) and δ_H 4.33 (2H) (polymer) shown in Figure 4.1. From the conversion data a linear first-order plot was generated (Figure 4.2), where the apparent rate constant, k_p^{app} was $1.3{\cdot}10^{-4}$ s^{-1}.

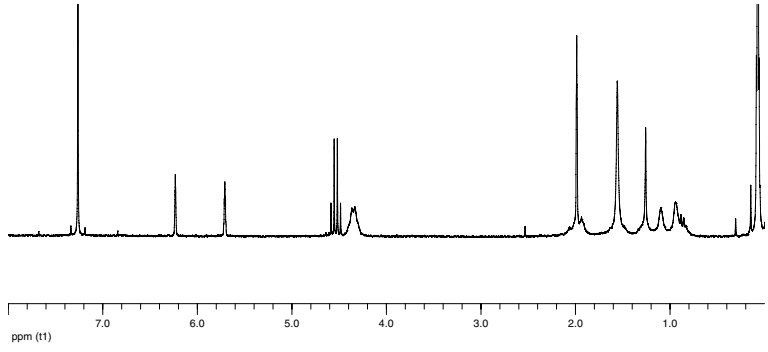

Figure 4.1. ^{1}H NMR ($CDCl_3$) spectrum for a sample taken during the homopolymerization of 3FM in bulk at 80°C (final sample). t = 100 min, conversion = 59 % determined from the signals at δ_H 4.49 (monomer) and δ_H 4.33 (polymer). [M]:[I]:[CuBr]:[n-Pr-1] = 300:1:1:2.

The extracted samples were analyzed by SEC to yield molecular weights, which were seen to increase with conversion. The polydispersities, however, also increased from 1.2 to 1.5 (fig. 4.3), which did not indicate an entirely controlled reaction mechanism. The final product of this reaction had a PDI of 1.32 and M_n of 45,700 g/mol (target 50,000 g/mol), which was the best result obtained in the homopolymerization of 3FM in this system. Reactions in dilute solution had indicated a controlled mecha-

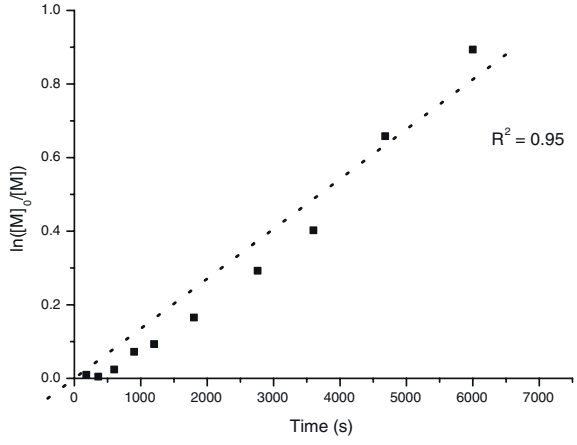

Figure 4.2. First order kinetic plot of the homopolymerization of 3FM at 80°C using ^{1}H NMR. [M]:[I]:[CuBr]:[ligand] = 300:1:1:2.

nism, so a ^{1}H NMR study in dilute solution could have been undertaken. This was not attempted, as the access to NMR apparatus was limited, which lead to the investigation of the use of a different analysis method, as described in the following.

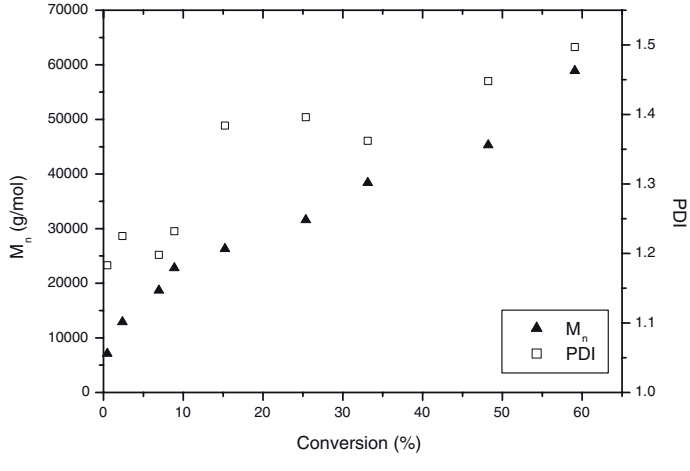

Figure 4.3. Evolution of M_n and PDI for the homopolymerization of 3FM at 80°C. [M]:[I]:[CuBr]:[n-Pr-1] = 300:1:1:2.

4.3 Monitoring Kinetics by Solid-Phase Microextraction

Although kinetics are commonly monitored by ^{1}H NMR analysis, any fast non-destructive quantitative analysis method can in principle be used. The use of solid-phase microextraction (SPME) [67] was attempted for the monitoring of residual monomer in samples taken during a polymerization reaction. No prior examples of the use of SPME in this field was known, thus this was a completely new approach to studying polymerization kinetics.

4.3.1 Analysis Theory

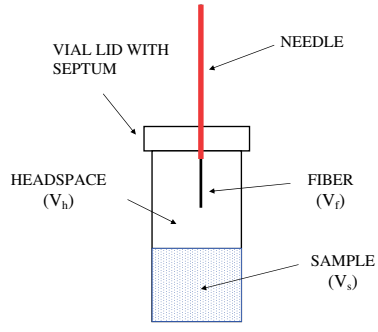

Figure 4.4. Sampling in solid-phase microextraction: A silica fiber is used to absorb volatile components from the headspace of a sample.

SPME is carried out using GC/MS apparatus for analysis. A needle with an absorbing fiber material (commonly silica fiber) is used to absorb volatile species from the headspace of a sample (see Figure 4.4). Desorption is obtained in the injector of the gas chromatograph by heating of the needle, whereby the analytes evaporate on to the column and are chromatographed. In the analysis of a polymerization by SPME the monomer and solvent will typically be absorbed on the needle and subsequently be analyzed, while formed polymer remains intact in the analysis sample.

If it is assumed that the theoretically absorbable volume in the needle is very large compared to the actual amount of absorbed sample, then it can also be assumed that the initial absorption rate is independent of the absorbed quantity. Thus, for very short absorption periods, the absorbed amount is proportional to the absolute quantity. The linear relationship between the absorbed amount of a species and the concentration of this component in the sample can be used to estimate the amount of residual monomer in a sample taken during polymerization. It is only required

that the absorption time is kept constant, but without reaching equilibrium. In order to obtain an absolute value in terms of concentration an internal standard is used. This is a compound that will be present during polymerization without interfering with the reaction and that will absorb on the needle along with the monomer.

The main advantage of the SPME analysis method is that contamination of the GC-column with solids can be avoided. Short absorbtion and analysis times speak in favor of this analysis method, which furthermore provides the possibility of on-line monitoring during polymerization.

4.3.2 SPME Experiments

4.3.2.1 Calibration Curve

The polymerizations of 3FM were performed in a mixture of TFT and xylene, where TFT had the role of both cosolvent and internal standard. A calibration curve was generated by preparing samples with varying volume fractions of 3FM, TFT and xylene. Total volume was kept at 500 μl with 100 μl of TFT. Volume of 3FM was varied from 1 μl to 40 μl reducing the volume of xylene equivalently. The signals of 3FM and TFT were well separated and the relative concentration of 3FM was determined by comparing the peak area of 3FM with the peak area of the internal standard, TFT. The precision of the method is demonstrated in Figure 4.5 by the very low standard deviation (R^2=0.997) of the generated calibration curve.

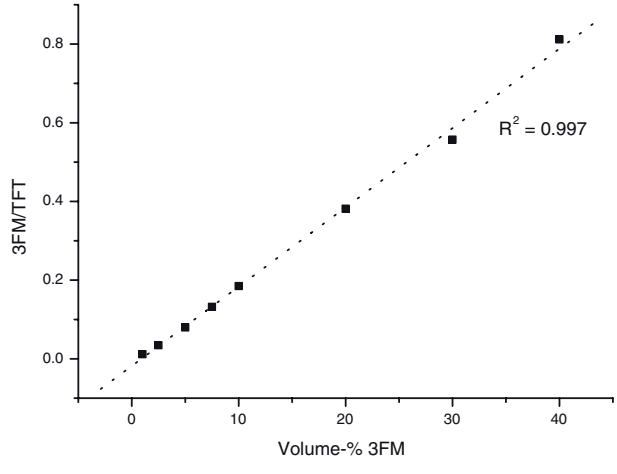

Figure 4.5. Calibration curve generated for the analysis of reaction kinetics of 3FM by SPME. The value 3FM/TFT is found by comparing peak areas in the chromatogram of these two compounds.

4.3.2.2 Polymerizations

Polymerizations were conducted at temperatures from 70 to 110 °C for different time intervals with sample extraction during reaction. Sample extraction was conducted under nitrogen and the extracted volume was approx. 200 μl. Extracted samples were transferred to vials containing 0.5 ml xylene to keep sample and headspace volumes constant (V_s and V_h, respectively). The structures of the polymers were confirmed by ^{1}H NMR analysis, while the final products were analyzed by SEC. The specific details of instrumentation are given in Chapter 10.

4.3.2.3 Results

The molecular weights and polydispersities of the final products are shown in Table 4.1. Initially a number of reactions were carried out at 80 °C to optimize the analysis process, when this seemed to be under control, polymerizations were performed at the other temperatures. One of the best results is shown in Figure 4.6, which shows the kinetic plot for a reaction at 100 °C (entry 7, Table 4.1). The first order kinetic plot was linear and the polymeric product obtained in this reaction had a relatively narrow polydispersity (1.32). A well-controlled product was also obtained, when repeating this experiment (entry 8, Table 4.1). The first-order kinetic plot was, however, not remotely linear as seen in Figure 4.7. Apparently no reaction took place at 70 °C (Figure 4.8), which was evidenced by a constant monomer concentration throughout reaction (over 2 days!) and only traces of oligomer in SEC and ^{1}H NMR.

Table 4.1. Polymerization of 3FM - final products of SPME kinetic study.

Sample	Time (h)	Temperature (°C)	Yield (%)	PDI	$M_{n,SEC}$ (g/mol)
1	51.5	70	0	-	-
2	6	80	9	1.32	17,500
3	8	80	33	1.39	32,300
4	24	80	94	1.53	49,600
5	25	80	90	1.64	50,400
6	12.5	90	28	1.90	44,500
7	6.5	100	41	1.32	33,000
8	6.5	100	18	1.26	21,000
9	4	110	29	1.33	24,100

[M]:[I]:[CuBr]:[ligand] = 300:1:1:2. Monomer concentration: 40 vol% in xylene (40 vol%)/TFT (20 vol%).

4.3.2.4 Sources of Error

The reproducibility of results using SPME was poor, which was surprising due to the accuracy of the analysis exhibited initially in the generation

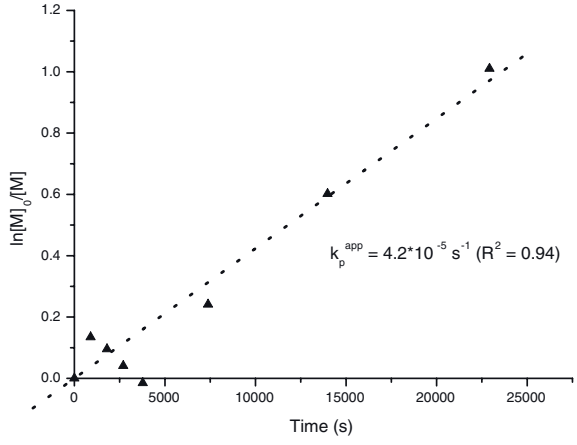

Figure 4.6. First-order kinetic plot of the homopolymerization of 3FM at 100 °C (entry 7, Table 4.1) using SPME. [M]:[I]:[CuBr]:[ligand] = 300:1:1:2.

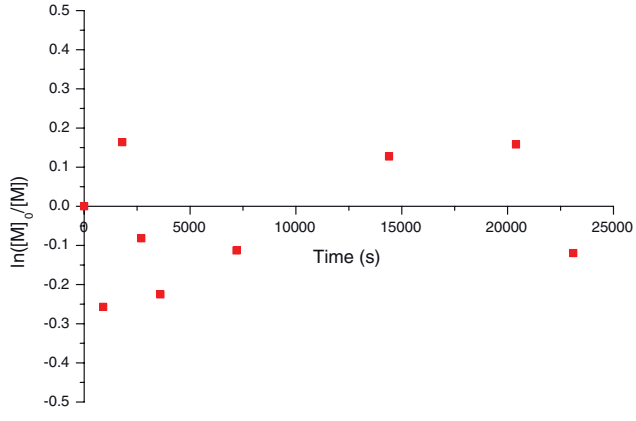

Figure 4.7. First-order kinetic plot of the homopolymerization of 3FM at 100 °C (entry 8, Table 4.1) using SPME. [M]:[I]:[CuBr]:[ligand] = 300:1:1:2.

of the calibration curve. The peaks of 3FM, TFT and xylene were all well separated in the chromatogram, so the source of error was not to be found there. A number of other factors could, however, have influenced the results. The injection of samples for analysis was manual, which gives different exposure times of the needle in headspace and injector. There was furthermore lack of temperature control of samples during analysis. Typically all samples were brought to ambient temperature and analyzed, but the room temperature could vary. The exposure time of the needle

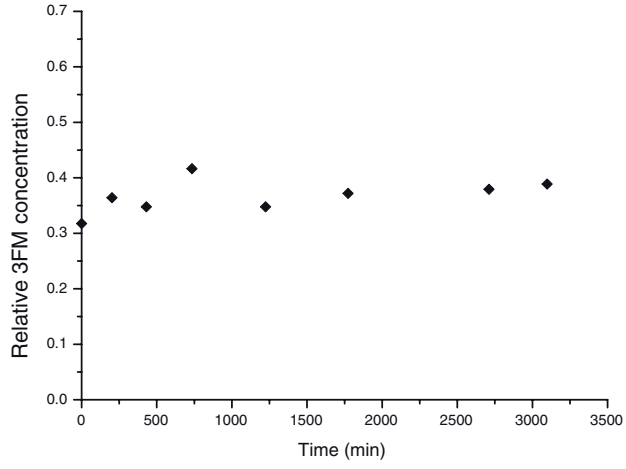

Figure 4.8. Relative concentration of 3FM with time at a reaction temperature of 70 °C (entry 1, Table 4.1) using SPME. [M]:[I]:[CuBr]:[ligand] = 300:1:1:2.

to the headspace may have been too long, thereby overloading the needle. These effects were, however, not observed during the generation of the calibration curve. Another possibility could be the fact that extractions were manual resulting in varying extraction volumes and consequently varying headspaces. Evaporation of volatiles was also possible during sampling. It is furthermore possible that the SPME needle was contaminated with solids (polymer or catalyst) from the samples, which could lead to less absorption from the headspace than anticipated. Finally and most likely the inhomogeneity of the polymerization samples may have resulted in an absorption on the fiber of the needle differing from the behavior observed during the generation of the calibration curve. This could be due to the polymer influencing the measured components, 3FM and TFT, by acting as a reservoir for one or both in which case the absorbed amounts would no longer be proportional.

In spite of initially holding great promise the use of SPME was discontinued due to lack of time for further optimization.

4.4 Monitoring Kinetics by ^{1}H NMR - II

4.4.1 Kinetics of 3FM

A second kinetic study of 3FM utilizing ^{1}H NMR analysis was performed, when the use of NMR equipment was realized. The specific details of the polymerizations can be found in Appendix 4. The system was a slightly different from the one utilized for the SPME studies, as toluene was used as

solvent (50 vol% monomer concentration) and no internal standard was needed. Homopolymerization of 3FM was undertaken at temperatures from 80 to 110 °C. The polymerization proceeded in a controlled fashion at all temperatures with linear first-order kinetic plots, molecular weights increasing with conversion and PDIs of less than 1.4 throughout reaction. The first-order kinetic plots for all the homopolymerizations are shown in Figure 4.9, while an example of molecular weight evolution is given in Figure 4.10.

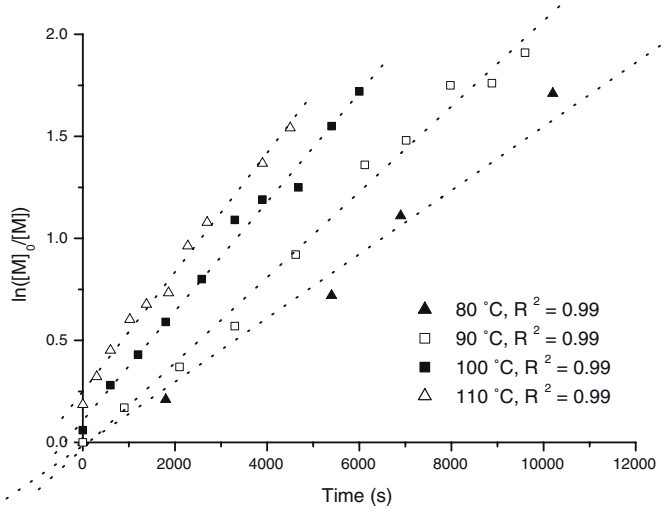

Figure 4.9. First-order plots of homopolymerizations of 3FM at 80 °C, 90 °C 100 °C and 110 °C. [M]:[I]:[Cu(I)Br]:[n-Pr-1] = 120:1:1:2. For the polymerization at 80 °C only data up to t = 12,000 s is shown.

Table 4.2. Polymerization of 3FM - final products of ^{1}H NMR kinetic study.

Sample	Temperature (°C)	Time (min)	Conversion (%)	$M_{n,SEC}$ (g/mol)	PDI	k_p^{app} (10^{-4} s^{-1})
1	80	320	94	9900	1.35	1.6
2	90	160	85	8800	1.38	2.1
3	100	100	82	7900	1.34	2.7
4	110	75	79	6200	1.28	2.9

Solvent: toluene, monomer concentration: 50 vol%,
[M]:[I]:[Cu(I)Br]:[n-Pr-1] = 120:1:1:2.

The kinetic study exhibited a clear temperature dependency demonstrated by the acceleration of the polymerization reaction with increasing temperature. Apparent rate constants of reactivity, k_p^{app} ranging from

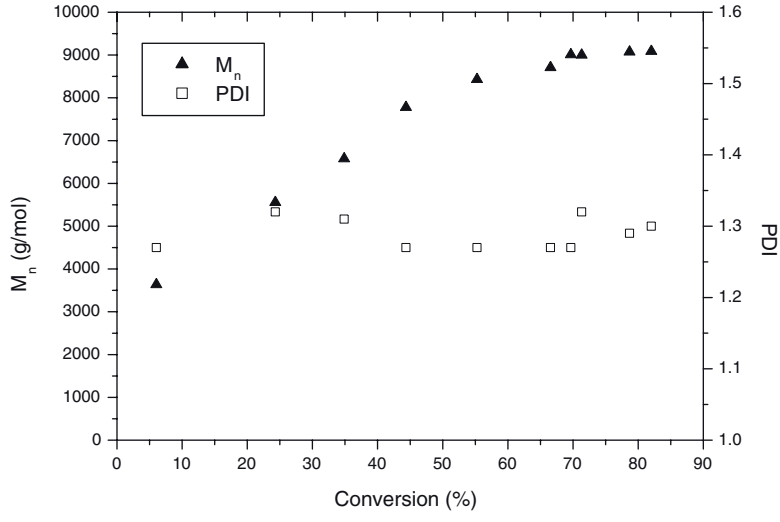

Figure 4.10. Evolution of M_n and PDI for the synthesis of P3FM at 100 °C (entry 3, Table 4.2). [M]:[I]:[Cu(I)Br]:[n-Pr-1] = 120:1:1:2.

$1.6{\cdot}10^{-4}$ s^{-1} to $2.9{\cdot}10^{-4}$ s^{-1} were found, which is in accordance with the value of $1.2{\cdot}10^{-4}$ s^{-1} previously found for MMA at 90 °C in an identical reaction system [61]. The polymerization rate of 3FM was seen to be faster than for MMA, which has also been the observation for a number of fluoro-substituted styrenes compared to styrene in ATRP [54, 62, 63]. Furthermore the value of $1.6{\cdot}10^{-4}$ s^{-1} is in relative good agreement with the value of $1.3{\cdot}10^{-4}$ s^{-1} found in the initial ^{1}H NMR study. The activation energy, E_a of the reaction can be found from the Arrhenius plot shown in Figure 4.11, where the slope is equivalent to -E_a/R according to the Arrhenius equation (4.7), where R is the gas constant, T is the absolute temperature, k is k_p^{app} and A is a constant.

$$lnk = lnA - \frac{E_a}{RT} \tag{4.7}$$

From the Arrhenius plot E_a is found to be 24 kJ/mol. This is a significantly lower value than the one found by Haddleton *et al.* in the homopolymerization of MMA in toluene (25 % solution): 61.3 kJ/mol [68].

4.4.2 Kinetics of 8FM

The second kinetic study of 3FM utilizing ^{1}H NMR for determining conversion was successful. This lead to an attempt at the same approach for the monomer 8FM, which has a longer fluorinated pendant alkyl chain than 3FM. A molecular weight of 15,000 g/mol was targeted in a ho-

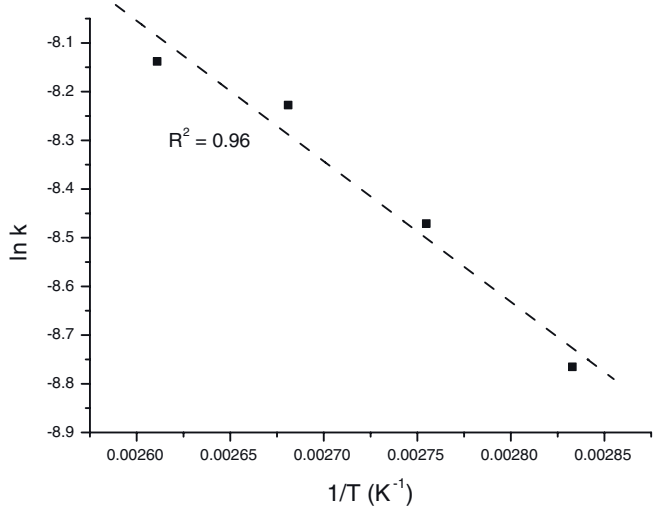

Figure 4.11. Arrhenius plot of the rate constants of reactivity for the homopolymerization of 3FM in toluene (50 vol%). [M]:[I]:[Cu(I)Br]:[n-Pr-1] = 120:1:1:2.

mopolymerization with the reaction conditions being the same as those used for 3FM. The first-order kinetic plot is seen in Figure 4.12, which clearly shows that the plot is not entirely linear. This is believed to be mainly due to solubility problems and not non-linear kinetics. The samples extracted at 170 and 230 minutes, respectively were initially too concentrated to be analyzed by ^{1}H NMR and were therefore diluted before analysis (smaller volumes were withdrawn from the reaction mixture for the following samples). Dilution (and handling) obviously lead to a large degree of error, as the conversion at 230 min can not possibly be higher than at the completion of reaction after 370 min.

The first few samples analyzed by SEC showed the expected tendency with increasing molecular weights and decreasing polydispersities (M_n = 14.800 g/mol, PDI = 1.07 at 43 % conversion). At higher conversions, however, the samples were not completely soluble in chloroform, the solvent used for analysis by SEC. Only the data for the soluble fraction of polymer were therefore obtained giving very misguiding results with very low molecular weights (∼5000 g/mol) and PDI∼1.3. It was concluded that this method was not suited for this particular monomer due to the low solubility. A different analysis method for estimating molecular weights could most probably have been found, if we had wished to do so. It was however our goal to synthesize polymers that could be dissolved in non-fluorinated solvents, which made further studies of P8FM superfluous. For the same reason a kinetic study of 17FM was not attempted.

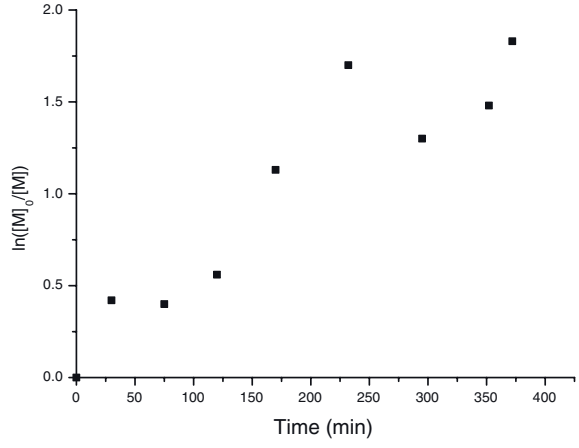

Figure 4.12. First-order plot of homopolymerization of 8FM at 80 °C. [M]:[I]:[Cu(I)Br]:[n-Pr-1] = 50:1:1:2.

4.5 Comparison of Analysis Methods

In spite of numerous attempts at using SPME for the kinetic studies of homopolymerizations of 3FM, optimization of this method to give reproducible results was fruitless. Instead the second kinetic study by ^{1}H NMR proved that this monomer follows first-order kinetics and reacts in a controlled manner at the given reaction conditions to give molecular weights close to target and low PDIs. The use of the same protocol for 8FM gave less conclusive results, as the low solubility of the product made analysis impossible. For the highly fluorinated monomers 8FM and 17FM SPME would have been an ideal analysis method, had it been successful. Here the solubility of the product would not have been a problem, as the analysis only involves the residual monomer and not the polymer.

5

Synthesis of Fluorinated Block Copolymers

There are several possible routes to obtain fluorinated materials by copolymerization of fluorinated monomers with non-fluorinated monomers. In this work the main focus has been on block copolymers, which can be obtained by either sequential addition or by the macroinitiator approach as discussed in Chapter 2 and demonstrated in Chapter 3. A number of studies involving random copolymerization have previously been undertaken [20, 21, 48] with good results. These are, however, of less relevance for this study and the few cases of block copolymerization of fluorinated methacrylates found in the literature have therefore been focused upon in the following.

5.1 Fluorinated Block Copolymers Synthesized by ATRP

The incorporation of fluorinated monomer 1H,1H-perfluorooctyl methacrylate (FOMA) in block copolymers was undertaken only shortly after the advent of ATRP [44]. For the polymerization of this monomer macroinitiators of poly(2-hydroxyethyl methacrylate)(PHEMA), poly(2-hydroxyethyl acrylate) (PHEA), PMMA, and poly(*tert*-butyl acrylate) (P*t*BA) were synthesized by ATRP. Polymerization of FOMA was conducted at 110 °C in TFT using CuBr as catalyst and bipy as ligand. Polydispersities of 1.3, 1.5 and 1.6 were obtained for the synthesis by PMMA, PHEMA and P*t*BA, respectively.

Perfluoroalkyl acrylate FAEM (see Figure 3.1), which consists of a mixture of acrylates was copolymerized by Li *et al.* [4] with butyl methacrylate (BMA). FAEM has a pendant alkyl chain -CH_2-CH_2-$(CF_2)_n$-CF_3 with n = 5 - 13 (average n $\sim$ 8.6). PBMA macroinitiators were synthesized (M_n = 6900 - 25,000 g/mol) and utilized for the polymerization of FAEM. The polymerization of the fluorinated acrylate was conducted in cyclohexanone at 100 °C for 72 hours using CuBr/PMDETA as catalyst/ligand complex obtaining conversions between 62 and 95 %, and PDIs from 1.29 to 1.44. The weight content of fluorine ranged from 3 to 23 weight-% and the copolymers exhibited surface activity both in solution and in solid state.

Random copolymers of styrene and acrylonitrile (PSAN) were used as macroinitiators for FOMA with polymerization taking place at 100 °C in a mixture of TFT and THF (4:1 v/v) [47]. The final random-block-copolymers had narrow molecular weight distributions (<1.2) and molecular weights of approximately 20,000 g/mol determined by ^{1}H NMR, while values of around 9000 g/mol were obtained by SEC analysis.

A tetra-armed star polymer of FEMA was synthesized to 89 % conversion within 3 hours from a tetrafunctional macroinitiator generated from pentaerythritiol and 2-bromoisobutyryl bromide [21] (Figure 5.1). The star polymer of FEMA was polymerized in a mixture of benzene and TFT at 114 °C, and the product was analysed by ^{13}C NMR, as it was not soluble in other than highly fluorinated solvents, which made SEC unfeasible. It was possible to synthesize a PEGMA-armed star by the same protocol, which was used as macroinitiator for FEMA to achieve a tetra-armed star with diblock copolymer arms. The latter reaction was run under the same conditions as the star-FEMA and gave 75 % conversion of monomer in 30 minutes with an initiator efficiency of 97 %. The star (co)polymers were analysed by ^{1}H and ^{13}C NMR and the spectral data from the latter analysis were used to estimate molecular weights. All the star polymers had molecular weights close to the theoretical ones indicating controlled reactions.

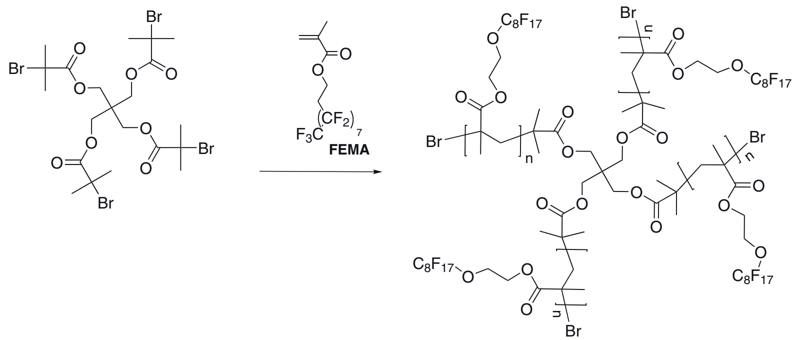

Figure 5.1. Synthesis of tetra-arm star polymer with arms of PFEMA [21].

5.2 Synthesis of Fluorinated Block Copolymers by ATRP

The aim of the polymerizations referred to in this Chapter was to synthesize amphiphilic block copolymers using the fluorinated methacrylates 3FM, 8FM and 17FM in combination with non-fluorinated monomers. The polymerization conditions developed earlier (Chapter 3) were utilized with the minor change of solvent from xylene to toluene. The approach

was initially to copolymerize the fluorinated methacrylates with MMA to ascertain whether this was possible and furthermore how the fluorinated pendant chain influences the reactivity of the fluoromonomers. Novel copolymers of the fluorinated methacrylates would then be synthesized with monomers 2-methoxyethyl acrylate (MEA) and poly(ethylene glycol) methyl ether methacrylate (PEGMA), both of which are hydrophilic and biocompatible.

In the copolymerizations in this and the following chapters, the overall conversion has been calculated according to equation (5.1).

$$p_{total} = p_1 n_1 + p_2 n_2 \tag{5.1}$$

where p_1 and p_2 are the individual conversions of the monomers, while n_1 and n_2 are the mole fractions of the two monomers in the feed. Weight fractions of the two polymers in the final product have been calculated from ^{1}H NMR spectra by comparing areas of characteristic peaks. The theoretical molecular weights have been calculated from equation (5.2).

$$M_{n,theory} = p_1 M_{n,M_1} + p_2 M_{n,M_2} \tag{5.2}$$

where M_{n,M_1} and M_{n,M_2} are the target molecular weights of the two respective monomers at 100 % conversion.

5.2.1 Copolymerization of 3FM and MMA

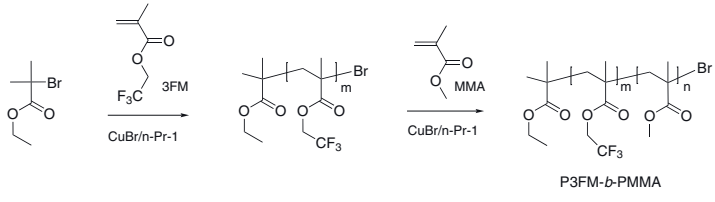

Figure 5.2. Synthesis of block copolymers of 3FM and MMA.

The monomer with the lowest amount of fluorine, 3FM is the most soluble and therefore studies were initially undertaken with this monomer in copolymerization with MMA. Conversions were estimated from ^{1}H NMR analysis using the peaks at δ_H 4.49 (q) and δ_H 4.33 for 3FM. Similarly the conversion of MMA was determined from the shift of the OC$\underline{H}_3$-group from δ_H 3.72 (s) (monomer) to δ_H 3.59 (polymer)[1].

5.2.1.1 Sequential Polymerization

In the sequential polymerizations the second monomer was added at relatively high conversions of the first monomer, with both monomers continuing to polymerize after addition, as observed by ^{1}H NMR to give a

[1] An example of a ^{1}H NMR spectrum of a P3FM/PMMA copolymer is shown in Appendix 4

gradient copolymer herein referred to as a block copolymer. The polymerization of MMA from P3FM was initially undertaken performing two experiments differing only in the method of addition of the second monomer i.e. MMA. In the first experiment MMA was added by syringe, while cannulation[2] was used for the second polymerization. In both cases the first-order kinetic plot showed an induction period for the initiation of the second monomer as seen in Figure 5.3. Adding the second monomer by cannulation is a slower process than when using a syringe, where addition can be almost instantaneous. The cannula needle can, however, easily be degassed and the risk of introducing oxygen upon addition of the second monomer is thereby minimized. The addition time was approximately 2 minutes by cannula, which is negligible compared to the total reaction time, therefore this addition procedure was chosen for all the following copolymerizations.

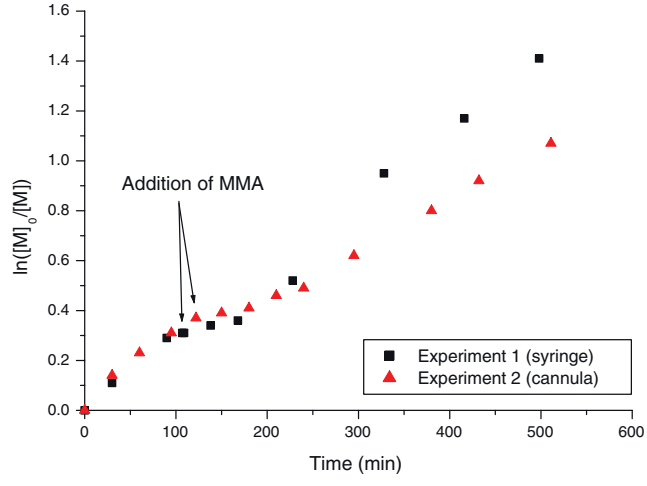

Figure 5.3. First-order kinetic plots of the synthesis of P3FM-*b*-PMMA in toluene at 90 °C. Addition of the second monomer was either performed with syringe or by cannulation.

SEC-analysis showed a bimodal distribution for both polymerizations of P3FM-*b*-PMMA (Figure 5.4) indicating that some termination took place with the addition of the second monomer. This may be due to the low solubility of P3FM in the solvent impeding further reaction. The bimodal distributions lead to polydispersities around 1.3 (see Table 5.1), however, all the distributions are comparable with those found for the homopolymerization of 3FM, which indicates that these are the optimal results achievable with the given system.

[2]The term cannulation is used here to describe the transfer of monomer/solvent mixture from one Schlenk tube to another via a double tipped needle using an increased flow of gaseous nitrogen to facilitate transfer.

Table 5.1. Copolymers of MMA and fluorinated monomers, 3FM, 8FM and 17 FM.

Sample	M_1	M_2	$[M_1]$:$[M_2]$	[I]:$[M_1]$	Time (h)	M_1;M_2[a]	m_1;m_2[b]	$M_{n,theory}$ (g/mol)	$M_{n,SEC}$ (g/mol)	PDI
1	3FM	MMA	1:1	1:113	8.3	0.56 ; 0.44	68 ; 32	25,800	10,000	1.32
2	3FM	MMA	1:1	1:113	8.5	0.52 ; 0.48	64 ; 36	22,900	7900	1.30
3[c]	3FM	MMA	1:1	1:113	4.5	0.52 ; 0.48	64 ; 36	23,600	9200	1.50
4	PMMA	3FM[d]	1:100	-	4	0.24 ; 0.76	16 ; 84	27,800	25,300	1.12
5	MMA	3FM	1.7:1	1:100	7	0.68 ; 0.32	56 ; 44	15,000	9200	1.08
6	MMA	8FM	2.5:1	1:100	7	0.75 ; 0.25	50 ; 50	16,500	9300	1.18
7[c]	MMA	17FM	4.7:1	1:100	7	0.87 ; 0.13	45 ; 55	17,000	10,300	1.24

[I]:[Cu(I)Br]:[n-Pr-1] = 1:1:2, Reaction temperature: 80 °C.

Table 5.2. Copolymers of 3FM and hydrophilic monomers MEA and PEGMA.

Sample	M_1	M_2	$[M_1]$:$[M_2]$	Ligand	[I]:$[M_1]$	Time (h)	M_1;M_2[a]	m_1;m_2[b]	$M_{n,theory}$ (g/mol)	$M_{n,SEC}$ (g/mol)	PDI
8	PEGMA[e]	3FM	1:3	n-Pr-1	1:42	11.3	0.70 ; 0.30	45 ; 55	29,900	16,500	1.18
9	3FM	PEGMA	3:1	n-Pr-1	1:113	27.9	0.83 ; 0.17	63 ; 37	26,200	17,500	1.22
10	MEA	3FM	1:1	HMTETA	1:150	5.5	0.53 ; 0.47	47 ; 53	33,200	10,400	1.57
11	3FM	MEA	1:1	HMTETA	1:113	10	0.62 ; 0.38	68 ; 32	31,100	10,300	1.42
12	3FM	MEA	1:1	HMTETA	1:113	9.3	0.89 ; 0.11	91 ; 9	20,800	27,400	1.56

[I]:[Cu(I)Br]:[n-Pr-1] = 1:1:2, [I]:[Cu(I)Br]:[HMTETA] = 1:1:1, Reaction temperature: 90 °C.

[a] *Molar fractions of the two monomers incorporated in the copolymer*
[b] *Weight-% of the two monomers incorporated in the copolymer.*
[c] *Polymerization was conducted at 90 °C.*
[d] *3FM polymerized from MMA-macroinitiator [I]:[M]=1:100.*
[e] *PEGMA polymerized at 50 °C.*

A third attempt at polymerizing MMA from P3FM was undertaken at a higher reaction temperature, 90 °C. This, however, only lead to a broader molecular weight distribution (PDI = 1.50). The results of the copolymerizations of 3FM and MMA are shown in Table 5.1.

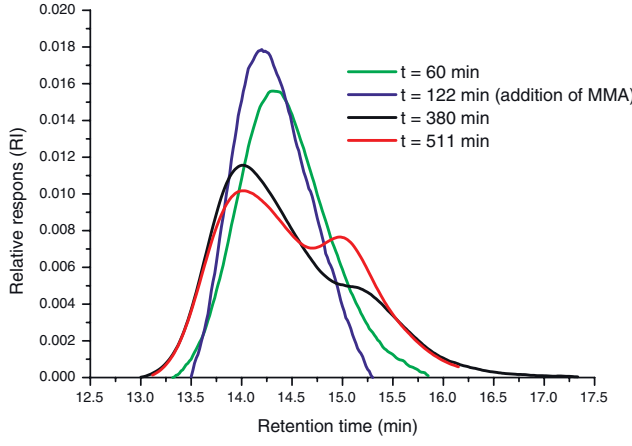

Figure 5.4. SEC-traces for the synthesis of P3FM-*b*-PMMA (entry 2, Table 5.1).

The converse approach i.e. polymerizing 3FM from PMMA was more successful (entry 5, Table 5.1), as the first-order kinetic plot of the synthesis of PMMA-*b*-P3FM was linear. Furhermore evolution of molecular weight was linear with conversion, PDIs were low throughout reaction (<1.3), and SEC-traces were monomodal evidencing a controlled reaction mechanism.

5.2.1.2 Macroinitiator Approach

Utilizing sequential polymerization is a fairly uncomplicated means of synthesizing block copolymers with the only drawback being the lack of absolute control of the polymer structure due to the presence of two monomers during reaction resulting in gradient copolymers instead of "true" block copolymers. One attempt was made at synthesizing a "true" block copolymer using a PMMA-macroinitiator for the polymerization of 3FM (entry 4, Table 5.1). The polymerization proceeded in a controlled fashion with a linear first-order kinetic plot, molecular weight increasing with conversion and low PDI throughout reaction (<1.2). SEC-analysis, however, showed residual macroinitiator, which was not the case with the sequential addition. This could be due to a lowering of the initiator efficiency through the formation of a high molecular weight macroinitiator. Exchange of the bromine of the end-groups during work-up resulting in

non-initiating macroinitiator species could be another explanation for the result.

The molecular weight of the PMMA-macroinitiator could be determined absolutely by SEC and ^{1}H NMR and could therefore be used to estimate the molecular weight of the PMMA-*b*-P3FM copolymer. The molecular weight of 27,800 g/mol found by ^{1}H NMR corresponded well with the value of 25,300 g/mol found by SEC, although both values were somewhat higher than the theoretical value, which can be explained by macroinitiator efficiencies lower than 100 % consistent with the observations in SEC. Comparison between the two polymerization methods deems the sequential to be faster and more efficient with the disadvantage of lower structure control, whereas the macroinitiator method has supreme control over structure, but is much more time-consuming due to the increased amount of work-up. The former polymerization method was therefore chosen for the remainder of the copolymerizations due to the tight schedule.

5.2.2 Copolymerization of MMA with 8FM and 17FM

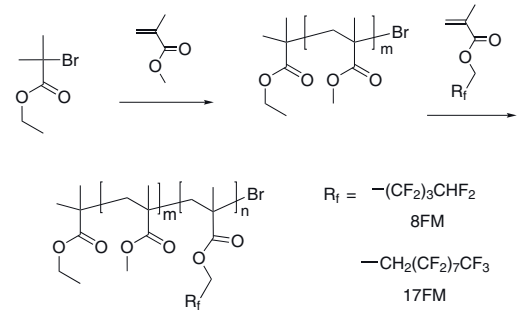

Figure 5.5. Synthesis of block copolymers of MMA and fluorinated methacrylates 8FM and 17FM.

The conversion of the first monomer was always the highest in the sequential copolymerizations, as the polymerization was normally terminated at an overall conversion of approx. 80 %. This resulted in a larger incorporation of the first monomer in the final product cf. eq. (5.2), which the results in Table 5.1 also indicate. While the homopolymerization of 3FM could be monitored by ^{1}H NMR (in $CDCl_3$), it was not possible to use this technique for the homopolymerization of 8FM due to low solubility of the polymer in the solvent (see Chapter 4.4.2) and it was assumed to be the case for P17FM as well. Polymeric products that can only be solubilized in fluorinated solvents have limited use, therefore only block copolymers generated from PMMA were synthesized i.e. PMMA-*b*-P8FM and PMMA-*b*-P17FM to avoid highly fluorinated polymers. Conversions were estimated from ^{1}H NMR analysis using the peak for C$\underline{H}_2$-CF_2 in the

fluorinated methacrylates: δ_H 4.60 (q) (monomer) and δ_H 4.44 (polymer) for 8FM and δ_H 4.39 (q) (monomer) and δ_H 4.24 (polymer) for 17FM. The first-order kinetic plots were similar to those acquired for the synthesis of PMMA-*b*-P3FM and were linear for both polymerizations as illustrated in Figure 5.6 (data for PMMA-*b*-P17FM). Evolution of molecular weight of the copolymeric products was observed to be linear with conversion as seen in Figure 5.7 (data for PMMA-*b*-P8FM) and SEC-analysis showed monomodal curves with low PDIs evidencing a controlled reaction mechanism. Figure 5.8 shows the SEC-traces for the polymerization of 8FM from PMMA. Polymerization results are shown in Table 5.1.

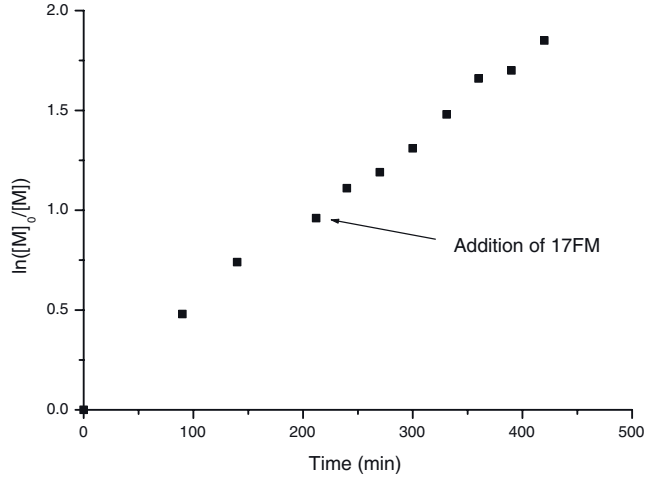

Figure 5.6. First-order kinetic plot of the copolymerization of MMA and 17FM.

Comparison of the kinetics of the three fluoromonomers indicates that the fluorinated pendant chain does not influence the rate of polymerization as long as the product is soluble under the given reaction conditions. In Figure 5.9 the first-order kinetic plots for the synthesis of the block copolymers of MMA and the fluorinated methacrylates are shown. There are no significant differences between the curves evidencing similar reactivity of the fluorinated monomers, thereby proving the influence of the fluorinated segment only to be important in terms of solubility. Table 5.1 shows the incorporated amount of MMA and fluorinated monomers in the final copolymeric products, which confirms the similarities of the fluorinated methacrylates. It is seen that the molar ratios are close to the feed ratios in all cases with only slightly higher levels of MMA in the products (due to higher conversion of MMA for all polymerizations), which can be explained by comparable reaction kinetics of the fluoromonomers.

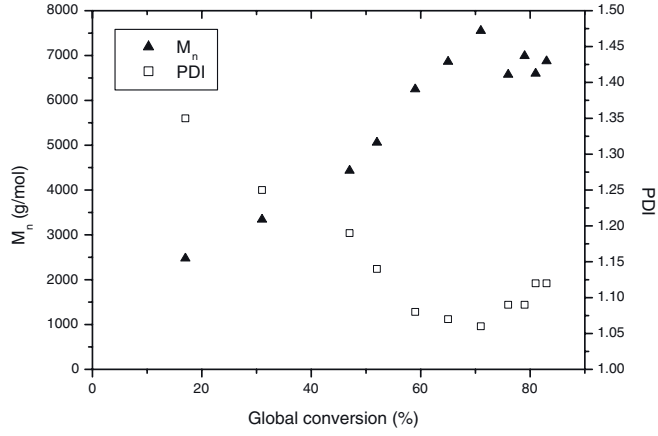

Figure 5.7. Evolution of M_n and PDI as a function of overall conversion for the synthesis of PMMA-*b*-P8FM.

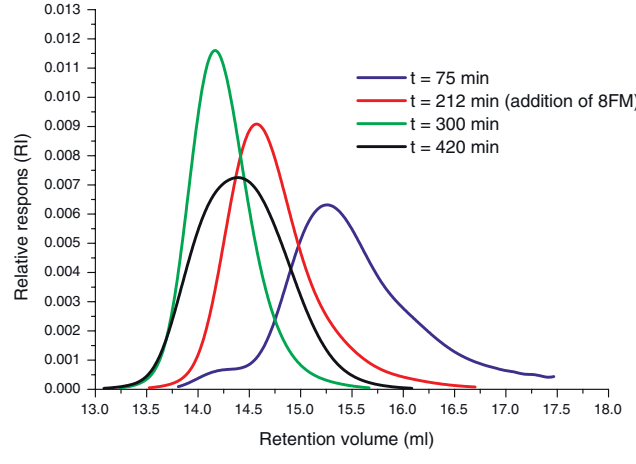

Figure 5.8. SEC-traces for the synthesis of PMMA-*b*-P8FM.

5.2.3 Copolymerization of 3FM and PEGMA

The hydrophilic monomer PEGMA has been shown not be polymerizable to high conversions (>60 %) at elevated temperatures [69], therefore different reaction temperatures were chosen for the reactions of 3FM and PEGMA during copolymerization of these two monomers. A reaction temperature of 50 °C was chosen for PEGMA, while 3FM was polymerized at 90 °C. Conversions of 3FM were estimated as previously mentioned, while conversions of PEGMA were found by comparing the residual monomer

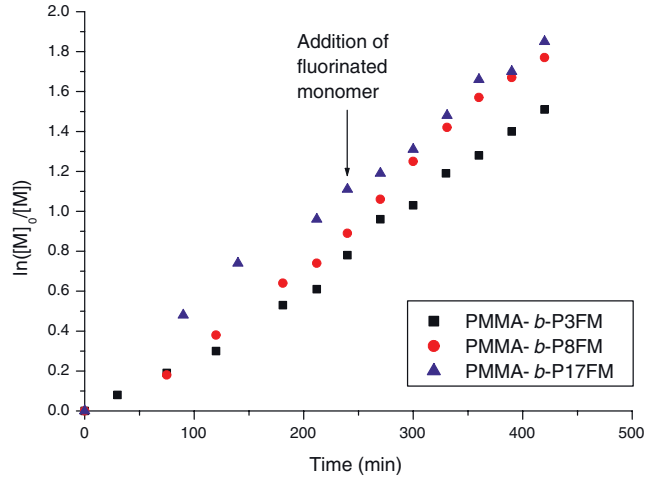

Figure 5.9. First-order kinetic plots of the synthesis of block copolymers of MMA and fluorinated methacrylates 3FM, 8FM and 17FM.

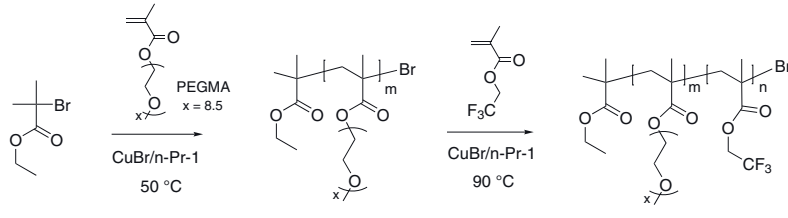

Figure 5.10. Synthesis of block copolymers of PEGMA and 3FM.

peaks (δ_H 6.14 and δ_H 5.55) with the peak at δ_H 4.12 deriving from CO-O-C$\underline{H}_2$ in the polymer. The original peak at δ_H 4.28 (dd) in the monomer is hidden under the peak for P3FM during copolymerization (see Figure 5.11) introducing an element of uncertainty for the calculated conversions.

The synthesis of PPEGMA-*b*-P3FM proceeded as anticipated with the propagation of 3FM from the PPEGMA-species, and also with an increased rate of polymerization of PEGMA at the elevated temperature[3]. Molecular weights increased with conversion and polydispersities were relatively low (< 1.2). For the converse approach polymerization of PEGMA from P3FM, no reaction was seen when the temperature was lowered to 50 °C, the temperature utilized for the first successful copolymerization. After leaving the reaction overnight without any further conversion, the temperature was increased to 90 °C again resulting in continued polymerization (Figure 5.12). This indicates a thermal barrier for the transforma-

[3]Figure shown in Appendix 4.

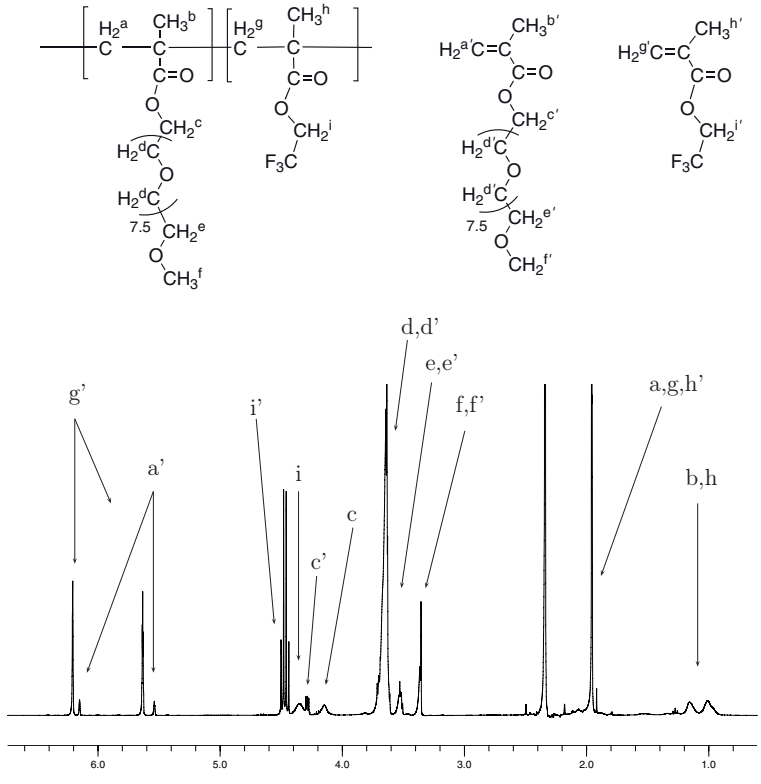

Figure 5.11. ^{1}H NMR spectrum of PPEGMA-*b*-P3FM (entry 8, Table 5.2) after 590 min. The conversion of PEGMA is 67 %, while the conversion of 3FM is 28 %. Assignments according to the the structure above are indicated by the arrows. The conversion of PEGMA is determined from the signals **a'** and **c** while the conversion of 3FM is estimated from **g'** and **i** (subtracted the signals c' and i').

tion of the P3FM-macroinitiator from dormant to activated state rather than for the propagation of the second monomer. This is in good correspondence with previous observations in the kinetic studies of 3FM, where no polymerization took place at 70 °C (Chapter 4.3.2.3). Possibly the copolymerization from P3FM could have been undertaken by cooling the reaction mixture after the propagation of PEGMA, which could be monitored by ^{1}H NMR. This was not investigated further, but could potentially have led to a broad molecular weight distribution obtaining a mixture of unreacted P3FM and copolymer. It must therefore be concluded that copolymerization of PEGMA and 3FM was only controlled under the given reaction conditions, when starting from the former monomer.

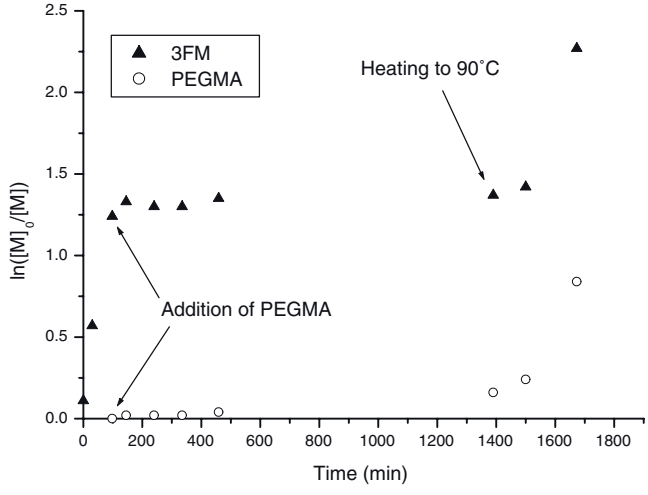

Figure 5.12. First-order kinetic plot generated from the individual conversions of 3FM and PEGMA in the synthesis of P3FM-*b*-PPEGMA.

5.2.4 Copolymerization of 3FM and MEA

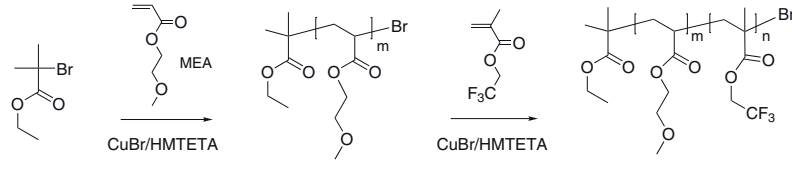

Figure 5.13. Synthesis of block copolymers of 3FM and MEA.

The polymerization of MEA with the Cu(I)Br/n-Pr-1 catalytic system had not been carried out before, therefore a test polymerization of MEA utilizing this system was undertaken. Conversions of MEA were found by comparing the residual monomer peaks (δ_H 5.74 (dd), 6.15 (dd) and 6.43 (dd)) with the peak at δ_H 3.54, which derives from CO-O-C$\underline{H}_2$ in both monomer and polymer, as there is no significant shift for this particular signal during polymerization. Kinetic results were highly unsatisfactory, as the conversion leveled off and did not exceed 40 %, although the polydispersities were relatively low with the final product having a M_n of 7500 g/mol and PDI of 1.23. The polymerization of MEA using HMTETA as ligand, which has previously proved to be efficient [70], yielded better results. First-order kinetics were linear and proceeded to conversions over 90 %, while the evolution of molecular weight was linear with conversion and PDI was low throughout reaction (Figure 5.14).

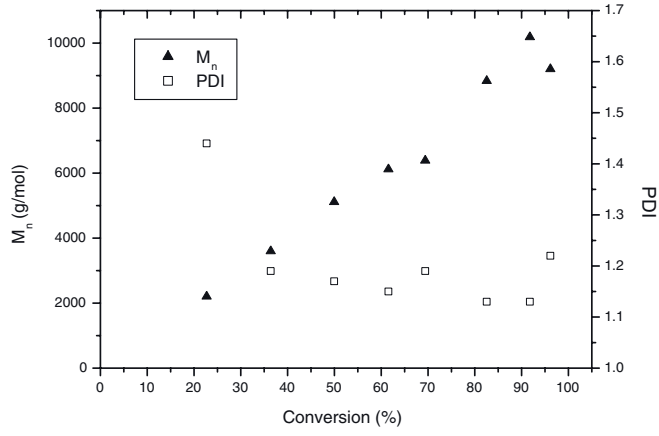

Figure 5.14. Evolution of M_n and PDI in the polymerization of MEA at 90 °C. [M]:[I]:[CuBr]:[HMTETA] = 150:1:1:1.

During the preliminary polymerizations 3FM had been polymerized using HMTETA as ligand with mediocre results (Table 3.3). A second attempt was made in the setup utilized for MEA, which was more successful with linear first-order kinetics and relatively low PDIs. As seen in Figure 5.15 the evolution of molecular weight was linear with conversion, although it did not proceed from the origin. The final PDI of 1.37 was comparable to the values found, when using n-Pr-1 as ligand.

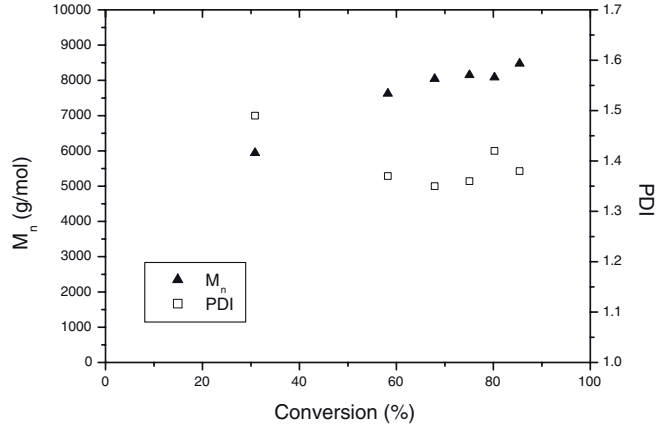

Figure 5.15. Evolution of M_n and PDI in the polymerization of 3FM at 90 °C. [M]:[I]:[CuBr]:[HMTETA] = 120:1:1:1.

Copolymerizations were undertaken starting with the polymerization of 3FM from PMEA. A linear first-order kinetic plot was found for this reaction (Figure 5.16), where both monomers continued to polymerize after the addition of 3FM, but with an obvious faster polymerization of this monomer. Evolution of molecular weight with overall conversion was linear, but PDI increased from 1.17 to 1.61 after the addition of 3FM and did not decrease significantly at higher conversions. This indicates loss of control over the reaction, perhaps by incomplete initiation of 3FM. The broadening of the molecular weight distribution was observed by Hvilsted *et al.* during the copolymerization of MEA and MMA [70]. An explanation could be the different nature of the two monomers, as MEA is relatively hydrophilic, while 3FM is highly hydrophobic, which makes them incompatible.

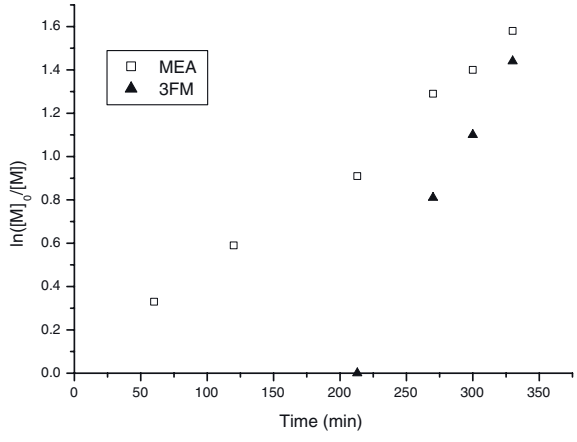

Figure 5.16. First-order kinetic plot of the individual conversions of MEA and 3FM in the synthesis of PMEA-*b*-P3FM.

The converse polymerization approach was also undertaken i.e. polymerization of MEA from P3FM. Two experiments were conducted and they both showed relatively linear first-order kinetics (Figure 5.17). The kinetics based on the individual conversions indicated that the faster reaction of 3FM made the polymerization of MEA difficult, when using sequential addition. High polydispersities (>1.3 in all instances) were recorded for both experiments and evolution of molecular weight was only linear with conversion in one case (shown in Figure 5.18). The lack of reproducibility of the polymerization results (entries 4 and 5, Table 5.2) was also illustrated by the difference in monomer ratios in the final products (0.62/0.38 vs. 0.89/0.11). It can be concluded that the two monomers 3FM and MEA are not compatible and can not be copolymerized by ATRP in a controlled manner at the chosen reaction conditions.

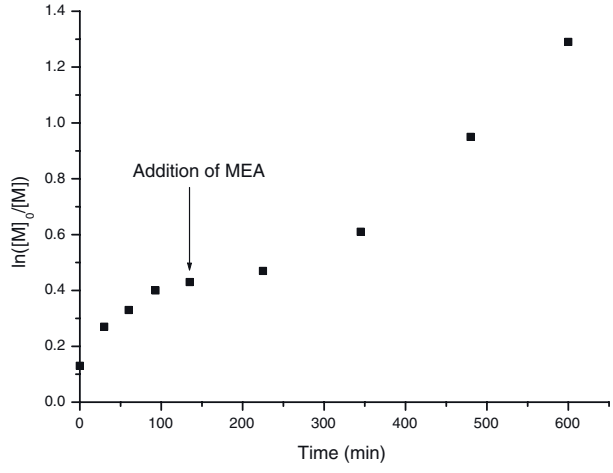

Figure 5.17. First-order kinetic plot for the synthesis of P3FM-*b*-PMEA (entry 11, Table 5.2).

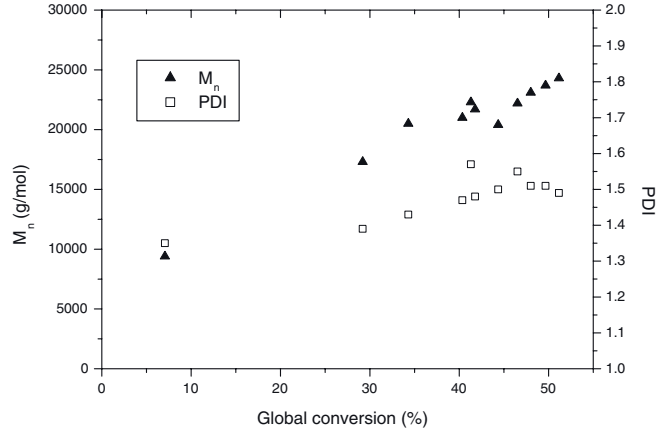

Figure 5.18. Evolution of M_n and PDI in the synthesis of P3FM-*b*-PMEA (entry 12, Table 5.2) at 90 °C. [I]:[CuBr]:[HMTETA] = 1:1:1.

5.3 Conclusions

Block copolymers of MMA and fluorinated methacrylates were polymerized by ATRP. It was possible to synthesize block copolymers starting from 3FM, although the converse approach yielded better results. P3FM-*b*-PMMA block copolymers synthesized at 80 °C showed bimodal distributions in SEC analysis with PDIs $\sim$ 1.3, while SEC-traces for PMMA-*b*-P3FM were monomodal with PDI = 1.08. A "true" block copolymer was furthermore synthesized from a PMMA-macroinitiator to yield PMMA-*b*-P3FM with a molecular weight of 25,000 and PDI = 1.12. Well-defined block copolymers of MMA and 8FM and 17FM, respectively were synthesized obtaining M_ns $\sim$ 17,000 and PDIs $\sim$ 1.2. Kinetic experiments evidenced that the length of the fluorinated pendant chain does not influence the reactivity in ATRP. Novel block copolymers of 3FM and PEGMA were synthesized by ATRP in toluene, which has not previously been done. Results were better starting from PPEGMA, as P3FM did not initiate the polymerization of PEGMA at the chosen reaction temperature: 50 °C. Copolymerization of 3FM and MEA was possible, even though the reaction conditions rendered a non-controlled polymerization. The synthesis of PMEA-*b*-P3FM exhibited linear evolution of molecular weight, but broad molecular weight distributions were obtained, PDI = 1.6. The converse approach indicated a lack of reproducibiliy and uncontrolled reaction with non-linear evolution of molecular weights and PDI $>$ 1.4.

6

ATRP utilizing a fluorinated macroinitiator

The incorporation of fluorinated monomers into block copolymers is a possible route to obtain partially fluorinated polymers, while an alternative approach is to use commercially available fluorinated compounds as macroinitiators for non-fluorinated monomers. The former approach was described in Chapters 3 and 5, while the latter approach will be described in the following after a short introduction of the work in the literature.

6.1 Examples of Fluorinated Macroinitiators

Various fluoropolymers, both commercially available and synthesized in small scale, have previously been used as macroinitiators in ATRP. Macroinitiators based on polyvinylidene fluoride (PVDF) have in particular been studied in connection with the formation of block-copolymers [71, 72] as well as graft-copolymers [18, 73]. The focus herein was, however, on a fluorinated macroinitiator previously used by Perrier *et al.* for the synthesis of semifluorinated MMA and PS copolymers [20, 48]. Several initiators derived from commercially available compounds were used in said study. The initiators were three fluorinated bromoisobutyryl esters prepared by esterification of various fluorinated telomers: perfluoroalkyl ethanol, 2-perfluoroalkyl ethyl-co-poly(ethylene glycol), or a dihydroxy functional telomer based on trimethylol propane (Figure 6.1). These α-perfluoroalkyl initiators provided well-defined copolymers in the ATRP of MMA at 90 °C utilizing the CuBr/*N*-(*n*-pentyl)-2-pyridyl-methanimine catalyst system in toluene. Copolymers with molecular weights between 9000 and 26,000 were obtained, while PDIs ranged from 1.08 to 1.30. The presence of the fluorinated moiety did not interfere detrimentally with the controlled polymerization mechanism. In fact the same first-order kinetics were observed for EBB and the 2-perfluoroalkyl ethyl-copoly(ethylene glycol) based initiator.

Shemper and Mathias [21] used the same methology as Perrier *et al.* for synthesizing an equivalent poly(ethylene glycol) containing fluorinated macroinitiator. The initiator was in this instance employed for the homopolymerization of poly(propylene glycol) methacrylate (PPGM) at 80 °C in methyl ethyl ketone (CuBr/PMDETA)(Figure 6.2). The resulting

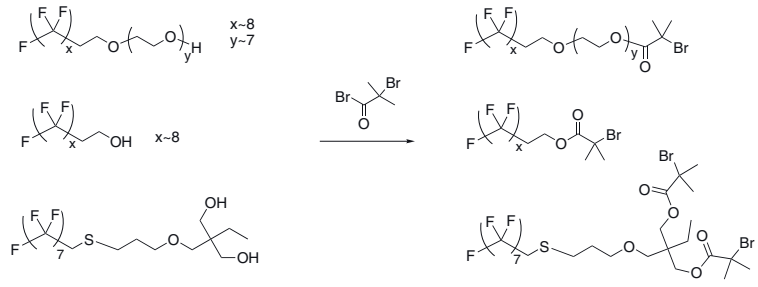

Figure 6.1. Synthesis of fluorinated macroinitiators by transesterification with 2-bromoisobutyryl bromide performed by Perrier *et al.* [20].

polymer had a molecular weight of 5200 g/mol (DP = 10) determined by ^{13}C NMR, which corresponded well with the theoretical value indicating a controlled polymerization mechanism. The molecular weight distribution could, however, not be determined, as the resulting polymer was not dissolvable in THF, the chosen eluent for SEC.

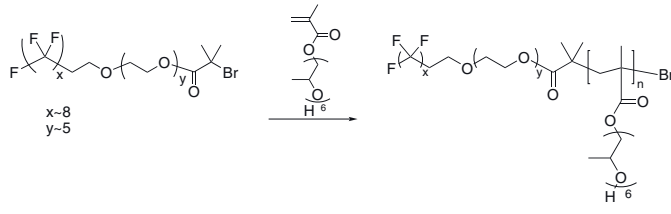

Figure 6.2. Polymerization of poly(propylene glycol) methacrylate utilizing a fluorinated macroinitiator [21].

6.2 Polymerizations Utilizing a Fluorinated Macroinitiator

In this work the hydroxyl terminated surfactant Zonyl FSO-100® used in the above mentioned work was converted to a macroinitiator species by transesterification according to the methology of Jankova *et al.* [64] (Figure 6.3). The structures of the surfactant Zonyl FSO-100® and the synthesized fluorinated macroinitiator, FMI were confirmed by ^{1}H, ^{13}C and ^{19}F NMR. The initial polymerizations were performed with MMA with three different initiator to monomer ratios. Novel functionalized polymers were subsequently synthesized by polymerization of the monomers MEA and PEGMA (Figure 6.4). Monomer conversions were determined by ^{1}H NMR as described in Chapter 5 and kinetics were in all instances compared to EBB initialized polymerizations.

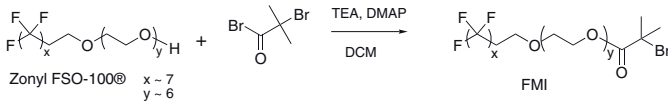

Figure 6.3. Synthesis of fluorinated macroinitiator, FMI from Zonyl FSO-100® by transesterification with 2-bromoisobutyryl bromide.

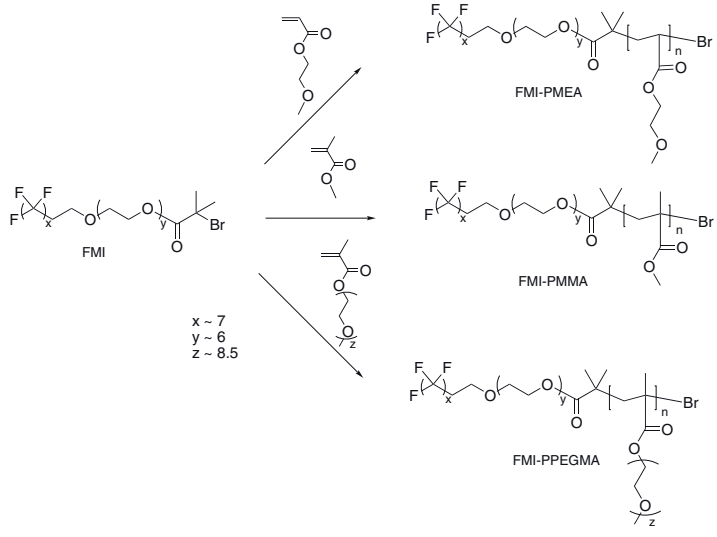

Figure 6.4. Polymerization of MEA, MMA and PEGMA utilizing the fluorinated macroinitiator, FMI.

6.2.1 Polymerization of MMA with FMI

Three different molecular weights were targeted in the polymerization of MMA with FMI: 5000; 10,000 and 20,000 g/mol. The kinetic plots (Figure 6.5) show that polymerization proceeds as a first-order reaction in all cases indicating a controlled mechanism with rates of polymerization increasing with increasing initiator to monomer ratio. For the three polymerizations apparent rates of propagation, k_p^{app}, were found to be $2.1{\cdot}10^{-4}$ s^{-1}, $1.1{\cdot}10^{-4}$ s^{-1} and $8.3{\cdot}10^{-5}$ s^{-1} for the target weights of 5, 10 and 20 kg/mol, respectively. Evolution of molecular weights were linear with conversion in all cases (see Figure 6.6), and PDIs were low (<1.25) evidencing the living nature of the reactions (Table 6.1). SEC-analysis showed monomodal curves, however, a high molecular weight shoulder was seen at high conversions, which was thought to be due to the surfactant nature of the initiator resulting in aggregation of the polymer. The molecular weights of the FMI-PMMA polymers were further estimated by ^{1}H NMR using the signal from the poly(ethylene glycol) functionality in the macroinitiator δ_H

3.62 and comparing with the signal from the monomer at δ_H 3.58 ($OC\underline{H}_3$). The results obtained by ^{1}H NMR were lower than those found by SEC-analysis in all cases, but in both cases the degree of polymerization was proportional to the initial ratio of monomer to initiator. Polymerization of MMA (target 10,000 g/mol) using EBB as initiator gave an apparent rate of propagation of $2.1 \cdot 10^{-4}$ s^{-1}, which was higher than for FMI. This result could be expected due to the difference in size and solubility of the two initiators. On the contrary almost identical polymerization rates for these two initiators were found by Perrier *et al.* [20].

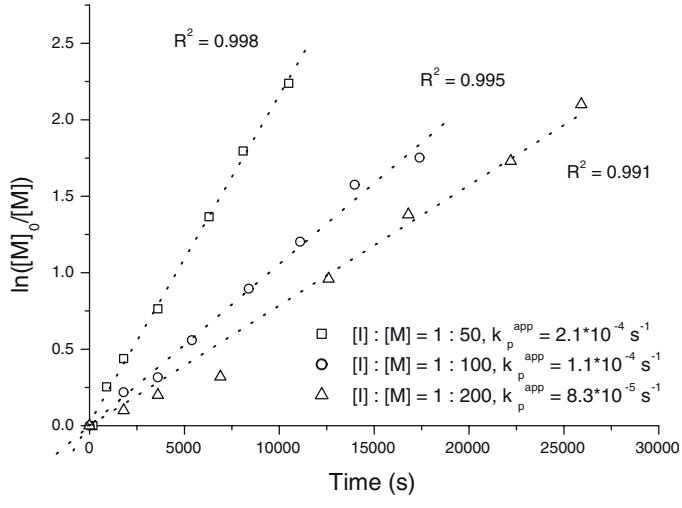

Figure 6.5. First-order kinetic plots of the polymerization of MMA from FMI at 90 °C, [I]:[Cu(I)Br]:[n-Pr-1] = 1:1:2.

6.2.2 Polymerization of PEGMA with FMI

The polymerization of PEGMA from FMI was conducted at 90 °C, which was necessary for later copolymerization with PMMA, although PEGMA was expected not to exhibit a first-order mechanism at this temperature [69]. The first-order kinetic plot was initially linear, until about 30 % conversion, but levelled off at higher conversions. Evidently PEGMA initially reacts in the same fashion as the other monomers, but due to increased viscosity and reduced solubility further reaction is impeded. The evolution of molecular weights was linear with conversion and the polydispersities were low (<1.2), which provides evidence for the fact that the reaction is controlled. A polymerization of PEGMA using EBB as initiator was also conducted and this showed faster kinetics than for FMI. The first-order kinetic plot of this reaction was also initially linear reaching a maximum

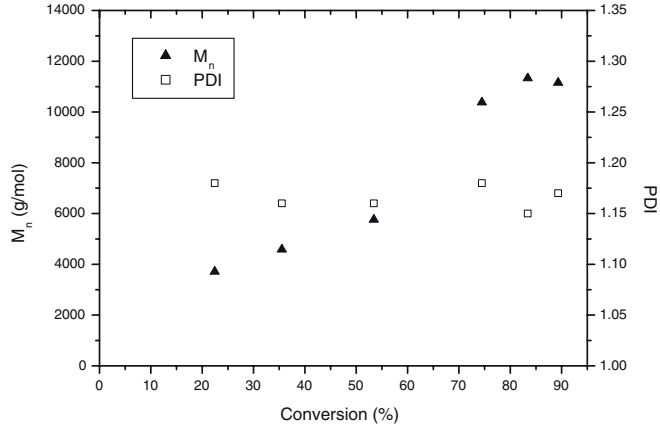

Figure 6.6. Evolution of M_n and PDI for the polymerization of MMA from FMI. [M]:[I]:[Cu(I)Br]:[n-Pr-1] = 50:1:1:2.

value, which was, however, significantly higher than for the reaction initiated by FMI (Figure 6.7). The conversion of PEGMA reached a value of 59 % when using EBB, while it was limited to 48 % with FMI.

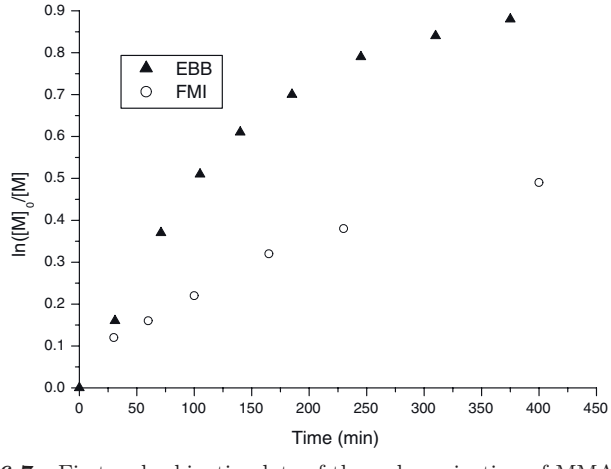

Figure 6.7. First-order kinetic plots of the polymerization of MMA at 90 °C, [I]:[Cu(I)Br]:[n-Pr-1] = 1:1:2. Polymerization from EBB ([M]:[I] = 44:1) and FMI ([M]:[I] = 42:1).

Table 6.1. Polymers synthesized using fluorinated macroinitiator, FMI.

Sample	M_1	M_2	[I]:[M_1]:[M_2]	Time (h)	Conversion (%)	$M_{n,theory}$ (g/mol)	$M_{n,SEC}$ (g/mol)	$M_{n,NMR}$ (g/mol)	PDI
1	MMA	-	1:50	3	89	5300	9200	5500	1.17
2	MMA	-	1:100	5	83	9200	12,400	7900	1.21
3	MMA	-	1:200	7	88	18,500	24,000	13,900	1.24
4	PEGMA	-	1:42	26	47	10,300	16,300	-[c]	1.20
5	MMA	PEGMA	1:100:24	26	91/49	15,900	21,600	-[c]	1.57
6[a]	MEA	-	1:230	20	77	24,000	24,400[b]	-[c]	1.21

[I]:[Cu(I)Br]:[n-Pr-1] = 1:1:2, Reaction temperature: 90 °C.

[a] *Ligand = HMTETA, [I]:[Cu(I)Br]:[HMTETA] = 1:1:1.*
[b] *SEC performed in THF.*
[c] *End-group not detectable by* ^{1}*H-NMR.*

6.2.3 Copolymerization of MMA and PEGMA with FMI

The synthesis of a block copolymer of MMA and PEGMA from FMI was undertaken as a sequential reaction at 90 °C. The first-order kinetic plots of the two monomers in Figure 6.8 shows that the polymerization rate of MMA is reduced with the addition of PEGMA. This is believed to be due to both the reduction in relative concentration of MMA and the increased viscosity of the reaction mixture. The leveling off in the conversion of PEGMA is seen as before with the maximum value of 49 %. Despite the non-linear first-order kinetics, the evolution of molecular weights was linear with conversion and the polydispersities were low (<1.25) up to an overall conversion of 72 %. Between an overall conversion of 72 and 81 % PDI leaps from 1.23 to 1.68, which indicates that the reaction was controlled until this point. SEC-curves were monomodal with the high molecular weight shoulder also observed in the SEC traces of FMI-PMMA.

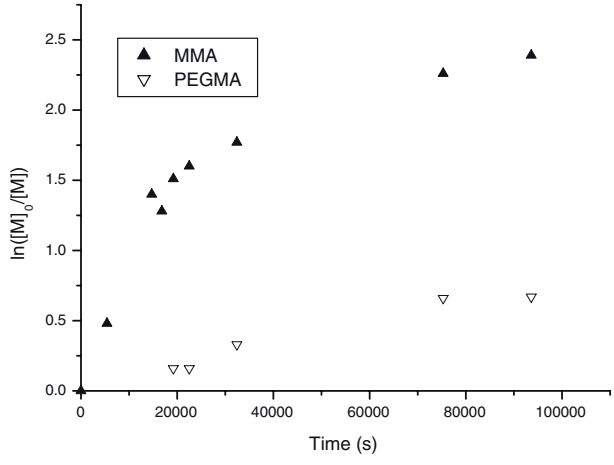

Figure 6.8. First-order kinetic plots of the conversions of MMA and PEGMA during the synthesis of FMI-PMMA-*b*-PPEGMA. Reaction temperature: 90 °C, $[M_1]$:$[M_2]$:[I]:[Cu(I)Br]:[n-Pr-1] = 100:42:1:1:2.

6.2.4 Polymerization of MEA with FMI

HMTETA was chosen as ligand for the synthesis of PMEA, due to the fact that preliminary experiments showed that the polymerization of MEA was controlled, when using this ligand as opposed to n-Pr-1 (see Chapter 5.2.4). The first-order kinetic plot for the polymerization of MEA from FMI was linear as seen in Figure 6.9. The evolution of molecular weights with conversion was furthermore linear with low polydispersities through-

out reaction evidencing a controlled reaction. Polydispersities increased slightly during reaction starting at 1.08 and ending at 1.21. As was the case for FMI-PMMA a shoulder in the high molecular weight part of the SEC trace was also seen for FMI-PMEA (Figure 6.10) substantiating that the initiator is responsible for this phenomenon, since no such observation was made, when using EBB as initiator.

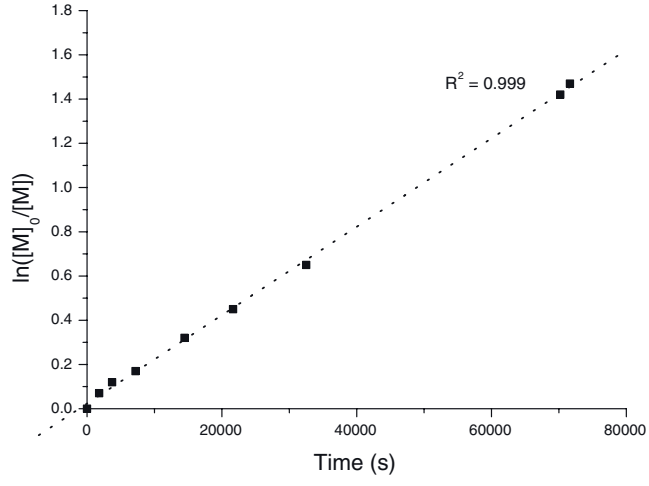

Figure 6.9. First-order kinetic plot for the polymerization of MEA from FMI at 90 °C, [M]:[I]:[Cu(I)Br]:[HMTETA] = 230:1:1:1.

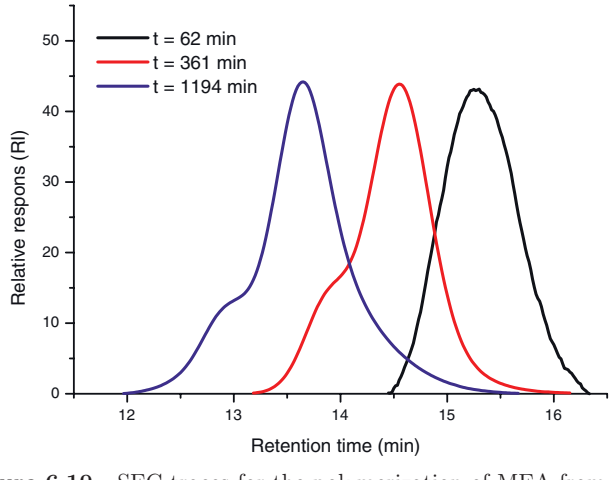

Figure 6.10. SEC-traces for the polymerization of MEA from FMI.

6.2.5 Copolymerization of MMA and MEA

The copolymerization of MMA and PEGMA from FMI was successful and therefore the combination of MMA and MEA seemed obvious. A preliminary copolymerization of these two monomers from EBB was undertaken and the first-order kinetic plot is relatively linear as seen in Figure 6.11. The evolution of molecular weights and PDI (Figure 6.12) indicated a controlled reaction, although there was an increase in PDI at the highest overall conversions (81 and 82 %) to around 1.3. The synthesis of FMI-PMMA-*b*-PMEA would therefore presumeably have been possible with good results, but was unfeasible due to the given time frame.

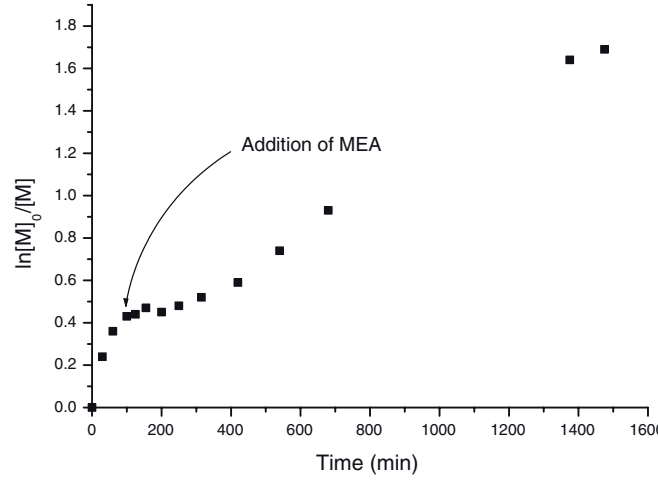

Figure 6.11. First-order kinetic plot for the sequential polymerization of PMMA-*b*-PMEA.

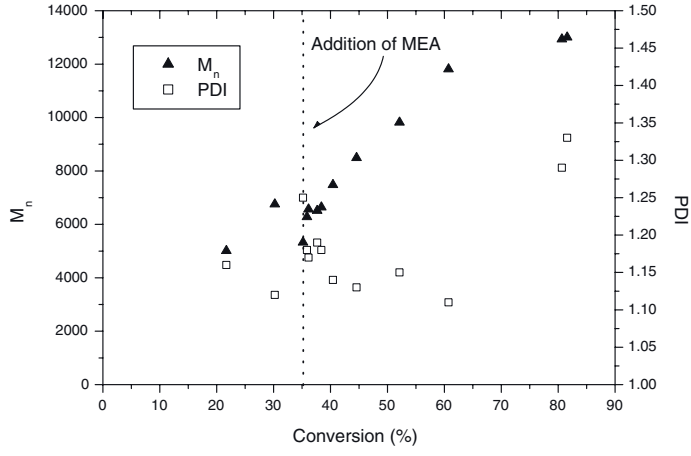

Figure 6.12. Evolution of M_n and PDI for the synthesis of PMMA-*b*-PMEA by sequential addition.

6.3 Conclusions

Controlled polymerizations of MMA, MEA and PEGMA using fluorinated macroinitiator, FMI were achieved with excellent results: molecular weights close to target and PDIs lower than 1.25 in all cases. Three molecular weights of FMI-PMMA were targeted and from reaction kinetics k_p^{app} was estimated to be $2.1{\cdot}10^{-4}$ s^{-1}, $1.1{\cdot}10^{-4}$ s^{-1} and $8.3{\cdot}10^{-5}$ s^{-1} for [M]:[I] of 50, 100 and 200, respectively. FMI was used to polymerize PEGMA by a controlled reaction (M_n = 16,300 , PDI = 1.20) and it was furthermore possible to synthesize the block copolymer FMI-PMMA-*b*-PPEGMA by sequential addition with good control over reaction until an overall conversion of 72 %. The hydrophilic monomer MEA was polymerized to a molecular weight of 24,400 g/mol, close to target, with a PDI of 1.21. Although the macroinitiator resulted in slower reaction kinetics than the conventional EBB for all the monomers, the obtained results were comparable in terms of molecular weight distributions. In conclusion the used methology is a simple and effective means of incorporating fluorine in a polymer.

7

Polymer Properties

Polymers containing fluorine are commonly more thermally resistant than their non-fluorinated analogues. Low surface energy is furthermore characteristic of films cast from fluorinated polymers. The thermal properties as well as the surface activity of cast films were studied for all the synthesized polymers and copolymers. In the following these properties are presented and discussed.

7.1 Contact Angle Measurements

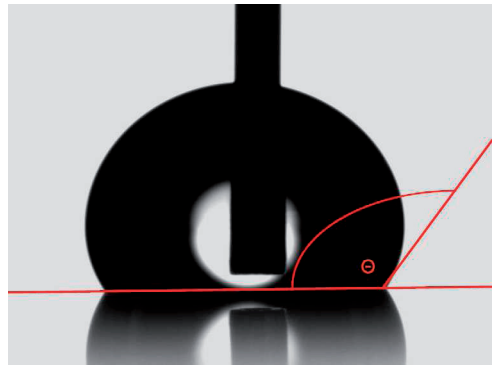

Figure 7.1. Definition of the contact angle, Θ, used herein. The shown sample is a film of PMMA-*b*-P17FM with a water contact angle of 118°.

Contact angles of water (Θ) were measured on the surfaces of films cast from solutions of the synthesized (co)polymers. The contact angle was defined as the angle within the droplet as indicated in Figure 7.1. Advancing contact angles were found by expanding a drop on the surface and measuring the angle at the commencement of expansion. This was done with the syringe needle inside the droplet. Similarly, receding contact angles were found by removing water from the droplet with the needle and measuring the angle at contraction. With the given definition of the contact angle, high contact angles are measured for hydrophobic surfaces and low contact angles for hydrophilic surfaces.

7.2 Copolymers from PEG-macroinitiators

7.2.1 Thermal Properties

The triblock copolymers synthesized from PEG-macroinitiators, as described in Chapter 3, were studied by differential scanning calorimetry (DSC) to observe their thermal transitions[1]. The results are shown in Table 7.1.

Table 7.1. Thermal transitions of P3FM-*b*-PEG-*b*-P3FM copolymers.

Sample[a]	Macroinitiator	PDI	$M_{n,SEC}$ (g/mol)	T_g (°C)	T_m (°C)
7	PEG2000	1.51	6240	-	29
2	PEG2000	1.50	19,100	27	-
1	PEG2000	1.60	23,700	46	-
9	PEG2000	1.50	27,600	52	-
4	PEG2000	1.39	29,900	42	-
8	PEG4600	1.23	12,000	-	41
3	PEG4600	1.88	28,500	66	27
6	PEG4600	1.29	31,700	67	36

[a] *Sample numbers here and in the following are the same as used in Table 3.5.*

The macroinitiators exhibited crystalline behavior with melting temperatures (T_m) of 39 and 50 °C for PEG2000 and PEG4600, respectively, while crystallization peaks at 20 and 33 °C, respectively were seen upon cooling. T_g of P3FM was observed to be 69 °C for a sample with a molecular weight of 8600 g/mol (PDI = 1.35).

For each of the low molecular weight samples (7 and 8) a single melting temperature was determined: 29 and 41 °C, respectively. A crystallization peak was additionally seen at 18 °C upon cooling for sample 8. The glass transition temperature (T_g) was not seen for these samples, which may be due to signal overlap with the broad peaks for T_m. The results indicate that the short fluorinated blocks do not hinder the formation of crystalline domains consisting of PEG. Samples 3 and 6 displayed T_gs for P3FM at 66 and 67 °C, respectively in addition to T_m for the PEG block at 27 and 36 °C, respectively. This is consistent with the results of Hussain *et al.* [9], who reported the lowering of T_m as well as the crystallization temperature of the PEO block by the presence of the fluorinated end-blocks in triblock copolymers.

All the high molecular weight triblock copolymers with a PEG2000 middle block exhibited amorphous behavior with a single T_g and no crystalline melting. The results were similar except for the value obtained for sample 2, which had a significantly lower T_g than the chemically equivalent samples 1, 4 and 9. The lower molecular weight of sample 2 could be the

[1] The scanning cycle was started at -50 °C close to the T_gs of the PEG-macroinitiators, therefore T_g was not observed in most cases and has not been reported.

reason for the difference in T_gs, as the size of the PEG block is relatively larger in this copolymer resulting in a depression of T_g. The decrease of 20 °C in T_g compared to the other samples is, however, more significant than expected.

7.2.2 Thermal Stability

Table 7.2. Thermogravimetric data for P3FM-*b*-PEG-*b*-P3FM copolymers.

Sample	(Co)polymer	$M_{n,SEC}$ (g/mol)	T(°C)[a] 10 %	50 %	90 %
	P3FM	8600	219	273	392
	PEG2000	2280[b]	286	376	416
	PEG4600	4920[b]	331	389	416
7	P3FM-*b*-PEG2000-*b*-P3FM	6240	276	389	419
4	P3FM-*b*-PEG2000-*b*-P3FM	29,900	226	373	394
8	P3FM-*b*-PEG4600-*b*-P3FM	12,000	262	384	407
3	P3FM-*b*-PEG4600-*b*-P3FM	28,500	270	373	400
6	P3FM-*b*-PEG4600-*b*-P3FM	31,700	168	355	391

[a] *Temperature at weight loss of 10, 50 and 90 %.* [b] *M_n estimated by ^1H NMR.*

Thermal stabilities of representative samples of the triblock copolymers of PEG and 3FM were determined by thermogravimetric analysis (TGA). The results were similar for most of the copolymers regardless of the molecular weights of macroinitiator and final product. This is illustrated in Table 7.2, where the degradation temperature at weight losses of 10, 50 and 90 % are shown. The PEG-macroinitiators were both thermally stable until approx. 250 °C, where degradation set in. P3FM exhibited a different behavior, as several characteristic degradation steps were seen. The first decay was believed to derive from the cleavage of part of the fluorinated alkyl chain from the backbone. Scission was deduced to take place in the pendant alkyl chain with a weight loss of 36 % at 185 to 250 °C from cleavage of the bond between CH_2 and CF_3. This peak partially overlapped with a second degradation peak ending at 305 °C and a weight loss of 56 %. This was presumed to be the scission of the ester group, as the weight loss coincided with the elimination of O-CH_2-CF_3.

Sample 6 had a different degradation pattern from the other samples, as two distinct decays were seen (Figure 7.2). The narrow molecular weight distribution of this copolymer could be the reason for this observation, as the thermal stability of the polymeric blocks differ and this copolymer mirrors the degradation behavior of P3FM. In all cases the thermal stability of the triblock copolymers was lower than for the PEG-macroinitiators.

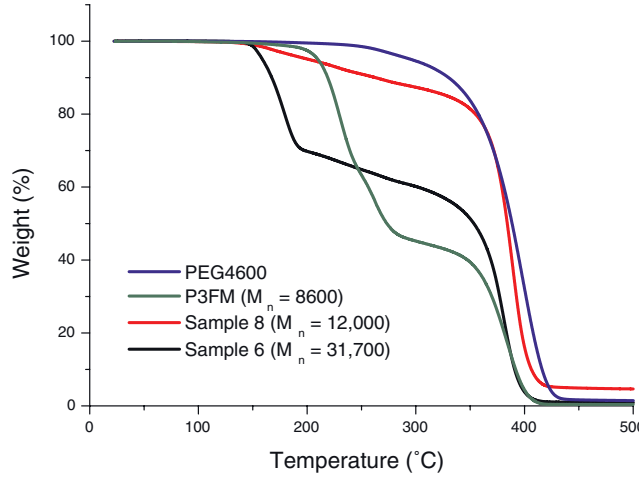

Figure 7.2. TGA-curves for P3FM, PEG4600, and P3FM-*b*-PEG4600-*b*-P3FM with two different molecular weights.

7.2.3 Surface Activity

Surface activities of several P3FM-*b*-PEG-*b*-P3FM copolymers were studied by measuring dynamic contact angles of water on flat films of the copolymers that had been spincoated on glass slides followed by annealing. The results are shown in Table 7.3.

Table 7.3. Dynamic contact angles of water on triblock copolymers synthesized from PEG-macroinitiators.

Sample	(Co)polymer	$M_{n,SEC}$	w%F[a]	Θ_{adv}	Θ_{rec}
	P3FM	8600	34	95 (± 4)	81 (± 8)
	PEG2000	2280[b]	0	18 (± 4)[c]	-[d]
	PEG4600	4920[b]	0	26 (± 6)[c]	-[d]
7	P3FM-*b*-PEG2000-*b*-P3FM	6240	22	90 (± 2)	31 (± 4)
2	P3FM-*b*-PEG2000-*b*-P3FM	19,100	30	81 (± 3)	48 (± 3)
4	P3FM-*b*-PEG2000-*b*-P3FM	29,900	31	97 (± 2)	79 (± 2)
8	P3FM-*b*-PEG4600-*b*-P3FM	12,000	20	96 (± 2)	54 (± 3)
6	P3FM-*b*-PEG4600-*b*-P3FM	31,700	29	93 (± 2)	73 (± 4)

[a] *Weight% fluorine calculated from* $M_{n,SEC}$. [b] M_n *determined by* ^{1}*H-NMR.*
[c] *Static contact angle.* [d] *Not detectable.*

It was not possible to measure the advancing (Θ_{adv}) or receding (Θ_{rec}) water contact angles on the surface of the films cast from the two PEG-macroinitiators. Due to the hydrophilic nature of these compounds, the applied water droplets spread out instantaneously on the films, which

made the determination of Θ_{adv} impossible. The values of Θ_{rec} were too low to be measured reliably by the given method ("needle-in"). Hence, the initial static contact angle has been used as an estimate of Θ_{adv} for the comparison with the triblock copolymers. Θ_{adv} and Θ_{rec} on a film of pure P3FM were 95° and 81°, respectively.

All of the triblock copolymers exhibited hydrophobic behavior independent of the fluorine content indicating a fluorine enrichment of the surface. The migration of the fluorinated segments to the surface during annealing has previously been observed [55, 74]. Sample 4 displaying the highest Θ_{adv} with a value of 97°, while sample 2 had an inexplicable Θ_{adv} of 81°. Θ_{rec} was dependent on the length of the fluorinated blocks, as the copolymers with the highest molecular weights, samples 6 and 4, exhibited values of 73 and 79°, respectively, while sample 7 displayed the most hydrophilic behavior with a Θ_{rec} of 31°.

7.3 Films with Honeycomb Structures

The formation of structured membranes by solvent casting solutions of star-shaped copolymers was discovered in 1994 by Francois *et al.* [75]. The structures are seen as highly regular porosities in films, when casting a solution of polymer in a volatile solvent under humid conditions. The evaporation of the volatile solvent leads to a decrease in the temperature of the solution and water droplets will start to condense onto the solution surface. These water droplets will organize themselves into a hexagonal array, which the polymer precipitates around. When the solvent and water have evaporated an ordered hexagonally packed polymeric structure will remain (see Figures 7.3 (top) and 7.4) [76].

Initially, the formation of honeycomb structures was assumed to be a phenomenon exclusively correlated with star-shaped copolymers. Later studies have shown that other copolymers also form honeycomb structures [77]. Fluorinated copolymers have previously been used to form honeycomb structured films by Yabu and coworkers [78], who cast films from a commercially obtained random copolymer of MMA and 1,1,2,2-tetrahydro-perfluorodecyl acrylate (1:1 ratio, see inset Figure 7.3). The films were highly hydrophobic and static contact angles of water up to 145° could be obtained for these films. The surface roughness was increased by peeling off the upper layer of the film with Scotch tape to obtain a pincushion structure (Figure 7.3). This increased the hydrophobic characteristics and for these structures contact angles of water up to 170° were measured.

7.3.1 Casting of Films with Honeycomb Structures

Films of three of the synthesized diblock copolymers were cast to observe, whether honeycomb structures could be formed. Block copolymers

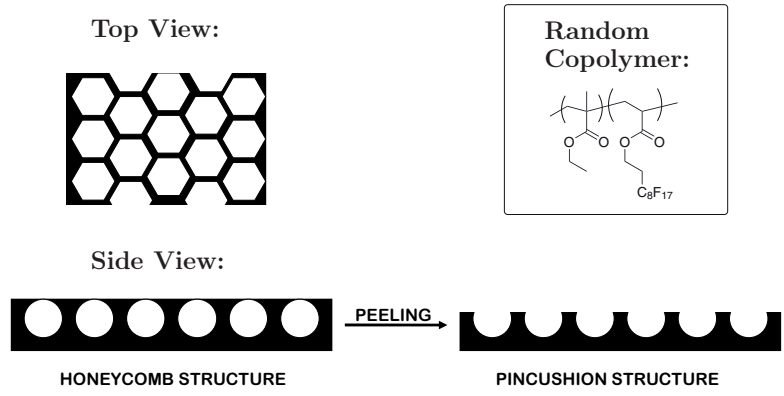

Figure 7.3. Schematic illustration of the honeycomb structured polymeric films prepared by Yabu *et al.* [78] seen from above and from the side. Peeling the top layer off with tape results in the formation of a pincushion structure. Inset: the chemical composition of the random copolymer used to cast the films.

of 3FM and MMA were chosen (Samples 1 and 5, Table 5.1) as well as the "true" block copolymer PMMA-*b*-P3FM (Sample 4, Table 5.1). The films were cast under humid conditions to form opaque films with isoporous honeycomb structures as seen in Figure 7.4. The formed pores were observed to have diameters in the micrometer range by means of an optical microscope.

Static contact angles of water were measured at minimum three different positions on the films and the results are shown in Table 7.4. Measurements were performed on the pristine film (Θ_{Cast}) as well as on the same films peeled with tape (Θ_{Peel}), where only half of the surface was peeled for this purpose. The films were annealed at 60 °C before measuring static contact angles of water on the film surfaces again, referred to as Θ_{Anneal} and $\Theta_{Peel\&Anneal}$, respectively.

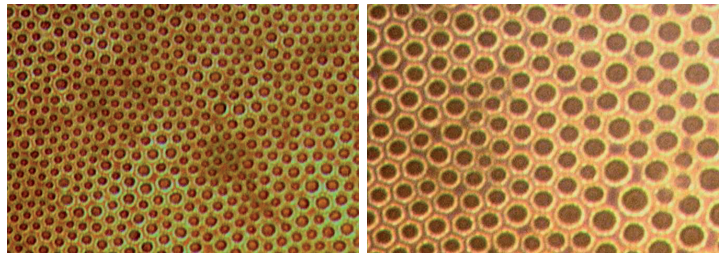

Figure 7.4. Honey-comb structures of P3FM-*b*-PMMA magnification of 500 (left) and 1000 (right) in an optical microscope. The formed pores are between 3 and 9 μm.

Generally, annealing lead to higher contact angles, which was also the case with peeling. $\Theta_{Peel\&Anneal}$ as high as 144° was found for film II as seen in Figure 7.5, while slightly lower values were found for film III. There was no direct correlation between contents of fluorine and contact angles, as the copolymer used to form film II had the lowest fluorine content and the highest measured contact angles. The formed films were brittle and relatively small (approx 1 cm^2), which made peeling of half the surface difficult. The peeling of film I was unsuccessful, as the entire film peeled off the glass slide, therefore annealing followed by further contact angles measurement was superfluous. The distribution of the copolymers at the surface of the honeycomb films is not known and the contact angles are influenced by both the chemical composition and the topography of the film surface i.e. the roughness, which may be influenced by the pore size. Further studies of honeycomb formation with the fluorinated copolymers were planned, but not accomplished due to difficulties coordinating efforts, when working in different locations.

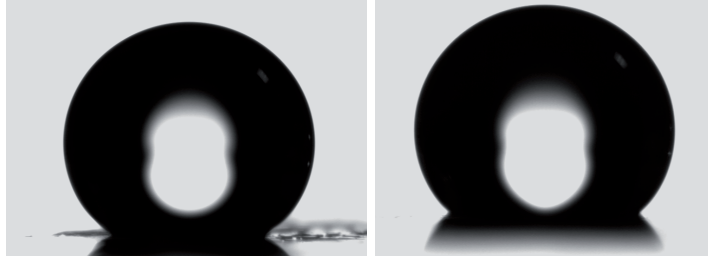

Figure 7.5. Static contact angles of water on the surfaces of PMMA-*b*-P3FM copolymer films with honeycomb structures. Films II (left) and III (right) have been cast, air dried, peeled with Scotch tape, and annealed at 60 °C overnight before measurements. The shown contact angles are 144° (left) and 133° (right).

Table 7.4. Static contact angles of water on polymer films with honeycomb structures.

Film	Copolymer[a]	Θ_{Cast}	Θ_{Anneal}	Θ_{Peel}	$\Theta_{Peel\&Anneal}$
I	P3FM-*b*-PMMA	108 (±3)	117 (±5)	-[b]	-[b]
II	PMMA-*b*-P3FM	135 (±9)	123 (±4)	127 (±14)	140 (±5)
III	PMMA-*b*-P3FM	101 (±3)	113 (±3)	134 (±4)	132 (±3)

[a] Polymers for films I and II are gradient copolymers (entries 1 and 5, respectively from Table 5.1), while III is cast from a "true" block copolymer (entry 4, Table 5.1). [b] Peeling was unsuccessful.

7.4 Copolymers from Fluorinated Methacrylates

7.4.1 Thermal Properties

T_gs of the fluorinated methacrylic copolymers described in Chapter 5 were measured by DSC and are shown in Table 7.5. Only one transition temperature was measured for each copolymer, which is characteristic of gradient copolymers.

Table 7.5. Glass transition temperatures of fluorinated diblock copolymers.

Sample[a]	(Co)polymer	PDI	$M_{n,SEC}$ (g/mol)	T_g (°C)
	P3FM		8600	59
	P8FM	-	-	27
	PMMA[b]	1.16	4400	69
	PMMA	1.18	18,600	101
	PMEA	1.23	7500	-49
	PPEGMA	1.11	7600	-65
1	P3FM-*b*-PMMA	1.32	10,300	67
2	P3FM-*b*-PMMA	1.30	7900	80
4	PMMA-*b*-P3FM	1.12	25,300	83
5	PMMA-*b*-P3FM	1.08	11,300	66
6	PMMA-*b*-P8FM	1.18	9300	66
7	PMMA-*b*-P17FM	1.24	10,300	95
8	PPEGMA-*b*-P3FM	1.18	16,500	-51
9	P3FM-*b*-PPEGMA	1.22	17,500	-62
10	PMEA-*b*-P3FM	1.60	10,400	-31;13
11	P3FM-*b*-PMEA	1.42	10,300	-6
12	P3FM-*b*-PMEA	1.56	27,400	68

[a] *Sample numbers here and in the following are the same as used in Tables 5.1 and 5.2.* [b] *PMMA-macroinitiator.*

Values of T_g between 66 and 83 °C were determined for the copolymers of MMA and 3FM, which coincides with the T_g of 101 °C found for PMMA as well as the previously determined value of 59 °C found for P3FM. Only one T_g was detectable for the "true" block copolymer PMMA-*b*-P3FM (entry 4), although two values were anticipated. This could be explained by the proximity of the T_g-values of the two homopolymers due to the size of the PMMA block, although the value of 83 °C was unexpectedly high. PMMA-*b*-P8FM exhibited a T_g of 66 °C, which is intermediate compared to the values of 101 and 27 °C for the homopolymers. The T_g of PMMA-*b*-P17FM was determined to be 95 °C, which is close to the value for PMMA. A homopolymer of 17FM did not show any glass transition, but displayed a crystalline melting temperature (T_m) of 88 °C, which was not observed in the copolymer. A single transition was found for the two copolymers of

3FM and PEGMA and in both cases values were close to T_g of PPEGMA: -51 and -62 °C. The copolymer PMEA-*b*-P3FM exhibited block copolymer behavior with two distinct T_gs of -31 and 13 °C. The first T_g is closer to T_g for PMEA, while the second is intermediary compared to the values for the two homopolymers. The relatively low value of 13 °C found for the second T_g is probably due to the presence of PMEA in the P3FM block. For one P3FM-*b*-PMEA copolymer (entry 11) a single T_g of -6 °C was found, while a value of 68 °C was found for the other (entry 12). This apparent inconsistency derives from the difference in composition, as the latter copolymer consists mainly of P3FM.

7.4.2 Thermal Stability

Most of the diblock copolymers exhibited more than one characteristic degradation step. In order to compare the thermal stabilities of the polymers the residual weight percent (w%) at temperatures of 200, 300 and 400 °C are therefore reported (Table 7.6). Homopolymers of the fluorinated monomers 8FM and 17FM exhibited similar degradation behavior to P3FM with several distinct degradation peaks. For P8FM scission appears to take place between the oxygen and the fluorinated chain (loss of 64 w%) possibly by the formation of a 5-membered ring, while the degradation mechanism of P17FM was more complex with multiple steps. The degradation patterns were also seen in the TGA-analysis of the copolymers of 3FM and MMA as well as the copolymers PMMA-*b*-P8FM and PMMA-*b*-P17FM. The fluorinated homopolymers P3FM, P8FM and P17FM had a lower thermal stability than PMMA, as the former polymers exhibited excessive degradation between 200 and 300 °C, while PMMA only had a minor weight loss in this temperature interval, 13 w%. The fluorinated block copolymers containing PMMA had intermediate thermal stabilities compared to the two equivalent homopolymers.

The thermal behavior of copolymers of 3FM and PEGMA was close to that exhibited by PPEGMA, indicating that the thermal stability was not decreased by the less thermally stable fluoropolymer. The same tendency was observed for the three copolymers of MEA and 3FM, where the latter component only to a lesser extent reduced the thermal stability compared to PMEA. The most fluorinated copolymer P3FM-*b*-PMEA (entry 12) was the least thermally stable with a degradation of 36 w% at 300 °C, while PMEA is almost intact at this temperature (residual 98 w%).

7.4.3 Surface Activity

Dynamic contact angles of water were measured on films that had been spincoated on glass slides followed by annealing. Results of the block copolymers of the fluorinated monomers and MMA are shown in Table 7.7. Θ_{adv} found for the copolymers of 3FM and MMA, 92° to 94°, were very close to the value for P3FM, while Θ_{rec} was slightly lower in all

Table 7.6. Thermogravimetric data for fluorinated diblock copolymers.

Sample	(Co)polymer	$M_{n,SEC}$	Weight[a]		
		(g/mol)	200 °C	300 °C	400 °C
	P3FM	8600	97	45	4
	PMMA	18,600	96	92	35
1	P3FM-*b*-PMMA	10,300	90	75	10
2	P3FM-*b*-PMMA	7900	97	84	13
3	P3FM-*b*-PMMA	9200	90	83	35
4	PMMA-*b*-P3FM	25,300	98	50	8
5	PMMA-*b*-P3FM	9600	75	56	22
	P8FM	-[b]	98	36	11
6	PMMA-*b*-P8FM	9300	99	72	28
	P17FM	-[b]	79	62	12
7	PMMA-*b*-P17FM	10,300	95	85	26
	PPEGMA	7600	96	88	27
8	PPEGMA-*b*-P3FM	16,500	95	81	12
9	P3FM-*b*-PPEGMA	17,500	96	82	10
	PMEA[c]	18,200	99	98	42
10	PMEA-*b*-P3FM	10,400	100	87	26
11	P3FM-*b*-PMEA	10,300	99	86	12
12	P3FM-*b*-PMEA	27,400	96	64	4

[a] *Residual weight% at temperatures of 200, 300 and 400 °C.* [b] *M_n could not be determined.* [c] *This polymer was synthesized previously [70]*

cases. The PMMA block is responsible for the reduction in Θ_{rec} and since PMMA is a relatively hydrophobic polymer, this reduction is small. The distribution of the two monomers in the copolymer did not influence the surface activity noticeably, as there was no significant difference between the results for copolymers 1, 4 and 5. The high surface activity can be explained by the migration of the fluorinated chains to the surface resulting in a fluorine enriched film surface as seen for the triblock copolymers. The film of PMMA-*b*-P8FM appeared not to be coherent, but the contact angles, $\Theta_{adv} = 92°$ and receding $\Theta_{rec} = 77°$, obtained for this copolymer were comparable to results for the P3FM/PMMA copolymers. The highest Θ_{adv} was found for PMMA-*b*-P17FM: 118°, while Θ_{rec} for this polymer films was 76°. The formation of coherent films of P8FM and P17FM was not possible under the same conditions as for the other films due to the low solubility of these polymers. No contact angle data are therefore given for these homopolymers.

The flat films of polymers 1, 4 and 5 were obviously less hydrophobic in comparison with the honeycomb structured films I, II and III (Table 7.4) cast from the same copolymers. This demonstrates the influence of surface structure, primarily surface roughness, on the contact angles of water.

Table 7.7. Dynamic contact angles of water on surfaces of copolymers of MMA with 3FM, 8FM, and 17FM.

Sample	(Co)polymer	$M_{n,SEC}$	w%F[a]	Θ_{adv}	Θ_{rec}
	PMMA	11,000	0	73 (± 1)	58 (± 2)
	P3FM	8600	34	95 (± 4)	81 (± 8)
1	P3FM-*b*-PMMA	10,300	23	96 (± 4)	84 (± 2)
4	PMMA-*b*-P3FM	25,300	29	94 (± 6)	73 (± 9)
5	PMMA-*b*-P3FM	9600	15	93 (± 6)	75 (± 2)
6	PMMA-*b*-P8FM	9300	25	92 (± 4)	77 (± 5)
7	PMMA-*b*-P17FM	10,300	27	118 (± 3)	76 (± 2)

[a] *w% fluorine calculated from the chemical composition found by* ^1H *NMR.*

Dynamic contact angles measured for the copolymers of 3FM and the hydrophilic monomers MEA and PEGMA are shown in Table 7.8. For the copolymers PPEGMA-*b*-P3FM and P3FM-*b*-PPEGMA Θ_{adv} was almost the same, 99° and 95°, respectively, while Θ_{rec} was markedly lower for the former copolymer (52° vs. 80°). This is most probably due to the fact that this copolymer has a pure PPEGMA block, which can form hydrophilic domains resulting in a low Θ_{rec}. The same tendency was seen for copolymers of MEA and 3FM, where both PMEA-*b*-P3FM and P3FM-*b*-PMEA had a Θ_{adv} of 96°, while Θ_{rec} had values of 44° and 81°, respectively. The hysteresis[2] of the copolymeric films was comparable to that observed for the fluorinated triblock copolymers.

Table 7.8. Dynamic contact angles of water on surfaces of copolymers of 3FM with MEA and PEGMA.

Sample	Copolymer	$M_{n,SEC}$	w%F[a]	Θ_{adv}	Θ_{rec}
	PPEGMA	7600	0	42 (± 6)	19 (± 3)
	PMEA	7500	0	55 (± 9)	11 (± 3)
8	PPEGMA-*b*-P3FM	16,500	15	99 (± 2)	52 (± 4)
9	P3FM-*b*-PPEGMA	17,500	21	95 (± 1)	80 (± 2)
10	PMEA-*b*-P3FM	10,400	18	96 (± 1)	44 (± 5)
11	P3FM-*b*-PMEA	10,300	23	96 (± 2)	81 (± 2)

[a] *w% fluorine calculated from the chemical composition found by* ^1H *NMR.*

[2]Hysteresis refers to the difference between Θ_{adv} and Θ_{rec}

Table 7.9. Glass transition temperatures and thermal stabilities of polymers initiated by FMI.

Sample[a]	Polymer	$M_{n,SEC}$ (g/mol)	T_g (°C)	T(°C)[b] 10 %	50 %	90 %
	PMMA	11,000	101	340	393	415
1	FMI-PMMA	9200	64	277	387	414
2	FMI-PMMA	12,400	73	275	389	415
3	FMI-PMMA	24,000	90	283	384	407
	PPEGMA	7600	-65	291	376	418
4	FMI-PPEGMA	16,300	-70	259	369	414
5	FMI-PMMA-*b*-PPEGMA	21,600	-37;33	329	381	413
	PMEA[c]	18,200	-37	363	396	422
6	FMI-PMEA	24,400	-38	370	411	439

[a] *Sample numbers here and in the following are the same as used in Table 6.1.*
[b] *Temperature at weight loss of 10, 50 and 90 %.*
[c] *This polymer was synthesized previously [70]*

7.5 Polymers from Fluorinated Macroinitiator

7.5.1 Thermal Properties

The glass transition temperatures of the polymers synthesized from the fluorinated macroinitiator, FMI are presented in Table 7.9. The FMI itself exhibited three thermal transitions: Glass transition at -71 °C, crystallization at -48 °C and melting at 8 °C.

In the FMI-PMMA polymers, it is obvious that the fluorinated macroinitiator performs as a plasticizer and also that the effect diminishes with increasing molecular weight of the polymer, as would be expected. For the FMI-PMMA with a molecular weight of approx. 30,000 g/mol the T_g is reduced by only 10 °C, whereas the lower molecular weight FMI-PMMAs have reductions in T_g of 28 and 37 °C, respectively. For the hydrophilic polymers PMEA and PPEGMA the fluorinated moiety gives rise to only small changes in T_g, as both polymers already have T_gs well below ambient temperature. The most pronounced difference between the fluorinated and non-fluorinated polymers of PPEGMA was that a crystallization peak was observed for the latter at 117 °C, whereas the former did not crystallize. The presence of the fluorinated macroinitiator evidently suppresses crystallization. The copolymer FMI-PMMA-*b*-PPEGMA has two transitions, the lower one at -37 °C being very evident, whereas the other at 33 °C is less distinct. Thus, this copolymer provides evidence of microphase separation as could be expected from the amphiphilic composition. The presence of PMMA in the PPEGMA block gives rise to an increase in T_g from -65 °C to -37 °C, whereas the T_g of 33 °C assigned to the PMMA block is low due to the small size of the block.

7.5.2 Thermal Stability

Analysis of FMI by TGA showed that the thermal stability of this was lower than for any of the synthesized polymers. Only a single degradation step was observed in all cases except for FMI-PMMA-*b*-PPEGMA, where two steps were seen. The temperature at weight losses of 10, 50 and 90 %, respectively are reported in Table 7.9 from which the thermal stabilities can be compared.

The onset of degradation of FMI-PPEGMA began somewhat earlier than for a homopolymer of PEGMA indicating a lower thermal stability of the fluorinated polymer. The three FMI-PMMA polymers exhibited a similar behavior, as they were less thermally stable than PMMA homopolymer, which was seen at the onset of degradation, which began around 275 °C for the FMI-PMMAs, i.e. 65 °C lower than for PMMA. The block copolymer FMI-PMMA-*b*-PPEGMA had a delayed degradation onset compared to both fluorinated polymers (FMI-PMMA and FMI-PPEGMA), whereas at

higher temperatures (>375 °C) the difference was negligible. The introduction of the fluorinated moiety had a minor positive effect on PMEA, as it did not reduce the thermal properties in contrast to the case for the other tested polymers.

7.5.3 Surface Activity

Dynamic contact angles of water on the polymers were measured on flat films that had been spincoated on glass slides followed by annealing. The results are shown in Table 7.10.

Table 7.10. Dynamic contact angles of water on surfaces of polymers initiated by FMI.

Sample	Polymer	$M_{n,SEC}$	w%F[a]	Θ_{adv}	Θ_{rec}
	PMMA	11,000	0	73 (± 1)	58 (± 2)
	PPEGMA	7600	0	42 (± 6)	19 (± 3)
	PMEA	7500	0	55 (± 9)	11 (± 3)
1	FMI-PMMA	9200	5	83 (± 2)	59 (± 3)
2	FMI-PMMA	12,400	3	90 (± 1)	39 (± 4)
3	FMI-PMMA	24,000	2	82 (± 3)	57 (± 2)
4	FMI-PPEGMA	16,300	2	67 (± 6)	22 (± 4)
6	FMI-PMEA	24,400	1	92 (± 4)	64 (± 8)

[a] *w% fluorine calculated from* $M_{n,SEC}$.

In general the incorporation of the fluorinated macroinitiator into the three different (meth)acrylic polymers increased the advancing contact angle of water (Θ_{adv}) as compared to the non-fluorinated analogues. Apparently the fluorinated segments migrated to the surface during annealing, as seen for the fluorinated copolymers. Thus, Θ_{adv} of FMI-PMMA was increased by 10° or more from 73° observed for the relatively hydrophobic PMMA. The effect on Θ_{adv} from the introduction of FMI was more pronounced for PMEA, which is an intermediate hydrophilic polymer, as well as for the hydrophilic PPEGMA. For PMEA Θ_{adv} of 92° and 55° were found for the partly fluorinated and non-fluorinated polymers, respectively. This is a difference of more than 35°, which mirrors the significant change in the nature of the polymer surface from intermediate hydrophilic to hydrophobic imparted by the fluoroalkoxy tail. The polymers containing PEGMA formed inhomogeneous films due to low solubility. Results obtained for these polymers are therefore estimates, as the difference between measurements was considerable. The presence of the fluorinated chain end resulted in larger contact angles of water on the film surfaces with the Θ_{adv} increasing from 42° to 67°. The change in the receding contact angle was virtually non-existent (19° versus 22°), which was a different behavior than seen for PMEA. The hydrophobic properties induced by FMI in the polymers of MMA and MEA were comparable to

those obtained by copolymerization with 3FM, although Θ_{adv} was lower in all cases.

7.6 Comparison of Polymerization Strategies

7.6.1 Synthesis

Using the PEG-macroinitiators for the polymerization of 3FM was a time consuming method partly due to the preparation of the macroinitiators. The products were relatively well-defined, but residual macroinitiator was found in all cases. The triblock copolymers could probably have been isolated by fractionation, which would, however, give a more elaborate workup procedure.

Synthesizing diblock copolymers by sequential addition was an efficient way of obtaining fluorinated copolymers. The disadvantage was the reduced control over the copolymer structure due to the presence of both monomers during reaction. In some cases sequential polymerization was a disadvantage, as the optimal reaction conditions of the two monomers were not the same, especially when copolymerizing 3FM with the hydrophilic monomers MEA and PEGMA.

For both types of copolymerization relatively large amounts of the fluorinated monomer(s) were needed, which increases the overall cost of the reaction, due to the high cost of these compounds.

Using the fluorinated macroinitiator for polymerizing non-fluorinated monomers was more time consuming than the sequential polymerization. The initiator efficiency was high, which made this method more feasible than polymerization from the PEG-macroinitiators. Compared to the other two approaches, this technique was relatively inexpensive, as the fluorinated macroinitiator could be synthesized from a commercially available surfactant.

7.6.2 Properties

Combining 3FM with the PEG-macroinitiators resulted in an increased operation temperature compared to the latter compounds, as T_g of P3FM was higher than the crystalline melting point of the PEG-macroinitiators. The thermal stability was, however, reduced at elevated temperatures compared to the original PEG-polymers. The fluorinated triblock copolymers were very surface active with high contact angles of water. When the fluorinated blocks were sufficiently long, purely hydrophobic behavior was seen in terms of high advancing and receding contact angles.

The diblock copolymers of MMA and the fluorinated methacrylates had intermediate thermal properties compared to the homopolymers in terms of T_g and thermal stability. The copolymers of 3FM and PEGMA had thermal properties close to those of PPEGMA, resulting in a very low

application temperature, due to the low T_g (< -50 °C). Combination of 3FM with MEA resulted in an increase in T_g compared to PMEA with only a minor reduction in thermal stability. The application temperature of the copolymers containing hydrophilic segments was significantly lower than for the P3FM-*b*-PEG-*b*-P3FM copolymers. For all copolymers the introduction of 3FM, 8FM or 17FM resulted in hydrophobic behavior of flat films.

The fluorinated macroinitiator performed as a plasticizer in all the synthesized polymers, while it also reduced the thermal stability of PMMA and PPEGMA, whereas the thermal stability of PMEA was virtually unaffected. Flat films cast from the fluorinated polymers exhibited increased hydrophobicity compared to the parent polymers. For PMEA the surface activity was comparable with that of the P3FM/PMEA copolymers, while the effect was smaller for FMI-PPEGMA. Seen in relation to the total fluorine content ($\leq$ 5 w%) in these polymers the effect was much larger than for the fluorinated copolymers.

7.7 Conclusions

For all the synthesized polymers and copolymers the introduction of the fluorinated moiety lead to a reduction in the thermal stability. This was probably due to the ester groups in the fluorinated monomers as well as the macroinitiator. T_gs were increased for copolymers of 3FM with MEA, PEGMA and from the PEG-macroinitiators, while the opposite was seen for polymers initiated by FMI. The hydrophobic properties of flat films were also increased for all synthesized (co)polymers with FMI having the largest effect seen in terms of total fluorine content. Therefore utilizing the fluorinated macroinitiator approach is considered the most profitable, if the obtained product fulfills the needed requirements.

8

Conclusion

Three different fluorinated methacrylates: 2,2,2-trifluoroethyl methacrylate (3FM), 2,2,3,3,4,4,5,5-octafluoropentyl methacrylate (8FM) and 1,1,-2,2-tetrahydroperfluorodecyl methacrylate (17FM) were utilized in ATRP. Preliminary homopolymerizations of 3FM and 17FM indicated low solubility of the fluorinated products and some lack of control over polymerization. Triblock copolymers were, however, synthesized by the developed protocol utilizing two different terminally functionalized poly(ethylene glycol)s (PEGs) as macroinitiators. Macroinitiators with molecular weights of 2000 and 4600 g/mol were chosen and successfully used to polymerize 3FM to obtain amphiphilic triblock copolymers. Different lengths of the fluorinated blocks were targeted and molecular weights between 6000 and 32,000 g/mol with PDIs of 1.2 to 1.9 were obtained. Low molecular weight triblock copolymers exhibited crystalline behavior with no glass transition, and for PEG4600 containing copolymers a T_m was detectable even at $M_n > 30{,}000$ g/mol. The P3FM-*b*-PEG2000-*b*-P3FM copolymers had T_gs of 27 to 42 °C and crystallinity was suppressed by the presence of the fluorinated end blocks at high molecular weights (∼20,000 g/mol).

It was attempted to use solid-phase microextraction (SPME) for kinetic studies of homopolymerizations of 3FM. The results of this study were disappointing, as reproducible results could not be obtained. A kinetic study monitoring monomer conversion by ^{1}H NMR indicated that 3FM follows first-order kinetics and reacts in a controlled manner to give molecular weights close to target and low PDIs with the lowest values being around 1.2. The use of ^{1}H NMR analysis for 8FM gave less conclusive results, as the low solubility of the polymeric product made analysis by ^{1}H NMR and SEC impossible.

Block copolymers of methyl methacrylate (MMA) and the three fluorinated methacrylates were polymerized by ATRP. Sequential addition was used in most instances and it was possible to synthesize block copolymers of MMA and 3FM starting from either monomer. The polymerization of MMA followed by 3FM yielded better results exhibiting low polydispersity and a linear evolution of molecular weights with conversion. The same behavior was seen for the polymerization of 3FM from a PMMA-macroinitiator, where a "true" block copolymer with a molecular weight of 25,000 g/mol and PDI of 1.12 was obtained. Block copolymers of MMA and 8FM and 17FM, respectively were synthesized by sequential addition with MMA as the first monomer. First-order kinetics indicated that

the length of the fluorinated pendant chain does not influence the reactivity in polymerization by ATRP. Novel block copolymers of 3FM and poly(ethylene glycol) methyl ether methacrylate (PEGMA) were synthesized by ATRP in toluene. Polymerization starting with PEGMA at 50 °C gave the best results (M_n = 16,500, PDI = 1.18), while the initiation of PEGMA from P3FM at 50 °C was not possible. Copolymerization of 3FM and 2-methoxyethyl acrylate (MEA) was possible, but polymerizations were not entirely controlled, presumably due to the different natures of the two monomers, evidenced by high polydispersities (>1.4) and lack of reproducibility in the composition of the obtained copolymers.

The fluorinated macroinitiator, FMI based on a 2-perfluoroalkyl ethyl-co-poly(ethylene glycol) surfactant was utilized in controlled polymerizations of MMA, MEA and PEGMA. Excellent results were achieved with MMA, which exhibited first-order kinetics, linear evolution of molecular weights and low polydispersities (PDI < 1.25) for three different monomer to initiator ratios: 50, 100 and 200. Similar results were obtained for the polymerization of MEA with M_n = 24,400 g/mol close to target and PDI = 1.21. Polymerization of PEGMA from FMI did not proceed in an entirely first-order manner, however, polydispersities were low throughout reaction (PDI < 1.2) and the evolution of molecular weight was relatively linear. This made it possible to synthesize the block copolymer FMI-PMMA-*b*-PPEGMA by sequential addition. The polymerization results obtained using FMI were comparable in terms of molecular weight distributions with those found using the conventional initiator ethyl-2-bromoisobutyrate (EBB), making this a method with great potential for incorporating fluorine in a polymer. In most cases the fluorinated macroinitiator performed as a plasticizer in the synthesized polymer.

The introduction of the fluorinated monomers lead to a reduction in the thermal stability of all the synthesized polymers and copolymers, which was also the case for the polymers initiated by FMI.

Flat films cast from the fluorinated copolymers and polymers exhibited increased hydrophobicity compared to the parent polymers. The diblock copolymers were the most hydrophobic with advancing contact angles above 90° in all cases with the highest value of 118° found for PMMA-*b*-P17FM. Honeycomb structured films were cast from copolymers of 3FM and MMA to yield highly hydrophobic surfaces with static contact angles of up to 144°.

9

Outlook

During the work on this Ph.D. a number of novel fluorinated polymers and copolymers were successfully synthesized. It was proposed that these compounds held potential as biocompatible materials for uses such as drug delivery. The surface activities have been studied, and the positive effect of the fluorine moiety was substantiated. There was, however, no proof of the postulated biocompatibility. In the following a number of options for continued work are given including both improvements on the work already completed as well as suggestions for further studies including test of the biocompatibility of the synthesized polymers.

9.1 Continuation of Present Work

9.1.1 Synthesis Work

Most of the proposed polymeric compositions were synthesized as planned. In several cases, however, optimization could most probably have improved the results in terms of control over molecular weights and distributions of these. Optimizations of the existing system might include changes in temperature, solvent and ligand. Changing to a fluorinated solvent might have improved the results for the fluorinated monomers, although a decrease in solubility of the hydrophilic comonomers in the same instance seems probable. This could have been circumvented by using the macroinitiator approach for performing the copolymerizations i.e. performing the polymerizations in two different solvents. A complete change in polymerization system could also have been undertaken, as the monomers in question hold potential for polymerization by RAFT. This approach would have been very time consuming, as we would have had to obtain knowledge on the practical aspects of this technique e.g. the synthesis of a suitable RAFT agent. Alternative analysis methods could have been sought such as SEC in a different solvent or with a different detector, but this was not possible with the current equipment.

9.1.2 SPME

Given time, an optimization of the SPME technique would have been relevant. If successful, kinetic studies of the monomers 8FM and 17FM could then have been undertaken, as it was determined by preliminary experiments that the signals of 8FM and 17FM, respectively were well separated from both TFT and xylene in the chromatogram. Analysis by SPME would have been an option for monitoring kinetics as an alternative to ^{1}H NMR analysis, which was shown not to be feasible for these monomers.

Part of an optimization process might have included studying a more homogeneous polymerization system i.e. polymerization of a non-fluorinated monomer to observe whether the inhomogeneity of the samples was the main source of error.

9.1.3 Honeycomb Structures

A few of the synthesized fluorinated block copolymers were used to form films with honey-comb structures. No examples of honeycomb formation with fluorinated block copolymers had been published at the time, making our work potentially relevant for publication. Lack of time was the limiting factor in these studies. If the relationship between chemical composition and block structure (gradient vs. "true" block) in regards to the size and distribution of pores could have been established, this would have been extremely interesting. The upper limit of the contact angles of water could also have been studied further.

9.2 Suggestions for Further Studies

9.2.1 Filmforming Properties

The ability of the synthesized fluorinated (co)polymers to form films was established in all instances. The strength of these films and their abilities to act as e.g. diffusion barriers have yet to be studied. The formation of free films would for many applications be necessary and it would have been interesting to see, whether these films could withstand extensive handling and how they then would perform in diffusion studies. The migration of components from the films would also have been important to study, if these were to be used in the medico industry.

9.2.2 Biocompatibility

The key to determine whether the synthesized polymers are useful for the proposed application is to test the biocompatibility. This could for example be done by animal testing, other preliminary testing would, however, be advisable, as animal testing is expensive and for ethic reasons should

only be used for products with great potential. Such tests could be in vitro experiments, where the reactions of cells or tissue to polymer films were studied. An important issue is whether the complete removal of the Cu(I)Br catalyst could be achieved in order to avoid the toxicological effect of this.

9.2.3 Bulk Properties

The study of the surfaces of the formed films could have been undertaken using XPS. This could have substantiated our assumption of the orientation of fluorinated segments on the film surfaces. The molecular packing in solid phase could have been determined by scattering (SANS or SAXS). By these methods the formation of microdomains might have been indicated, which we did not manage to demonstrate by DSC.

9.2.4 Behavior in Solution

It could be relevant to study the behavior of the (co)polymers in different solvents to determine both the stability and the solubility. This includes studying the aggregation of the (co)polymers in solution e.g. the formation of micelles, which could be important in drug delivery uses. Here the difference, if any, between the gradient and "true" block copolymers might have been observed.

10

Experimental

10.1 Instrumentation

10.1.1 Nuclear Magnetic Resonance Spectroscopy

The structures of the final products were confirmed by ^{1}H NMR, which was performed on either a 250 MHz or a 400 MHz Bruker apparatus using $CDCl_3$ as solvent.

10.1.2 Size Exclusion Chromatography

Molecular weights were determined by SEC performed on a Viscotek 200 instrument equipped with a PL guard column and two PL mixed D-columns (Polymer Laboratories). RI-detection was used with THF as eluent (1 ml/min, irganox as flow rate marker) at ambient temperature utilizing PMMA standards (2000 - 240,000 g/mol).

The fluorinated homopolymers described in Chapter 4.4 were analyzed on a system with a PL gel 5 μm guard column and two PL gel 5 μm mixed D-columns (Polymer Laboratories). Chloroform/triethylamine 95:5 was used as eluent (flow rate 1 ml/min, toluene as flow rate marker) with PMMA-standards (200 to 1,000,000 g/mol).

10.1.3 Infrared Spectroscopy

The FT-IR analysis were performed on a PerkinElmer Spectrum One model 2000 Fourier transform infrared system with a universal attenuated total reflection sampling accessory on a ZnSe/diamond composite. Sixteen scans were used for all samples with a resolution of 4 cm^{-1} in the range from 525 to 4000 cm^{-1}.

10.1.4 Solid-Phase Microextraction

For SPME, the vials were head-space-extracted for 0.02 min[1] using a SPME needle (Supelco, 57334-U, 85 mm Carboxen/PDMS Stableflex) shortened to 0.2 cm mounted in a Varian 8200Cx autosampler. This needle automatically extracts components from the sample and transfers the

[1] Fraction of 100 for all chromatograph time data

needle to the injector block of the GC. The GC parameters were as follows:

- Carrier gas: He 99.9995%
- GC: Varian 3400Cx
- Head pressure: 1.7 bar (25 psi)
- Injector: on-column SPI
- Injector temperature programming: 130 °C for 0.1 min, 130 - 250 °C (300 °C/min), 250 °C for 3 min.
- GC oven temperature programming: 40 °C for 3 min, 40 - 200 °C (20 °C/min), 200 °C for 1 min.

The analytical column was a Restek Stabilwax-DA, 30 m, 0.25 mm i.d., coating 0.25 mm. The transfer line to the MS was mounted with an SGE No-Vent module at a temperature of 230°C. The MS used was a Saturn 2000 instrument with Silcosteel treated ion-trap electrodes (190°C). The MS scanned continuously from m/z 19 to 249, averaging of two scans every 0.5 s with SIS to allow filtering of m/z 28 and 32. The prescan target for the ion trap was 5000.

10.1.5 Differential Scanning Calorimetry

The glass transition temperatures were measured with a DSC Q1000 system from TA Instruments. The samples were heated up to 150 °C (10 °C/min) and cooled to -50 °C to remove any effects induced by prior treatment. The glass transition temperature was then measured upon consecutive heating from -50 °C to 200 °C at a rate of 10 °C/min. For PEGMA containing polymers as well as copolymers of PMEA cooling to -100 °C was applied.

10.1.6 Thermogravimetric Analysis

Thermogravimetric measurements were performed on a TGA Q500 from TA Instruments heating the polymer sample from ambient temperature to 600 °C at a rate of 20 °C/min under nitrogen atmosphere.

10.1.7 Contact Angle Measurements

Measurements were performed on an OCA15plus Contact Angle System apparatus from Dataphysics with contact angles attained by the sensile drop method.

10.1.7.1 Honeycomb Films

Samples for contact angle measurements were dissolved in dichlormethane (20 mg/ml) and cast on glass slides under humid conditions. The films were air dried further and half the film surface was peeled with Scotch tape. Stationary contact angles were measured by placing a water droplet on the film surface and measuring the angle after approximately 30 seconds, when a steady state was reached. The films were annealed at 60 °C overnight before conducting the second set of contact angle measurements.

10.1.7.2 Flat Films

Samples were dissolved in dichlormethane in a concentration of 20 mg/ml and spincoated (1000 rpm) on glass slides. The films were annealed for 24 hours at 110 °C before measurement. Dynamic contact angles were measured by the "needle-in" method.

10.2 General Procedures

10.2.1 Experimental Setup

Polymerizations took place in a Schlenk tube connected to a manifold, which can ensure inert conditions through flushing with nitrogen or alternatively be evacuated by using a vacuum pump. Reaction mixtures were degassed before polymerization by placing the reaction vessel (Schlenk tube) in liquid nitrogen under nitrogen flow until it was completely frozen (5-10 min). The Schlenk tube was evacuated and concurrently thawed to ambient temperature under nitrogen. This freeze-pump-thaw cycle was performed 3-5 times before placing the Sclenk tube on an oil bath at the chosen reaction temperature. The setup used for the polymerizations by ATRP is shown in figure 10.1.

10.2.2 Materials

2,2,2-Trifluoroethylene methacrylate (3FM), 2,2,3,3,4,4,5,5-octafluoropentyl methacrylate (8FM) and 1,1,2,2-tetrahydroperfluorodecyl methacrylate (17FM) were kindly supplied by Osaka Chemicals. The monomers were passed through a column of inhibitor remover (Sigma Aldrich) or neutral Al_2O_3 to remove inhibitor before polymerization. For the homopolymerizations 3FM and 17FM were stored over CaH_2 and distilled before use. α,α,α-trifluorotoluene (TFT), dichloromethane (DCM), toluene, Cu(I)Br, 4-dimethylamino-pyridine (DMAP), triethylamine (TEA), ethyl-2-bromoisobutyrate (EBB) (Sigma Aldrich) and *N*-(*n*-propyl)-2-pyridylmethanimine (n-Pr-1) (Warwick Polymer Labs) were used as received. Xylene was distilled and kept over molecular sieves until used.

Figure 10.1. Experimental setup used for the polymerizations by ATRP. The manifold has two lines, the upper line is connected to a pump, which ensures evacuation. The lower line can be flushed continuously with nitrogen for inert conditions.

10.3 Synthesis Procedures

10.3.1 Synthesis of Me_6TREN Ligand

20 ml of formaldehyde (37 %) (0.27 mol) and 24 ml (98 %) (0.61 mol) of formic acid were placed in a round-bottomed flask equipped with stirrer and condenser. 5 ml (0.034 mol) of tris(2-aminoethyl)amine (TREN) and 10 ml of distilled water were added dropwise to the flask at 0 °C followed by additional 20 ml of distilled water. After heating to 100 °C the reaction was left to reflux overnight. The volatiles were removed by rotary evaporation and the reaction mixture was neutralized with saturated NaOH solution followed by extraction with DCM (3 times). The combined organic phases were dried with $MgSO_4$ and the product was recovered by rotary evaporation as light yellow crystals. m = 6.8 g (89 % yield). ^{1}H NMR($CDCl_3$): δ 2.60 (t, 6H), δ 2.40 (t, 6H), δ 2.25 (s, 18H).

10.3.2 Synthesis of PEG-macroinitiators

The synthesis of the PEG-macroinitiators were performed by Master student Maria V. Juhl [65] by the following protocol:

10 g of PEG2000 was dissolved in 100 ml anhydrous THF in a 250 ml two-necked round-bottomed flask equipped with a stirrer and a condenser with a gas inlet (N_2). 183 mg (1.5 mmol) of DMAP and 2.1 ml (15 mmol) of TEA were added under nitrogen. The temperature was lowered to 0 °C and 1.85 ml (15 mmol) of 2-bromoisobutyryl bromide in 20 ml THF was added dropwise to the reaction over a period of 15 min followed by thawing to ambient temperature. After 20 hours the reaction mixture was filtered and solvent was removed in vacuo. The recovered solids were dissolved in DCM and washed with a saturated $NaHCO_3$-solution followed by water until pH of 7 was obtained. The organic phase was dried with $MgSO_4$, filtered and the product was isolated by rotary evaporation (m = 8.2 g, 71 % yield, M_n = 2260 g/mol, PDI = 1.02).

PEG4600 macroinitiator was synthesized using the same protocol.

10.3.3 Homopolymerization of MMA

The preliminary polymerizations of MMA were performed using the procedure described in the following:

5 ml (47 mmol) of MMA and 30 ml of xylene were charged to a Schlenk tube equipped with a magnetic stirrer and sealed with a glass stopper. 35 mg (0.24 mmol) of Cu(I)Br, 46 mg (0.27 mmol) of PMDETA, and 35 μl (0.24 mmol) of EBB were added, and 3 freeze-pump-thaw cycles were conducted to degas the reaction mixture. After the last cycle the reactants were thawed to ambient temperature and placed on an oil bath at 80°C. Reactions were terminated by cooling the Schlenk tube in liquid nitrogen. The product was isolated by filtration (filter paper) and precipitation in methanol (M_n = 15,400 g/mol, PDI = 1.07).

10.3.4 Homopolymerization of 3FM and 17FM

Most homopolymerizations took place using the procedure described in the following, although in a few cases a larger volume of the monomer (2 or 5 ml) or a different monomer concentration (15 or 100 %) was utilized.

1.0 ml (7.0 mmol) of 3FM, 1.0 ml of xylene, 9.0 mg (0.06 mmol) of Cu(I)Br and 11 mg (0.06 mmol) of PMDETA were charged to a Schlenk tube equipped with a magnetic stirrer and sealed with a glass stopper. 9 μl (0.06 mmol) of EBB was added and 3 freeze-pump-thaw cycles were carried out. After the last cycle the reactants were thawed to ambient temperature and placed on an oil bath at 80°C. Reactions were terminated by cooling the Schlenk tube in liquid nitrogen. The product was isolated by precipitation in hexane. (M_n = 8,600 g/mol, PDI = 1.37).

Homopolymerizations of 17FM were conducted using the same protocol.

10.3.5 Polymerization of 3FM using PEG-macroinitiators

The polymerization of 3FM from a PEG-based macroinitiator was conducted in the following manner:

1 ml (7 mmol) of 3FM, 1 ml of xylene, 17 mg (0.12 mmol) of Cu(I)Br and 135 mg (0.06 mmol) of PEG2000-macroinitiator were placed in a Schlenk tube equipped with a magnetic stirrer and sealed with a glass stopper. The reaction mixture was stirred at a slightly elevated temperature (up to 40 °C) until the macroinitiator was dissolved. 35 μl (0.22 mmol) of n-Pr-1 was added, 5 freeze-pump-thaw cycles were conducted, the reactants were thawed to ambient temperature and placed on an oil bath at 80 °C. Reactions were terminated by cooling the Schlenk tube in liquid nitrogen. Products were purified by precipitation in hexane from THF. (M_n = 29,900, PDI = 1.39).

10.3.6 Polymerization of 3FM for SPME Analysis

A typical polymerization was performed as follows:

3.0 ml (21 mmol) of 3FM, 1.5 ml (12 mmol) of TFT and 3.0 ml of xylene were charged to a Schlenk tube equipped with a magnetic stirrer and sealed with a rubber septum. 10 mg (0.07 mmol) of Cu(I)Br, 25 μl (0.16 mmol) of n-Pr-1 and 11 μl (0.07 mmol) of EBB were added, and 5 freeze-pump-thaw cycles were performed. After the last cycle the reactants were thawed to ambient temperature and placed on an oil bath at the reaction temperature (70-110 °C). Reactions proceeded under inert conditions. Samples ($\sim$ 200 μl) were withdrawn by syringe under nitrogen at regular intervals, dissolved in xylene and stored in the freezer (-20 °C) until analysis. Samples were brought to ambient temperature before analysis by SPME. The final product was purified by precipitation in hexane from THF and characterized by ^{1}H NMR and SEC. (M_n = 32,300, PDI = 1.39).

10.3.7 Homopolymerization of 8FM

5 ml (24 mmol) of 8FM and 5 ml of toluene were charged to a Schlenk tube equipped with a magnetic stirrer and sealed with a rubber septum. 69 mg (0.48 mmol) of Cu(I)Br and 70 μl (0.48 mmol) of EBB were added, and 5 freeze-pump-thaw cycles were carried out. The reaction mixture was thawed to ambient temperature, 150 μl (0.96 mmol) of degassed n-Pr-1 was added and the reaction was conducted at 80 °C for 6 hrs. Samples were withdrawn by syringe under nitrogen at regular intervals for analysis by ^{1}H NMR and SEC. Catalyst was removed on a column of activated neutral Al_2O_3 using DCM as solvent. The product was recovered as a

white solid after removal of solvent in vacuo.

10.3.8 Polymerization of 3FM with HMTETA (Chapter 5)

5 ml (35 mmol) of 3FM and 5 ml of toluene were charged to a Schlenk tube equipped with a magnetic stirrer and sealed with a rubber septum. 42 mg (0.29 mmol) of Cu(I)Br and 80 μl (0.29 mmol) of HMTETA were added, and 5 freeze-pump-thaw cycles were carried out. The reaction mixture was thawed to ambient temperature, 45 μl (0.31 mmol) of degassed EBB was added and the reaction proceeded at 90 °C for 160 min. Samples were withdrawn by syringe under nitrogen at regular intervals for analysis by ^{1}H NMR and SEC. The product was precipitated in water from methylenechloride and recovered by filtration. (M_n = 8500, PDI = 1.37).

10.3.9 Polymerization of MEA with n-Pr-1

5 ml (39 mmol) of MEA and 5 ml of toluene were charged to a Schlenk tube equipped with a magnetic stirrer and sealed with a rubber septum. 39 mg (0.27 mmol) of Cu(I)Br and 40 μl (0.27 mmol) of EBB were added, and 5 freeze-pump-thaw cycles were carried out. The reaction mixture was thawed to ambient temperature, 80 μl (0.51 mmol) of degassed n-Pr-1 was added and the reaction was run at 90 °C for 9 hrs. Samples were withdrawn by syringe under nitrogen at regular intervals for analysis by ^{1}H NMR and SEC. Catalyst was removed on a column of activated neutral Al_2O_3 using ethyl acetate as eluent. The product was recovered as a light yellow highly viscous substance after removal of solvents in vacuo. (M_n = 7500, PDI = 1.23).

10.3.10 Polymerization of MEA with HMTETA

5 ml (39 mmol) of MEA and 5 ml of toluene were charged to a Schlenk tube equipped with a magnetic stirrer and sealed with a rubber septum. 37 mg (0.26 mmol) of Cu(I)Br and 70 μl (0.26 mmol) of HMTETA were added, and 5 freeze-pump-thaw cycles were carried out. The reaction mixture was thawed to ambient temperature, 40 μl (0.27 mmol) of degassed EBB was added and the reaction was run at 90 °C for 5 hrs. Samples were withdrawn by syringe under nitrogen at regular intervals for analysis by ^{1}H NMR and SEC. Catalyst was removed on a column of activated neutral Al_2O_3 using ethyl acetate as eluent and precipitated directly in petrol ether. The product was recovered as a light yellow highly viscous substance by filtration. (M_n = 9200, PDI = 1.22).

10.3.11 Copolymerization of MMA and MEA

3.0 ml (28 mmol) of MMA and 3 ml of toluene were charged to a Schlenk tube equipped with a magnetic stirrer and sealed with a rubber septum. 40 mg (0.28 mmol) of Cu(I)Br, and 75 μl (0.28 mmol) of HMTETA were added, and 3 freeze-pump-thaw cycles were carried out. Reactants were thawed to ambient temperature, 40 μl (0.27 mmol) of degassed EBB was added and reaction was allowed to proceed at 90 °C. 5 ml (39 mmol) of degassed MEA (50 % V/V solution in toluene) was cannulated into the reaction after 1.5 hrs. Samples were withdrawn by syringe under nitrogen at regular intervals for analysis by ^{1}H NMR and SEC. Catalyst was removed on a column of activated neutral Al_2O_3 and the product was recovered as a white, highly viscous substance after removal of solvent in vacuo. (M_n = 15,100, PDI = 1.41).

References

[1] N. Wisniewski and M. Reichert. Methods for reducing biosensor membrane fouling. *Colloids Surf. B: Biointerfaces*, 18:197–219, 2000.

[2] R.D. Johnson and L.G. Bachas. Ionophore-based ion-selective potentiometric and optical sensors. *Anal. Bioanal. Chem.*, 376:328–341, 2003.

[3] V.G. Gavalas, M.J. Berrocal, and L.G. Bachas. Enhancing the blood compatibility of ion-selective electrodes. *Anal. Bioanal. Chem.*, 384:65–72, 2006.

[4] K. Li, P. Wu, and Z. Han. Preparation and surface properties of fluorine-containing diblock copolymers. *Polymer*, 43:4079–4086, 2002.

[5] F. Wang, H. Li, Z.B. Zhang, C.P. Hu, and S.S. Wu. Synthesis and surface properties of fluorinated block copolymers containing sulfonic groups. *J. Polym. Sci. Part A:Polym. Chem.*, 42:4809–4818, 2004.

[6] S. Villarroya, J. Zhou, C.J. Duxbury, A. Heise, and S.M. Howdle. Synthesis of semifluorinated block copolymers containing poly(ϵ-caprolactone) by the combination of ATRP and enzymatic ROP in $scCO_2$. *Macromolecules*, 39:633–640, 2006.

[7] M. Eberhardt and P. Théato. RAFT polymerization of pentafluorophenyl methacrylate: Preparation of reactive linear diblock copolymer. *Macromol. Rapid Commun.*, 26:1488–1493, 2005.

[8] K.T. Lim, M.Y. Lee, M.J. Moon, G.D. Lee, S.S. Hong, J.L. Dickson, and K.P. Johnston. Synthesis of fluorine-containing block copolymers via ATRP 2. Synthesis and characterization of semi-fluorinated di- and triblock copolymers. *Polymer*, 43:7043–7049, 2002.

[9] H. Hussain, H. Budde, S. Höring, K. Busse, and J. Kressler. Synthesis and characterization of poly(ethylene oxide) and poly(perfluorohexylethyl methacrylate) containing triblock copolymers. *Macromol. Chem. Phys.*, 203:2103–2112, 2002.

[10] Y. Inoue, J. Watanabe, M. Takai, S.I. Yusa, and K. Ishihara. Synthesis of sequence-controlled copolymers from extremely polar and apolar monomers by living radical polymerization and their phase-separated structures. *J. Polym. Sci. Part A:Polym. Chem.*, 43:6073–6083, 2005.

[11] V. Roche, F. Vacandio, D. Bertin, and Y. Massiani. Corrosion performance of lamellae nanostructured fluorinated organic coating applied on steel. *J. Electroceram.*, 16:41–47, 2006.

[12] D. Plackett, K. Jankova, H. Egsgaard, and S. Hvilsted. Modification of jute fibers with polystyrene via atom transfer radical polymerization. *Biomacromolecules*, 6:2474–2484, 2005.

[13] L. Andruzzi, A. Hexemer, X. Li, C.K. Ober, E.J. Kramer, G. Galli, E. Chiellini, and D.A. Fischer. Control of surface properties using fluorinated polymer brushes produced by surface-initiated controlled radical polymerization. *Langmuir*, 20:10498–10506, 2004.

[14] A.M. Granville, S.G. Boyes, B. Akgun, M.D. Foster, and W.J. Brittain. Synthesis and characterization of stimuli-responsive semifluorinated polymer brushes prepared by atom transfer radical polymerization. *Macromolecules*, 37:2790–2796, 2004.

[15] A.M. Granville and W.J. Brittain. Stimuli-responsive semifluorinated polymer brushes on porous silica substrate. *Macromol. Rapid Commun.*, 25:1298–1302, 2004.

[16] R. Chen, W. Feng, S. Zhu, G. Botton, B. Ong, and Y. Wu. Surface-initiated atom transfer radical polymerization grafting of poly(2,2,2-trifluoroethyl methacrylate) from flat silicon wafer surfaces. *J. Polym. Sci. Part A:Polym. Chem.*, 44:1252–1262, 2006.

[17] L. Ying, W.H. Yu, E.T. Kang, and K.G. Neoh. Functional and surface-active membranes from poly(vinylidene fluoride)-*graft*-poly(acrylic acid) prepared via RAFT-mediated graft copolymerization. *Langmuir*, 20:603–6040, 2004.

[18] S. Holmberg, P. Holmlund, C.E. Wilén, T. Kallio, G. Sundholm, and F. Sundholm. Synthesis of proton-conducting membranes by the utilization of preirradiation grafting and atom transfer radical polymerization techniques. *J. Polym. Sci. Part A:Polym. Chem.*, 40:591–600, 2002.

[19] Z.Q. Shi and S. Holdcroft. Synthesis and proton conductivity of partially sulfonated poly([vinylidene difluoride-*co*-hexafluoropropylene]-*b*-styrene) block copolymers. *Macromolecules*, 38:4193–4201, 2005.

[20] S. Perrier, S.G. Jackson, D.M. Haddleton, B. Ameduri, and B. Boutevin. Preparation of fluorinated methacrylic copolymers by copper mediated living radical polymerization. *Tetrahedron*, 58:4053–4059, 2002.

[21] B.S. Shemper and L.J. Mathias. Synthesis and characterization of statistical and block fluorinated copolymers with linear and star-like architectures via ATRP. *Eur. Polym. J.*, 40:651–665, 2004.

[22] G. Lu, S. Zhang, and X. Huang. Synthesis and characterization of a novel ABA triblock copolymer via 4,4 '-bis(trifluorovinyloxy)biphenyl and methyl methacrylate. *J. Polym. Sci. Part A:Polym. Chem.*, 44:5438–5444, 2006.

[23] M. Kato, M. Kamigaito, M. Sawamoto, and T. Higashimura. Polymerization of methyl methacrylate with the carbon tetrachloride/dichlorotris(triphenylphosphine)ruthenium(II)/methylaluminium bis(2,6-di-*tert*-butylphenoxide) initiating system: Possibility of living radical polymerization. *Macromolecules*, 28:1721–1723, 1995.

[24] J.S. Wang and K. Matyjaszewski. Controlled/"living" radical polymerization - atom transfer radical polymerization in the presence of transition-metal complexes. *J. Am. Chem. Soc.*, 117:5614–5615, 1995.

[25] T.R. Darling, T.P. Davis, M. Fryd, A.A. Gridnev, D.M. Haddleton, S.D. Ittel, R.R. Matheson Jr., G. Moad, and E. Rizzardo. Living polymerization: Rationale for uniform terminology. *J. Polym. Sci. Part A:Polym. Chem.*, 38:1706–1708, 2000.

[26] M. Szwarc. Living polymers. Their discovery, characterization, and properties. *J. Polym. Sci. Part A:Polym. Chem.*, 36:ix–xv, 1998.

[27] M. Szwarc, M. Levy, and R. Milkovich. Polymerization initiated by electron transfer to monomer. A new method of formation of block copolymers. *J. Am. Chem. Soc.*, 78:2656–2657, 1956.

[28] N. Hadjichristidis, H. Iatrou, S. Pispas, and M. Pitsikalis. Anionic polymerization: High vacuum techniques. *J. Polym. Sci. Part A:Polym. Chem.*, 38:3211–3234, 2000.

[29] M. Miyamoto, M. Sawamoto, and T. Higashimura. Living polymerization of isobutyl vinyl ether with the hydrogen iodide/iodine initiating system. *Macromolecules*, 17:265–268, 1984.

[30] Joseph P. Kennedy and Béla Iván. *Carbocationic Macromolecular Engineering*. Hanser Publishers, 1992.

[31] M.K. Georges, R.P.N. Veregin, P.M. Kazmaier, and G.K. Hamer. Narrow molecular weight resins by a free-radical polymerization process. *Macromolecules*, 26:2987–2988, 1993.

[32] G. Moad, E. Rizzardo, and D.H. Solomon. Selectivity of the reaction of free radicals with styrene. *Macromolecules*, 15:909–914, 1982.

[33] C.J. Hawker, A.W. Bosman, and E. Harth. New polymer synthesis by nitroxide mediated living radical polymerizations. *Chem. Rev.*, 101:3661–3688, 2001.

[34] O. Lagrille, N.R. Cameron, P.A. Lovell, R. Blanchard, A.E. Goeta, and R. Koch. Novel acyclic nitroxides for nitroxide-mediated polymerization: Kinetic, electron paramagnetic resonance spectroscopy, X-ray diffraction, and molecular modeling investigations. *J. Polym. Sci. Part A:Polym. Chem.*, 44:1926–1940, 2006.

[35] K. Matyjaszewski. Transition metal catalysis in controlled radical polymerization: Atom transfer radical polymerization. *Chem. Eur. J.*, 11:3095–3102, 1999.

[36] J. Chiefari, Y. K. (Bill) Chong, F. Ercole, J. Krstina, J. Jeffery, T.P.T. Le, R.T.A. Mayadunne, G.F. Meijs, C.L. Moad, G. Moad, E. Rizzardo, and S.H. Thang. Living free-radical polymerization by reversible addition-fragmentation chain transfer: The RAFT process. *Macromolecules*, 31:5559–5562, 1998.

[37] G. Moad, R.T.A. Mayadunne, E. Rizzardo, M. Skidmore, and S.H. Thang. Synthesis of novel architectures by radical polymerization with reversible addition fragmentation chain transfer (RAFT polymerization). *Macromol. Symp.*, 192:1–12, 2003.

[38] K. Matyjaszewski and J. Xia. Atom transfer radical polymerization. *Chem. Rev.*, 101:2921–2990, 2001.

[39] Y. Chen, D. Liu, Q. Deng, X. He, and X. Wang. Atom transfer radical polymerization directly from poly(vinylidene fluoride): Surface and antifouling properties. *J. Polym. Sci. Part A:Polym. Chem.*, 44:3434–3443, 2006.

[40] G. David, C. Boyer, J. Tonnar, B. Ameduri, P. Lacroix-Desmazes, and B. Boutevin. Use of iodocompounds in radical polymerization. *Chem. Rev.*, 106:3936–3962, 2006.

[41] M. Kamigaito, T. Ando, and M. Sawamoto. Metal-catalyzed living radical polymerization. *Chem. Rev.*, 101:3689–3745, 2001.

[42] E.J. Ashford, V. Naldi, R. O'Dell, N.C. Billingham, and S.P. Armes. First example of the atom transfer radical polymerization of an acidic monomer: direct synthesis of methacrylic acid copolymers in aqueous media. *Chem. Commun.*, 999:1285–1286, 1999.

[43] Y. Shen, H. Tang, and S. Ding. Catalyst separation in atom transfer radical polymerization. *Prog. Polym. Sci.*, 29:1053–1078, 2004.

[44] D. Betts, T. Johnson, C. Anderson, and J.M. DeSimone. Controlled radical polymerization methods for the synthesis of non-ionic surfactants for CO_2. *Polymer Preprints*, 38:760–761, 1997.

[45] D.E. Betts, T. Johnson, D. LeRoux, and J.M. DeSimone. Controlled radical polymerization methods for the synthesis of nonionic surfactants for CO_2. In K. Matyjaszewski, editor, *New Materials by Controlled Radical Polymerization, ACS Symposion Series, vol. 685; American Chemical Society; Washington, DC*, pages 418–432. 1998.

[46] J. Xia, T. Johnson, S.G. Gaynor, K. Matyjaszewski, and J. DeSimone. Atom transfer radical polymerization in supercritical carbon dioxide. *Macromolecules*, 32:4802–4805, 1999.

[47] Y. Yang, Z. Wang, Y. Gao, T. Liu, C. Hu, and Q. Dong. Synthesis of fluorinated diblock copolymer by ATRP and its application of PAVAc polymerization in scCO_2. *J. Appl. Polym. Sci.*, 102:1146–1151, 2006.

[48] S. Perrier, S.G. Jackson, D.M. Haddleton, B. Améduri, and B. Boutevin. Preparation of fluorinated copolymers by copper-mediated living radical polymerization. *Macromolecules*, 36:9042–9049, 2003.

[49] H. Hussain, K. Busse, and J. Kressler. Poly(ethylene oxide)- and poly(perfluorohexylethyl methacrylate)-containing amphiphilic block copolymers: Association properties in aqueous solution. *Macromol. Chem. Phys.*, 204:936–946, 2003.

[50] Z. Ma and P. Lacroix-Desmazes. Synthesis of hydrophilic/CO_2-philic poly(ethylene oxide)-*b*-poly(1,1,2,2-tetrahydroperfluorodecyl acrylate) block copolymers via controlled/living radical polymerizations and their properties in liquid and supercritical CO_2. *J. Polym. Sci. Part A:Polym. Chem.*, 42:2405–2415, 2004.

[51] Z.B. Zhang, S.K. Ying, and Z.Q. Shi. Synthesis of fluorine-containing block copolymers via ATRP 2. Synthesis and characterization of semi-fluorinated di- and triblock copolymers. *Polymer*, 40:5439–5444, 1999.

[52] Z.B. Zhang, S.K. Ying, Q.H. Hu, and X.D. Xu. Semifluorinated ABA triblockcopolymers: Synthesis, characterization, and amphiphilic properties. *J. Appl. Polym. Sci.*, 83:2625–2633, 2002.

[53] H. Li, Z.B. Zhang, C.P. Hu, S.K. Ying, S.S. Su, and X.D. Xu. Synthesis and characterization of fluorinated block copolymers containing carboxylic or sulfonic groups. *React. Func. Polym.*, 56:189–197, 2003.

[54] K. Jankova and S. Hvilsted. Preparation of poly(2,3,4,5,6-pentafluorostyrene) and block copolymers with styrene by ATRP. *Macromolecules*, 36:1753–1758, 2003.

[55] S. Borkar, K. Jankova, H. W. Siesler, and S. Hvilsted. New highly fluorinated styrene-based materials with low surface energy prepared by ATRP. *Macromolecules*, 37:788–794, 2004.

[56] K. Jankova, P. Jannasch, and S. Hvilsted. Ion conducting solid polymer electrolytes based on polypentafluorostyrene-*b*-polyether-*b*-polypentafluorostyrene prepared by atom transfer radical polymerization. *J. Mater. Chem.*, 14:2902–2908, 2004.

[57] K. Jankova and S. Hvilsted. Novel fluorinated block copolymer achitectures fuelled by atom transfer radical polymerization. *J. Fluor. Chem.*, 126:241–250, 2005.

[58] J. Queffelec, S.G. Gaynor, and K. Matyjaszewski. Optimization of atom transfer radical polymerization using Cu(I)/tris(2-(dimethylamino)ethyl)amine as a catalyst. *Macromolecules*, 33:8629–8639, 2000.

[59] M. Ciampolini and N. Nardi. Five-coordinated high-spin complexes of bivalent cobalt, nickel, and copper with tris(2-dimethylaminoethyl)amine. *Inorg. Chem.*, 5:41–44, 1966.

[60] J. Xia, S.G. Gaynor, and K. Matyjaszewski. Controlled/"living" radical polymerization. Atom transfer radical polymerization of acrylates at ambient temperature. *Macromolecules*, 31:5958–5959, 1998.

[61] D.M. Haddleton, M.C. Crossman, B.H. Dana, D.J. Duncalf, A.M. Heming, D. Kukulj, and A.J. Shooter. Atom transfer polymerization of methyl methacrylate mediated by alkylpyridylmethanimine type ligands, copper(I) bromide, and alkyl halides in hydrocarbon solution. *Macromolecules*, 32:2110–2119, 1999.

[62] J. Qiu and K. Matyjaszewski. Polymerization of substituted styrenes by atom transfer radical polymerization. *Macromolecules*, 30:5643–5648, 1997.

[63] S. Hvilsted, S. Borkar, H.W. Siesler, and K. Jankova. Novel fluorinated polymer materials based on 2,3,5,6-tetrafluoro-4-methoxystyrene. In K. Matyjaszewski, editor, *Advances in Controlled/Living Radical Polymerization, ACS Symposion Series, vol. 854; American Chemical Society; Washington, DC*, pages 936–946. 2003.

[64] K. Jankova, X. Chen, J. Kops, and W. Batsberg. Synthesis of amphiphilic PS-*b*-PEG-*b*-PS by atom transfer radical polymerization. *Macromolecules*, 31:538–541, 1998.

[65] M.V. Juhl. *Master Thesis: Preparation of block copolymers with amphiphilic properties.* Technical University of Denmark, DK, 2004.

[66] S. Perrier and D.M. Haddleton. Initiating efficiency of poly(ethylene glycol)-based initiators for transition metal mediated living radical polymerization. *Eur. Polym. J.*, 40:2277–2286, 2004.

[67] R. Belardi and J. Pawliszyn. The application of chemically modified fused silica fibers in the extraction of organics from water matrix samples and their rapid transfer to capillary columns. *Water Pollut. Res. J. Can.*, 24:179–191, 1989.

[68] D.M. Haddleton, D. Kukulj, D.J. Duncalf, A.M. Heming, and A.J. Shooter. Low-temperature living "radical" polymerization (atom transfer polymerization) of methyl methacrylate mediated by copper(I) *N*-alkyl-2-pyridylmethanimine complexes. *Macromolecules*, 31:5201–5205, 1998.

[69] F. Lecolley. *Ph.D. Thesis: New polymers from living radical polymerisation for biological applications. Chapter 3: Synthesis and characterization of N-succinimidyl ester functionalized poly(mPEGMA).* University of Warwick, UK, 2004.

[70] M. Bednarek, K. Jankova, and S. Hvilsted. Novel polymers based on atom transfer radical polymerization of 2-methoxyethyl acrylate. *J. Polym. Sci. Part A:Polym. Chem.*, 45:333–340, 2007.

[71] M. Destarac, K. Matyjaszewski, E. Silverman, B. Ameduri, and B. Boutevin. Atom transfer radical polymerization initiated with vinylidene fluoride telomers. *Macromolecules*, 33:4613–4615, 2000.

[72] Z.Q. Shi and S. Holdcroft. Synthesis of block copolymers possessing fluoropolymer and non-fluoropolymer segments by radical polymerization. *Macromolecules*, 37:2084–2089, 2004.

[73] J.F. Hester, P. Banerjee, Y.W. Won, A. Akthakul, M.H. Acar, and A.M. Mayes. ATRP of amphiphilic graft copolymers based on PVDF and their use as membrane additives. *Macromolecules*, 35:7652–7661, 2002.

[74] J.G. Wang and C.K. Ober. Self-organizing materials with low surface energy: The synthesis and solid-state properties of semifluorinated side-chain ionenes. *Macromolecules*, 30:7560–7567, 1997.

[75] G. Widawski, M. Rawiso, and B. François. Self-organized honeycomb morphology of star-polymer polystyrene films. *Nature*, 369:387–389, 1994.

[76] O. Pitois and B. François. Crystallization of condensation droplets on a liquid surface. *Colloid Polym. Sci.*, 277:574–578, 1999.

[77] M.H. Stenzel, C. Barner-Kowollik, and T.P. Davis. Formation of honeycomb-structured, porous films via breath figures with different polymer architectures. *J. Polym. Sci. Part A:Polym. Chem.*, 44:2363–2375, 2006.

[78] H. Yabu, M. Takebayashi, M. Tanaka, and M. Shimomura. Superhydrophobic and lipophobic properties of self-organized honeycomb and pincushion structures. *Langmuir*, 21:3235–3237, 2005.

Appendices

Appendix 1

Fluoropolymer Materials and Architectures Prepared by Controlled Radical Polymerizations

Available online at www.sciencedirect.com
ScienceDirect
European Polymer Journal 43 (2007) 255–293
EUROPEAN POLYMER JOURNAL
www.elsevier.com/locate/europolj

Review article

Fluoropolymer materials and architectures prepared by controlled radical polymerizations

Natanya M.L. Hansen, Katja Jankova, Søren Hvilsted *

Danish Polymer Centre, Department of Chemical Engineering, Technical University of Denmark, Building 423, DK-2800 Kgs. Lyngby, Denmark

Received 31 October 2006; accepted 8 November 2006
Available online 4 January 2007

Abstract

This review initially summarizes the mechanisms, merits and limitations of the three controlled radical polymerizations: nitroxide mediated polymerization (NMP), atom transfer radical polymerization (ATRP) or metal catalyzed living radical polymerization, and reversible addition–fragmentation chain transfer (RAFT) polymerization. This is followed by two

Abbreviations: AA, acrylic acid; AFM, atomic force microscopy; AIBN, azo-bis-isobutyronitrile; ATRP, atom transfer radical polymerization; ATR-SCVCP, atom transfer radical self-condensing vinyl copolymerization; BMA, *n*-butyl methacrylate; bipy, 2,2′-bipyridine; BIEA, 2-(2-bromoisobutyryloxy)ethyl acrylate; BMS, *p*-bromomethylstyrene; CA, contact angle; CL, ε-caprolactone; CMS, *p*-chloromethylstyrene; CRP, controlled radical polymerization; CTA1, cumyldithiobenzoate; CTA2, cyanopentanoic acid dithiobenzoate; DBX, α,α′-dibromo-*p*-xylene; DEA, *N*,*N*-diethylacrylamide; DEPN, *N*-*tert*-butyl-1-diethylphosphono-2,2-dimethylpropyl nitroxide; di-penta, dipentaerythritol; DLS, dynamic light scattering; DMAEMA, 2-dimethylaminoethyl methacrylate; DMAP, 4-(dimethylamino)pyridine; DMSO, dimethyl sulfoxide; DMF, dimethyl formamide; DP, degree of polymerization; DSC, differential scanning calorimetry; DVB, divinylbenzene; EA, ethyl acrylate; EBB, ethyl 2-bromoisobutyrate; EGMAFO, ethylene glycol monomethacrylate monoperfluorooctanoate; FABu, butyl α-fluoroacrylate; FAEM, perfluoroalkyl acrylate; FDA, 1,1,2,2-tetrahydroperfluorodecyl acrylate; FEMA, 1H,2H,2H-heptadecafluorodecyl methacrylate; FPI, fluorinated polyimide; FMA, pentafluorophenyl methacrylate; F-MADIX, ethyl-2-(*O*-trifluoroethylxanthyl)propionate; FNEMA, 2-[(perfluorononenyl)oxy] ethyl methacrylate; FOA, 1H,1H-perfluorooctyl acrylate; FOMA, 1H,1H-perfluorooctyl methacrylate; FS, 2,3,4,5,6-pentafluorostyrene; FS_1, (1H,1H-perfluoro-2,5-dimethyl-3,6-dioxanonan-1-yl)styrene; FS_2, (1H,1H,2H,2H-perfluorooctan-1-yl)styrene; GMA, glycidyl methacrylate; HEA, 2-hydroxyethyl acrylate; HEMA, 2-hydroxyethyl methacrylate; HFP, hexafluoropropene; MA, methyl acrylate; MI, macroinitator; MF, microfiltration; MMA, methyl methacrylate; MPC, 2-methacryloyloxyethyl phosphorylcholine; MPEG, monomethoxy poly(ethylene glycol); NAM, *N*-acryloylmorpholine; NaPSS, poly (sodium 4-styrenesulfonate); NaSS, sodium 4-styrenesulfonate; NMR, nuclear magnetic resonance spectroscopy; NIPAAM, *N*-isopropylacrylamide; NMP, nitroxide mediated polymerization; PDI, polydispersity index; PDMS, polydimethylsiloxane; PEG, poly(ethylene glycol); PEGMA, poly(ethylene glycol) methyl ether methacrylate; penta$(TEG)_4$, tetraethyleneglycol extended pentaerytrithol; PFA, 2,2,3,3,3-pentafluoropropyl acrylate; PhEBr, 1-phenylethyl bromide; PMDETA, *N*,*N*,*N*,*N*′,*N*″-pentamethyldiethylenetriamine; PPGM, poly(propylene glycol) methacrylate; PS, polystyrene; PTFE, poly(tetrafluoroethylene); RAFT, reversible addition–fragmentation transfer; $scCO_2$, supercritical carbon dioxide; SEM, scanning electron microscopy; St, styrene; *t*-BA, *tert*-butyl acrylate; TEA, triethylamine; TEM, transmission electron microscopy; TEMPO, 2,2,6,6-tetramethyl-1-piperidinyloxy; TFEMA, 2,2,2-trifluoroethylene methacrylate; TFT, α,α,α-trifluorotoluene; TF(F_5)S, 2,3,5,6-tetrafluoro-4-(2,2,3,3,3-pentafluoropropoxy)styrene; TF(F_{15})S, poly(2,3,5,6-tetrafluoro-4-(2,2,3,3,4,4,5,5,6,6,7,7,8,8,8-pentadecafluorooctaoxy)styrene); TFMS, 2,3,5,6-tetrafluoro-4-methoxystyrene; T_g, glass transition temperature; THF, tetrahydrofuran; THFOMA, 1H,1H,2H,2H-tetrahydroperfluorooctyl methacrylate; *t*-BMA, *tert*-butyl methacrylate; VDF, vinylidene fluoride; XPS, X-ray photoelectron spectroscopy.

* Corresponding author. Tel.: +45 45 252 965.
E-mail address: sh@kt.dtu.dk (S. Hvilsted).

doi:10.1016/j.eurpolymj.2006.11.016

parts, one dealing with homo- and copolymerizations of fluorinated methacrylates and acrylates, and a second where fluorinated styrenes, alone or in combination with other monomers, are the main issues. In these parts, initiators (including multifunctional and macroinitiators), ligands and other reaction conditions as well as some kinetics and conversions are discussed. Numerous possibilities for preparation of a variety of different block copolymers where one or more blocks are fluorinated are devoted particular attention. The advantageous properties and functionalities that can be obtained from these novel fluorinated materials and architectures are especially emphasized. Thus, various amphiphilic, biocompatible or low energy materials, fluorinated nanoparticles and nanoporous films/membranes as well as materials for submicron and nanolevel electronics have been fabricated. In addition, the possible fluorination of various surfaces through surface initiation is highlighted. A final part deals with the use of fluorine containing initiators and macroinitiators, and the applications on the novel materials derived thereof.

Keywords: Fluorinated (co)polymers; Fluorinated monomers; Surface initiated polymerization; Amphiphilic polymers; Biomaterials; Characterizations

Contents

1. Introduction

Fluorinated polymers have always attracted significant attention due to high thermal stability, superb chemical resistance, excellent mechanical properties at extreme temperatures, superior weatherability, oil and water repellence and low flammability in addition to low refractive index. The development of fluoropolymers began with the invention of polytetrafluoroethylene (PTFE) in 1938 by Dr. Roy Plunkett of DuPont Company, continuing in 1992 when a soluble perfluoropolymer (Teflon® AF) was invented, while fluoroplastics polymerized in supercritical carbon dioxide were introduced in 2002. Besides these commercially important examples many other routes [1] toward fluorinated materials have been researched intensively by both academic and industrial teams. These efforts have led to the emergence of various functional materials with notable properties: biomaterials, surfactants, lubricants, insulators, ion conducting materials (e.g. for Li-ion batteries) and proton conducting materials (e.g. for membranes for fuel cells). A number of materials such as paints and coatings as well as materials for the optic and electronic industries have additionally been developed.

The outstanding contribution in the past decade of the controlled radical polymerization (CRP) methods [2] allowed for development of advanced well-defined copolymers with various architectures (block, star, dendritic, alternating or graft) having predictable molecular weights and low molecular weight distributions. These techniques also permit advanced fluorinated materials to be synthesized. The newest review involving fluorinated organic compounds in controlled polymerizations [3] dates from 2002, followed by a comprehensive book [4] from 2004 on well-architectured fluoropolymers, both of these being from the CNRS group in Montpellier, France. Since then a lot of new contributions have emerged, which we propose to cover in this review. Extensive research engaging the three main controlled radical polymerisation techniques, namely atom transfer radical polymerisation (ATRP), nitroxide-mediated radical polymerization (NMP) and reversible addition–fragmentation chain-transfer (RAFT), have furnished various fluorinated materials and architectures, where ATRP has been the dominating technique, as will be seen on the following pages. In order to summarize the achievements on the synthesis of well-defined fluorinated copolymers using the three above-mentioned techniques, and being involved in ATRP of fluoromonomers, we found the time opportune to make this review. After a short introduction to each of the used methods: NMP, ATRP and RAFT, the synthesis of various fluorinated materials and architectures is subdivided by polymer type, i.e. poly(meth)acrylates, polystyrenes, other polymers and fluorinated initiators. The latter are included, since they convey characteristics of fluorinated polymers to the non-fluorinated (co)polymers for which they are used. Fluoromonomers can be polymerized by CRP methods in bulk or in solution in common solvents, which are often involved for the

copolymerisation with non-fluorinated monomers. Specific fluorinated solvents, ionic liquids and supercritical CO_2 have also been employed as reaction media. Sometimes also another part of the catalytic system (e.g. ligands in ATRP) is preferred to be fluorinated. CRP methods generally rely on a reversible activation–deactivation process between dormant and active polymer chains, and as the double bond of monomers containing fluorine is additionally activated by the electron withdrawing group, this sometimes leads to considerably higher rates of polymerisation compared to the non-fluorinated analogues. This in turn allows for the possibility of using either the macroinitiator method or the sequential monomer addition method for the synthesis of F-containing copolymers. In order to clarify the structures of the discussed monomer structures or the (co)polymer architectures, we have taken the liberty of redrawing and including many of the chemical structures in the review. We have also included an extensive list of abbreviations. However, in order to limit the list, abbreviations of all polymers are omitted, when the polymer abbreviation is simple P in combination with the relevant monomer abbreviation (e.g. only MMA not PMMA will be in the list).

1.1. Living/controlled polymerization

The definition of living polymerization is a polymerization reaction, where no unwanted side reactions such as transfer or termination take place, and where all polymer chains are initiated simultaneously. This means that the growing ends of the polymer chains are active indefinitely and that an ideally living system should yield polymers with polydispersities of 1.0. In reality no such reactions have been found, but some systems are not far from achieving this goal. For these reaction systems a number of terms have been used including "living", pseudo-living, quasi-living and living/controlled, which has led to confusion and frustration among researchers in the field [5]. We prefer the term controlled polymerization, which will be used to describe reactions that fulfil the following criteria:

- Kinetics are first order with respect to the monomer.
- Degree of polymerization is directly proportional to the initial monomer to initiator ratio.
- Narrow molecular weight distributions are obtained.
- After consumption of monomer the reaction can continue by addition of new monomer.

In free radical polymerization the active polymer chains can react with one another either by radical combination or by disproportionation, which can lead to broad molecular weight distributions, furthermore chain transfer often plays a disturbing role. For some applications a narrow molecular weight distribution in the polymer is necessary, which has led to the development of a number of techniques whereby control of the polymerization reaction is obtained, termed controlled radical polymerization reactions.

The strategy for eliminating undesirable termination reactions has been to ensure that only a fraction of the polymer in question is activated at a time, i.e. present as an active radical, while the majority of polymer chains are in a dormant/inactivated state. A dynamic equilibrium between the two states must exist in order for the growth of the polymer chains to be equal.

1.2. Nitroxide mediated polymerization

The first step toward a controlled polymerization reaction involving radicals was nitroxide mediated polymerization (NMP), which was undertaken in 1993 by Georges and coworkers [6], inspired by the work done by Moad and Rizzardo [7] on using nitroxides as radical trapping agents. Georges used the nitroxide, 2,2,6,6-tetramethyl-1-piperidinyloxy (TEMPO) to control the polymerization of styrene, where the reaction was initiated by a free radical initiator, benzoyl peroxide. During reaction the nitroxide efficiently end-capped the growing polymer chains by a reversible termination reaction ensuring equal growth of all chains, while suppressing termination reactions almost completely. Using alkoxyamines has proved to be a more efficient way to perform NMP, as these compounds are able to function as both initiator and end-capping group as outlined in Fig. 1, giving full control over the concentration of intiating radicals. Upon heating, the alkoxyamine is homolytically cleaved to the initiating radical $^{\cdot}R_3$ and the stabilized, persistent radical $^{\cdot}ONR_1R_2$ that are both only present for a short time period, ideally long enough for a monomer unit (M) to react with the initiating radical before recombination takes place.

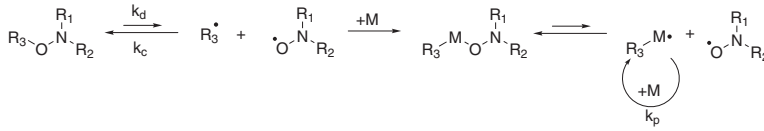

Fig. 1. Mechanism of nitroxide mediated polymerization utilizing an alkoxyamine as initiator and end-capping group [8].

1.2.1. Monomers

The TEMPO-type nitroxides (piperidine structure) have mainly been used for styrenic monomers, but new types of nitroxides have made the polymerization of acrylates, acrylamides, 1,3-dienes and acrylonitrile monomers by NMP possible. Different functional groups are tolerated in NMP such as amino, carboxylic acid and glycidyl [9].

1.2.2. Nitroxides

The nitroxides employed in NMP can either be used in combination with a free radical initiator (bicomponent system) or act as both initiator and rate controlling species (monocomponent system). Different nitroxides have been developed and used for NMP, many of which have proved to be far superior to the TEMPO type, giving better molecular weight distributions in addition to faster polymerizations. Polymerization of non-styrenic monomers by NMP was made possible with the development of second generation acyclic nitroxides such as 2,2,5-trimethyl-4-phenyl-3-azahexane nitroxide (TIPNO) (Fig. 2, **1**) and *N-tert*-butyl-1-diethylphosphono-2,2-dimethylpropyl nitroxide (DEPN) also called SG1 (Fig. 2, **2**). In some cases coordination between the oxygen and the side groups is believed to be the reason for the elevated reactivity, which is the case for nitroxide **3** (Fig. 2), where hydrogen bonding takes place with the hydroxyl group through a six-membered ring intermediate [10]. Other factors that influence the reactivity of the nitroxide (i.e. the equilibrium between dormant and active nitroxide species) are polarity as well as steric factors. Large substituents normally have a positive effect on the performance of the nitroxide although only to a certain extent, which was recently studied for nitroxide **4** (Fig. 2) and derivatives thereof [11].

1.2.3. Reaction conditions

Originally NMP reactions had to take place at high temperatures (>100 °C), which is best suited for bulk or solution polymerization. Seen from an industrial viewpoint NMP is an advantageous polymerization method, as one species can be used for both initiation and process control. Aqueous media is however preferred in the industry due to reduced costs and hazards, which has led to an increased effort to develop NMP in emulsion, miniemulsion, dispersion and suspension. Nitroxides that can be used in mini-emulsion have been developed and with these compounds reactions can be run at temperatures under 100 °C and under non-pressurized conditions [15]. Recently emulsion polymerization by NMP has also been undertaken among others by Charleux et al. [16].

1.2.4. Limitations of NMP

The main limitation of NMP is the range of potential monomers, as the method works best for styrenes and acrylates. Methacrylates can not be homopolymerized by NMP, due to the competing

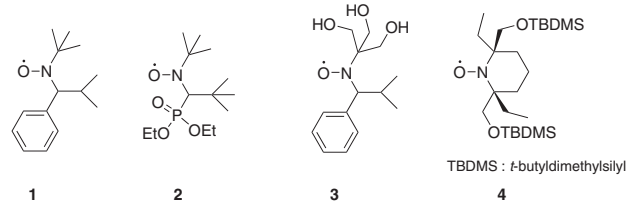

Fig. 2. Examples of alkoxyamines used for NMP [10,12–14].

dispropotionation reaction, where abstraction of hydrogen from the α-methyl group leads to an alkene on the polymer chain end. Methyl methacrylate has however recently been polymerized in a controlled manner [17] by addition of low concentrations of styrene (4.4%) using DEPN.

1.2.5. Copolymers by NMP

Block copolymers can be synthesized by NMP and the alkoxyamine group can withstand reaction conditions of other controlled radical polymerization methods such as ATRP and RAFT, making it possible to synthesize polymers by combining NMP with other reaction pathways. Different functionalities can also be incorporated in the nitroxide to give endfunctionalized polymers. NMP has been used for design of complex architectures such as star, graft and dendritic polymers.

1.3. Atom transfer radical polymerization

Reactions, where metal catalysts were utilized in combination with aromatic ligands yielding well-controlled structures and narrow molecular weight distributions, were concurrently carried out in 1995 by research groups headed by Matyjaszewski [18] and Sawamoto [19]. The term Atom Transfer Radical Polymerization was coined by Matyjaszewski, whereas Sawamoto's groups termed this type of reaction Metal Catalyzed Living Radical Polymerization. The mechanism involves the transfer of a halogen atom from the dormant polymer chain to a metal catalyst yielding an active chain end (a radical), hence the term Atom Transfer Radical Polymerization (ATRP). Reaction is outlined in Fig. 3 and takes place through a reversible redox reaction involving the transition metal catalyst (Mt), which is oxidized as the polymer is converted from the dormant state (P–X) to the active species (P•) through the transfer of the halogen (X). The metal catalyst is bound in a complex with a multidentate ligand (L), which assists in binding the halogen. In the equilibrium the deactivation reaction is kinetically favored ($k_d \gg k_a$) thus rendering only a small concentration of active radical species present at a given time. Ideally, this eliminates the possibility of two activated polymer chain ends encountering to give termination, while in practice termination does occur.

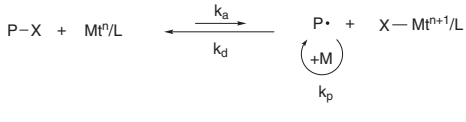

Fig. 3. Mechanism of atom transfer radical polymerization [20].

1.3.1. Monomers

ATRP can be carried out with monomers that have a group, which can stabilize the propagating radical. The most common monomers include styrene, (meth)acrylates, (meth)acrylamides and acrylonitrile. Monomers with highly labile or reactive groups have been polymerized by ATRP including functionalities such as epoxides, lactones, and dienes. For each monomer the rates of activation and deactivation (k_a and k_d) are unique, and these in combination with the rate of propagation k_p determine the polymerization rate.

1.3.2. Initiators

Initiators for ATRP must have a halogen (Br or Cl) and a functional group that can stabilize the formed radical, e.g. carbonyl, cyano or phenyl. The initiator is normally chosen so that the structure mimics the structure of the monomer with the aim of making the rate of initiation and propagation equivalent ($k_i = k_p$). Different functionalities can be incorporated in the initiator and a number of functional groups can be tolerated including epoxide, hydroxyl, cyano and lactone [21]. Multifunctional initiators can be used to synthesize more advanced structures such as star polymers.

1.3.3. Catalysts

The catalyst consists of a transition metal and a halogen, with the metal being a transition metal such as copper, nickel, ruthenium, palladium, rhodium or iron. The criteria for the metal are that it has two oxidation steps separated by one electron step that it has an affinity for halogen and finally that it can complex strongly with the ligand. The main criterion for the halogen is that it can migrate rapidly between the growing chain and the catalyst, and that the bonds with both these species are broken homolytically. The halogen is normally bromine or chlorine, but pseudohalogens have also been used [21]. The catalyst is susceptible to oxidation to the higher oxidation step during reaction, which can be avoided by operating under inert conditions.

1.3.4. Ligands

The primary function of the ligand is to ensure solubilization of the metal catalyst in the solvent, but the reactivity of the metal catalyst is highly influenced by the steric and electronic properties of the ligand as well. Bulky side groups on the ligand can hinder bond formation with the halogen, while electron withdrawing groups can hinder the homolytic cleavage of the halogen–metal bond.

While nitrogen ligands are used for copper-based ATRP, phosphorus-based ligands are used for most other transition metals in ATRP [21]. A few examples of the ligands used are given in Fig. 4.

1.3.5. Solvents

ATRP can be run in bulk, but often a solvent is required to ensure dissolution of the catalyst/ligand complex and reduce viscosity at high conversions. Traditionally used solvents such as toluene, xylene, acetone, diphenyl ether, dimethyl formamide and various alcohols can be used for ATRP, but polymerization can also take place in water and supercritical carbon dioxide, which has attracted attention because of environmental friendliness and cost reduction.

1.3.6. Limitations of ATRP

A number of functional groups are not tolerated in ATRP including carboxylic acid and certain ionic groups, which react with the catalyst, thereby impeding the establishment of the equilibrium. However, carboxylic acid groups can be introduced by polymerization of the carboxylic acid salt instead. Other monomers can not be polymerized by this method, because the formed radical is not stabilized enough, which is the case for monomers such as vinyl acetate and halogenated alkenes. The main problem in using ATRP for syntheses, industrial or otherwise, is removal of the catalyst. The metal catalyst–ligand complex is undesired in the product, as the transition metal induces aging in the polymer, but also for aesthetic (coloration) and toxicological reasons removal is important. Catalyst removal is both difficult and costly, but several methods are presently in use. One procedure is to immobilize the catalyst by having it attached to solid supports during reaction, but this can give loss of control, perhaps due to reduced mobility. Other purification methods include running the raw product on an alumina column, precipitation of polymer and use of an absorbant [22].

1.3.7. Copolymers synthesized by ATRP

The product of an ATRP reaction is a potential initiator for yet another reaction, as it still has the halogen moiety in the growing chain end, which allows reactivation of the chain end using the initially synthesized polymer as macroinitiator for a second polymerization reaction either by sequential addition or reinitiation. Industrially produced polymers have also been functionalized and used as macroinitiators for ATRP. A number of different polymer architectures have been synthesized by ATRP including star-shaped, graft and dendritic polymers.

1.4. Reversible addition–fragmentation transfer polymerization

One of the newest methods of controlling molecular structure when employing radical mechanisms

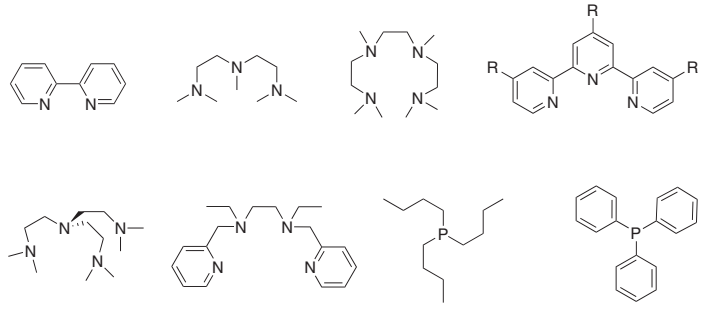

Fig. 4. Examples of ligands used for ATRP [21].

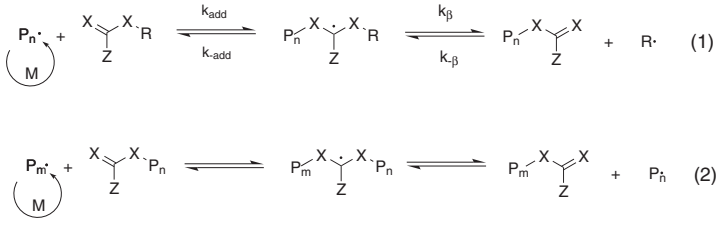

Fig. 5. Mechanism of polymerization by reversible addition–fragmentation transfer [24].

is Reversible Addition–Fragmentation Transfer Polymerization, RAFT, which was introduced by Rizzardo et al. in 1998 [23]. The polymerization reaction is controlled via a dithio compound, the RAFT agent, which is transferred between the active and dormant chains by a reversible addition–fragmentation reaction. During reaction the active polymer formed by initiation adds to the RAFT agent to form a radical species (see Fig. 5), which fragments into a new active radical and a dormant polymer-RAFT adduct. The new radical can either be the species $R^{\cdot}$, which can start a new polymer chain (Fig. 5(1)), or be another polymer chain $P_n^{\cdot}$, that can continue growing (Fig. 5(2)). Rapid transfer between the different radical species ensures the formed polymers grow to equal lengths.

The correct choice of RAFT agent for the utilized monomer ensures that the exchange reaction is significantly faster than the propagation reaction, so in combination with a high ratio of RAFT agent to initiator, a polymer product with a narrow molecular weight distribution is obtained. When reaction is completed the polymer product contains the RAFT agent functionality (commonly thiocarbonylthio). Using this method a small amount of termination products derived from the initiator can not be avoided.

1.4.1. Monomers

RAFT is tolerant of a number of functional groups in the monomer including carboxylic acids, carboxylic acid salts, hydroxyl groups, amides and tertiary amines. Most monomers polymerizable by free radical methods can be used, but most commonly styrenes, (meth)acrylates and vinyl acetates have been polymerized [24].

1.4.2. RAFT agents

As shown in Fig. 5 the RAFT agent has three functional reactive groups, X, Z and R, with X most commonly being sulphur, R is a free radical leaving-group that also must be able to reinitiate polymerization, while Z mainly modifies the activity of the RAFT agent. The used RAFT agent should be consumed during the initial stages of reaction to ensure the same degrees of polymerization. The transfer constant C_{tr} (k_{tr}/k_p[1]) of the RAFT agent is dependent on Z and R as well as the monomer, and must be high (>2), in order to keep the polydispersity low. For this reason the Z-group is chosen to give a less stable intermediate than the used monomer. Molecular weights are dependent on the ratio of RAFT agent to monomer.

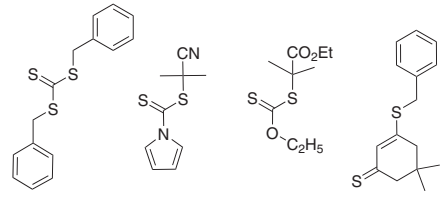

Fig. 6. Examples of compounds used as RAFT agents [24].

RAFT agents include trithiocarbonates, dithiobenzoates and xanthates (dithiocarbonates) as shown by a few examples in Fig. 6.

1.4.3. Initiators

As there is no generation of new radicals in the reversible chain transfer, a free radical source must be utilized. Here the RAFT method has an advantage over both NMP and ATRP namely that virtually the same reaction conditions as for free radical polymerization can be used. This includes using free radical initiators such as azo-bis-isobutyronitrile (AIBN) and dibenzoyl peroxide.

[1] $k_{tr} = k_{add} \cdot \frac{k_\beta}{k_{-add}+k_{-\beta}}$

1.4.4. Reaction conditions

A number of reaction conditions can be used: bulk, solution, emulsion, mini-emulsion and suspension. Reaction can also take place over a wide range of temperatures (ambient to 140 °C). RAFT-reactions can take place in most conventional solvents as well as in protic solvents such as alcohols and water. Super-critical carbon dioxide and ionic liquids have also successfully been used as polymerization media [25].

Some RAFT-reactions have been conducted under high pressure, as this slows radical–radical termination, thereby making formation of well-defined polymers with higher molecular weights possible.

1.4.5. Limitations of RAFT

Only a few RAFT agents are commercially available, therefore it is often necessary to synthesize a suitable agent before polymerization can be undertaken. There have however been developed dependable methods for doing this.

Many functional groups can be incorporated in the RAFT agent and are tolerated in the monomer as well, but monomers containing primary or secondary amines cannot be polymerized, as these functionalities react with the RAFT agent in unwanted side reactions.

Another disadvantage of RAFT is that the products contain the thiocarbonylthio-moiety giving colored polymers, which for some applications is unacceptable. There are however a number of methods for converting the RAFT-endgroup, which is possible in most cases.

1.4.6. Copolymers by RAFT

Block copolymers can be synthesized using RAFT by simple sequential addition, if the same RAFT agent can be utilized for both monomers. More sophisticated methods can be employed to yield complex structures such as graft and star polymers, using compounds with multiple thiocarbonylthio functionalities to synthesize the latter. Endgroup functionalized polymers can easily be synthesized by incorporating the group in question (OH, COOH or SO_3^-) in either R or Z of the RAFT agent.

RAFT is especially well-suited to make microgels from block copolymers having two blocks of different nature (e.g. hydrophilic–hydrophobic) that self-assemble in a given media, where incorporated unreacted double bonds can be crosslinked to yield a star microgel [25].

2. Fluorinated methacrylates and acrylates

In the literature a number of fluorinated or perfluorinated methacrylic and acrylic monomers have been studied in the synthesis of block copolymers by controlled radical polymerization methods. The most extensive work has been done in the field of ATRP witnessed by the number of monomers studied in this area (a few examples are shown in Fig. 7 with the abbreviations used). The following will therefore give an insight into the use of ATRP for fluorinated (meth)acrylates, succeeded by a account of (meth)acrylates polymerized by RAFT and NMP.

2.1. Fluorinated methacrylates and acrylates synthesized by ATRP

2.1.1. Homopolymerization and copolymerization with similar monomers

Homopolymerizations of different fluorinated acrylates and methacrylates have been conducted with the ultimate goal of synthesizing block copolymers with non-fluorinated monomers. Numerous reports of di- and triblock copolymers combining a fluorinated polymer with another hydrophobic monomer such as styrene, methacrylate or acrylate by ATRP can be found in the literature.

As early as 1997 DeSimone and coworkers reported the polymerization of the 1H,1H-perfluorooctyl

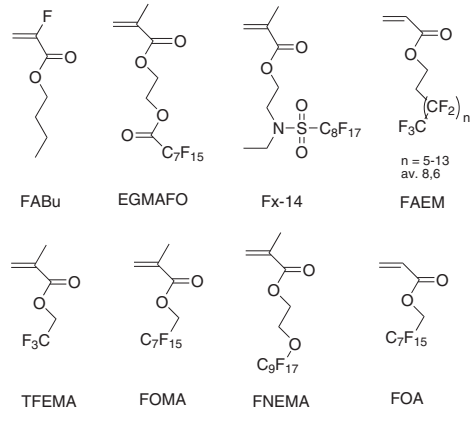

Fig. 7. Examples of fluorinated and perfluorinated monomers polymerized by ATRP.

methacrylate (FOMA) by ATRP [26]. For the polymerization of this monomer macroinitiators of poly(2-hydroxyethyl methacrylate) (PHEMA), poly (2-hydroxyethyl acrylate) (PHEA), poly(methyl methacrylate) (PMMA), polystyrene (PS) and poly (*tert*-butyl acrylate) (P*t*BA) were synthesized also by ATRP. Reactions of the fluorinated monomers were run at 110 °C in trifluorotoluene (TFT) using CuBr as catalyst and 2,2′-bipyridine (bipy) as ligand. Polydispersities of 1.3, 1.5 and 1.6 were obtained for the synthesis by PMMA, PHEMA and P*t*BA, respectively (no results for PS are given). The PHEA macroinitiator was employed at 100 °C yielding copolymers with polydispersities of 1.1 for a large range of molecular weights (35–100 kg/mol). PHEMA and PHEA were polymerized by ATRP in the protected form of trimethylsilanes (TMS) (as shown in Fig. 8) with deprotection after the polymerization of FOMA. In the same study other fluorinated methacrylates and acrylates were polymerized by the iniferter technique among these the equivalent acrylate to FOMA; 1H,1H-perfluorooctyl acrylate (FOA). The products obtained by this method had relatively high polydispersities; 1.5 and above.

The work with FOMA and FOA was later continued [27] and these monomers were successfully polymerized in supercritical CO_2 ($scCO_2$) at 85 °C (4900 psi). Carbon dioxide was chosen as the solvent, as it is environmentally friendly and because fluoropolymers are "CO_2-philic" rendering a system, where both monomer and polymer are solubilized during reaction. CuCl was used as catalyst, while Cu(0) was added to accelerate the reaction, and three different ligands were tested: bipy, 4,4′-di(5-nonyl)-2,2′-bipyridine (dNbipy) and 4,4′-di(tridecafluoro-1,1,2,2,3,3-hexahydrononyl)-2,2′-bipyridine (dR_{f6}bipy) (see Fig. 9). Phase separation was seen when using bipy or dNbipy as ligands, and relatively low conversions were obtained: 54% and 64%, respectively. The best results were obtained

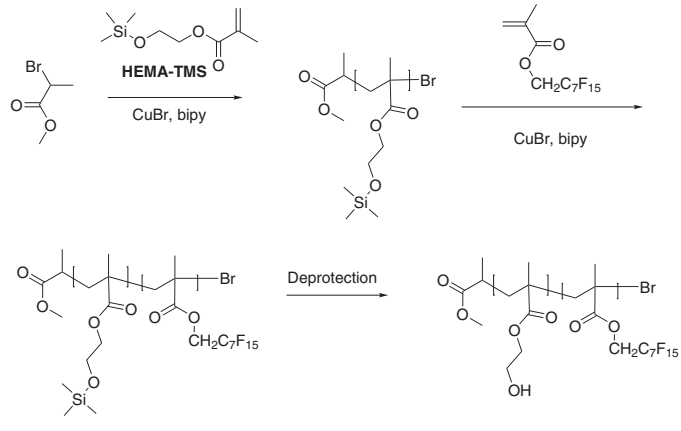

Fig. 8. Synthesis of PHEMA-*b*-PFOMA by use of TMS-protected HEMA [26].

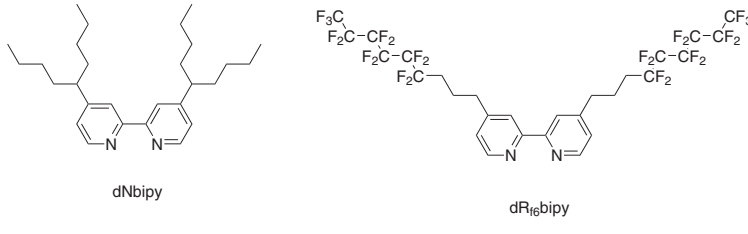

Fig. 9. Ligands used by Xia et al. [27] for the synthesis of FOMA and FOA.

in polymerization of FOMA using the fluorinated ligand dR_{f6}bipy: $M_{n,calculated} = 16{,}800$ g/mol, $M_{n,NMR} = 19{,}000$ g/mol, $M_{w,LS} = 17{,}000$ g/mol, and a monomer conversion of 83%. This homopolymer was used as a macroinitiator for polymerizations of MMA and 2-(dimethylamino)ethyl methacrylate (DMAEMA) (Fig. 10) using the same reaction conditions. The choice of solvent makes this strategy possible, as in commonly used organic solvents the solubility of the fluorinated macroinitiator probably would not be complete thereby reducing control over reactivities. Two glass transition temperatures (48 and 124 °C) were observed for PFOMA-*b*-PMMA indicating microphase separation in solid state. A triblock copolymer was synthesized from a difunctional macroinitiator of PFOA polymerizing PMMA with almost equal amounts of the two polymers. It is deemed that this type of copolymers may potentially be used as fluorinated thermoplastic elastomers. PFOA was also used as a stabilizer for ATRP of MMA in CO_2, where a colloidal dispersion was formed, resulting in a fairly well controlled reaction ($M_n = 13{,}400$, PDI = 1.41).

The sulfonamide functionalized methacrylate, Fx-14 (Fig. 11) has been polymerized by Li et al. [28]. Homopolymers as well as diblock copolymers with styrene and MMA were synthesized. The latter were made by synthesizing a macroinitiator and then polymerizing the fluoromonomer as the second block. Size exclusion chromatography (SEC) traces showed two peaks for both types of diblock copolymers, which was taken as an indication of aggregation with the high-molecular weight peak being the aggregated molecules and the low-molecular weight peak being the free polymer. Surprisingly, thermogravimetric analysis (TGA) showed that P(Fx-14) was less thermally stable than both PS and PMMA.

Perfluoroalkyl acrylate FAEM was copolymerized by Li et al. [29] with butyl methacrylate (BMA) as the first polymer block in the diblock. FAEM is a mixture of acrylates (Fig. 7), where the average chain length of the CF_2-alkyl chain is 8.6 units. The polymerization of the acrylate was conducted in cyclohexanone at 100 °C for 72 h using CuBr/PMDETA as catalyst/ligand complex obtaining conversions between 62% and 95%, and PDI's from 1.29 to 1.44.

The surface properties of the synthesized diblock copolymers were studied by contact angle measurements. The dependency of surface activity on the amount of fluorine present in the copolymers was examined by varying the length of the fluorinated block for a given PBMA size, which showed a consistency between fluorine block length and surface activity. Subsequently the fluorinated block size was held constant, while changing the PBMA-block size, which showed no significant difference. It could

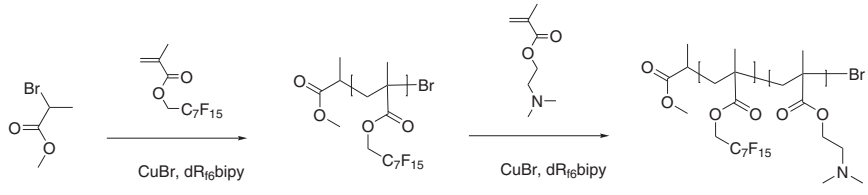

Fig. 10. Synthesis of diblock copolymer using PFOMA as macroinitiator for DMAEMA [27].

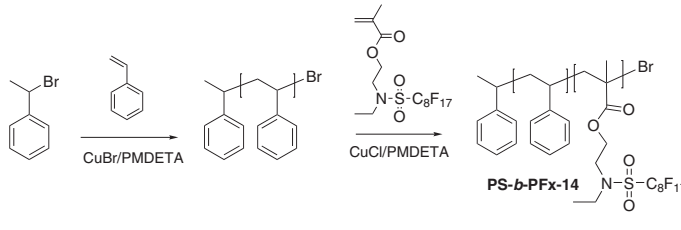

Fig. 11. Diblock copolymer PS-*b*-PFx-14 synthesized by Li et al. [28].

therefore be concluded that the surface activity was solely dependent on the total amount of fluorine present in the polymer. The incorporation of mere 7.6 wt.% FAEM created water and oil-repellent surfaces (contact angles of >100° for water and >75° for paraffin oil). At higher fluorine content surface tensions were comparable to PTFE.

Haddleton and coworkers have studied both ATRP of fluorinated monomers using aliphatic initiators as well as the synthesis of methacrylates with fluorinated macroinitiators [30,31]. The monomers 2,2,2-trifluoroethylene methacrylate (TFEMA) and 1H,1H,2H,2H-heptadecafluorodecyl methacrylate (FEMA) were polymerized by ATRP in toluene at 90 °C. CuBr was used as catalyst, while *N*-(*n*-pentyl)-2-pyridylmethamine was the ligand employed. It was possible to homopolymerize TFEMA using ethyl-2-bromoisobutyrate (EBB) as initiator. Kinetics of the reaction showed a gradual loss of reactive species through irreversible termination, but in spite of this, polydispersities as low as 1.06 were obtained for low molecular weights ($M_n = 6200$ g/mol) and below 1.3 for higher molecular weights ($M_n =$ 20,000 g/mol).

FEMA was synthesized from the equivalent fluoroalcohol and methacryloyl chloride and consequently it was attempted to polymerize this monomer by the method previously described, but phase separation took place during reaction and the resulting homopolymer was only soluble in fluorinated solvents, which severely limits the usefulness of the product. Instead, statistical copolymerizations of FEMA with MMA and styrene, respectively, with phenyl-2-bromoisobutyrate as initiator were attempted with good results. Reaction with MMA was relatively fast (over 95% conversion of FEMA in 4 h) with polydispersities as low as 1.06 and in all cases lower than 1.2. Styrene and FEMA reacted markedly slower (50–60% conversion of FEMA in 20 h), but still with good control of the product (PDI < 1.3 in most cases). For both types of copolymerization the reaction rate was slightly elevated with increasing concentration of the fluorinated methacrylate; for MMA k_{app} increased from 7×10^{-3} s^{-1} to 1.3×10^{-2} s^{-1} with the addition of 20% FEMA, similarly k_{app} of styrene was raised from 4.8×10^{-4} s^{-1} to 7.8×10^{-4} s^{-1} under the same conditions. Conversions of MMA and FEMA were almost the same throughout the reaction and no irreversible termination was observed. For the copolymerization with styrene irreversible termination possibly takes place at concentrations of FEMA above 20%.

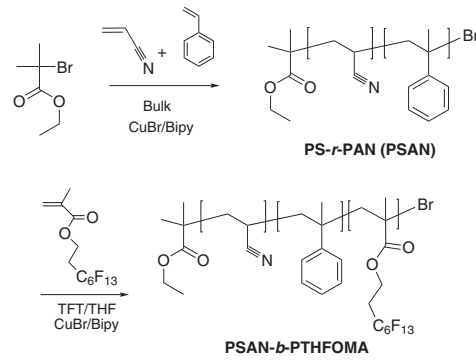

Fig. 12. Synthesis of block copolymer from random copolymer PSAN (PS-*r*-PAN) and PTHFOMA [32].

Contact angle measurements of the PMMA-*r*-PFEMA copolymers coated on glass plates showed a relationship between fluorine contents and surface activity, and also indicated that the fluorinated chains migrate to the surface to give highly hydrophobic properties.

Random copolymers of styrene and acrylonitrile (PSAN) were used as macroinitiators for 1H, 1H,2H,2H-tetrahydroperfluorooctyl methacrylate (THFOMA) with polymerization taking place at 100 °C in a mixture of TFT and THF (4:1 v/v) [32]. The final *random-block*-copolymers (Fig. 12) had narrow molecular weight distributions (<1.2) and molecular weights of approximately 20,000 g/mol (determined by nuclear magnetic resonance spectroscopy (^{1}H NMR)). The PSAN-*b*-PTHFOMA copolymers were used as stabilizers in dispersion polymerizations of acrylonitrile–vinylacetate in $scCO_2$, where their presence resulted in the formation of spherical particles with a narrow size distribution as well as higher molecular weights and yields for the synthesized polymers. The best results were obtained with a PTHFOMA-block of about 17,000 and a PSAN-block of 4500 g/mol.

2.1.2. Copolymerization with hydrophilic monomers

Shemper and Mathias [33] have taken the work of Haddleton's groups further synthesizing both linear and star-shaped polymers containing FEMA. Statistical copolymers were synthesized with FEMA and poly(ethylene glycol) methyl ether methacrylate (PEGMA) ($M_n \sim 300$ g/mol) or poly(propylene glycol) methacrylate (PPGM) (structures shown in Fig. 13). Polymerization took place in methyl ethyl

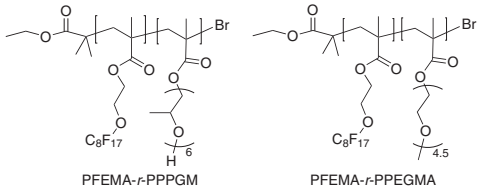

Fig. 13. Random copolymers of fluoromethacrylate FEMA with poly(ethylene glycol) methyl ether methacrylate (PEGMA) and poly(propylene glycol) methacrylate (PPGM) [33].

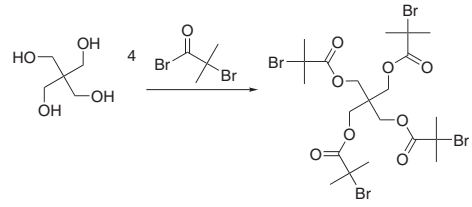

Fig. 14. Initiator synthesized from pentaerythritiol and 2-bromoisobutyryl bromide used for design of star-shaped polymers of PFEMA, PPEGMA and PPEGMA-*b*-PFEMA [33].

ketone at 80 °C (one experiment was conducted at 88 °C) using CuBr/PMDETA as catalyst/ligand and EBB as initiator. (A homopolymer of FEMA was also synthesized, but during reaction phase separation was seen as previously observed [30].) The copolymers of FEMA with PPGM and PEGMA were synthesized with a 50/50 molar feed, and PEGMA/FEMA were also reacted at a 90/10 ratio.

The statistical copolymer of PPGM and FEMA could not be analyzed by SEC due to aggregation in THF and it was not possible to separate signals from initiator and polymer in ^{13}C NMR. The PPEGMA-*r*-PFEMA copolymer with only 10% FEMA could be analyzed by SEC (PDI = 1.09), but some aggregation was observed. Kinetic studies of this copolymer (analysis by SEC) showed that although the reaction was first-order, the presence of FEMA reduced the propagation rate of PEGMA to half the value compared to a homopolymerization of PEGMA under similar conditions. The authors could not give an explanation of this phenomenon.

The molecular weights of both copolymers of PPEGMA-*r*-PFEMA were estimated by ^{1}H NMR and the compositions were equivalent to feed ratios indicating similar reactivity rates of the monomers, as expected.

Tetra-armed homopolymer stars of PEGMA or FEMA were synthesized with high conversions (100% and 89%) within 3 h from a tetrafunctional macroinitiator generated from pentaerythritiol and 2-bromoisobutyryl bromide (Fig. 14). The star polymer of FEMA was polymerized in a mixture of benzene and TFT at 114 °C, and the product was analysed by ^{13}C NMR, as it was not soluble in other than highly fluorinated solvents, which made SEC unfeasible. It was possible to use the PPEGMA four-armed star to polymerize FEMA to achieve a tetraarmed diblock copolymer. This reaction was run under the same conditions as the star-FEMA and gave 75% conversion of monomer in 30 min with an initiator efficiency of 97%. The product was analysed by ^{1}H and ^{13}C NMR and the spectral data from the latter analysis were used to estimate molecular weights. All the star polymers had molecular weights close to the theoretical ones indicating controlled reactions.

The amphiphilic star block copolymer changed behavior depending on the solvent, which was observed during ^{1}H NMR-analysis, where the ratio of the signals of the two blocks differed depending on which solvent was used ($CDCl_3$ versus TFT) indicating a change of mobility of the two segments with solvent. These polymers were not soluble in water and were only partially soluble in THF despite the relatively low content of FEMA (33%). In triflurotoluene micelles with a diameter of 137 nm were observed by dynamic light scattering (DLS).

Lim et al. [34] have synthesized amphiphilic block copolymers utilizing a poly(ethylene oxide) (PEO) macroinitiator (M_n = 2000 and 5000 g/mol) for the polymerization of the fluoromethacrylates, FOMA and THFOMA (Fig. 15). Reactions took place in a mixture of TFT and benzene at 120 °C using CuCl/bipy giving high conversions (85–95%) with very high initiator efficiencies (>90%). It was, however, impossible to analyze the products by SEC, as the amphiphilic polymers aggregated in THF even at low concentrations, therefore the polydispersities were not found. Kinetics of the two monomers were very similar and differences in the obtained products, if any, have not been commented upon by the authors. Measurements of interfacial activity of the block copolymers using a high pressure pendant drop apparatus showed that the polymers lower the surface tension to a degree that allows emulsion formation of water in $scCO_2$. The formation of micelles in solution was ascertained by dynamic laser

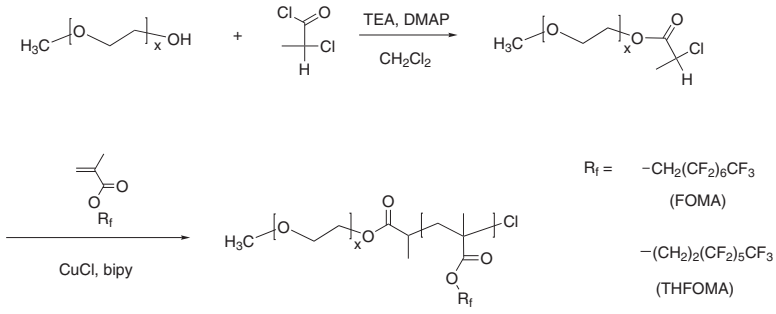

Fig. 15. Synthesis of diblock copolymers of perfluorinated methacrylates with poly(ethylene oxide) macroinitiator [34].

light scattering and the micelle size was in the nanometer range (50–150 nm) in both water and chloroform. Analysis of the micelles by transmission electron microscopy (TEM) showed formation of both spherical and cylindrical aggregates dependent on the length of the two polymer blocks with all micelles having PEO in the shell and fluorinated polymer cores.

PEO-based macroinitiators have also been utilized by Hussain et al. [35,36] to synthesize di- and triblock copolymers with THFOMA. PEO was converted to a macroinitiator with 2-bromopropionyl bromide and used for polymerization of THFOMA at 80 °C in butyl acetate using CuBr as catalyst with bipy or PMDETA as ligand. The authors do not give information on yields or initiator efficiency, but polydispersities as low as 1.1 were found by SEC and monomodal curves were generated in all cases. A certain degree of aggregation of the copolymers during analysis was observed, as a lower molecular weight than for the initial macroinitiator was found in some cases. Poly(ethylene oxide)s having different molecular weights were used in this study: 2, 6, 10 and 20 kg/mol. Exhaustive studies of the block copolymers in both bulk and solution were performed to determine their behavior. The copolymers were soluble in water and surface tension measurements of aqueous solutions showed that the critical micelle concentration decreased with fluorine content. The formation of micelles in solution was further proved by DLS, which also indicated that the aggregation behavior of the diblock copolymer was very different from the triblock copolymers. While the diblock copolymers were nearly fully extended in the micelles, the triblock copolymers folded in loops forming flowerlike micelles. Micelle size was shown to be independent of temperature.

The use of the copolymers of THFOMA and PEO as coating for metals was investigated by mixing aqueous solutions of colloidal gold with polymer solution. TEM investigations confirmed the formation of nanoparticles as anticipated, also a number of different morphologies (micelle, fibrous network and irregular) of the block copolymers were found by this method dependent on the initial concentration. Differential scanning calorimetry (DSC) showed that the block copolymers formed different ordered melt morphologies as well, however the PEO-chains crystallized on cooling destroying this order except with very long fluorinated chains.

The combination of ATRP and enzymatic ring-opening polymerization has been utilized by Villarroya et al. to synthesize copolymers of THFOMA and ε-caprolactone (CL) (Fig. 16) [37]. Reactions were carried out in $scCO_2$ (1500–1700 psi) at 45 °C using CuBr/bipy for the ATRP of THFOMA and Novozym-435 for the enzymatically catalysed polymerization of CL. Block copolymers were synthesized by either initiation of THFOMA from a PCL-macroinitiator or by a two-step one-pot synthesis method. In both cases a bifunctional initiator capable of initiating both monomers was utilized for polymerization of CL first and THFOMA subsequently. Addition in the reverse order did not succeed, since CL polymerized via initiation by water and not by the PTHFOMA-macroinitiator resulting in two homopolymers instead of one block copolymer. Molecular weights ranged from 13,000 to 30,000 g/mol with polydispersities from 1.2 with the highest values for the one-pot approach being 1.51 (RI-detector). DSC indicated microphase separation with two distinct T_g's in most cases; −60 °C for PCL and 46 °C for PTHFOMA.

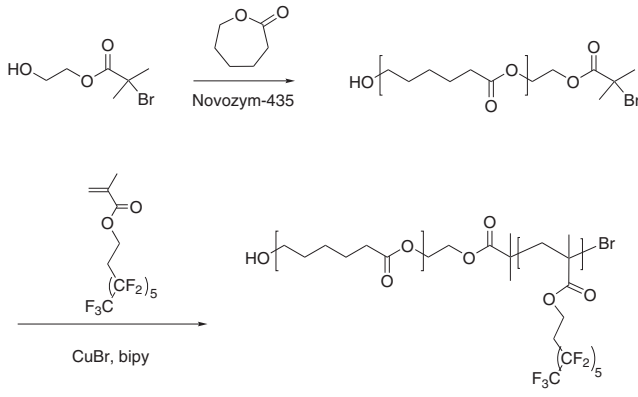

Fig. 16. Synthesis of block copolymer of polycaprolactone and PTHFOMA by sequential performance of enzymatic ring-opening polymerization and ATRP, respectively [37].

2.1.3. Fluorinated methacrylate ethers and esters

Block copolymers of methacrylic monomers with a fluorinated pendant ether or ester chain instead of an alkyl have also been synthesized by ATRP.

2-[(Perfluorononenyl)oxy] ethyl methacrylate (FNEMA) and ethylene glycol monomethacrylate monoperfluorooctanoate (EGMAFO) were used for synthesis of di- and triblock copolymers by Zhang et al. [38,39]. The fluorofunctionalized monomers were copolymerized with styrene, methyl acrylate and butyl acrylate (BA), respectively, polymerizing the non-fluorinated block first (Fig. 17). 1-Phenylethyl bromide (PhEBr) was used as monofunctional initiator for the synthesis of diblocks, while α,α'-dibromo-*p*-xylene (DBX) was used for the triblock copolymers in a similar fashion. The polymerizations were conducted in TFT at 100 °C using CuBr/bipy.

Conversions for the methacrylate ether FNEMA were between 50% and 60% with polydispersities from 1.27 to 1.49 including results of both di- and triblock copolymerisation. The results for the ester EGMAFO were similar for conversions (48–68%), but the polydispersities were quite high ranging from 1.70 to 2.41. The authors believe the broad distribution of molecular weights to be due to termination by combination, as the same phenomenon was observed in homopolymerisation of EGMAFO.

Triblock copolymers consisting of fluoropolymer and styrene were studied by DSC, which showed two distinct glass transition temperatures indicating phase separation due to immiscibility of the two

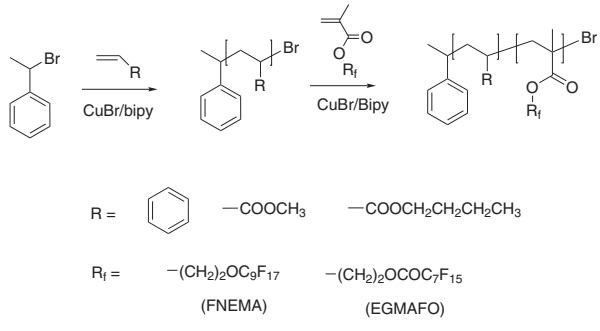

Fig. 17. Synthesis of diblock copolymers of fluorinated methacrylate ester (EGMAFO) and ether (FNEMA) with styrene, methyl acrylate and butyl acrylate [38].

polymers. Surface activity in solution (Wilhelmy plate method) and solid state (contact angle) was studied, showing high surface activity in solution and low surface energy in solid state, implying that these materials can potentially be applied as efficient surfactants as well as low energy materials.

Amphiphilic diblock copolymers containing ionic groups were successfully synthesized by Hu and coworkers [40,41] using the methacrylate ether FNEMA. The ionic moieties studied in this work were carboxylic and sulfonic groups. The former products were obtained by polymerization of *tert*-butyl methacrylate (*t*BMA) followed by hydrolysis of the ester to the carboxylic acid (Fig. 18). The latter products were synthesized by polymerization of styrene and subsequent sulfonation of the *para*-position with lauroyl sulfate or acetyl sulfate (Fig. 19). In both cases FNEMA was polymerized as the second monomer before converting the first polymer block to yield the ionic species (less than 100% conversion for all reactions) (this strategy was employed due to the fact that the ATRP method is not tolerant of ionic species). Synthesis took place in TFT at 100 °C employing CuBr as catalyst and either PMDETA as ligand (P*t*BMA-macroinitiator) or bipy (PS-macroinitiator). Polydispersities between 1.35 and 1.41 were obtained for the block copolymers containing carboxylic groups, and values ranging from 1.21 to 1.60 for those with sulfonic groups. The sulfonated copolymers (PSSF) were studied more closely regarding solubility and surface activity revealing that the sulfonic groups enabled these compounds to dissolve in non-fluorinated solvents such as THF, acetone and *N*-methyl pyrrolidone. The latter solvent was therefore used for studies of surface activity in solution along with aqueous solutions. Most of the synthesized polymers were soluble in water, but did not reduce the surface tension to a very large extent, which on the contrary was the case for the *N*-methyl pyrrolidone solutions. Wetting of thin films showed that the surface activity was similar to that of PTFE.

An extensive study of the use of PATF as a surface modifying agent for polyurethaneurea-acrylate (PUA) by the same authors [42] shows that even a small amount (2 wt.%) can modify the surface of the otherwise hydrophilic PUA-film to exhibit hydrophobic surface properties. Measurements (attenuated total reflection spectroscopy (ATR) and X-ray photoelectron spectroscopy (XPS)) indicate that during the film formation process the fluorinated groups in PATF enrich the air side surface. The use of the sodium salt of PATF did not have the same effect.

2.1.4. α-Fluorinated acrylates

Otazaghine et al. [43] have undertaken the polymerization of butyl α-fluoroacrylate (FABu) by ATRP with good results (PDI < 1.17). Reactions took place in anisole at 90 °C using HMTETA as

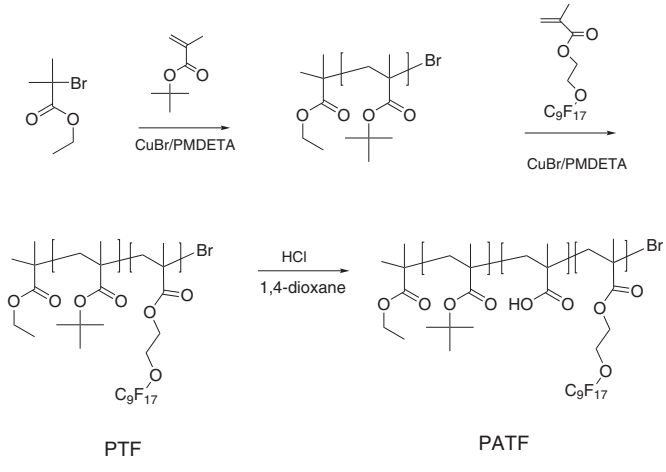

Fig. 18. Synthesis of diblock copolymer of FNEMA and *t*BMA containing carboxylic groups derived from the partial hydrolysis of *t*BMA. The carboxylic groups are randomly distributed [40].

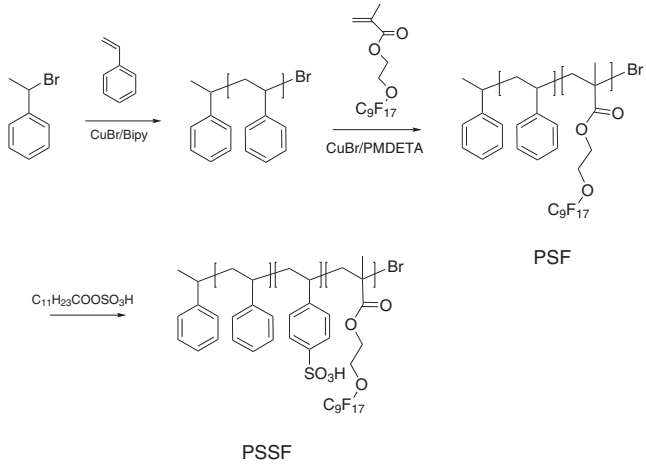

Fig. 19. Synthesis of diblock copolymer of FNEMA and styrene containing sulfonic groups derived from the partial *para*-sulfonation of PS. The sulfonic groups are randomly distributed [40].

ligand and CuBr or CuCl as catalyst. The experiments showed that the α-fluorinated acrylate was much more reactive than the non-fluorinated equivalent. FABu was synthesized from the equivalent acid chloride (Fig. 20). A silylated initiator was used to determine the true molecular weights by ^{1}H NMR and these results were used to generate a universal calibration curve for SEC. A study of the coupling reaction of FABu oligomers under ATRP conditions was later performed showing that the coupling rate was not quantitative (74–81%) [44].

Poly(α-fluorinated acrylate)s generally show better thermal stability and a higher glass transition temperature than their methacrylic homologues as well as low absorption in the near-infrared area, giving materials suited for applications in optics.

2.1.5. Surface initiated ATRP of fluorinated methacrylates and acrylates

Granville and Brittain [45] have performed surface initiated polymerization of 2,2,3,3,3-pentafluoropropyl acrylate (PFA) to form polymer brushes of PMA-*b*-PPFA on a porous silica substrate. The silica layer was treated with (11-(2-bromo-2-methyl)propionyloxy)-undecyltrichlorosilane to obtain a bromoisobutyrate initiator on the surface utilized to initiate the polymerization of MA, which could be used as macroinitiator for the second block (Fig. 21). CuBr/PMDETA was used as catalyst/ligand system for both polymerizations and while polymerization of MA took place in anisole, PFA was reacted in TFT. The generated brushes were subjected to selective solvents, as well as thermal treatments, to induce surface rearrangement. The rearrangement resulted in the creation of an ultrahydrophobic surface by either thermal treatment (60 °C for 6 min) or solvent treatment with TFT (static contact angle, $\theta = 135°$). Similar studies were performed by the same research group [46] polymerising brushes of polystyrene and fluorinated acrylates on a silica substrate and comparing with the PMA-*b*-PPFA-brushes. The fluorinated monomers were polymerized in the previously employed fashion and the chosen acrylates were heptadecafluorodecyl acrylate, pentafluoropropyl acrylate and trifluoroethyl acrylate. Advancing con-

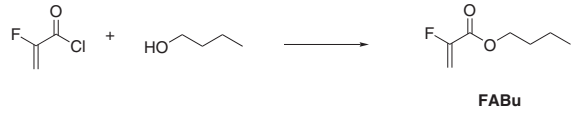

Fig. 20. The synthesis of fluorinated acrylate FABu used by Otazaghine et al. [43]

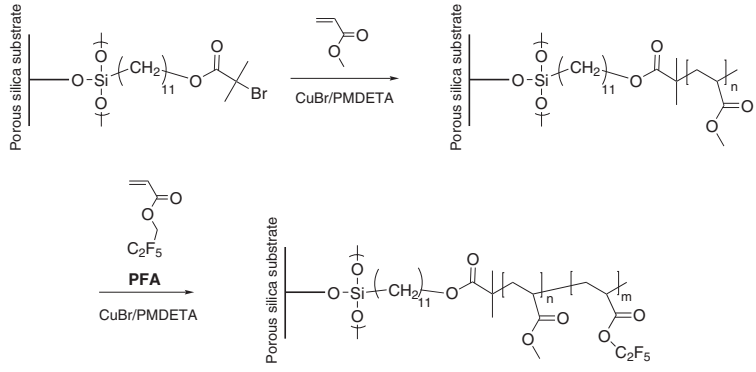

Fig. 21. The synthesis of PMA–PPFA diblock brushes on a silica substrate [45].

tact angles were generally higher for the surfaces with block copolymer brushes versus the PS-brushes (up to 15° difference). Increasing the amount of fluorine from 3 to 17 fluorine groups also resulted in an increase in advancing contact angles (102–126°). Solvent induced rearrangements of the diblock brushes showed a lower degree of rearrangement than for the PMA-tethered grafts, which was believed to be due to the lower ability of PS to rearrange.

Silicon wafers were also used by Chen et al. [47] to carry out surface-initiated polymerization of TFEMA (90 °C in TFT using CuCl/dNbipy) to yield brushes that were used to polymerize MMA. In a test run under the mentioned conditions a linear homopolymer of TFEMA with a PDI of 1.15 was obtained. Both mono- and difunctional initiators were used on the surface and the latter almost doubled the grafting densities. Wafers with a thin layer of brushes had rough surfaces (large difference between receding and advancing contact angles) and showed contact angles of approx. 94°, while this was reduced after copolymerization with MMA (up to 25°).

2.2. Fluorinated methacrylates and acrylates synthesized by RAFT

While there are numerous reports of fluorinated (meth)acrylates polymerized by ATRP, the examples of polymerizations by NMP or RAFT are very few.

A polymerization study of 1,1,2,2-tetrahydroperfluorodecyl acrylate (FDA) comparing ATRP and RAFT polymerization was undertaken by Ma and Lacroix-Desmazes [48]. For polymerization a macroinitiator (MI) or RAFT agent (DTA1 and DTA2) based on PEO was synthesized (Fig. 22). ATRP of FDA was performed in cyclohexanone at 100 °C using CuBr/HMTETA as catalyst/ligand system, while RAFT polymerizations took place in TFT at 65 °C using AIBN as initiator. The molecular weights could not be estimated by SEC due to low solubility, instead ^{1}H NMR was employed, and when using DTA1 also UV–vis analysis could be performed. The values found for the crude products corresponded well with theoretical values (targets of up to 25,000 g/mol). To purify the block copolymer product extraction with trichlorotrifluoroethane was carried out, which yielded products of much higher molecular weight (up to 150,000 g/mol) consisting only of copolymers rich in PFDA. PEO–PFDA block copolymers could be used to stabilize an emulsion in CO_2–water mixtures (water in CO_2).

RAFT polymerization of pentafluorophenyl methacrylate (FMA) was carried out by Eberhardt and Théato [49] in the presence of cumyldithiobenzoate (CTA1) and cyanopentanoic acid dithiobenzoate (CTA2), respectively (Fig. 23). Polymerizations took place in dioxane using AIBN as initiator yielding homopolymers with narrow molecular weight distributions (PDI < 1.3 (CTA1) and <1.15 (CTA2)). Amphiphilic block copolymers were also synthesized using PFMA as macroinitiator for MMA, *N*-acryloylmorpholine (NAM) and *N*,*N*-diethylacrylamide (DEA), respectively. PNAM was chosen for high solubility and non-toxicity, while PDEA is important for medical purposes, as

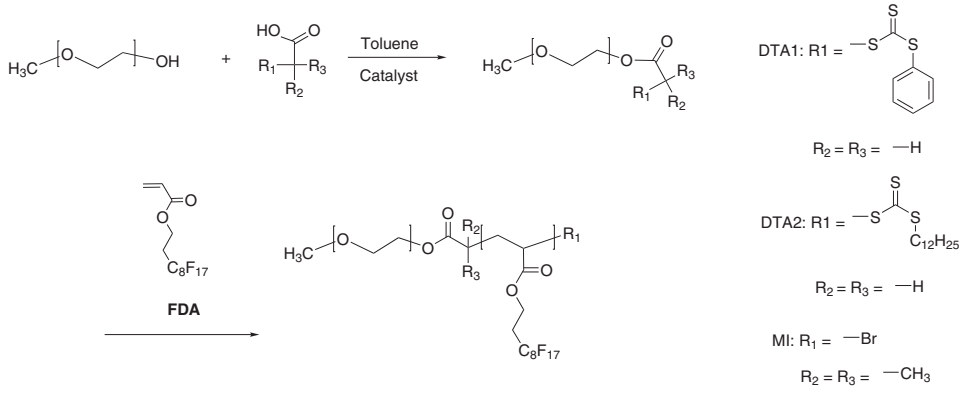

Fig. 22. Polymerization of fluoroacrylate FDA with PEO-macroinitiator (ATRP) or degenerative transfer agent of PEO (RAFT) [48].

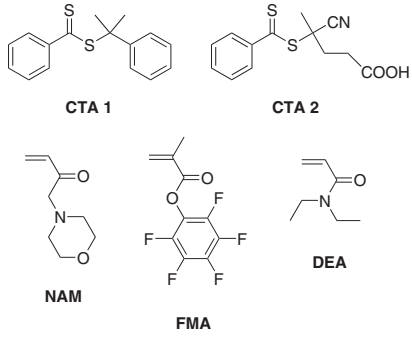

Fig. 23. RAFT agents and monomers used by Eberhardt and Théato [49].

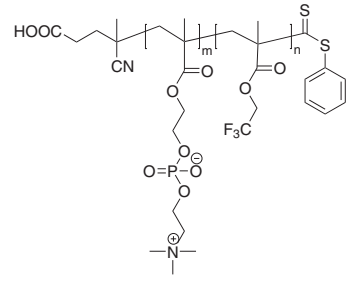

Fig. 24. Poly(MPC-*co*-TFEMA) synthesized as diblock, gradient and random copolymer by RAFT [50].

it possesses a lower critical solution temperature (LCST), between 25 and 36 °C. The previously used reaction conditions were employed for the synthesis of the diblock copolymers. CTA2 gave narrower molecular weight distributions for the diblock copolymers (<1.30) for higher molecular weights (up to 50,000), whereas CTA1 again gave broader distributions (<1.4) for lower molecular weights (20,000–40,000).

Block, gradient and random block copolymers of TFEMA and 2-methacryloyloxyethyl phosphorylcholine (MPC) were copolymerized using RAFT by Inoue et al. (Fig. 24) [50]. These materials have great potential as biomaterials, as MPC is a highly hydrophilic and biocompatible compound, which has a structure that mimics phospholipids, polar groups located on the outer surface of a cell. CTA2 was the used RAFT agent with AIBN as initiator and polymerizations took place at 70 °C. For the diblock copolymers one glass transition was observed for PTFEMA, which was expected, as MPC does not have a T_g. The observation of T_g for PTFEMA indicates the formation of microdomains in the block copolymers, while the statistical and gradient copolymers did not display this behaviour. Static contact angles decreased with an increase in bulk concentration of MPC.

2.3. Fluorinated methacrylates and acrylates synthesized by NMP

Lacroix-Desmazes et al. [51] have polymerized FDA by NMP using DEPN as nitroxide. Reactions were run in cyclohexanone at 123 °C using AIBN as initiator to increase reaction rates (reaction time

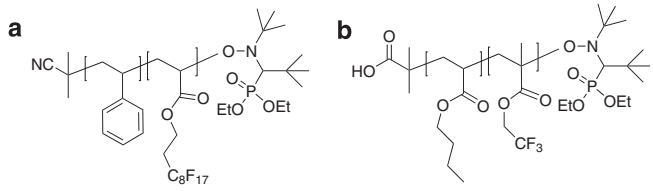

Fig. 25. Structure of PS-*b*-PFDA: (a) [51] and PBA-*b*-PTFEMA; (b) [52] synthesized by NMP.

approximately 7 h). For homopolymers of PFDA good yields were realized (84–91%) for molecular weights of 40,000–76,000 g/mol. Due to insolubility SEC was not performed on the fluorohomopolymers, instead composition was confirmed by elemental analysis. PS-DEPN macroinitiators (4000–10,000 g/mol) with narrow molecular weigths (<1.14) were obtained utilising the AIBN/DEPN bicomponent initiator system and block copolymers of various lengths synthesized of FDA using these PS-DEPN macroinitiators (Fig. 25) were subsequently analysed by elemental analysis, SEC (TFT as solvent with PS-standards) and ^{1}H NMR (TFT). Narrow molecular weights distribution were found in all cases (<1.15) for the relatively large polymers (43,000–50,000 g/mol) and DSC-analysis showed only a single melting peak (71–74 °C), while no glass transition was observed presumably due to the high crystallinity of PFDA and relatively low PS-content.

PS–PFDA block copolymers formed micelles in CO_2 and could be used as a stabilizer of PS particles in dispersion. Surface and bulk properties of PS-*b*-PFDA showed the same surface tension as for the PFDA homopolymer indicating enrichment of this block at the surface. Bulk microstructured morphology was observed, but no long-range order existed.

DEPN was also the nitroxide of choice for Roche et al. [52] for the synthesis of block copolymers of BA and TFEMA (Fig. 25). BA was used as macroinitiator for the fluorinated monomer to yield polymers with molecular weights of 30,000 and 70,000 g/mol aiming at different ratios of the two monomers varying the size of the BA-block. The block copolymers were deposited by solution casting on steel surfaces as a protective layer against corrosion. Lamellar structure was observed for copolymers having similar weight fractions of the two monomers and these coatings also had the best adhesion to the steel surface. Coating thickness (35–265 nm) had a great influence on corrosion resistance with the thickest coating exhibiting good corrosion resistance for 8 months measured by electrochemical impedance.

3. Fluorinated polystyrenes

Mono- as well as pentafluorostyrenes are commercially available; also mono-substituted trifluoromethyl styrenes exist. Furthermore, the labile *p*-fluorine can relatively easy be replaced by nucleophilic substitution [53,54] with alkoxides making a variety of *p*-substituted 2,3,5,6-tetrafluorostyrenes available. The majority of the efforts in controlled polymerization of fluorinated styrenes have been in the field of ATRP, but NMP has also been utilized for polymerization of these compounds. The following will therefore mainly be a study of the use of ATRP for synthesizing fluorinated polystyrenes including kinetics, while the few cases of NMP found will be covered as well.

3.1. Fluorinated polystyrenes synthesized by ATRP

3.1.1. Kinetics of fluorinated polystyrenes in ATRP

A series of mono-substituted fluorine-containing styrenes were polymerized by ATRP [55] with PhEBr initiation and CuBr ligated with bipy catalysis in diphenyl ether at 110 °C. Based on the monomer conversion data a first order relationship was established in all cases; furthermore the molecular weight increased linearly with monomer conversion, and the polydispersities were relatively low ($M_w/M_n < 1.3$). Thus all the criteria for a controlled polymerization were fulfilled. From the derived linear monomer conversion relationships the apparent rate coefficients, $k_p^{app} = -d(\ln[M])/dt$, listed in Table 1 were calculated. Whereas a single fluorine substituent (4-F) only had a neglectable effect on k_p^{app} as compared to non-substituted styrene, the electron-withdrawing substituents, 3-CF_3 and 4-CF_3, had a clear enhancing effect. On the other hand, when all five aromatic hydrogens were replaced by five electron-withdrawing fluorines [56]

Table 1
Apparent rate coefficients in ATRP of fluoro-substituted styrenes

Substitution	$k_p^{app} \times 10^4$ (s^{-1})	Solvent	Reference
3-CF_3	1.44	DPE[a]	[55]
4-CF_3	1.33	DPE[a]	[55]
4-F	0.39	DPE[a]	[55]
None	0.44	DPE[a]	[55]
2,3,4,5,6-F_5	3.0	None	[56]
2,3,5,6-F_4-4-OCH_3	6.9	None	[54]
None	1.41	None	[54]

$[M]_0$:$[PhEBr]_0$:$[CuBr]_0$:$[bipy]_0$ = 100:1:1:3 at 110 °C.
[a] DPE: diphenyl ether, $[M]_0 = 4.37$ M.

the rate of polymerization (3.0×10^{-4} s^{-1}) of 2,3,4,5,6-pentafluorostyrene (FS) more than doubled as compared to that of styrene (1.41×10^{-4} s^{-1}) in bulk as seen from Table 1. However, nucleophilic substitution of the 4-F in FS with an electron-donating methoxy group resulting in 2,3,5,6-tetrafluoro-4-methoxystyrene (TFMS) had an even more dramatic effect, since the rate of polymerization of TFMS [54] increased to 6.9×10^{-4} s^{-1}. Previously a single 4-OCH_3 had been demonstrated to exert a slight retarding effect on the rate of polymerization of styrene [55]. Apparently some beneficial but still unexplained synergistic effect on polymerization rate arises by the substitution of four electron-withdrawing F atoms and one electron-donating 4-OCH_3 group in TFMS. In summary, the kinetics and the molecular weight investigations have shown that all these fluorinated styrenes can be polymerized in a controlled manner by ATRP.

3.1.2. Copolymerization with styrene

Numerous different approaches have been employed in the design of novel block copolymer materials where especially poly(pentafluorostyrene) (PFS) but also other fluorinated styrenes constitute one or more blocks. A schematic survey of the applied ATRP protocols is presented in Table 2.

The controlled characteristics of PFS and PTFMS have first been exploited by Hvilsted et al. [54,56] to prepare hydrophobic diblock copolymers with PS. The conservation of the bromine reactivity in the isolated homopolymers was indirectly proved through the efficient ability to act as macroinitiators (MIs). Thus, all combinations of block copolymers among these three monomers are possible and the sequence of the consecutive ATRPs is of less importance. Moreover, PTFMS can be demethylated and the resulting poly(2,3,5,6-tetrafluoro-4-hydroxystyrene) have been derivatized to form liquid crystalline azobenzene side chain polymers [54].

Other semifluorinated block copolymers with PS have been developed. 2,3,5,6-tetrafluoro-4-(2,2,3,3,3-pentafluoropropoxy)styrene (TF(F_5)S) and 2,3,5,6-tetrafluoro-4-(2,2,3,3,4,4,5,5,6,6,7,7,8,8,8-pentadecafluorooctaoxy)styrene (TF(F_{15})S) were applied in conjunction with styrene to produce block copolymers by ATRP [53]. In case of TF(F_5)S the block copolymers could be synthesized by use of both blocks as MI. The block copolymers with the minority phase being >10% exhibited phase separation mirrored in two glass transition temperatures (T_g) that reflect the T_g of the individual blocks. The fluorinated side chains of PTF(F_5)S and PTF(F_{15})S enrich the surfaces of thin films, as evidenced by XPS, with resulting high advancing water contact angles of 117° and 122°, respectively. Even thin films of block copolymers with only 10 mol% of PTF(F_5)S or PTF(F_{15})S had considerably higher contact angles (105° and 111°, respectively) than that of thin PS films (95°).

Similar block copolymers were prepared from (1H,1H-perfluoro-2,5-dimethyl-3,6-dioxanonan-1-yl) styrene (FS_1) and (1H,1H,2H,2H-perfluorooctan-2,5-1-yl)styrene (FS_2) that in turn were applied as comonomers in ATRP [68]. Initially styrene was initiated in the conventional ATRP protocol with PhEBr, CuBr and bipy at 110 °C then FS_1 or FS_2 was added. Also these block copolymers demonstrated microphase separation and low glass transition temperatures ~−44 °C (PS-*b*-PFS_1). These materials hold promise as low surface-energy additives or surfactants for $scCO_2$ applications.

Hydrophobic triblock copolymers with a central PS block and two flanking PFS blocks were produced [57] in two sequential ATRPs. The difunctional initator, DBX, was first employed for preparation of the PS block, which was then used as MI for the FS polymerization. Symmetrical and hydrophobic pentablock copolymers [57] were designed by use of two individual ATRPs initially with styrene and then with FS. The PS was initiated by use of a dibromoester prepared from the fluorinated initiator: 1H,1H′,10H,10H′-perfluorodecane-1,10-diol, which can be considered as a short fluorinated middle block. The outer PFS blocks could subsequently be added by employing the isolated, triblock copolymer PS-macroinitiator.

Four and six arm star-shaped PFS were prepared from bromoesters initially based on a tetraethyleneglycol extended pentaerytrithol (penta($TEG)_4$) or a

Table 2
ATRP protocols for fluorinated styrene monomers employed in block copolymers architectures

Parent styrene	R	Abbreviation	Initiator or MI	Comonomer	Catalyst	Ligand	Solvent	Temperature (°C)	Reference
$CH_2{=}CHC_6F_5$		FS	PhEBr	St	CuBr	Bipy	Xylene	110	[56]
			PhEBr	TFMS	CuBr	Bipy	Xylene	110	[54]
			PEGPG, PEG		CuBr	Bipy	Xylene	110	[57,58]
			DBX		CuBr	Bipy	Xylene	110	[57]
			Dipenta/PS		CuBr	Bipy	Bulk	110	[57]
			Penta$(TEG)_4$		CuBr	Bipy	Bulk	110	[57]
			EBB	*t*-BA	CuBr	Bipy	Xylene	90	[59]
			EBB	MMA	CuBr	Bipy	Xylene	90	[60]
			PDMS		CuBr	Bipy	Bulk	110	[57]
			PVDF		CuBr	Bipy	Bulk	130	[70]
			Si/SiO_2/PS		CuBr/$CuBr_2$	PMDETA	*o*-Xylene	110	[72]
			Si/CMS	MMA	CuCl/$CuCl_2$	Bipy	DMSO[a]	80	[61]
			Ge/CMS	DMAEMA	CuCl/$CuCl_2$	Bipy	DMSO[a]	90	[62]
			CMS, BMS	CMS, BMS	CuCl/$CuCl_2$	Bipy	C_6H_5F	65	[63]
			EBB	GMA, *t*-BA	CuBr	PMDETA	Bulk[b]	110	[64]
			FPI		CuBr	PMDETA	DMF[c]	110	[65]
			PhEBr, PMMA	MMA	CuBr/$CuBr_2$	PMDETA	Anisole	110	[66]
$CH_2{=}CHC_6F_4R$	OMe	TFMS	PhEBr	St, FS	CuBr	Bipy	Xylene	110	[54]
	$OCH_2CF_2CF_3$	$TF(F_5)S$	PhEBr	St, FS	CuBr	Bipy	Xylene	110	[53]
	$OCH_2(CF_2)_6CF_3$	$TF(F_{15})S$	PS		CuBr	Bipy	Xylene	110	[53]
$CH_2{=}CHC_6H_4R$	F	4-F	PhEBr PMA	MA	CuBr	PMDETA	Toluene	91	[67]
	$CH_2OCH_2[CF(CF_3)OCF_2]_2CF_2CF_3$	FS_1	PS		CuBr	Bipy	Toluene/TFT	110	[68]
	$CH_2O(CH_2)_2(CF_2)_5CF_3$	FS_2	PS		CuBr	Bipy	Toluene/TFT	110	[68]

[a] DMSO: dimethyl sulfoxide.
[b] GMA and *t*-BA polymerizations performed in THF.
[c] DMF: dimethyl formamide.

ditrimethylolpropane (DiTMP) core and a dipentaerythritol (dipenta), respectively [57]. (The latter structure is shown in Fig. 26) All star-shaped PFS were prepared in bulk with the molar ratios of initiating groups:CuBr:bipy equal to 1:1:2. Normally the polymerizations were stopped at low monomer conversions to avoid star–star coupling, this was especially important in case of the six arm stars. Star PFS in a large molecular weight range 3000–70,000 were prepared that all demonstrated relatively low $M_w/M_n < 1.30$ (SEC). The tetraethyleneglycol core based four arm star PFS with as little as 8–10 wt.% TEG_4 demonstrated amphiphilic behaviour resulting in micelle formation in THF/water solutions [57]. The six arm PFSs, on the other hand, appear as super hydrophobic nanoparticles resisting all attempts to degrade the hexaester core with strong bases. A similar behaviour was demonstrated by a six arm segmented block copolymer prepared from dipenta and PS followed by PFS, in this case PFS forms a shell around a PS core.

Hyperbranched FS copolymers were prepared by atom transfer radical self-condensing vinyl copolymerization (ATR-SCVCP) of an inimer, either *p*-bromomethylstyrene (BMS) or *p*-chloromethylstyrene (CMS), and FS (Fig. 27) [63]. The conventional bipy was employed in combination with the catalysts CuCl or CuBr. Number average molecular weights from 3000–260,000 (polydispersities from 1.8 to 4.8) with degrees of branching typically 30% were obtained when the FS: inimer ~1–2. Solubility tests indicated that the polymers were soluble in a broad range of organic solvents, when extensive biradical coupling was avoided.

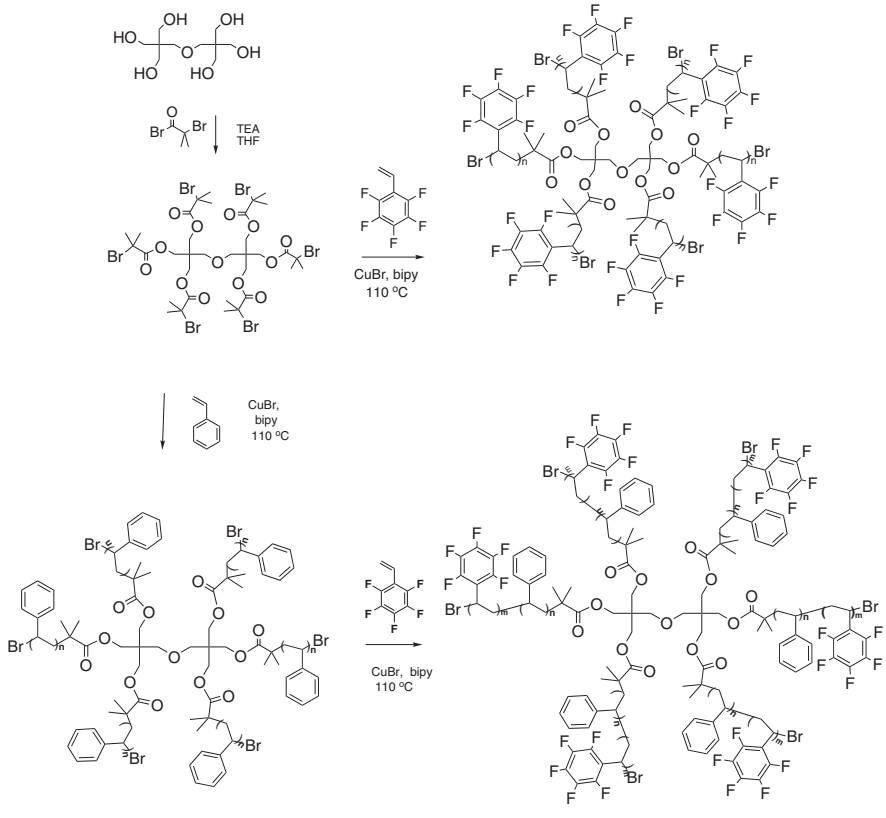

Fig. 26. Synthesis of star-shaped polymers on a dipentaerythritol core having six arms consisting of either PFS or PS-*b*-PFS [57].

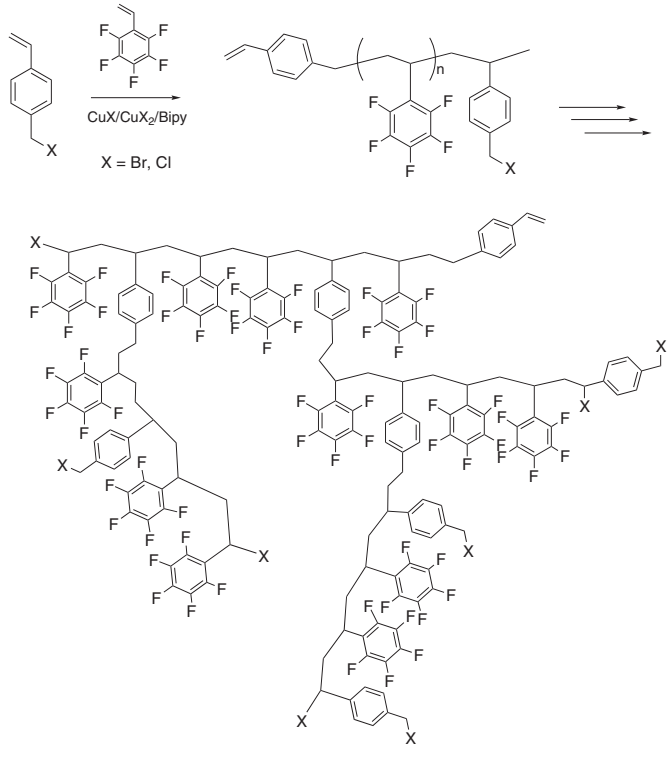

Fig. 27. Example of a hyperbranched structure synthesized by polymerization of FS using a BMS or CMS inimer [63].

3.1.3. Copolymerization with acrylic and methacrylic monomers

Amphiphilic block copolymers were obtained by sequencial ATRP of 4-fluorostyrene initiated by PhEBr and then employing the resulting poly(4-fluorostyrene) as MI for methyl acrylate [67], however, the reversed order was also employed. After hydrolysis the block copolymers assembled into micelles that were converted into shell-crosslinked nanoparticles by covalent stabilization of the acrylic acid residues in the shell.

Block copolymers of PFS and poly(*tert*-butyl acrylate) (P*t*BA), PFS-*b*-P*t*BA, were prepared by polymerization of *t*BA from a PFS-macroinitiator via ATRP [59]. Amphiphilic block copolymers of PFS and polyacrylic acid (PAA), PFS-*b*-PAA, were subsequently produced by hydrolysis of the P*t*BA blocks. The amphiphilic PFS-*b*-PAA copolymers could be cast into porous membranes by phase inversion in aqueous media. Three-dimensionally ordered membranes with well-defined pores of sizes in the micrometer range were obtained as a result of inverse micelle formation. The pH of the aqueous media for the phase inversion and the PAA content in the PFS-*b*-PAA copolymers could be used to adjust the pore size of the membranes.

PFS-*b*-PMMA was prepared by Kang et al. [60] from a conventionally ATRP synthesized PFS-MI and employed in the production of nanoporous PFS films after selective UV decomposition of the PMMA blocks. Nanoporous PFS films with pore sizes in the range 30–50 nm and porosity in the range 15–40% were obtained from PFS-*b*-PMMA copolymers with different PMMA content. Dielectric constants approaching 1.8κ have been realized in the nanoporous PFS films with a pore volume larger than 0.3 mL g^{-1}.

Both possible block copolymers of PFS and PMMA with narrow polydispersities (<1.15) were prepared by Bucholz and Loo [66]. The synthesized

copolymers showed well-ordered, periodic nanostructures upon annealing (cylindrical and lamellar structures dependent on the ratio of the two blocks). The segregation behavior was studied thoroughly (scanning electron microscopy (SEM) and small-angle X-ray scattering (SAXS)) and it was concluded that PFS/PMMA copolymers surprisingly are only twice as aggregating as PS/PMMA copolymers, which is believed to be due to the cancellation of polarity of the *ortho* and *meta* fluorine substituents.

Rod-coil (or tadpole-shaped) *block–graft* copolymers based on a PFS block and a glycidyl methacrylate polymer (PGMA) block with grafted P*t*BA side chains were synthesized by consecutive ATRPs [64]. Hydrolysis of the P*t*BA side chains in the *block–graft* copolymer into PAA side chains created an amphiphilic PFS-*b*-(PGMA-*g*-PAA) macromolecule with a brush-shaped hydrophilic head (rod) and a hydrophobic fluoropolymer tail (coil) (Fig. 28). The postulated macromolecular architecture was suggested by atomic force microscopy (AFM) images and micelle formation.

3.1.4. Copolymerization with other monomers and polymerization by macroinitiators

In the design of symmetrical block copolymers or star-shaped polymers initiators originally based on hydroxyl compounds ($M_n \sim 5000$–$12{,}000$ g/mol) that are converted quantitatively to bromoesters are often employed [69]. Thus very amphiphilic triblock copolymers based on various hydroxyl-terminated polyethers of different lengths were converted to MIs by reaction with bromo acids (Fig. 29) [58]. From these a number of triblock copolymers with very short PFS end blocks were prepared by ATRP. The amphiphilic triblock copolymers have very interesting material properties such as good Li^+ complexation while preserving excellent film forming capabilities. Since the Li^+ conductivity is high, such materials seem prospective for solid-state electrolyte applications in batteries.

Hydroxyl terminated polydimethylsiloxane (PDMS) was converted to a bromine ester and utilized in ATRP for FS [70]. PDMS with varying degrees of polymerization (DP) $\sim$ 15–50 was prepared by living anionic polymerization and the resulting PDMS-*b*-PFS polymers had M_ns of 12,000–25,000 ($M_w/M_n \sim 1.13$–1.18) and contained 9–33 wt.% PDMS. The synthesized PDMS-*b*-PFS copolymers were intended as precursors for nanoporous materials after removing the PDMS block by selective etching with HF [71].

Comb-shaped copolymers consisting of a rigid fluorinated polyimide (FPI) backbone and well-defined PFS side-chains (FPI-*g*-PFS) were synthesized from a bromide-containing FPI MI by ATRP

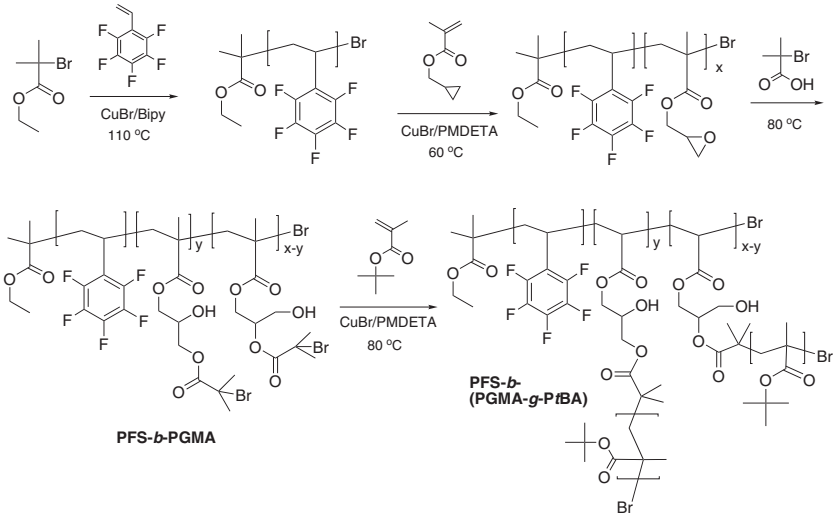

Fig. 28. Synthesis of tadpole-shaped copolymer PFS-*b*-(PGMA-*g*-P*t*BA) [64]. After hydrolysis the amphiphilic copolymer PFS-*b*-(PGMA-*g*-PAA) is formed, when the *t*BA ester is converted to a carboxylic acid group.

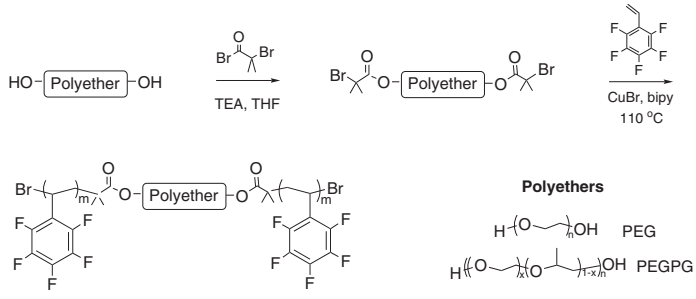

Fig. 29. Functionalized polyethers utilized as macroinitiators for the synthesis of triblock copolymers with PFS end-blocks [58].

[65] (Fig. 30). When the FPI backbone consists of 14 repeating units and the PFS side chains contained 32–93 repeating units, ordered arrays of the comb-shaped macromolecules, consisting of rigid FPI rods of 20–30 nm in length and flexible PFS brushes (side chains) of 4–6 nm in width, were imaged by AFM. In addition to having a dielectric constant (κ) as low as 2.1, the resulting comb-shaped FPI-*g*-PFS copolymer also exhibited good solution processability and good thermal stability up to 470 °C. The FPI-*g*-PFS copolymer is therefore suggested as a potential ultralow-κ material for submicron and nanolevel electronics.

Fluorinated diblock copolymers with PFS have been prepared by ATRP initiated by CCl_3-terminated poly(vinylidene fluoride) (PVDF) blocks derived by telomerization [72]. The traditional ATRP protocol with CuBr and bipy was employed in xylene solution at 130 °C when PVDF-CCl_3 had DP = 15, whereas the polymerization initiated by the insoluble PVDF-CCl_3 with DP of approx. 70 ($M_n \sim 4600$) was performed in bulk. Block copolymers with PVDF content between 12 and 19 wt.% and M_n from 5000 to 15,700 ($M_w/M_n \sim 1.14$–1.34) were prepared. These novel PVDF-*b*-PFSs demonstrated higher thermal resistance compared to the PVDF block and were intended as novel piezoelectrical material candidates with improved thermal resistance.

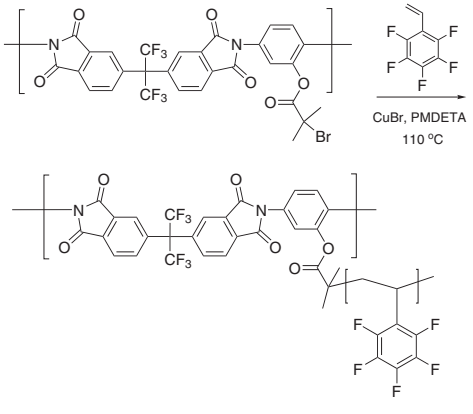

Fig. 30. Comb-shaped copolymers with a rigid FPI-backbone and PFS graft side chains [65].

3.1.5. Surface initiated ATRP of fluorinated styrenes

Trichloro(4-chloromethylphenyl)silane was immobilized on the surface of SiO_2 nanoparticles and employed for consecutive ATRP of FS and divinylbenzene (DVB) [73]. The resulting SiO_2-*g*-PFS-*b*-PDVB nanoparticles were allowed to agglomerate on a silicon substrate to form 2–4 μm films that were UV irradiated. Crosslinking of the residual double bonds in the outer PDVB layer of the core shell nanospheres strengthen the films. The silica cores were removed by HF etching producing nanoporous fluoropolymer films having dielectric constants as low as 1.7κ.

Surface initiated ATRP has also been used to produce stimuli-responsive semifluorinated polymer brushes on a silica substrate [46]. The brushes consisted of a PS inner block and a PFS outer block. Solvent-induced diblock rearrangement experiments were performed using a selective solvent (cyclohexane) for the PS block to generate a fluorine-deficient surface. The diblock system exhibited a water contact angle typical for PS blocks after this solvent treatment. Tensiometric data indicated that the polymer brush layers rearranged reversibly to form

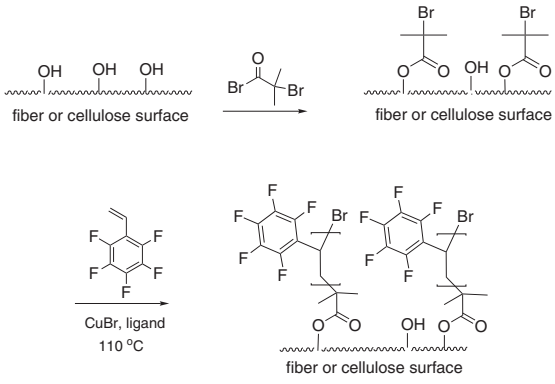

Fig. 31. The principal route for ATRP of FS on a fiber surface [74,76].

either a PS or a PFS enriched air–polymer interface depending upon the nature of the solvent (treatment with cyclohexane or fluorobenzene, respectively).

Linear, branched and highly branched (arborescent) PFS-silicon hybrids were prepared via surface initiated ATRP from the CMS inimer and sulfonyl chloride-modified CMS immobilized on hydrogen-terminated Si(100), or SiH, surfaces [61]. Kinetics investigations indicated that the chain growth of PFS from the functionalized silcon surfaces was consistent with a controlled process. AFM images revealed that the surface-initiated ATRP of PFS had proceeded uniformly on the Si-CMS surface to provide a dense and molecularly flat surface coverage of the linear brushes. The uniformity of surfaces with branched brushes was controlled by varying the feed ratio of the monomer and the CMS inimer. Furthermore, the active PFS ends were used as MIs for MMA polymerization producing diblock copolymer brushes. In a somewhat similar approach UV-induced attachment (hydrogermylation) of CMS on the hydrogen-terminated Ge(100) (Ge–H) surface provided a stable Ge–C bonded initiator monolayer for the surface initiated ATRP of FS [62]. Well-defined PFS-Ge hybrids, consisting of covalently tethered PFS brushes were prepared. In this case subsequent surface initiated block copolymerization with DMAEMA could be performed in a controlled manner.

Surface-initiated ATRP of FS [74] has recently been performed onto five different cellulose surfaces and fibers: cotton, jute and hemp fibers in addition to microcrystalline cellulose and filter paper. Hydroxyl groups on the specific surfaces were transformed to corresponding 2-bromoisobutyrates or 2-bromopropionates, which were then employed as initiating groups for ATRP of different monomers [74–76] (Fig. 31). The ATRP of FS was conducted either in bulk or in toluene solution and catalyzed using CuBr/bipy, CuBr/PMDETA or CuBr/Tris[2-(dimethylamino)ethyl]amine (Me_6TREN) with or without a sacrificial initiator. In the latter case no polymer was created in the bulk, whereas in the former the separately initiated bulk PFS was used to analyze the molecular-weight characteristics by SEC, as it should mimic the properties of the attached polymer. Analytical flash pyrolysis in combination with GC/MS [76] offered the possibility to estimate the chain length of the grown polymer. In the case of FS it was estimated that 1000 monomer units were attached on the surface of the jute fibers, whereas in the case of ATRP of styrene only 100 units were found. Depending on the surface area of the used virgin sample ATRP of FS resulted in the attachment of 3–47 wt.% PFS. The initially hydrophilic fibers became extremely hydrophobic after grafting with PFS. Additionally, attachment of the fluorinated polymer imparted the high thermostability and chemical resistance of fluoropolymers to the fibers (TGA). Possible applications of the novel materials could be as reinforced corrosion resistant gaskets.

3.2. Fluorinated polystyrenes synthesized by NMP

Hydrophobic di- and triblock copolymers of PS and *p*-substituted fluoroalkoxy methylstyrene were prepared by nitroxide-mediated controlled

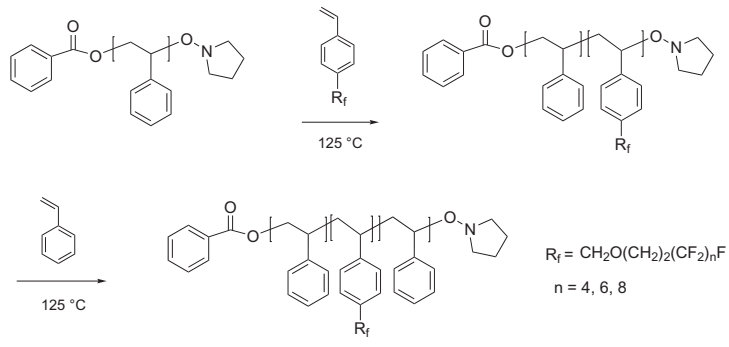

Fig. 32. NMP utilized for synthesis of triblock copolymers of PS with a middle block consisting of *p*-substituted PS [77].

polymerization by Andruzzi et al. (Fig. 32) [77]. The block copolymers demonstrated a tendency to form layered mesophases in the bulk. When the length of the fluorocarbon chains was increased the degree of order of the mesophase enhanced from a disordered smectic to an ordered pseudohexagonal smectic. This was attributed to the interplay between the rod-like nature of the fluorinated chains and the phase separation on the molecular level of the different incompatible components in the polymer. In addition, an unexpected enhancement of the surface organization was observed, which was ascribed to the aromatic groups [78]. Furthermore, block copolymer films exhibited rather high advancing water contact angles (up to 130°), which were constant over time. Near-edge X-ray absorption fine structure (NEXAFS) studies were used to probe the surface coverage of the fluorinated segments. This strongly supports that the fluorinated block copolymers form fluorine enriched film surfaces and the polymer design points to a route to engineer low surface energy polymers.

The above-mentioned work was continued to include studies of polymerization of diblock copolymers of PS and *p*-substituted fluoroalkoxy methylstyrene by NMP on planar silicon oxide surfaces [79]. By angle-resolved XPS and water contact angles studies it was shown that the second block (used to produce the copolymer brushes) was always exposed at the polymer–air interface regardless of its surface energy. Furthermore, it was strongly evidenced that the brushes were stretched and therefore created a layer so dense that the outermost block in all cases completely covered the surface. Moreover, it was concluded that these block copolymer brushes can be employed to accurately tailor the physicochemical properties of a polymer film, allowing precise control over surface stability, molecular structure, and behavior.

4. Fluorinated alkenes

MA has been randomly copolymerized with the fluorinated alkenes F-hexene, F-octene and F-decene (see Fig. 33) by ATRP [80]. The resulting copolymers had PDIs lower than 1.33 and the length of the fluorinated alkyl chain did not seem to influence the reaction rate of the monomers relative to each other, although the perfluorinated monomers in all cases reacted faster than the parent 1-alkenes. XPS-analysis showed segregation of the fluorinated chains at the surfaces of polymer films cast on glass.

5. Fluorine-containing initiators and macroinitiators

This part is devoted to a survey on controlled radical polymerizations where fluorine-containing

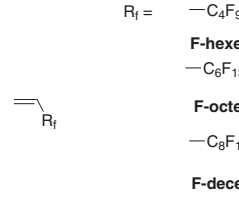

Fig. 33. Fluorinated alkenes polymerized by ATRP by Borkar and Sen [80].

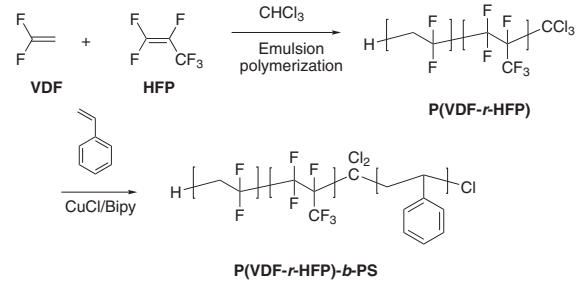

Fig. 34. P(VDF-*r*-HFP) used as macroinitiator for styrene by Shi and Holdcroft [84].

initiators have been employed. This includes commercially available as well as synthesized fluoropolymers that have been functionalized and subsequently employed as macroinitiators to prepare semifluorinated block copolymers, as well as smaller compounds utilized in the same fashion. Finally, this part also has examples of fluorinated compounds used to assist in controlled radical polymerizations e.g. as transfer agents in RAFT.

5.1. Fluorine-containing initiators and macroinitiators in ATRP

5.1.1. PVDF-based macroinitiators

PS-*b*-PVDF-*b*-PS block copolymers have in principle been prepared by a combination of telomerization and ATRP of styrene, starting from a $BrCF_2$-terminated vinylidene fluoride (VDF) difunctional telomer [82]. However, the reaction times extended over several days, molecular weights were uncontrolled, and the polydispersities were large.

On the other hand, by use of α-trichloromethylated VDF telomers (with number average degrees from 1 to 11) as initiators new PVDF-based block copolymers with PS, PMA and PMMA have been synthesized [83]. The initiators, resulting from telomerization of VDF with chloroform, promoted fast initiation relative to propagation in ATRP of styrene and (meth)acrylates. By varying the telomer molecular weight and the ratio between telomer and monomer in ATRP, respectively, the chain length of both blocks and copolymer composition could be predetermined.

Shi and Holdcroft chose to incorporate hexafluoropropene (HFP) in VDF by random copolymerization to avoid crystallization of the latter [84]. Trichloromethyl-terminated P(HFP-*r*-VDF) with molecular weights up to 25,000 were obtained by emulsion polymerization in the presence of chloroform and subsequently used to initiate the ATRP of MMA and styrene (Fig. 34). The P(VDF-*r*-HFP)-*b*-PS and P(VDF-*r*-HFP)-*b*-PMMA demonstrated phase-separated morphology in the solid state and possessed distinct T_gs associated with fluoropolymer, PS and PMMA domains. The PS-block of P(VDF-*r*-HFP)-*b*-PS was later partially *para*-sulfonated and showed great potential as a proton conducting membrane having a performance comparable to Nafion [85]. The high proton conductivity was believed to be partially due to the microphase separation of the two polymer blocks, which led to the formation of channel networks in the membranes. Further studies (small-angle neutron scattering (SANS) and TEM) showed a greater degree of large-scale ordering for membranes from copolymers with a partially sulfonated block compared to a fully sulfonated, while the internal structure of the PS-domain determines the conductivity [86].

Direct initiation of the secondary fluorinated site of high molecular weight PVDF has been exploited in the preparation of amphiphilic graft copolymers by ATRP [87]. The hydrophilic comonomers were either poly(ethylene glycol) methyl ether methacrylate (PEGMA, $M_n = 475$) or *tert*-butyl methacrylate in the ATRP step, where the latter was employed as a precursor for poly(methacrylic acid). Surface segregation of PVDF-*g*-PEGMA additives in PVDF was examined as a route to wettable, fouling-resistant surfaces on PVDF filtration membranes. Only 5 wt.% copolymer in the membrane with 3.4 wt.% PEGMA exhibited a near-surface PEGMA concentration of 42 wt.% as measured by XPS.

PVDF-*g*-PCMS membranes have been prepared by preirradition grafting of CMS solutions in toluene onto 80 μm PVDF films [88]. These membranes

were employed for ATRP of styrene with CuCl or CuBr and bipy at 120 °C. The polymerization increased linearly with time up to at least 400% PS grafting. This implicated first-order kinetics and a controlled radical polymerization. Finally, the membranes became proton-conducting after sulfonation of the PS grafts. The highest conductivity measured for the prepared membranes was 70 mS/cm, which is comparable to the values normally measured for commercial Nafion® membranes. SEM/energy-dispersive X-ray results implied that the membranes had to be grafted throughout the matrix with both PCMS and PS to become proton-conducting after sulfonation.

Films of PVDF were treated by Liu et al. [89,90] with LiOH to generate oxygen-containing functionalities on the polymer chains by elimination of HF followed by reduction, ultimately forming a PVDF functionalized with OH-groups on the surface. This was in turn reacted with EBB yielding a macroinitiator for ATRP equipped for fashioning polymer brushes on the film surface. Brushes of MMA and PEGMA ($M_n \sim 300$ g/mol) were synthesized successfully using CuBr/HMTETA and $CuCl/CuCl_2$/bipy, respectively. DMAEMA was further copolymerized onto the PMMA and PEGMA brushes (CuBr/HMTETA) forming block copolymer grafts on the PVDF surface. The static contact angle of water on the films was reduced from 93° to 84° by the introduction of PMMA-brushes, while PEGMA and/or PDMAEMA brushes gave values around 60°.

The above-mentioned research group [91] attempted a slightly different strategy to acquire hydrophilic polymer brushes on a PVDF film surface: direct polymerization from the fluorinated sites. Using this approach, brushes of PEGMA ($M_n \sim 300$ g/mol) and DMAEMA were attached to PVDF films, and PS was also added as a second block to the brushes. The PVDF-*g*-PEGMA showed an enhanced resistance to protein fouling (BSA).

2-(2-Bromoisobutyryloxy)ethyl acrylate (BIEA) was polymerized on the surface of ozone-pretreated PVDF and further used as macroinitiator for functional monomers sodium 4-styrenesulfonate (NaSS) and PEGMA ($M_n \sim 360$ g/mol) to yield branched graft copolymers (Fig. 35) [92]. Membranes of PVDF-*g*-PBIEA-*g*-NaPSS cast in 1 M aq. NaCl solution were enriched in NaPSS side chains on the surface and had larger pore sizes compared to membranes cast in water (phase inversion). Porous PVDF-*g*-PBIEA membranes were used to run ATRP of PEGMA and the resulting PVDF-*g*-PBIEA-*g*-PPEGMA copolymer membranes exhibited substantially improved antifouling properties in protein adsorption studies (γ-globulin). DMAEMA was also polymerized by ATRP from a porous PVDF-*g*-PBIEA membrane [93] albeit to a very low conversion (<5%). The PDMAEMA pendants were quarternized utilizing hexylbromide thereby forming cations both on the surface and in the pores. Membranes of PVDF-*g*-PBIEA-*g*-PDMAEMA functionalized in

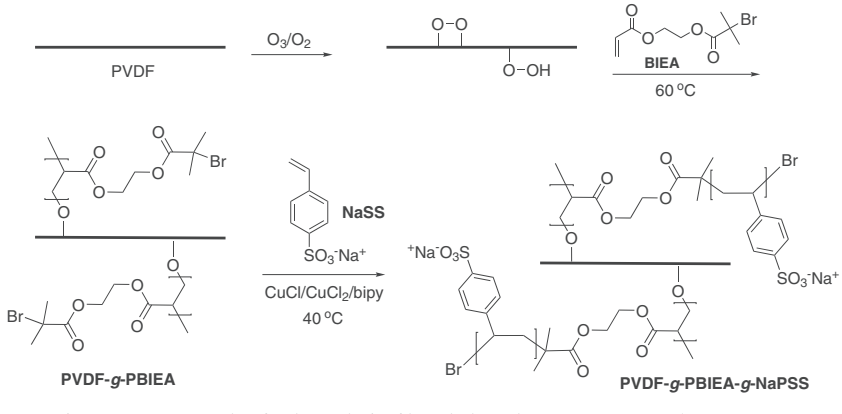

Fig. 35. PVDF as template for the synthesis of branched copolymers PVDF-*g*-PBIEA-*g*-NaPSS [92].

this fashion inhibited bacterial growth on the membrane surface (*E. Coli*).

5.1.2. Other fluorinated initiators and macroinitiators

Semifluorinated PMMA and PS copolymers were obtained by incorporating fluorinated moieties by the use of fluorinated initiators [30,31]. The initiators were different fluorinated bromoisobutyryl esters prepared by esterification of various fluorinated telomers: perfluoroalkyl ethanol, 2-perfluoroalkyl ethyl-copoly(ethylene glycol), or a dihydroxy functional telomer based on trimethylol propane (Fig. 36). These α-perfluoroalkyl initiators provided well-defined block copolymers in the ATRP of MMA at 90 °C utilizing the CuBr/*N*-pentyl-2-pyridinalmethanimine catalyst system in toluene. The important finding is that the presence of the fluorinated organics does not interfere detrimentally with the controlled polymerization mechanism. Furthermore, this approach is also strongly advocated as a versatile route to a range of interesting surface active materials.

The same approach was used for synthesizing the fluorinated initiator containing a poly(ethylene glycol)-segment mentioned above. The initiator was in this instance [33] employed for the homopolymerization of PPGM at 80 °C in methyl ethyl ketone (CuBr/PMDETA). The resulting polymer had a molecular weight of 5200 g/mol (DP = 10) determined by ^{13}C NMR, which corresponded well with the theoretical value.

Perfluorobutyl iodide (F_9-I), 1H,1H-heptafluorobutyl iodide (F_7-I) and 1,4-diiodo-perfluorobutane (I-F_8-I) with $–CF_2CH_2I$ or $–CF_2CF_2I$ end groups were initially used as model initiators for ATRP of MMA [81]. The homopolymerization of MMA with the initiators was slow, when the system F_7-I/CuBr/bipy was used, but the first order kinetic plot showed linearity. The ATRP proceeded rapidly when the perfluorinated F_9-I was used in conjunction with CuCl(or Br)/bipy complex and slowly when CuI was used instead. The best initiating efficiency was seen with the system using CuCl. The F_x-groups from the initiators employed in the PMMA homopolymers were detected by ^{19}F NMR. Regrettably the PVDF-I and I-PVDF-I applied as MIs for the production of block copolymers with MMA showed low initiator efficiency because the propagation rate was much faster than the initiation rate.

Perfluoropolyether (PFPE) with M_n of 1400 was the CO_2-philic anchor part of four stabilizer materials bearing different PMMA-philic head groups (PFPE-alcohol, PFPE-acetate, PFPE-methacrylate and PFPE-*b*-PMMA) [94]. The most effective stabilizer for the dispersion polymerization of MMA in $scCO_2$ was the block copolymer PFPE-*b*-PMMA, prepared by ATRP of MMA in solution of pentafluorobutane using PFPE-bromoester as macroinitiator (Fig. 37). The ratio of PFPE to PMMA could be varied by using PFPE-macroinitiators with various lengths on which block copolymers with different PMMA compositions could be positioned. The influence of the ratio of polymer-philic to CO_2-philic segment in a surfactant on the stabilizer efficiency was discussed. A ratio of 1.1 in the block copolymer ($M_n \sim 4000$ g/mol) led to the best result: high molecular weight PMMA in excellent yield with a very fine particle morphology.

A thorough study of surface characteristics is found in a contribution from Koh et al. [95], where incompletely condensed, fluorinated polyhedral oligomeric silsesquioxane (Fig. 38) with the highly reactive trisodium silanolate was used for the synthesis of an ATRP fluorine-initiator for MMA. In

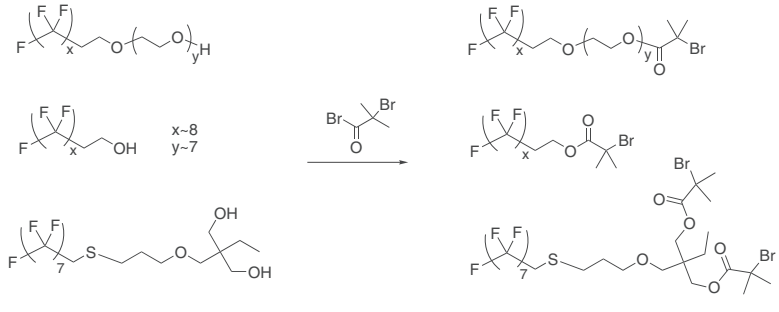

Fig. 36. Fluorinated macroinitiators synthesized by Perrier et al. [30] by esterification of hydroxyl-terminated fluorinated compounds.

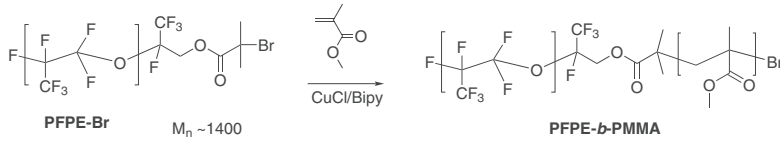

Fig. 37. PFPE-*b*-PMMA used as stabilizer for the dispersion polymerization of MMA in $scCO_2$ [94].

a blend of the resulting tadpole-shaped functional polymer with a matrix PMMA the functional polymer preferentially populated the air–polymer interface. The outermost layer of the film was almost completely covered by the fluorine-containing head (initiator moiety) due to its low surface energy. Additionally, strong resistance to ion etching (Ar^+) was found, owing to the unique polyhedral oligomeric silsesquioxane structure.

Triblock copolymers have been synthesized, where the central block was based on a perfluorocyclobutane polymer (PFCB), while the outer blocks consisted of PMMA [96]. The block copolymers had narrow molecular weight distributions (PDI < 1.3) and molecular weights up to 30,000 g/mol. Cycloaddition [2 + 2] of 4,4′-bis(trifluorovinyloxy)biphenyl led to the PFCB, which could in turn be transformed into a macroinitiator by functionalization with 2-bromo-1-(4-trifluorovinyloxyphenyl)-propan-1-one (Fig. 39). The latter compound was also successfully used as initiator for MMA to synthesize PMMA with a terminal fluorinated group. PFCB has lately come in to focus, as it has superior optical and processability properties compared to other fluoropolymers.

The authors of this review has previously found, that even short segments of fluorinated polystyrene in block copolymers with styrene impart highly hydrophobic characteristics for the materials even at low fluorine content [53]. Thus, we have synthesized different mono and difunctional aliphatic as well as aromatic F-initiators for ATRP by reacting

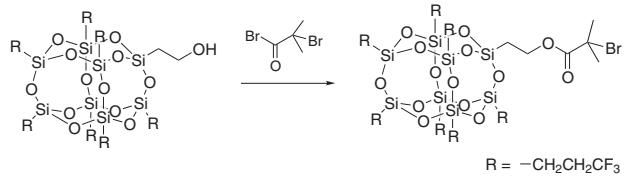

Fig. 38. Polyhedral oligomeric silsesquioxane used as macroinitiator for MMA [95].

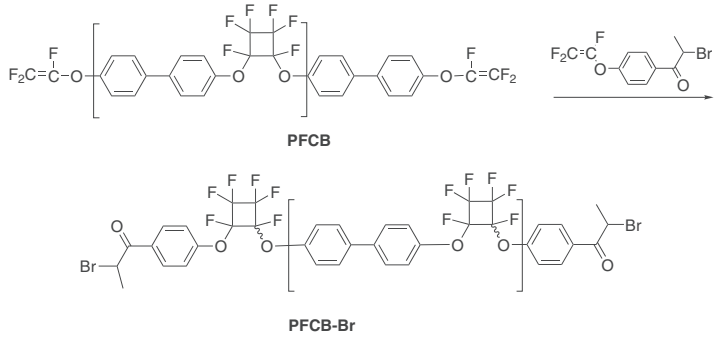

Fig. 39. Derivatization of the PFCB polymer by cycloaddition to yield a fluorinated macroinitiator for ATRP [96].

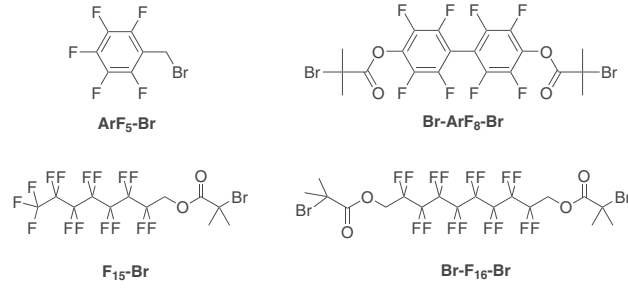

Fig. 40. Fluorinated mono and difunctional initiators used by Jankova et al. [97] for the homopolymerization of PS.

2-bromoisobutyrylbromide with the corresponding alcohols [57,69,97]. In this way a monofunctional F_{15}–Br initiator and two bifunctional initiators Br–F_{16}–Br and Br–ArF_8–Br were synthesized (structures shown in Fig. 40). Together with the commercial pentafluorophenyl ethylbromide (ArF_5–Br) these initiators were used for ATRP of styrene, which yielded chain-end- and in-chain-fluorine functionalized PSs. The five aromatic fluorine atoms (ArF_5–) are not sufficient to change the surface characteristics of PS (investigated by CA of water droplets). The functional PS from Br–ArF_{16}–Br probably possesses a quite stiff structure, hence no definite surface enrichment is seen even when decreasing the molecular weight (increasing relative fluorine content). Terminal aliphatic fluorine-containing groups generally seem more effective than internal, indicating that the former are more mobile. This influence is naturally dependent on the molecular weight, since the effect is reduced with increasing molecular weight.

5.2. Fluorine-containing initiators and macroinitiators in RAFT

5.2.1. PVDF-based macroinitiators

PVDF with "living" PEGMA ($M_n \sim 300$ g/mol) side chains (PVDF-*g*-PEGMA) was prepared through molecular graft copolymerization of the PEGMA macromonomer with ozone-preactivated PVDF backbone in a RAFT-mediated process [98]. Microfiltration (MF) membranes were fabricated from the amphiphilic PVDF-*g*-PEGMA comb copolymers by phase inversion in aqueous medium. Surface composition analysis revealed a substantial surface enrichment of the PEGMA graft chains with more uniform pore size distribution compared to similar membranes prepared by conventional radical polymerization without transfer agent. The PVDF-*g*-PEGMA MF membranes displayed substantial resistance to γ-globulin fouling, in comparison to the pristine hydrophobic PVDF MF membranes.

PVDF-*g*-poly(acrylic acid) (PVDF-*g*-PAA) copolymers with well-defined PAA side chains were synthesized by RAFT-mediated graft copolymerization of acrylic acid with ozone-pretreated PVDF [99]. MF membranes were prepared from the PVDF-*g*-PAA copolymers by phase inversion in an aqueous solution. The MF membranes were enriched with PAA on the surface, including the pore surfaces, and had a uniform pore size distribution. The PVDF-*g*-PAA membrane was further functionalized in a subsequent surface-initiated block copolymerization with *N*-isopropylacrylamide (NIPAAM). The resulting PVDF-*g*-PAA-*b*-PNIPAAM membranes exhibited both pH- and temperature-dependent permeability for aqueous solutions. This membrane was argued to provide reversible temperature-dependent permeability for model drug solutions as e.g. calcein and FI-TC dextran in phospate buffer (pH 7.4), with the most drastic change in drug permeability being observed in the temperature range between 27 and 32 °C.

5.2.2. Other fluorinated initiators and macroinitiators

Thermally initiated graft polymerization of PEGMA ($M_n \sim 300$ g/mol) with ozone-pretreated fluorinated polyimide (FPIDS) (Fig. 41) via RAFT was carried out by Chen et al. [100]. Two interesting materials were produced from these FPIDS-*g*-PEGMA comb copolymers: (i) Solution casting of the graft copolymers followed by thermal decomposition of the labile PEGMA side chains in air,

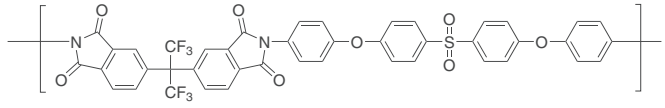

FPIDS

Fig. 41. Polyimide containing phenylsulfone groups in the backbone used by Chen et al. [100] for synthesizing FPIDS-*g*-PPEGMA comb polymers.

resulted in nanoporous FPIDS films with ultra-low dielectric constants (approaching 2.0). With porosities in the range of 2–10% and pore sizes in the range of 20–50 nm, these pores were more well-defined and the retention of the mechanical properties was better than when the corresponding nanoporous films were obtained from graft copolymers prepared by conventional free radical process [100]. (ii) Porous MF membranes were fabricated from the same amphiphilic graft copolymers FPIDS-*g*-PEGMA by phase inversion in aqueous media. XPS revealed a substantial surface enrichment of the hydrophilic component. The pore size distribution in this case was also found to be more uniform than that of the parent membranes from the conventional free radical process [90].

Surface modification of PTFE films by well defined comb copolymer brushes was carried out by Yu et al. [101]. Peroxide initiators were generated directly on the PTFE film surface, and PGMA brushes were generated by a surface-initiated RAFT in the presence of a chain transfer agent. The epoxy groups in PTFE-*g*-PGMA were transformed to initiating groups for ATRP by reaction with 2-bromo-2-methylpropionic acid. The resulting PTFE-*g*-PGMA–Br material was used as a macroinitiator for the ATRP of two hydrophilic vinyl monomers, thus including the PEGMA and sodium salt of poly(4-styrenesulfonic acid) in the comb copolymer brushes on the PTFE structure. Novel surface functionalities and molecular architectures arose in this way by introducing well-defined graft chains onto inert F-polymer films via surface-initiated CRP.

6. Fluorinated RAFT agents

Numerous species have been employed as RAFT agents [102]. Several groups have employed fluorine-containing compounds and proved their ability to act as transfer agents for RAFT of different monomers. The structures of tested fluorinated transfer agents are shown in Fig. 42. Good control of the polymerization of MA with cumyl *p*-fluorodithiobenzoate (CPFDB) was found and the fluorine-containing end groups were detected by electrospray ionization mass spectrometry [103]. Utilizing benzylfluorodithioformate (BFDF) in RAFT yielded well-defined PS and the experiments held promise for the development of a novel class of fluorinated RAFT agents [104]. The use of *O*-pentafluorophenyl *S*-benzyl xanthate (PFPBX) for the synthesis of PS by RAFT was attempted, but the obtained products had very broad molecular weight distributions (PDI > 1.6) [105]. The two xanthates F-MADIX and PF-MADIX were used to synthesize PS and PEA with good control over molecular weight distributions [106]. PF-MADIX showed the best performance yielding polymers with PDI as low as 1.09, but also required longer reaction times. F-MADIX was furthermore utilized in a RAFT-mediated ab initio emulsion polymerization of St with a good control [107]. The particle size could also be controlled by changing the F-MADIX concentration. It is argued that this happens because of a change of the F-MADIX living group's water solubility. Five original ω-perfluorodithioesters (ω-FTE) were employed in the RAFT of St, MMA, ethyl acrylate (EA) and 1,3-butadiene [108]. Block copolymers PMMA-*b*-PS and PEA-*b*-PS bearing these fluorinated moieties were also synthesized. Four dithioesters (φ-FTE) with fluorinated aromatic Z-groups were synthesized and utilized for RAFT of MMA with high yields and low polydispersities (<1.1) [109].

7. Fluorinated polymers by derivatization

Various fluorinated materials have been synthesized by postderivatization, i.e. modification of an existing (co)polymer by reacting different functional groups on the original material with smaller fluorine-containing molecules. We have found this type of work to be beyond the scope of this review, as we have chosen to concentrate on controlled polymeri-

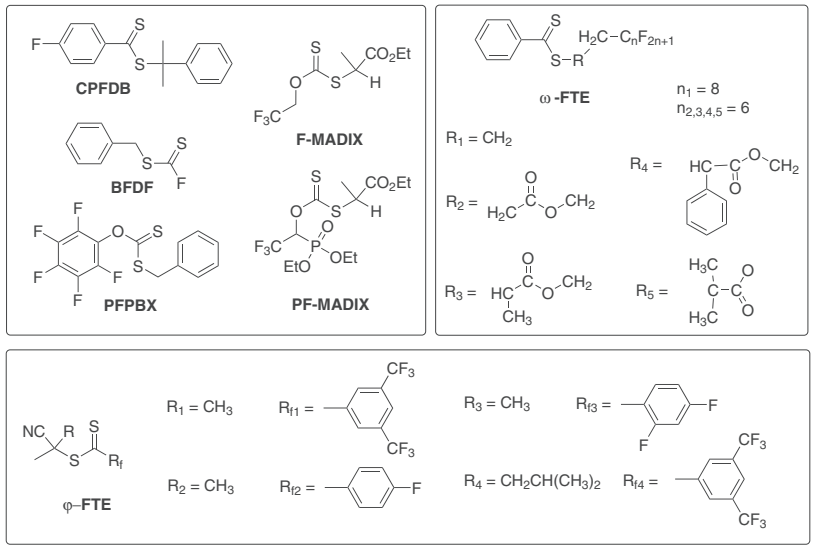

Fig. 42. Fluorinated RAFT agents used in the literature: CPFDB [103], BFDF [104], PFPBX [105], F-MADIX and PF-MADIX [106], ω-FTEs [108] and φ-FTEs [109].

zation reactions that directly involve fluorinated species.

8. Conclusions

The application of various fluorinated monomers, especially acrylates, methacrylates and styrenes that are particularly susceptible to different controlled radical polymerization protocols, have produced a large number of novel materials with unsurpassed and unique properties. The kinetics of several fluorinated monomers have been studied extensively in order to obtain information on the relationship between structure and reactivity. A number of different polymer architectures incorporating fluorinated polymers have been made possible through controlled radical polymerizations including star-shaped, graft, block and branched copolymers. The greatest challenge of synthesizing these novel materials is often the analysis of the final products due to their low solubility.

The very hydrophobic nature of fluoropolymer blocks has been exploited especially in the design of functional, amphiphilic block copolymers. Fluorinated block copolymers have been used to prepare low energy surfaces including water- and oil-repellent materials. Some polymers have also had the same effect, when used as additives in other polymers. Several fluorinated surface active compounds have been synthesized by controlled radical polymerizations and successfully used to assist polymerizations of non-fluorinated polymers in supercritical carbon dioxide. Biomimicking and potentially biocompatible copolymers have been introduced by combining inert fluoropolymers with biopolymers or polymers known to circumvent immunological rejection. Amphiphilic fluorinated copolymers have shown potential as coatings for metals by either instigating the formation of nanoparticles in a colloid solution or forming a corrosion-protective layer on a surface. The chemical inertness of fluorine has been exploited for synthesizing materials resistant to ion-etching. By forming covalent bonds in the outer layer of micelles of diblock copolymers in solution shell-crosslinked nanoparticles with a fluorinated core were engendered. Surface-initiated polymerizations of (co)polymer brushes on various surfaces have produced hydrophobic surfaces as well as materials that are tunable in hydrophobicity and permeability dependent on treatment in terms of change in pH, temperature, or solvent. A range of porous membranes with three-dimensionally ordered structures have been prepared and some have shown great potential as proton-conducting

materials for applications such as solid-state electrolytes in batteries. Low dielectric constant materials have also been realized in this fashion and seem prospective for uses in nanolevel electronics.

Fluorinated compounds including commercially available polymers have been used as macroinitiators for non-fluorinated monomers to incorporate a fluorinated species in this way. Focus in the area has especially been on tethering brushes of non-fluorinated polymers onto the fluoropolymer in this way benefiting from the inertness of the parent polymer and enhancing performance with respect to antifouling, conduction and/or permeability.

In conclusion the use of controlled radical polymerization methods for synthesizing fluorinated polymers has already realized numerous materials for various appliances and we envisage many more applications in the future.

Acknowledgements

Aage and Johanne Louis–Hansen's Foundation (DK), Materials Research, Danish Research Agency and Danish ministry of Science Technology and Innovation through grant 61,568: Polymetal-Centre for Selective Micro Metallization of Polymers are gratefully acknowledged for financial support. Novo Nordisk A/S and The Graduate School of Polymer Science are thanked for their support towards Ms. Hansen's Ph.D.-stipend.

References

[1] Ebnesajjad S, Khaladkar PR. Fluoropolymer applications in chemical processing industries. Norwich, NY: William Andrew, Inc.; 2005.
[2] Matyjaszewski K. Controlled/living radical polymerizations: from synthesis to materials. ACS, Washington, DC: Oxford University Press; 2006.
[3] Lacroix-Desmazes P, Ameduri B, Boutevin B. Use of fluorinated organic compounds in living radical polymerizations. Collect Czech Chem Commun 2002;67(10):1383.
[4] Ameduri B, Boutevin B. Well-architectured fluoropolymers: synthesis, properties and applications. Amsterdam: Elsevier; 2004.
[5] Darling TR, Davis TP, Fryd M, Gridnev AA, Haddleton DM, Ittel SD, et al. Living polymerization: rationale for uniform terminology. J Polym Sci, Part A: Polym Chem 2000;38(10):1706.
[6] Georges MK, Veregin RPN, Kazmaier PM, Hamer GK. Narrow molecular-weight resins by a free-radical polymerization process. Macromolecules 1993;26(11):2987.
[7] Moad G, Rizzardo E, Solomon DH. Selectivity of the reaction of free-radicals with styrene. Macromolecules 1982;15(3):909.
[8] Lagrille O, Cameron NR, Lovell PA, Blanchard R, Goeta AE, Koch R. Novel acyclic nitroxides for nitroxide-mediated polymerization: kinetic, electron paramagnetic resonance spectroscopic, X-ray diffraction, and molecular modeling investigations. J Polym Sci Part A: Polym Chem 2006;44(6):1926.
[9] Hawker CJ, Bosman AW, Harth E. New polymer synthesis by nitroxide mediated living radical polymerizations. Chem Rev 2001;101(12):3661.
[10] Harth E, Van Horn B, Hawker CJ. Acceleration in nitroxide mediated 'living' free radical polymerizations. Chem Commun 2001;1(9):823.
[11] Siegenthaler KO, Studer A. Nitroxide-mediated radical polymerization/increase of steric demand in nitroxides. How much is too much? Macromolecules 2006;39(4):1347.
[12] Benoit D, Chaplinski V, Braslau R, Hawker CJ. Development of a universal alkoxyamine for "living" free radical polymerizations. J Am Chem Soc 1999;121(16):3904.
[13] Benoit D, Grimaldi S, Robin S, Finet JP, Tordo P, Gnanou Y. Kinetics and mechanism of controlled free-radical polymerization of styrene and *n*-butyl acrylate in the presence of an acyclic beta-phosphonylated nitroxide. J Am Chem Soc 2000;122(25):5929.
[14] Knoop CA, Studer A. Hydroxy- and silyloxy-substituted TEMPO derivatives for the living free-radical polymerization of styrene and *n*-butyl acrylate: synthesis, kinetics, and mechanistic studies. J Am Chem Soc 2003;125(52):16327.
[15] Farcet C, Lansalot M, Charleux B, Pirri R, Vairon JP. Mechanistic aspects of nitroxide-mediated controlled radical polymerization of styrene in miniemulsion, using a water-soluble radical initiator. Macromolecules 2000; 33(23):8559.
[16] Nicolas J, Charleux B, Guerret O, Magnet S. Nitroxide-mediated controlled free-radical emulsion polymerization using a difunctional water-soluble alkoxyamine initiator. Toward the control of particle size, particle size distribution, and the synthesis of triblock copolymers. Macromolecules 2005;38(24):9963.
[17] Charleux B, Nicolas J, Guerret O. Theoretical expression of the average activation–deactivation equilibrium constant in controlled/living free-radical copolymerization operating via reversible termination. Application to a strongly improved control in nitroxide-mediated polymerization of methyl methacrylate. Macromolecules 2005;38(13):5485.
[18] Wang JS, Matyjaszewski K. Controlled/"Living" radical polymerization – atom transfer radical polymerization in the presence of transition–metal complexes. J Am Chem Soc 1995;117(20):5614.
[19] Kato M, Kamigaito M, Sawamoto M, Higashimura T. Polymerization of methyl methacrylate with the carbon-tetrachloride dichlorotris(triphenylphosphine)ruthenium(II) methylaluminum bis(2,6-di-*tert*-butylphenoxide) initiating system – possibility of living radical polymerization. Macromolecules 1995;28(5):1721.
[20] Matyjaszewski K. Transition metal catalysis in controlled radical polymerization: atom transfer radical polymerization. Chem Eur J 1999;5(11):3095.
[21] Matyjaszewski K, Xia JH. Atom transfer radical polymerization. Chem Rev 2001;101(9):2921.
[22] Kamigaito M, Ando T, Sawamoto M. Metal-catalyzed living radical polymerization. Chem Rev 2001;101(12): 3689.

[23] Chiefari J, Chong YK, Ercole F, Krstina J, Jeffery J, Le TPT, et al. Living free-radical polymerization by reversible addition–fragmentation chain transfer: the RAFT process. Macromolecules 1998;31(16):5559.
[24] Moad G, Mayadunne RTA, Rizzardo E, Skidmore M, Thang SH. Synthesis of novel architectures by radical polymerization with reversible addition fragmentation chain transfer (RAFT polymerization). Macromol Symp 2003;192:1.
[25] Moad G, Rizzardo E, Thang SH. Living radical polymerization by the RAFT process. Aust J Chem 2005;58(6):379.
[26] Betts D, Johnson T, LeRoux D, DeSimone JM. New materials by controlled radical polymerization – 25 – controlled radical polymerization methods for the synthesis of nonionic surfactants for CO_2. ACS Symp Series 1998;685:418.
[27] Xia JH, Johnson T, Gaynor SG, Matyjaszewski K, DeSimone J. Atom transfer radical polymerization in supercritical carbon dioxide. Macromolecules 1999;32(15): 4802.
[28] Li Y, Zhang W, Yu Z, Huang J. Synthesis of fluorine-containing diblock copolymers and their properties. Polym Prep 2000;41:202.
[29] Li K, Wu PP, Han ZW. Preparation and surface properties of fluorine-containing diblock copolymers. Polymer 2002; 43(14):4079.
[30] Perrier S, Jackson SG, Haddleton DM, Ameduri B, Boutevin B. Preparation of fluorinated methacrylic copolymers by copper mediated living radical polymerization. Tetrahedron 2002;58(20):4053.
[31] Perrier S, Jackson SG, Haddleton DM, Ameduri B, Boutevin B. Preparation of fluorinated copolymers by copper-mediated living radical polymerization. Macromolecules 2003;36(24):9042.
[32] Yang YJ, Wang Z, Gao Y, Liu T, Hu CP, Dong QZ. Synthesis of fluorinated diblock copolymer by ATRP and its application of PAVAc polymerization in $ScCO_2$. J Appl Polym Sci 2006;102(2):1146.
[33] Shemper BS, Mathias LJ. Syntheses and characterization of statistical and block fluorinated copolymers with linear and star-like architectures via ATRP. Eur Polym J 2004;40(4): 651.
[34] Lim KT, Lee MY, Moon MJ, Lee GD, Hong SS, Dickson JL, et al. Synthesis and properties of semifluorinated block copolymers containing poly(ethylene oxide) and poly(fluorooctyl methacrylates) via atom transfer radical polymerisation. Polymer 2002;43(25):7043.
[35] Hussain H, Busse K, Kressler J. Poly(ethylene oxide)- and poly(perfluorohexylethyl methacrylate)-containing amphiphilic block copolymers: association properties in aqueous solution. Macromol Chem Phys 2003;204(7):936.
[36] Hussain H, Budde H, Horing S, Kressler J. Synthesis and characterization of poly(ethylene oxide) and poly(perfluorohexylethyl methacrylate) containing triblock copolymers. Macromol Chem Phys 2002;203(14):2103.
[37] Villarroya S, Zhou JX, Duxbury CJ, Heise A, Howdle SM. Synthesis of semifluorinated block copolymers containing poly(epsilon-caprolactone) by the combination of ATRP and enzymatic ROP in $scCO_2$. Macromolecules 2006;39(2): 633.
[38] Zhang ZB, Ying SK, Shi ZQ. Synthesis of fluorine-containing block copolymers via ATRP 2. Synthesis and characterization of semifluorinated di- and triblock copolymers. Polymer 1999;40(19):5439.
[39] Zhang ZB, Ying SK, Hu QH, Xu XD. Semifluorinated ABA triblock copolymers: synthesis, characterization, and amphiphilic properties. J Appl Polym Sci 2002;83(12):2625.
[40] Li H, Zhang ZB, Hu CP, Ying SK, Wu SS, Xu XD. Synthesis and characterization of fluorinated block copolymers containing carboxylic or sulfonic groups. React Func Polym 2003;56(3):189.
[41] Wang F, Li H, Zhang ZB, Hu CP, Wu SS. Synthesis and surface properties of fluorinated block copolymers containing sulfonic groups. J Polym Sci Part A: Polym Chem 2004;42(19):4809.
[42] Li H, Zhang ZB, Hu CP, Wu SS, Ying SK. Surface composition and property of film prepared with aqueous dispersion of polyurethaneurea-acrylate including fluorinated block copolymer. Eur Polym J 2004;40(9):2195.
[43] Otazaghine B, Boutevin B, Lacroix-Desmazes P. Controlled radical polymerization of *n*-butyl alpha-fluoroacrylate. 1. Use of atom transfer radical polymerization as the polymerization method. Macromolecules 2002;35(20):7634.
[44] Otazaghine B, David G, Boutevin B, Robin JJ, Matyjaszewski K. Synthesis of telechelic oligomers via atom transfer radical polymerization, 1 – Study of styrene. Macromol Chem Phys 2004;205(2):154.
[45] Granville AM, Brittain WJ. Stimuli-responsive semi-fluorinated polymer brushes on porous silica substrates. Macromol Rapid Commun 2004;25(14):1298.
[46] Granville AM, Boyes SG, Akgun B, Foster MD, Brittain WJ. Synthesis and characterization of stimuli-responsive semifluorinated polymer brushes prepared by atom transfer radical polymerization. Macromolecules 2004;37(8):2790.
[47] Chen RX, Feng C, Zhu SP, Botton G, Ong B, Wu YL. Surface-initiated atom transfer radical polymerization grafting of poly(2,2,2-trifluoroethyl methacrylate) from flat silicon wafer surfaces. J Polym Sci Part A: Polym Chem 2006;44(3):1252.
[48] Ma Z, Lacroix-Desmazes P. Synthesis of hydrophilic/CO_2-philic poly(ethylene oxide)-*b*-poly(1,1,2,2-tetrahydroperfluorodecyl acrylate) block copolymers via controlled/living radical polymerization and their properties in liquid and supercritical CO_2. J Polym Sci Part A: Polym Chem 2004; 42(10):2405.
[49] Eberhardt M, Theato P. RAFT polymerization of pentafluorophenyl methacrylate: preparation of reactive linear diblock copolymer. Macromol Rapid Commun 2005; 26(18):1488.
[50] Inoue Y, Watanabe J, Takai M, Yusa S, Ishihara K. Synthesis of sequence-controlled copolymers from extremely polar and apolar monomers by living radical polymerization and their phase-separated structures. J Polym Sci Part A: Polym Chem 2005;43(23):6073.
[51] Lacroix-Desmazes P, Andre P, DeSimone JM, Ruzette AV, Boutevin B. Macromolecular surfactants for supercritical carbon dioxide applications: synthesis and characterization of fluorinated block copolymers prepared by nitroxide mediated radical polymerization. J Polym Sci Part A: Polym Chem 2004;42(14):3537.
[52] Roche V, Vacandio F, Bertin D, Massiani Y. Corrosion performance of lamellae nanostructured fluorinated organic coating applied on steel. J Electroceram 2006; 16(1):41.

[53] Borkar S, Jankova K, Siesler HW, Hvilsted S. New highly fluorinated styrene-based materials with low surface energy prepared by ATRP. Macromolecules 2004;37(3):788.
[54] Hvilsted S, Borkar S, Siesler HW, Jankova K. Novel fluorinated polymer materials based on 2,3,5,6-tetrafluoro-4-methoxystyrene. In: Advances in controlled/living radical polymerization. ACS Symposium Series 854. 2003. p. 236.
[55] Qiu J, Matyjaszewski K. Polymerization of substituted styrenes by atom transfer radical polymerization. Macromolecules 1997;30(19):5643.
[56] Jankova K, Hvilsted S. Preparation of poly(2,3,4,5,6-pentafluorostyrene) and block copolymers with styrene by ATRP. Macromolecules 2003;36(5):1753.
[57] Jankova K, Hvilsted S. Novel fluorinated block copolymer architectures fuelled by atom transfer radical polymerization. J Fluor Chem 2005;126(2):241.
[58] Jankova K, Jannasch P, Hvilsted S. Ion conducting solid polymer electrolytes based on polypentafluorostyrene-*b*-polyether-*b*-polypentafluorostyrene prepared by atom transfer radical polymerization. J Mater Chem 2004;14(19):2902.
[59] Fu GD, Kang ET, Neoh KG. Three-dimensionally ordered porous membranes prepared via self-assembly and reverse micelle formation from well-defined amphiphilic block copolymers. Langmuir 2005;21(8):3619.
[60] Fu GD, Yuan ZL, Kang ET, Neoh KG, Lai DM, Huan ACH. Nanoporous ultra-low-dielectric-constant fluoropolymer films via selective UV decomposition of poly (pentafluorostyrene)-*block*-poly(methyl methacrylate) copolymers prepared using atom transfer radical polymerization. Adv Funct Mater 2005;15(2):315.
[61] Xu FJ, Yuan ZL, Kang ET, Neoh KG. Branched fluoropolymer-Si hybrids via surface-initiated ATRP of pentafluorostyrene on hydrogen-terminated Si(100) surfaces. Langmuir 2004;20(19):8200.
[62] Xu FJ, Cai QJ, Kang ET, Neoh KG, Zhu CX. Well-defined polymer-germanium hybrids via surface-initiated atom transfer radical polymerization on hydrogen-terminated Ge(100) substrates. Organometallics 2005;24(7):1768.
[63] Cheng C, Wooley KL, Khoshdel E. Hyperbranched fluorocopolymers by atom transfer radical self-condensing vinyl copolymerization. J Polym Sci Part A: Polym Chem 2005;43(20):4754.
[64] Fu GD, Phua SJ, Kang ET, Neoh KG. Tadpole-shaped amphiphilic block–graft copolymers prepared via consecutive atom transfer radical polymerizations. Macromolecules 2005;38(7):2612.
[65] Fu GD, Kang ET, Neoh KG, Lin CC, Liaw DJ. Rigid fluorinated polyimides with well-defined polystyrene/poly(pentafluorostyrene) side chains from atom transfer radical polymerization. Macromolecules 2005;38(18):7593.
[66] Bucholz TL, Loo YL. Phase behavior of near-monodisperse semifluorinated diblock copolymers by atom transfer radical polymerization. Macromolecules 2006;39(18):6075.
[67] Becker ML, Remsen EE, Wooley KL. Diblock copolymers, micelles, and shell-crosslinked nanoparticles containing poly(4-fluorostyrene): tools for detailed analyses of nanostructured materials. J Polym Sci Part A: Polym Chem 2001;39(23):4152.
[68] Radhakrishnan K, Switek KA, Hillmyer MA. Synthesis of semifluorinated block copolymers by atom transfer radical polymerization. J Polym Sci Part A: Polym Chem 2004;42(4):853.
[69] Jankova K, Chen XY, Kops J, Batsberg W. Synthesis of amphiphilic PS-*b*-PEG-*b*-PS by atom transfer radical polymerization. Macromolecules 1998;31(2):538.
[70] Jankova K, Bednarek M, Hvilsted S. Unpublished results; 2004.
[71] Ndoni S, Vigild ME, Berg RH. Nanoporous materials with spherical and gyroid cavities created by quantitative etching of polydimethylsiloxane in polystyrene–polydimethylsiloxane block copolymers. J Am Chem Soc 2003;125(44):13366.
[72] Jankova K, Ameduri B, Hvilsted S. Unpublished results; 2003.
[73] Fu GD, Shang ZH, Hong L, Kang ET, Neoh KG. Nanoporous, ultralow-dielectric-constant fluoropolymer films from agglomerated and crosslinked hollow nanospheres of poly(pentafluorostyrene)-*block*-poly(divinylbenzene). Adv Mater 2005;17(21):2622.
[74] Jankova K, Lindquist J, Egsgaard H, Plackett DV, Malmstrom EE, Hvilsted S. Surface-initiated atom transfer radical polymerization as a tool for coating of various surfaces with fluoropolymers. In: 17th international symposium on fluorine chemistry, Shanghai, July 24–29; 2005.
[75] Carlmark A, Malmstrom EE. ATRP grafting from cellulose fibers to create *block*-copolymer grafts. Biomacromolecules 2003;4(6):1740.
[76] Plackett D, Jankova K, Egsgaard H, Hvilsted S. Modification of jute fibers with polystyrene via atom transfer radical polymerization. Biomacromolecules 2005;6(5):2474.
[77] Andruzzi L, Chiellini E, Galli G, Li XF, Kang SH, Ober CK. Engineering low surface energy polymers through molecular design: synthetic routes to fluorinated polystyrene-based block copolymers. J Mater Chem 2002;12(6):1684.
[78] Li XF, Andruzzi L, Chiellini E, Galli G, Ober CK, Hexemer A, et al. Semifluorinated aromatic side-group polystyrene-based block copolymers: bulk structure and surface orientation studies. Macromolecules 2002;35(21):8078.
[79] Andruzzi L, Hexemer A, Li XF, Ober CK, Kramer EJ, Galli G, et al. Control of surface properties using fluorinated polymer brushes produced by surface-initiated controlled radical polymerization. Langmuir 2004;20(24):10498.
[80] Borkar S, Sen A. Novel fluoroalkene-methyl acrylate copolymers by atom transfer radical polymerization. Macromolecules 2005;38(7):3029.
[81] Jol S-Y, Lee W-S, Ahn B-S, Park K-Y, Kim K-A, Rhee-Paeng I-S. New AB or ABA type block copolymers: atom transfer radical polymerization (ATRP) of methyl methacrylate using iodine-terminated PVDFs as (macro)initiators. Polym Bull 2000;44(1):1.
[82] Zhang ZB, Ying SK, Shi ZQ. Synthesis of fluorine-containing block copolymers via ATRP 1. Synthesis and characterization of PSt–PVDF–PSt triblock copolymers. Polymer 1999;40(5):1341.
[83] Destarac M, Matyjaszewski K, Silverman E, Ameduri B, Boutevin B. Atom transfer radical polymerization initiated with vinylidene fluoride telomers. Macromolecules 2000;33(13):4613.
[84] Shi ZQ, Holdcroft S. Synthesis of block copolymers possessing fluoropolymer and non-fluoropolymer segments

by radical polymerization. Macromolecules 2004;37(6): 2084.
[85] Shi ZQ, Holdcroft S. Synthesis and proton conductivity of partially sulfonated poly([vinylidene difluoride-*co*-hexafluoropropylene]-*b*-styrene) block copolymers. Macromolecules 2005;38(10):4193.
[86] Rubatat L, Shi ZQ, Diat O, Holdcroft S, Frisken BJ. Structural study of proton-conducting fluorous block copolymer membranes. Macromolecules 2006;39(2):720.
[87] Hester JF, Banerjee P, Won YY, Akthakul A, Acar MH, Mayes AM. ATRP of amphiphilic graft copolymers based on PVDF and their use as membrane additives. Macromolecules 2002;35(20):7652.
[88] Holmberg S, Holmlund P, Wilen CE, Kallio T, Sundholm G, Sundholm F. Synthesis of proton-conducting membranes by the utilization of preirradiation grafting and atom transfer radical polymerization techniques. J Polym Sci Part A: Polym Chem 2002;40(4):591.
[89] Liu DM, Chen YW, Zhang N, He XH. Controlled grafting of polymer brushes on poly(vinylidene fluoride) films by surface-initiated atom transfer radical polymerization. J Appl Polym Sci 2006;101(6):3704.
[90] Chen YW, Liu DM, Mang N. Surface modification of poly(vinylidene fluoride) films by controlled grafting polymer brushes. Surf Rev Lett 2005;12(5–6):709.
[91] Chen YW, Liu DM, Deng QL, He XH, Wang XF. Atom transfer radical polymerization directly from poly(vinylidene fluoride): surface and antifouling properties. J Polym Sci Part A: Polym Chem 2006;44(11):3434.
[92] Zhai GQ, Kang ET, Neoh KG. Inimer graft-copolymerized poly(vinylidene fluoride) for the preparation of arborescent copolymers and ''surface-active'' copolymer membranes. Macromolecules 2004;37(19):7240.
[93] Zhai GQ, Shi ZL, Kang ET, Neoh KG. Surface-initiated atom transfer radical polymerization on poly(vinylidene fluoride) membrane for antibacterial ability. Macromol Biosci 2005;5(10):974.
[94] Woods HM, Nouvel C, Licence P, Irvine DJ, Howdle SM. Dispersion polymerization of methyl methacrylate in supercritical carbon dioxide: an investigation into stabilizer anchor group. Macromolecules 2005;38(8):3271.
[95] Koh K, Sugiyama S, Morinaga T, Ohno K, Tsujii Y, Fukuda T, et al. Precision synthesis of a fluorinated polyhedral oligomeric silsesquioxane-terminated polymer and surface characterization of its blend film with poly(methyl methacrylate). Macromolecules 2005;38(4):1264.
[96] Lu GL, Zhang S, Huang XY. Synthesis and characterization of a novel ABA triblock copolymer via 4,4′-bis(trifluorovinyloxy)biphenyl and methyl methacrylate. J Polym Sci Part A: Polym Chem 2006;44(18):5438.
[97] Jankova K, Borkar S, Hvilsted S. Unpublished results; 2005.
[98] Chen YW, Ying L, Yu WH, Kang ET, Neoh KG. Poly(vinylidene fluoride) with grafted poly(ethylene glycol) side chains via the RAFT-mediated process and pore size control of the copolymer membranes. Macromolecules 2003;36(25):9451.
[99] Ying L, Yu WH, Kang ET, Neoh KG. Functional and surface-active membranes from poly(vinylidene fluoride)-*graft*-poly(acrylic acid) prepared via RAFT-mediated graft copolymerization. Langmuir 2004;20(14):6032.
[100] Chen YW, Wang WC, Yu WH, Kang ET, Neoh KG, Vora RH, et al. Ultra-low-kappa materials based on nanoporous fluorinated polyimide with well-defined pores via the RAFT-moderated graft polymerization process. J Mater Chem 2004;14(9):1406.
[101] Yu WH, Kang ET, Neoh KG. Controlled grafting of comb copolymer brushes on poly(tetrafluoroethylene) films by surface-initiated living radical polymerizations. Langmuir 2005;21(1):450.
[102] Moad G, Rizzardo E, Thang SH. Living radical polymerization by the RAFT process – A first update. Aust J Chem 2006;59(10):669.
[103] Vana P, Albertin L, Barner L, Davis TP, Barner-Kowollik C. Reversible addition–fragmentation chain-transfer polymerization: unambiguous end-group assignment via electrospray ionization mass spectrometry. J Polym Sci Part A: Polym Chem 2002;40(22):4032.
[104] Theis A, Stenzel MH, Davis TP, Coote ML, Barner-Kowollik C. A synthetic approach to a novel class of fluorine-bearing reversible addition–fragmentation chain transfer (RAFT) agents: F-RAFT. Aust J Chem 2005; 58(6):437.
[105] Chiefari J, Mayadunne RTA, Moad CL, Moad G, Rizzardo E, Postma A, et al. Thiocarbonylthio compounds (S=C(Z)S–R) in free radical polymerization with reversible addition–fragmentation chain transfer (RAFT polymerization). Effect of the activating group Z. Macromolecules 2003;36(7):2273.
[106] Destarac M, Bzducha W, Taton D, Gauthier-Gillaizeau I, Zard SZ. Xanthates as chain-transfer agents in controlled radical polymerization (MADIX): structural effect of the *O*-alkyl group. Macromol Rapid Commun 2002;23(17): 1049.
[107] Monteiro MJ, Adamy MM, Leeuwen BJ, van Herk AM, Destarac M. A ''living'' radical ab initio emulsion polymerization of styrene using a fluorinated xanthate agent. Macromolecules 2005;38(5):1538.
[108] Lebreton P, Ameduri B, Boutevin B, Corpart JM. Use of original omega-perfluorinated dithioesters for the synthesis of well-controlled polymers by reversible addition–fragmentation chain transfer (RAFT). Macromol Chem Phys 2002;203(3):522.
[109] Benaglia M, Rizzardo E, Alberti A, Guerra M. Searching for more effective agents and conditions for the RAFT polymerization of MMA: influence of dithioester substituents, solvent, and temperature. Macromolecules 2005;38(8): 3129.

Appendix 2

Synthesis of Fluorinated Block Copolymers by Living Radical Polymerization

SYNTHESIS OF FLUORINATED BLOCK COPOLYMERS BY LIVING RADICAL POLYMERIZATION

Natanya M.L. Hansen[1], Søren Hvilsted[1], Michael Gerstenberg[2], Daniel Nyström[3], David M. Haddleton[4]

[1]Danish Polymer Centre, Dept. of Chemical Engineering, Technical University of Denmark, Building 423, 2800 Kgs. Lyngby, Denmark
[2]Novo Nordisk A/S, Brennum Park, 3400 Hillerød, Denmark
[3]Royal Institute of Technology, Fibre and Polymer Technology, Teknikringen 56-58, 100 44 Stockholm, Sweden
[4]Department of Chemistry, University of Warwick, Coventry CV4 7AL, United Kingdom

Introduction

Fluorinated polymers are highly hydrophobic and are interesting due to a number of unique properties including high biocompatibility and low surface activity, as well as high chemical and thermal resistance. The aim of this work was to synthesize amphiphilic block copolymers utilizing fluorinated methacrylates. Atom transfer radical polymerization (ATRP) [1] was utilized mediated by copper(I) diimines catalysts. Our approach was to combine methyl methacrylate and a fluorinated methacrylate into a block copolymer (fig. 1). A number of fluorinated/perfluorinated methacrylic and acrylic monomers have been previously studied as block copolymers from ATRP including work with the monomer 2,2,2-trifluoroethylene methacrylate [2,3].

Experimental

Materials 2,2,2-Trifluoroethylene methacrylate (3FM) was kindly supplied by Osaka Chemicals. Methyl methacrylate (MMA) was purchased from Sigma Aldrich. The monomers were passed through a column of activated neutral Al_2O_3 before use to remove inhibitor. Ethyl-2-bromoisobutyrate (EIBr), chloroform and toluene (Sigma Aldrich) were used without further purification. Cu(I)Br was purified according to the method of Keller and Wycoff [4]. *N*-(n-Propyl)-2-pyridylmethamine (n-Pr-1) was synthesized as previously described [5].

Instrumentation

Molecular weights were determined by GPC performed on a system with two PL gel 5 µm columns mixed D-columns (300 x 7.5 mm) and a PL gel 5 mm guard column (50 x 7.5 mm) (Polymer Laboratories) using tetrahydrofuran/triethylamine 95:5 as eluent using PMMA-standards (flow rate 1 ml/min, toluene as flow rate marker). ^{1}H-NMR was performed on a Bruker DPX400 spectrometer using $CDCl_3$ as solvent. Polymer films were studied under an optical microscope.

Synthesis of P3FM-b-PMMA

5.0 ml (35 mmol) 3FM and 5.0 ml toluene were charged to a Schlenk tube equipped with a magnetic stirrer and sealed with a rubber septum. 42 mg (0.29 mmol) Cu(I)Br, and 45 µl (0.31 mmol) EIBr were added, and 5 freeze-pump-thaw cycles were carried out to deoxygenate the reaction mixture. Reactants were thawed to ambient temperature, 90 µl (0.58 mmol) of n-Pr-1 was added and reaction was run at 90 °C. 4 ml (37 mmol) of degassed MMA (50 % V/V solution in toluene) was added to the reaction by syringe after 2 hrs. Samples were withdrawn by syringe under nitrogen at regular intervals for analysis by NMR (^{1}H) and GPC. Catalyst was removed on a column of activated neutral Al_2O_3 and the product was recovered as a light green solid after removal of solvent in vacuo.

Synthesis of PMMA-b-P3FM

5.0 ml (47 mmol) MMA and 5 ml toluene were charged to a Schlenk tube equipped with a magnetic stirrer and sealed with a rubber septum. 69 mg (0.48 mmol) Cu(I)Br, and 70 µl (0.48 mmol) EIBr were added, and 3 freeze-pump-thaw cycles were carried out to deoxygenate the reaction mixture. Reactants were thawed to ambient temperature, 145 µl (0.93 mmol) of n-Pr-1 was added and reaction was run at 90 °C. 4 ml (28 mmol) of degassed 3FM (50 % V/V solution in toluene) was cannulated into the reaction after 3.5 hrs. Samples were withdrawn by syringe under nitrogen at regular intervals for analysis by NMR (^{1}H) and GPC. Catalyst was removed on a column of activated neutral Al_2O_3 and the product was recovered as a light green solid after removal of solvent in vacuo.

Filmcasting

20 mg of polymer was dissolved in 1 ml $CHCl_3$ and cast at ambient temperature on glass slides under humid conditions and air flow to yield opaque membranes.

Results and discussion

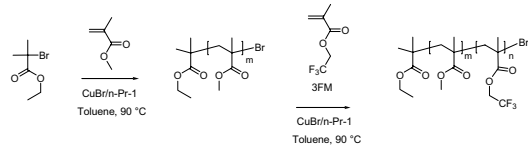

Figure 1. Scheme for the copolymerization of PMMA-b-P3FM

Polymerization of block copolymers. Conversions were estimated from ^{1}H-NMR-analysis using the peak for $C\underline{H}_2$-CF_3 in the fluorinated methacrylate: δ 4.49 (q) (monomer) and δ 4.33 (polymer) as shown in figure 2. Similarly the conversion of MMA was determined from the shift of the CH_3-group from δ 3.72 (s) in the monomer to δ 3.59 in the polymer. In the polymerizations of the block copolymers, the second monomer was added at relatively high conversions of the first monomer, with both monomers continuing to polymerize after addition, as observed by ^{1}H-NMR to give a gradient copolymer.

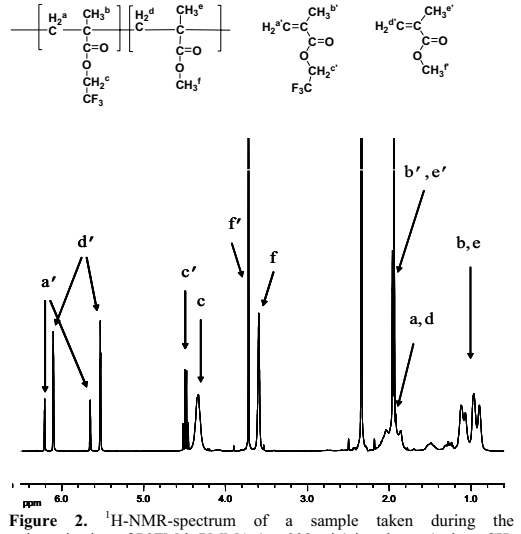

Figure 2. ^{1}H-NMR-spectrum of a sample taken during the polymerization of P3FM-b-PMMA (t = 328 min) in toluene (only φ-$C\underline{H}_3$ δ 2.34 (s) from the solvent shown). Assignments according to the structures above are indicated by the arrows.

Kinetic plots (fig. 3) were relatively linear indicating a low amount of termination. For the polymerization of MMA from P3FM a small induction period was observed for initiation of the second monomer. GPC-analysis showed that indeed some termination took place with the addition of the second monomer. Evolution of M_n of the copolymeric product was observed to be linear with conversion as seen in figure 4 and PDI's are low evidencing a controlled reaction mechanism (table 1). Narrower molecular weight distributions were obtained for the polymerization of 3FM from PMMA than for the converse approach. This may be due to the low solubility of P3FM in the solvent impeding further reaction.

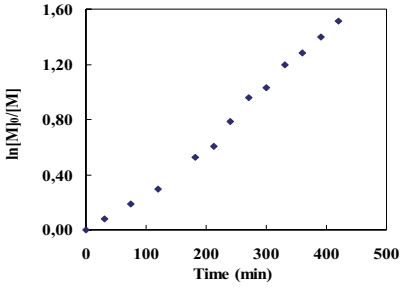

Figure 3. Kinetic plot of the copolymerization of PMMA-b-P3FM.

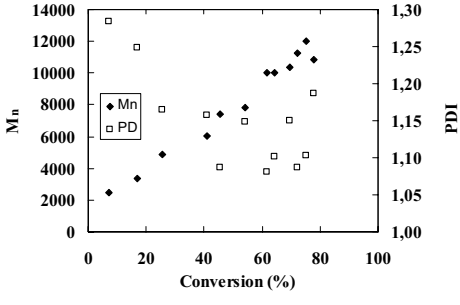

Figure 4. Evolution of M_n for the copolymerization of PMMA-b-P3FM.

Table 1.

Polymer	$[M_1]:[M_2]$	M_n[a]	PDI[a]
P3FM-b-PMMA	1 : 1	13,600	1.34
PMMA-b-P3FM	3 : 2	10,900	1.19

[a]From GPC-analysis
[I]:[Cu(I)Br]:[n-Pr-1] = 1:1:2

Film casting

Films of the synthesized block copolymers were cast to observe the bulk morphology. The films were cast under humid conditions to form so-called honey-comb structures. These structures seen as highly regular porosities in films were first discovered by Francois et al., who cast a solution of polymer and volatile solvent under humid conditions [6]. The evaporation of the volatile solvent leads to a decrease in solution temperature and water droplets start to condense onto the solution surface. These water droplets will organize themselves into a hexagonal array before the polymer precipitates around them and when the solvent and water have evaporated an ordered hexagonally packed polymeric structure will remain [7].

The synthesized block copolymers were cast to form opaque films with isoporous structures (fig. 5). The formed pores were 3-9 µm in diameter.

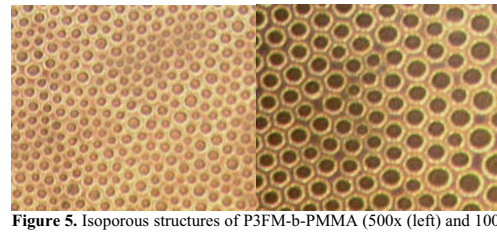

Figure 5. Isoporous structures of P3FM-b-PMMA (500x (left) and 1000x enlargement).

Conclusions

Block copolymers of MMA and fluorinated methacrylate were polymerized by controlled radical polymerization (ATRP). The synthesized copolymers could be cast to form films with isoporous structures, honeycomb structures, with porosities in the µm-range.

Acknowledgements. N. Hansen would like to thank Novo Nordisk A/S for supporting her project. D. Nyström would like to thank Wilhem Beckers Jubileumsfond and The Research Council of Norway for financial support within the NanoMat program, project ''Dendritic nanoporous materials with multifunctionality'' (no.163529/S10).

References

(1) (a) Kamigaito, M.; Ando, T.; Sawamoto, M. *Chem. Rev.* **2001**, *101*, 3689 (b) Wang, J. S. and Matyjaszewski, K. *J. Amer. Chem. Soc.* **1995,** *117(20)*, 5614
(2) Perrier, S., Jackson, S. G., Haddleton, D. M., Ameduri, B., and Boutevin, B. *Tetrahedron* **2002,** *58(20)*, 4053
(3) Chen, R. X., Feng, C., Zhu, S. P., Botton, G., Ong, B., and Wu, Y. L. *J. Polym. Sci A-Polym. Chem.* **2006,** *44(3)*, 1252
(4) Keller, R. N. and Wycoff, H. D *Inorg.Synth* **1947,** *2(1)*
(5) Haddleton, D. M., Crossman, M. C., Dana, B. H., Duncalf, D. J., Heming, A. M., Kukulj, D., and Shooter, A. J. *Macromolecules* **1999,** *32(7)*, 2110
(6) Widawski, G., Rawiso, M., and Francois, B. *Nature* **1994,** *369(6479)*, 387
(7) Pitois, O. and Francois, B. *Coll. and Polym. Sci.* **1999,** *277(6)*, 574

Appendix 3

Fluorinated Bio-acceptable Polymers via an ATRP Macroinitiator Approach

Fluorinated Bio-Acceptable Polymers Via an ATRP Macroinitiator Approach

NATANYA M. L. HANSEN,[1] DAVID M. HADDLETON,[2] SØREN HVILSTED[1]

[1]Danish Polymer Centre, Department of Chemical Engineering, Technical University of Denmark, Building 423, 2800 Kgs. Lyngby, Denmark

[2]Department of Chemistry, University of Warwick, Coventry CV4 7AL, United Kingdom

Received 9 March 2007; accepted 16 July 2007
DOI: 10.1002/pola.22326
Published online in Wiley InterScience (www.interscience.wiley.com).

ABSTRACT: Polymers derived from bio-acceptable poly(methyl methacrylate) (PMMA), poly(2-methoxyethyl acrylate) (PMEA), and poly(oligo(ethylene glycol) methyl ether methacrylate) (PPEGMA) have been prepared via atom transfer radical polymerization (ATRP) utilizing an initiator prepared from a fluoroalkoxy-terminated oligoethylene glycol. Polymerizations are controlled as seen by both linear first-order kinetics and molecular weight evolution coupled with low polydispersities (<1.25) with respect to conversion. A range of ligands have been used depending upon the nature of the monomer: *N*-(*n*-propyl)-2-pyridyl-methanimine with the methacrylates MMA and PEGMA and 1,1,4,7,10,10-hexamethyltriethylene tetramine (HMTETA) with MEA. In all cases the use of the fluorinated initiator results in a lower apparent rate of propagation (k_p^{app}) as compared with the more conventional and nonfluorinated initiator, ethyl 2-bromoisobutyrate. The initiator generally also serves as an internal plasticizer lowering the glass transition temperature from the parent polymers. The surface characteristics of the fluoroinitiator containing polymers are altered compared with the nonfluorinated analogues. This is reflected in a significant increase in the advancing water contact angles of all fluoro-containing polymers. © 2007 Wiley Periodicals, Inc. J Polym Sci Part A: Polym Chem 45: 5770–5780, 2007
Keywords: atom transfer radical polymerization (ATRP); biocompatibility; block copolymers; contact angle; kinetics (polymer); thermal properties

INTRODUCTION

Fluorinated polymers are very hydrophobic and are interesting due to a number of unique properties which include biocompatibility and low surface energy, as well as high chemical and thermal resistance. A recent relevant review[1] elaborates on the numerous novel fluoropolymer materials and architectures prepared by controlled radical polymerization techniques. Incorporation of fluorinated monomers into block copolymers is a viable and often used route to obtain partially fluorinated polymers, whilst a second and arguably more facile option is the use of commercially available fluorinated compounds as macroinitiators with nonfluorinated monomers. The latter approach was chosen in this present work, whereby a commercially available fluorinated surfactant was utilized as a macroinitiator for the polymerization of nonfluorinated monomers by atom transfer radical polymerization (ATRP).[2,3] Various fluoropolymers, both commercial and synthesized in-house, have previously been used as macroinitiators for ATRP

Correspondence to: S. Hvilsted (E-mail: sh@kt.dtu.dk)
Journal of Polymer Science: Part A: Polymer Chemistry, Vol. 45, 5770–5780 (2007)

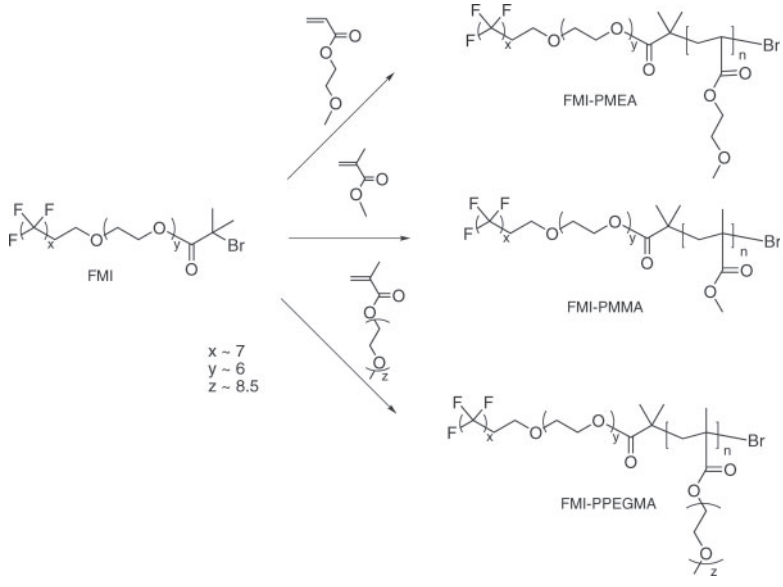

Scheme 1. Fluorinated macroinitiator, FMI, employed in the polymerization of MEA, MMA and PEGMA.

with mainly PVDF-type macroinitiators being studied for the formation of both block-copolymers[4–6] and graft-copolymers,[7–9] poly(2,3,4,5,6-pentafluorostyrene) has furthermore been used both as initiator and copolymer for styrenic monomers.[10–13] Perfluorinated macroinitiators derived from commercially available compounds have previously been utilized for the polymerization of MMA where the initiator was derived from either perfluoroalkyl ethanol or 2-perfluoroalkyl ethyl-*co*-poly(ethylene glycol).[14] The latter macroinitiator was also successfully used for the polymerization of a methacrylate-functionalized poly(propylene glycol).[15]

In this present work the surfactant Zonyl FSO-100® was transformed into a macroinitiator by transesterification, according to the methodology of Jankova et al.[16] Polymerizations of MMA were carried out with different ratios of initiator to monomer and the reaction kinetics compared with a conventional ATRP initiator. Novel copolymers were synthesized with 2-methoxyethyl acrylate (MEA) and poly(ethylene glycol) methyl ether methacrylate (PEGMA), both of which are hydrophilic and biocompatible. PMEA is biocompatible and demonstrates superior properties with respect to blood compatibility in comparison with polymers having similar structures.[17] The presence of "freezing bound water" in PMEA is thought to be the reason for the excellent blood compatibility, although the mechanism is not fully understood.[18,19] MEA has furthermore recently been polymerized successfully by living polymerization in our group,[20] which has given incentive to study the possibilities of combination with fluorinated compounds. This contribution describes the possibility for the preparation of biomedical materials via ATRP (Scheme 1) from a partly fluorinated macroinitiator (FMI) used for the controlled preparation of bio-acceptable polymers. Thus, the particular emphasis and novelty are on the flexibility and robustness of ATRP for the introduction of commercially available fluoro containing end groups into bioacceptable (meth)acrylate polymers with controlled molecular architectures.

EXPERIMENTAL

Materials

Zonyl FSO-100, methyl methacrylate (MMA), 2-methoxyethyl acrylate (MEA), and poly(ethylene glycol) methyl ether methacrylate (PEGMA) ($M_n \approx 475$ g/mol) were purchased from Sigma Aldrich. The monomers were passed through a

column of activated neutral Al_2O_3 before use to remove inhibitor. Ethyl-2-bromoisobutyrate (EBB), 2-bromoisobutyryl bromide, 4-dimethylaminopyridine (DMAP), triethylamine (TEA), dichlormethane (DCM), 1,1,4,7,10,10-hexamethyltriethylenetetramine (HMTETA), chloroform, petroleum ether, and toluene (Sigma Aldrich) were used without further purification. Cu(I)Br was purified according to the method of Keller and Wycoff.[21] *N*-(*n*-Propyl)-2-pyridylmethanimine (**n-Pr-1**) was synthesized as previously described and degassed immediately prior to use.[22]

Instrumentation

Molecular weights were determined by size exclusion chromatography (SEC) performed on a Polymer Laboratories (PL) modular system with a PL gel 5-μm guard column (50 $\times$ 7.5 mm^2) and two PL gel 5-μm mixed D-columns (300 $\times$ 7.5 mm^2) using chloroform/triethylamine 95:5 as eluent using PMMA-standards (flow rate 1 mL/min, toluene as flow rate marker) unless otherwise stated. ^{1}H NMR and ^{13}C NMR were performed on a Bruker DPX400 instrument, and ^{19}F NMR on a Bruker DPX300 spectrometer. $CDCl_3$ was used as solvent in all cases. Samples for contact angle measurements were dissolved in THF (20 mg/mL) and spin coated (1000 rpm) onto glass slides. Samples containing PPEGMA were dissolved in a mixture of ethyl acetate and toluene, 2:1 v/v %. Measurements were performed on an OCA15 plus contact angle system apparatus from Dataphysics with contact angles attained by the "needle-in" method. The glass transition temperatures (T_g's) were determined with a DSC Q1000 system from TA Instruments. Samples were heated to 150 °C (10 °C/min) and cooled to −50 °C (or −100 °C) to remove any effects induced by prior treatment. The T_g was then determined by consecutive heating from −50 °C (or −100 °C) to 200 °C at 10 °C/min. Cooling to −100 °C was only used for the polymers containing PMEA or PPEGMA, as these polymers have T_g's well below ambient temperature. Thermogravimetric analysis (TGA) was performed on a TGA Q500 from TA Instruments heating the polymer from ambient temperature to 600 °C at a rate of 20 °C/min in N_2 (g).

Synthesis of Fluorinated Macroinitiator

The fluorinated macroinitiator (FMI) was synthesized based on previously described work in the literature.[14,16] Zonyl FSO-100 was dissolved in toluene and dried by removal of water-toluene by azeotropic rotary evaporation. About 5.29 g (7.3 mmol) of anhydrous Zonyl FSO-100 was dissolved in 30 mL DCM and placed in a 100-mL three-necked round-bottomed flask equipped with stirrer, condenser, gas inlet (N_2), and rubber septum. About 0.0556 g (0.88 mmol) of DMAP and 1225 μL (8.8 mmol) of TEA were added under nitrogen. The temperature was lowered to 0 °C and 1100 μL (8.8 mmol) of 2-bromoisobutyryl bromide was added dropwise and the reaction was left stirring overnight. The reaction mixture was diluted in DCM and washed five times with saturated $NaHCO_3$-solution. The product was isolated by rotary evaporation (m = 5.48 g, 86% yield).

^{1}H NMR ($CDCl_3$): δ 4.30 (t, 2H), δ 3.73 (m, 2H), δ 3.71 (m, 2H), δ 3.62 (m, 22H), δ 2.40 (m, 2H), δ 1.91 (s, 6H). ^{13}C NMR ($CDCl_3$): δ 171.6; δ 70.7; δ 68.7; δ 65.1; δ 63,1; δ 55.6; δ 31.5 ^{19}F NMR ($CDCl_3$): δ −81.9 ($C\underline{F}_3$); δ −114.6; δ −122.9; δ −123.1; δ −124.1; δ −124.9; δ −127.3.

Synthesis of FMI-PMMA

About 5.0 mL (47 mmol) of MMA and 5.0 mL of toluene were charged to a Schlenk tube equipped with a magnetic stirrer and sealed with a rubber septum. About 42 mg (0.29 mmol) of Cu(I)Br, and 0.41 g (0.47 mmol) of FMI were added, and three freeze-pump-thaw cycles were carried out to deoxygenate the reaction mixture. Reactants were thawed to ambient temperature, 145 μL (0.93 mmol) of **n-Pr-1** was added and the reaction was run at 90 °C. Samples ($\sim$ 100 μL) were withdrawn by syringe under nitrogen at regular intervals for analysis by ^{1}H NMR and SEC. Catalyst residues were removed on a column of activated neutral Al_2O_3 and the product was recovered after removal of volatiles *in vacuo*.

Synthesis of FMI-PMEA

About 5.0 mL (39 mmol) of MEA and 5.0 mL of toluene were charged to a Schlenk tube equipped with a magnetic stirrer and sealed with a rubber septum. About 26 mg (0.18 mmol) of Cu(I)Br, 0.15 g (0.17 mmol) of FMI and 50 μL (0.18 mmol) of HMTETA were added and subsequently degassed via three freeze-pump-thaw cycles. Reactants were thawed to ambient temperature and the reaction was carried out at 90 °C. Samples were withdrawn by syringe under nitrogen at regular intervals for analysis

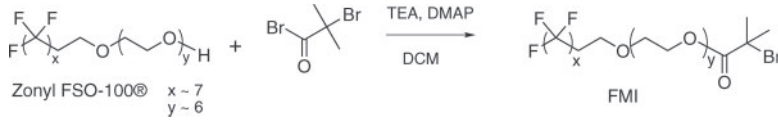

Scheme 2. Synthesis of fluorinated macroinitiator FMI from Zonyl FSO-100® by transesterification with 2-bromoisobutyrylbromide.

by ^{1}H NMR and SEC. The product was purified by precipitation in petroleum ether and removal of the volatiles by rotary evaporation.

Synthesis of FMI-PPEGMA

About 5.0 mL (11 mmol) of PEGMA and 5.0 mL of toluene were charged to a Schlenk tube equipped with a magnetic stirrer and sealed with a rubber septum. About 41 mg (0.29 mmol) of Cu(I)Br, and 0.25 g (0.29 mmol) of FMI were added and degassed via three freeze-pump-thaw cycles. Reactants were thawed to ambient temperature and 85 μL (0.55 mmol) of **n-Pr-1** added and the reaction allowed to proceed at 90 °C. Samples were withdrawn by syringe under nitrogen at regular intervals for analysis by ^{1}H NMR and SEC. Catalyst was removed on a column of activated neutral Al_2O_3 using ethyl acetate as eluent and the product was recovered as a highly viscous liquid after removal of volatiles *in vacuo*.

Synthesis of FMI-PMMA-PPEGMA

About 5.0 mL (47 mmol) of MMA and 5.0 mL of toluene were charged to a Schlenk tube equipped with a magnetic stirrer and sealed with a rubber septum. About 48 mg (33 mmol) of Cu(I)Br, and 0.40 g (0.46 mmol) of FMI were added and degassed via three freeze-pump-thaw cycles. The reaction mixture was thawed to ambient temperature prior to the addition of 145 μL (0.93 mmol) of **n-Pr-1.** The reaction was carried out at 90 °C. A total of 5 mL (11 mmol) of degassed PEGMA (50 % V/V solution in toluene) was cannulated into the reaction mixture after 4 h. Samples were withdrawn by syringe under nitrogen at regular intervals for analysis by ^{1}H NMR and SEC. The product was purified by precipitation from ethyl acetate in a 1:1 mixture of petroleum ether and diethylether, and isolated by removal of volatiles *in vacuo*.

RESULTS AND DISCUSSION

The structure of the synthesized FMI was confirmed by ^{1}H, ^{13}C and ^{19}F NMR analysis, Scheme 2.

Polymerization of MMA

Three different molecular weight PMMA were targeted from the FMI *viz.* 5000, 10,000, and 20,000 g mol^{-1}. Conversions were determined by ^{1}H NMR using the peaks from the OCH_3-group at δ_H 3.72 (s) from the monomer and δ_H 3.59 from the polymer. The kinetic plots for the poly-

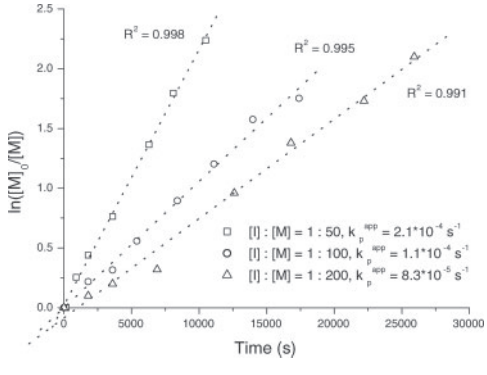

Figure 1. First-order kinetic plots for the polymerization of MMA from FMI in toluene solution. [I]:[Cu(I)Br]:[**n-Pr-1**] = 1:1:2, reaction temperature = 90 °C.

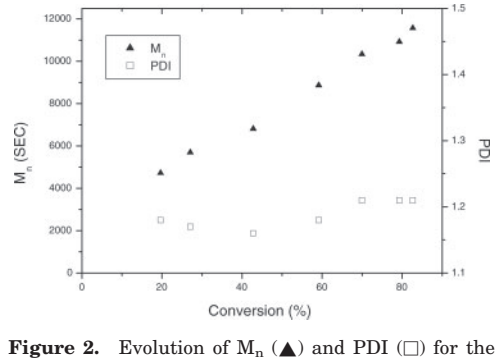

Figure 2. Evolution of M_n (▲) and PDI (□) for the polymerization of MMA from FMI. [M]:[I]:[Cu(I)Br]:[**n-Pr-1**] = 100:1:1:2 (entry II, Table 1).

Table 1. Polymers Synthesized from the Fluorinated Macroinitiator. [I]:[Cu(I)Br]:[**n-Pr-1**] = 1:1:2, Reaction Temperature: 90 °C

	M_1	M_2	[I]:[M_1]:[M_2]	Time (h)	Conversion (%)	$M_{n,theo}$ (g mol^{-1})	$M_{n,SEC}$ (g mol^{-1})	$M_{n,NMR}$ (g mol^{-1})	PDI
I	MMA	–	1:50	3	89	5000	9200	5500	1.17
II	MMA	–	1:100	5	83	10,000	12,400	7900	1.21
III	MMA	–	1:200	7	88	20,000	24,000	13,900	1.24
IV	MEA[a]	–	1:230	20	77	24,000	24,400[b]	–[c]	1.21
V	PEGMA	–	1:42	26	47	10,300	16,300	–[c]	1.20
VII	MMA	PEGMA	1:100:24	26	91/49	15,900	21,600	–[c]	1.57

[a] Ligand = HMTETA, [I]:[Cu(I)Br]:[HMTETA] = 1:1:1.
[b] SEC performed in THF.
[c] End-group not detectable by ^{1}H NMR.

merizations are shown in Figure 1, where the polymerizations proceed with first-order kinetics in all cases indicating a controlled mechanism. The rates of polymerization increased with decreasing monomer to initiator ratio as expected. For the three polymerizations apparent rates of propagation, k_p^{app}, were found to be 2.1×10^{-4} s^{-1}, 1.1×10^{-4} s^{-1}, and 8.3×10^{-5} s^{-1} for the target weights of 5, 10, and 20 kg mol^{-1}, respectively. The evolution of molecular weight was linear with conversion in all cases, Figure 2, and the PDIs low (<1.25) (Table 1). SEC-analysis showed monomodal curves (Fig. 3). However, a high molecular weight shoulder was seen at high conversions, which could possibly be due to the surface activity of the initiator resulting in aggregation of the polymer. The molecular weights of the FMI-PMMA polymers were further estimated by ^{1}H NMR using the signal from the —C$\underline{H}_2$C$\underline{H}_2$O— in the macroinitiator at δ 3.62 and comparing with the signal from the monomer at δ 3.58 (OC$\underline{H}_3$), Figure 4. Molecular weights obtained by NMR were difficult to obtain due to peak overlap. Results obtained by ^{1}H NMR were lower than those found by SEC-analysis in all cases, but showed the similar tendencies that is lower molecular weight at relatively higher concentration of initiator in accordance with theoretical values. Polymerization of MMA (target 10,000 g mol^{-1}) using ethyl 2-bromoisobutyrate (EBB) as initiator gave an apparent rate of propagation of 2.1×10^{-4} s^{-1}. In a very similar system Haddleton et al.[22] report k_p[Pol*] = 7.5×10^{-5} mol^{-1}(dm^3 s^{-1}). These new results indicate that the reactivity of FMI is comparable with EBB (Fig. 5). Almost identical polymerization rates for these two initiators were found by Perrier et al.[14] (k_p[Pol*] = 007 mol^{-1} dm^3 s^{-1}), when using the same type of system with a slightly different ligand (pentyl- vs. propylfunctionalized methanimine). In that case, however, an increase of the reaction rate was seen at higher conversions for the FMI which we did not observe.

Polymerization of MEA

Conversions of MEA were calculated by comparing the residual monomer peaks (δ_H 5.74 (dd), 6.15 (dd), and 6.43 (dd)) with the peak at δ_H 3.54, which derives from CO—O—C$\underline{H}_2$ in both monomer and polymer, as there is no significant shift in the signals during polymerization. The first-order kinetic plot for the polymerization of MEA from FMI is linear, Figure 6, with a k_p^{app} = 2.0×10^{-5} s^{-1}, lower than 8.3×10^{-5} s^{-1} obtained for MMA ([M]:[I] = 200). It is stressed that a direct comparison between the reactivity of the two monomers cannot be made, as different ligands have been used in these two polymerizations. HMTETA was chosen as ligand for

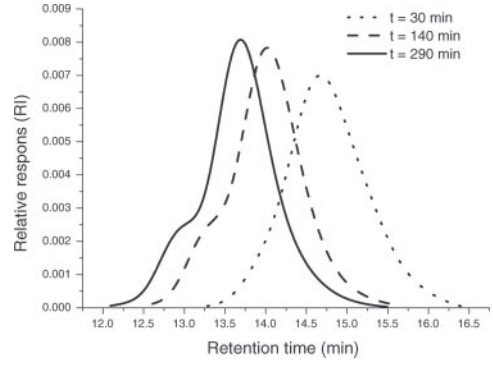

Figure 3. Development of the SEC-traces in the synthesis of FMI-PMMA (entry II, Table 1).

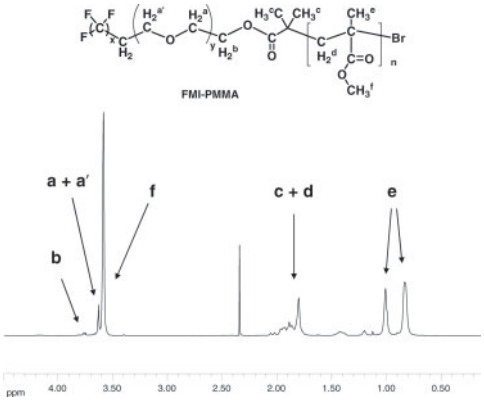

Figure 4. ^{1}H-NMR spectrum of the product FMI-PMMA (entry II, Table 1) in toluene (only φ-C$\underline{H}_3$ δ 2.34 (s) from the solvent shown). Assignments according to the structure above are indicated by arrows.

the polymerization of MEA as preliminary experiments indicated good control, relative to **n-Pr-1**. Polymerization of MEA from FMI gave a linear evolution of molecular weight with conversion with low polydispersities throughout reaction, Figure 7. Polydispersities increased during reaction from 1.08 to 1.21. As was the case for FMI-PMMA a shoulder in the high molecular weight part of the SEC trace was observed for FMI-PMEA. This effect is ascribed to the initiator as this was not observed when using EBB. Polymerization of MEA initialized with EBB showed the same tendency as for

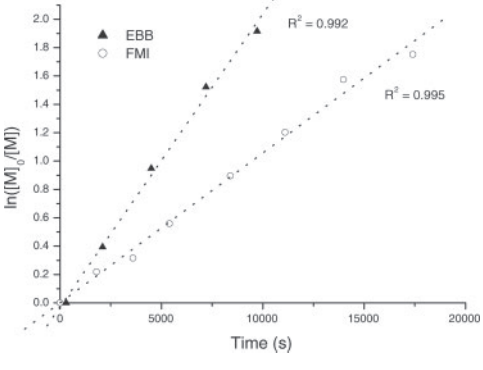

Figure 5. First-order kinetic plots for the polymerization of MMA from ethyl-2-bromoisobutyrate (EBB) (▲) and FMI (○) in toluene. [M]:[I]:[Cu(I)Br]:[**n-Pr-1**] = 100:1:1:2, Reaction temperature = 90 °C.

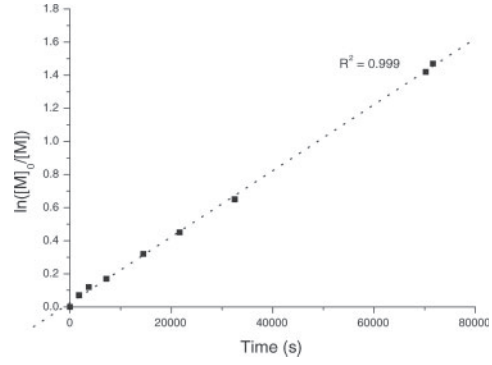

Figure 6. First-order kinetic plot for the polymerization of MEA from FMI in toluene. [M]:[I]:[Cu(I)Br]:[HMTETA] = 230:1:1:1, Reaction temperature = 90 °C.

MMA: the use of FMI resulted in a relatively slower reaction. Although the monomer to initiator ratio was changed slightly from 230 in the case of FMI to 150 with EBB there was a large difference between the two reactivity ratios, as k_p^{app} for the reaction initiated with EBB was $\sim 1.0 \times 10^{-4}$ s^{-1}, almost five times the value obtained with FMI. This could be due to the hydrophilic nature of the monomer, which might make it less compatible with the FMI.

We have not seen previous examples of the polymerization of MEA using a fluorinated (macro) initiator, and the polymerization results are comparable in terms of control of both molecular weights and polydispersities with those previously obtained.[20]

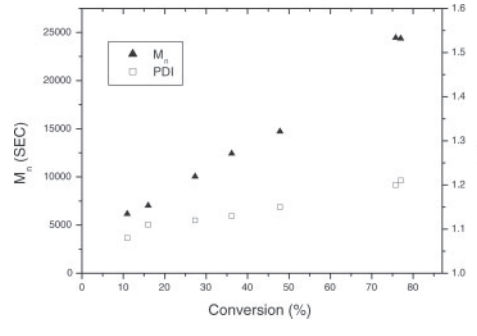

Figure 7. Evolution of M_n (▲) and PDI (□) for the polymerization of MEA from FMI. [M]:[I]:[Cu(I)Br]:[HMTETA] = 230:1:1:1 (entry IV, Table 1).

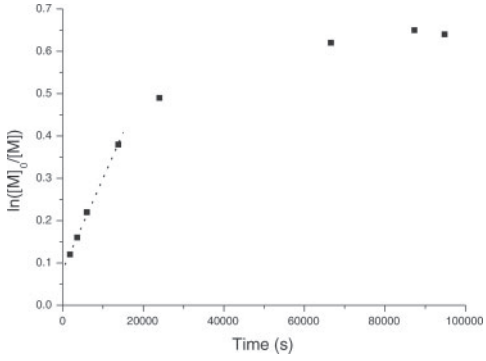

Figure 8. First-order kinetic plot for the polymerization of PEGMA from FMI in toluene solution. [M]:[I]:[Cu(I)Br]:[**n-Pr-1**] = 42:1:1:2, Reaction temperature: 90 °C.

Polymerization of PEGMA

Polymerization of PEGMA from FMI was carried out at 90 °C. It was necessary for the copolymerization with PMMA to polymerize at this elevated temperature therefore an experiment was conducted at 90 °C, although it was expected not to exhibit a first-order mechanism.[23] Conversions were found by comparing the peaks at δ_H 4.28 (dd) and δ_H 4.12 from CO—O—C<u>H</u>$_2$ in monomer and polymer, respectively. The first-order kinetic plot, Figure 8, is initially linear, until about 30% conversion, but levels off at higher conversions. Using only the first few data points of the kinetic plot, $k_p^{app} = 2.2 \times 10^{-5}$ s^{-1} could be estimated, close to the values found for MMA and MEA. Evidently PEGMA reacts initially at the same rate as the other monomers, but due to increased viscosity and reduced solubility further reaction is impeded. Evolution of molecular weights was linear with conversion and the PDI remained low (<1.2), Figure 9. SEC-curves were monomodal with a high molecular-weight shoulder, as seen in the polymerizations of MMA and MEA.

Shemper and Mathias[15] have reported the polymerization of poly(propylene glycol) methacrylate ($M_n \approx 300$ g mol^{-1}) using FMI as initiator with Cu(I)Br/PMDETA and conducting polymerization in methyl ether ketone at 80 °C. Here a much shorter reaction time was reported with the completion of reaction in only 2 h for [M]:[I] = 10, attaining target molecular weight of 5200 g mol^{-1} from NMR.

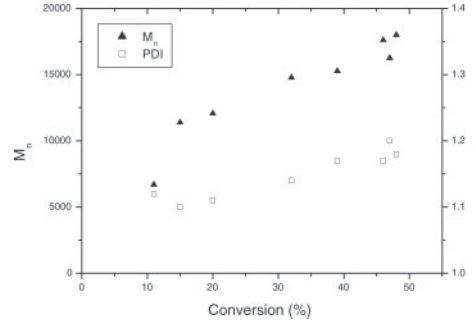

Figure 9. Evolution of M_n (▲) and PDI (□) for the polymerization of PEGMA from FMI. [M]:[I]:[Cu(I)Br]:[**n-Pr-1**] = 42:1:1:2 (entry V, Table 1). Reaction temperature = 90 °C.

Copolymerization of MMA and PEGMA

The synthesis of a block copolymer of MMA and PEGMA was undertaken as a sequential reaction at 90 °C in toluene. The first-order kinetic plot, Figure 10, is quite similar to that recorded for the homopolymerization of PEGMA. The evolution of molecular weights was reasonably linear with conversion and the PDI remained low (<1.25) up to a conversion of ~70%, Figure 11. Attempts to take the reaction to higher conversions resulted in side-reactions with the PDI increasing sharply (~1.7). SEC-curves were monomodal with the highmolecular-weight shoulder seen in the other polymerizations. Thus, it is possible to synthesize block

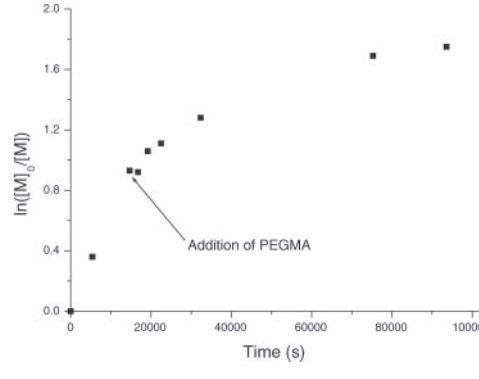

Figure 10. First-order kinetic plot for the sequential polymerization of MMA and PEGMA from FMI in toluene solution. [I]:[Cu(I)Br]:[**n-Pr-1**] = 1:1:2, Reaction temperature = 90 °C.

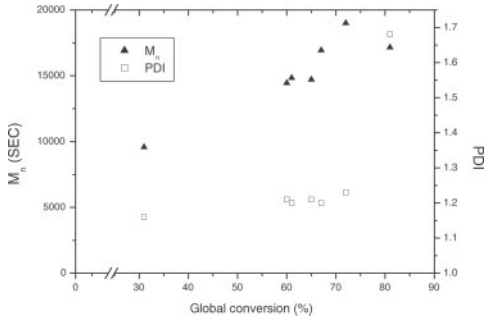

Figure 11. Evolution of M_n (▲) and PDI (□) for FMI-PMMA-*b*-PPEGMA. $[M_1]:[M_2]:[I]:[Cu(I)Br]:[$**n-Pr-1**$] = 100:42:1:1:2$ (entry V, Table 1).

copolymers in a controlled fashion up to 70% conversion after which molecular weight control is lost.

Thermal Properties

The glass transition temperatures of the polymers were determined by DSC, Table 2. The FMI exhibited three thermal transitions: $T_g = -71$ °C, crystallization at −48 °C, and $T_m = 8$ °C, Figure 12. The FMI performs as a plasticizer in the FMI-PMMA polymers with the effect diminishing with increasing molecular weight, as expected. For the FMI-PMMA with a molecular weight of ~30,000 g mol^{-1} the T_g is reduced by 10 °C, whereas for the lower molecular weight FMI-PMMAs reductions in T_g of 28 and 37 °C, respectively are seen. Part of this effect is attributed to the difference in molecular weights, but the terminal fluorinated group must primarily be responsible for this phenomenon.

For the hydrophilic polymers PMEA and PPEGMA the fluorinated moiety gives rise to only small changes in T_g, with both polymers already having T_g's well below ambient temperature. The introduction of the FMI leads to an increase in T_g for PMEA, which is not expected, as FMI has a lower T_g than PMEA. In addition FMI is anticipated to work as a plasticizer in this polymer. There is however only an increase in temperature of 11 °C, wherein effects from molecular weight differences furthermore are included.

The T_g's of FMI-PPEGMA and PPEGMA diverge by 5 °C, which is not surprising, as the T_g's of FMI and PPEGMA are −71 and −65 °C, respectively. The most pronounced difference between the fluorinated and nonfluorinated polymers of PPEGMA was that a crystallization peak was observed for the latter at 117 °C. The presence of the FMI suppresses crystallization. The copolymer FMI-PMMA-*b*-PPEGMA has two thermal transitions, the lower one at −37 °C being quite strong, while the second at 33 °C is less distinct. Thus, we see evidence of microphase separation with the discrepancy between the values for the homopolymers and the block copolymer ascribed to the fact that the copolymer is a gradient block copolymer. This still gives rise to two T_g's as in any phase separated

Table 2. Glass Transition Temperatures and Thermal Stabilities of Polymers Initiated by Fluorinated Macroinitiator

Entry[a]	Polymer	$M_{n,\,SEC}$ (g mol^{-1})	T_g (°C)	T (°C)		
				10 % wt loss	50 wt % loss	90 wt % loss
	FMI	–	−71	197	262	354
I	FMI-PMMA	5500[b]	64	277	387	414
II	FMI-PMMA	7900[b]	73	275	389	415
III	FMI-PMMA	29,900	90	283	384	407
	PMMA[c]	18,600	101	340	393	415
IV	FMI-PMEA	24,400	−38	370	411	439
	PMEA[c]	18,200	−37	363	396	422
V	FMI-PPEGMA	16,300	−70	259	369	414
	PPEGMA[c]	7600	−65	291	376	418
VII	FMI-PMMA-*b*-PPEGMA	21,600	−37; 33	329	381	413

[a] Entry numbers are equivalent to the ones used in Table 1.
[b] M_n estimated by ^{1}H NMR.
[c] Homopolymerization by ATRP initiated by EBB.

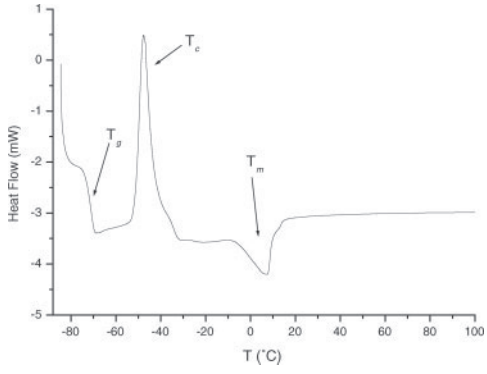

Figure 12. DSC analysis of FMI, second heating cycle from −90 to 200 °C (only data up to 100 °C shown). Glass transistion (T_g), crystallization (T_c) and melting (T_m) temperatures are indicated by arrows.

block copolymer, however these are found at intermediate temperatures compared with the homopolymers.

Thermal Stability

Fluorine content in polymers often increases thermal resistance. To compare the thermal stabilities of the polymers we report the temperature at weight losses of 10, 50, and 90%, Table 2. Nonfluorinated homopolymers synthesized for DSC were also used for comparison in TGA. Analysis of the macroinitiator showed that the thermal stability of this was lower than for any of the synthesized polymers. This is reflected by lower thermal stability of the PPEGMA polymers, as the onset of degradation of FMI-PPEGMA began earlier than for the PEGMA homopolymer, Table 2. The three FMI-PMMA polymers exhibited a similar behavior being less thermally stable than PMMA homopolymer with the onset of degradation beginning at 275 °C for the FMI-PMMAs, that is, 65 °C lower than for PMMA.

The block copolymer FMI-PMMA-*b*-PPEGMA had a delayed degradation onset compared with both fluorinated polymers (FMI-PMMA and FMI-PPEGMA), whereas at higher temperatures (>375 °C) the difference is negligible. The degradation to 90% of the original weight took place at ~363 °C for PMEA and 370 °C for FMI-PMEA, Figure 13. This indicates that the introduction of the fluorinated moiety had a minor positive effect on PMEA, as it did not reduce the thermal properties in contrast to the case for the other tested polymers.

Surface Activity

Contact angles of water on the polymers were measured on films that had formed by spin coating onto glass slides followed by annealing, Table 3.

In general, the incorporation of the FMI into the three different (meth)acrylic polymers increased the water advancing contact angle ($\Theta_{advancing}$) as compared with the nonfluorinated polymers. Thus, $\Theta_{advancing}$ of FMI-PMMA increased by 10° or more from $\Theta_{advancing} = 73°$ observed for the relatively hydrophobic PMMA. The hysteresis is much larger for the fluorinated polymers, implying that these can be viewed as copolymers consisting of a moderately hydrophobic and a highly hydrophobic block giving rise to an increased difference between $\Theta_{advancing}$ and $\Theta_{receding}$. The surface roughness also influences this factor, but there was no visible difference between the samples regarding this.

The effect of introducing FMI on $\Theta_{advancing}$ was more pronounced for PMEA, which has been classified an intermediate hydrophilic polymer[17] and the hydrophilic PPEGMA. For PMEA $\Theta_{advancing}$ of 92° and 55° were found for the partly fluorinated and nonfluorinated polymers, respectively, a difference of more than 35°, ascribed to the fluoroalkoxy tail. Apparently the fluorinated segments migrate to the surface during annealing, seen by the increase in both advancing and receding contact angles. The migration of the fluorinated segments to the surface during annealing has previously been observed.[12,24]

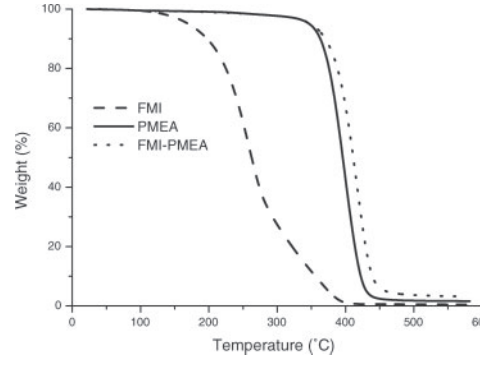

Figure 13. TGA-curves for FMI, PMEA and FMI-PMEA.

Table 3. Water Contact Angles of Polymers Initiated by Fluorinated Macroinitiator, FMI

Entry[a]	Polymer	$M_{n,\ SEC}$ (g mol^{-1})	$\Theta_{advancing}$	$\Theta_{receding}$
I	FMI-PMMA	5500[b]	83 (± 2)	59 (± 3)
II	FMI-PMMA	7900[b]	90 (± 1)	39 (± 4)
III	FMI-PMMA	29,900	82 (± 3)	57 (± 2)
	PMMA[c]	18,600	73 (± 1)	58 (± 2)
IV	FMI-PMEA	24,400	92 (± 4)	64 (± 8)
	PMEA[c]	7500	55 (± 9)	11 (± 3)
V	FMI-PPEGMA	16,300	67 (± 6)	22 (± 4)
	PPEGMA[c]	7600	42 (± 6)	19 (± 3)

[a] Entry numbers are equivalent to the ones used in Table 1.
[b] M_n estimated by ^{1}H NMR.
[c] Homopolymerization initiated by EBB.

The polymers containing PEGMA were not easily solubilized and the films formed from these polymers were not homogeneous containing particles consisting of nondissolved polymer. Results obtained for these polymers are therefore estimates, as the difference between measurements was considerable. It can, however be concluded that the presence of the fluorinated chain end resulted in larger contact angles of water on the film surfaces with the advancing contact angle increasing from 42° to 67°. The change in the receding contact angle was virtually nonexistent (19° vs. 22°), which lead to an increase in hysteresis that is the opposite behavior than seen for PMEA.

CONCLUSIONS

Controlled polymerizations of MMA, MEA, and PEGMA were achieved using a FMI based on the commercially available fluorinated surfactant Zonyl FSO-100. Although the macroinitiator resulted in slower reaction kinetics than the conventional ethyl-2-bromoisobutyrate the obtained results were comparable in terms of molecular weight distributions. The FMI functioned as a plasticizer in polymers of MMA by reducing T_g significantly especially for PMMA with low molecular weights. Thermogravimetric measurements showed that the introduction of the FMI lead to a decrease in thermal stability of polymers of MMA and PEGMA, while the thermal stability was unaltered in PMEA. All the synthesized polymers exhibited an increase in hydrophobicity with the introduction of the fluorinated moiety, which was especially pronounced for PMEA with an increase in the advancing contact angle of more than 35°.

N. Hansen would like to thank Novo Nordisk A/S for supporting her project as well as the following funds for supporting her stay at the University of Warwick: Ingeniørvidenskabelig Fond og G.A. Hagemanns Mindefond; Berg, Nielsens Legat; Knud Højgaards Fond & Otto Mønsteds Fond.

REFERENCES AND NOTES

1. Hansen, N. M. L.; Jankova, K.; Hvilsted, S. Eur Polym J 2007, 43, 255.
2. (a) Kato, M.; Kamigaito, M.; Sawamoto, M.; Higashimura, T. Macromolecules 1995, 28, 1721; (b) Wang, J. S.; Matyjaszewski, K. J Am Chem Soc 1995, 117, 5614.
3. (a) Kamigaito, M.; Ando, T.; Sawamoto, M. Chem Rev 2001, 101, 3689; (b) Matyjaszewski, K.; Xia, J. Chem Rev 2001, 101, 2921; (c) Limer, A.; Haddleton, D. M. Prog React Kinet 2004, 29, 187.
4. Destarac, M.; Matyjaszewski, K.; Silverman, E.; Ameduri, B.; Boutevin, B. Macromolecules 2000, 33, 4613.
5. Shi, Z. Q.; Holdcroft, S. Macromolecules 2004, 37, 2084.
6. Lu, G. L.; Zhang, S.; Huang, X. Y. J Polym Sci Part A: Polym Chem 2006, 44, 5438.
7. Hester, J. F.; Banerjee, P.; Won, Y. Y.; Akthakul, A.; Acar, M. H.; Mayes, A. M. Macromolecules 2002, 35, 7652.
8. Holmberg, S.; Holmlund, P.; Wilen, C. E.; Kallio, T.; Sundholm, G.; Sundholm, F. J Polym Sci Part A: Polym Chem 2002, 40, 591.
9. Chen, Y. W.; Liu, D. M.; Deng, Q. L.; He, X. H.; and Wang, X. F. J Polym Sci Part A: Polym Chem 2006, 44, 3434.

10. Jankova, K.; Hvilsted, S. Macromolecules 2003, 36, 1753.
11. Hvilsted, S.; Borkar, S.; Siesler, H. W.; Jankova, K. In Advances in Controlled/Living Radical Polymerization; Matyjaszewski, K. Ed.; ACS Symposion Series Vol. 854; American Chemical Society: Washington, DC, 2003; Chapter 17, pp 236–249.
12. Borkar, S.; Jankova, K.; Siesler, H. W.; Hvilsted, S. Macromolecules 2004, 37, 788.
13. Cheng, C.; Wooley, K. L.; Khoshdel, E. J Polym Sci Part A: Polym Chem 2005, 43, 4754.
14. Perrier, S.; Jackson, S. G.; Haddleton, D. M.; Ameduri, B.; Boutevin, B. Tetrahedron 2002, 58, 4053.
15. Shemper, B. S.; Mathias, L. J. Eur Polym J 2004, 40, 651.
16. Jankova, K.; Chen, X. Y.; Kops, J.; Batsberg, W. Macromolecules 1998, 31, 538.
17. Tanaka, M. Bio-Med Mater Eng 2004, 14, 427.
18. Tanaka, M.; Mochizuki, A. J Biomed Mater Res A 2004, 68, 684.
19. Li, G. F.; Shen, Y.; Morita, S.; Nishida, T.; Osawa, M. J Am Chem Soc 2004, 126, 12198.
20. Bednarek, M.; Jankova, K.; Hvilsted, S. J Polym Sci Part A: Polym Chem 2007, 45, 333.
21. Keller, R. N.; Wycoff, H. D. Inorg Synth 1946, 2, 1.
22. Haddleton, D. M.; Crossman, M. C.; Dana, B. H.; Duncalf, D. J.; Heming, A. M.; Kukulj, D.; Shooter, A. J. Macromolecules 1999, 32, 2110.
23. Lecolley, F. New Polymers from Living Radical Polymerisation for Biological Applications, Chapter 3: Synthesis and Characterization of *N*-succinimidyl ester functionalized Poly (mPEGMA), Ph.D. Thesis, 2004, University of Warwick, UK.
24. Wang, J. G.; Ober, C. K. Macromolecules 1997, 30, 7560.

Appendix 4

Synthesis of Fluorinated Copolymers by Controlled Radical Polymerization

SYNTHESIS OF FLUORINATED COPOLYMERS BY CONTROLLED RADICAL POLYMERIZATION

Natanya M.L. Hansen[1], Michael Gerstenberg[2], David M. Haddleton[3], Søren Hvilsted[1*]

[1]*Danish Polymer Centre, Dept. of Chemical Engineering, Technical University of Denmark, Building 423, DK-2800 Kgs. Lyngby, Denmark*

[2]*Novo Nordisk A/S, Brennum Park, DK-3400 Hillerød, Denmark*

[3]*Department of Chemistry, University of Warwick, Coventry CV4 7AL, United Kingdom*

*corresponding author: sh@kt.dtu.dk

Abstract

The partly fluorinated monomers, 2,2,2-trifluoroethylene methacrylate (3FM), 2,2,3,3,4,4,5,5-octafluoropentyl methacrylate (8FM), and 1,1,2,2-tetrahydroperfluorodecyl methacrylate (17FM) have been employed in the preparation of block copolymers with methyl methacrylate (MMA), 2-methoxyethyl acrylate (MEA), and poly(ethylene glycol) methyl ether methacrylate (PEGMA) by Atom Transfer Radical Polymerization (ATRP). A kinetic study of the 3FM homopolymerization initiated with ethyl bromoisobutyrate and Cu(I)Br/*N*-(*n*-propyl)-2-pyridylmethanimine as catalyst shows good living/controlled polymerization in the temperature range, 80 to 110°C, with apparent rate constants, k_p^{app}, from $1.6 \cdot 10^{-4}$ s^{-1} to $2.9 \cdot 10^{-4}$ s^{-1} and the activation energy, E_a = 24 kJ mol^{-1}. Various 3FM containing block copolymers with MMA are prepared by (random) sequential monomer addition or from a PMMA macroinitiator in all cases with controlled characteristics. Block copolymers of 3FM and PEGMA from random addition resulted in block copolymers with PDI < 1.22, whereas the block copolymers from 3FM and MEA have less controlled characteristics with PDI on the order of 1.6. Block copolymers based on MMA with 8FM and 17FM have PDI's < 1.30. The glass transition temperatures of the block copolymers are in almost all cases dominated by the majority monomer. Sequential monomer addition results in too short pure blocks to induce observable microphase separation by DSC in otherwise very amphiphilic monomer combinations. The thermal stability of the fluorinated poly(methacrylates) in inert atmosphere is less than that of the non-fluorinated poly((meth)acrylates) ascribed to cleavage of the fluoroalkoxy pendant chains. The presence of fluorinated blocks in all instances significantly increase the advancing water contact angle of thin films deposited on glass as compared to films of the non-fluorinated poly((meth)acrylates).

Introduction

Fluorinated polymers have received increased interest due to a number of unique properties related to the high hydrophobicity including good biocompatibility and low surface energy, in addition to high chemical and thermal resistance. Various controlled radical polymerization methods have been employed to synthesize fluorinated polymers for a wide range of applications[1], where the most recently reported include corrosion resistant surface coatings[2], solid-state electrolytes for batteries[3], materials for nanoscale electronics[4] as well as biocompatible materials for medico purposes[5,6].

The incorporation of fluorinated monomers in block copolymers is a possible route to obtain multifunctional fluorinated polymers. Atom transfer radical polymerization (ATRP)[7] is a versatile method for synthesizing block copolymers and only shortly after the advent of ATRP, fluorinated methacrylic monomers were copolymerized by this method[8]. Fluorinated (meth)acrylic monomers can be combined with a range of other monomers and have previously been copolymerized with monomers of similar character such as methyl methacrylate, butyl methacrylate as well as styrene[9,10,11]. The combination with the hydrophilic monomers 2-hydroxyethyl methacrylate[8] and 2-(dimethylamino)ethyl methacrylate[12] has been utilized to render amphiphilic and surface active copolymers. Another approach has been to convert a hydrophobic polymer (styrene or *tert*-butyl acrylate) to a more hydrophilic monomer by functionalization into an ionic species post polymerization[13]. Methacrylate-functionalized poly(ethylene glycol) and poly(propylene glycol) have been copolymerized with a fluorinated methacrylate to synthesize both linear and 4 arm star shaped copolymers[14]. Amphiphilic di- and triblock copolymers have also been synthesized utilizing poly(ethylene oxide)-macroinitiators for the polymerization of the fluorinated methacrylates yielding comb shaped di- and triblock copolymers[15,16]. The combination of ATRP and enzymatic ring-opening polymerization has recently been utilized to synthesize copolymers of fluorinated methacrylate and ε-caprolactone in super critical carbon dioxide[17]. A few cases of surface-initiated ATRP of fluorinated methacrylates (copolymer with MA or MMA) can be found in the literature[18,19]. The attachment of the highly hydrophobic polymers to the surfaces resulted in drastic changes in contact angles compared to the surface covered in non-fluorinated brushes.

In this present work amphiphilic block copolymers were synthesized using three different fluorinated methacrylates 2,2,2-trifluoroethylene methacrylate (3FM), 2,2,3,3,4,4,5,5-octafluoropentyl methacrylate (8FM) and 1,1,2,2-tetrahydroperfluorodecyl methacrylate (17FM) with pendant alkyl chains containing 3, 8 and 17 fluorine atoms, respectively. ATRP mediated by copper(I)/*N*-(*n*-propyl)-2-pyridylmethanimine catalyst was used for polymerization. Our approach was to initially copolymerize the fluorinated methacrylates with methyl methacrylate (MMA) (Scheme 1) to ascertain how the fluorinated pendant chain influences the reactivity of the monomers. A kinetic study of the homopolymerization of 3FM was also undertaken to optimize reaction conditions. Fluorinated solvents are commonly used as reaction media, but here toluene was chosen, as this is an inexpensive and relatively benign solvent. Herein a method of polymerizing well-defined block copolymers from both the fluorinated monomer and the non-fluorinated is proposed, which has not previously been reported for systems in non-fluorinated organic solvents. Novel block copolymers of 3FM and hydrophilic monomers 2-methoxyethyl acrylate (MEA) and poly(ethylene glycol) methyl ether methacrylate (PEGMA), respectively have been synthesized (Scheme 2 & 3). These copolymers are highly amphiphilic and could hold potential for biomedical applications. PMEA is biocompatible and demonstrates superior properties with respect to blood compatibility in comparison with polymers having similar structures[20]. The presence of "freezing bound water" in PMEA is thought to be the reason for the excellent blood compatibility, although the mechanism is not fully understood[21,22]. MEA has recently been polymerized successfully by ATRP in our group[23,24], which has given further incentive to study the possibilities of copolymerization with fluorinated compounds.

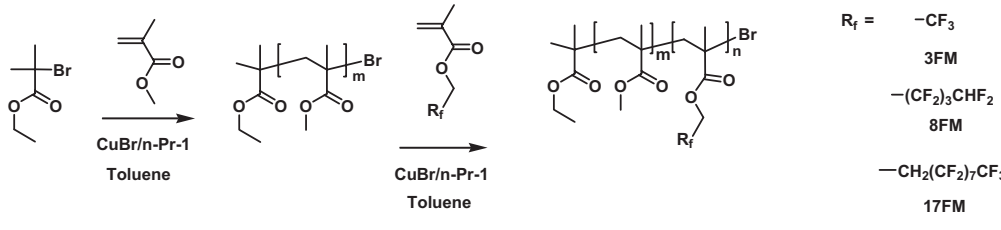

Scheme 1. Outline of the synthesis of PMMA-*b*-PxFM copolymers.

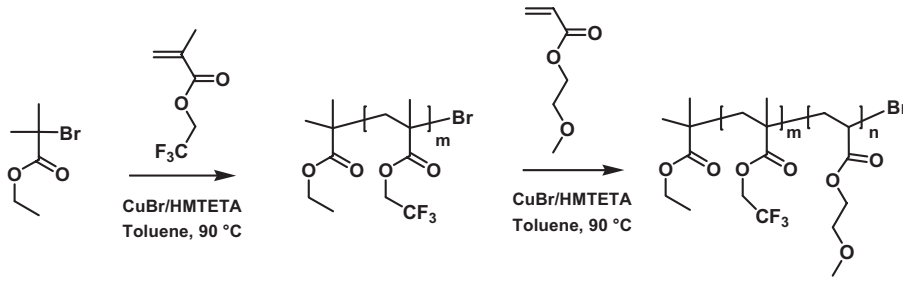

Scheme 2. Outline of the synthesis of P3FM-*b*-PMEA.

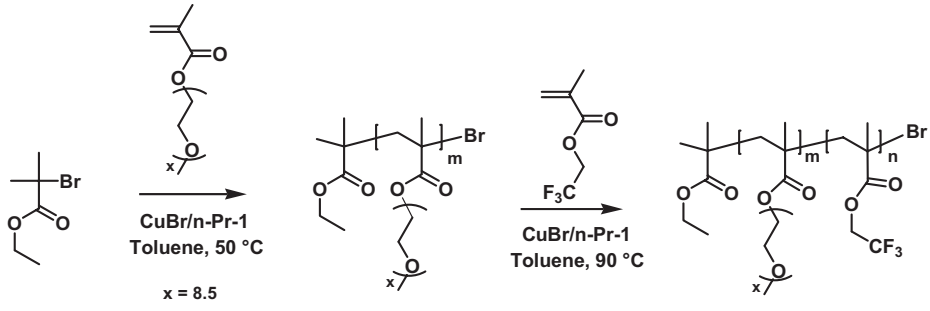

Scheme 3. Outline of synthesis of PPEGMA-*b*-P3FM.

Experimental

Materials

2,2,2-Trifluoroethylene methacrylate (3FM), 2,2,3,3,4,4,5,5-octafluoropentyl methacrylate (8FM) and 1,1,2,2-tetrahydroperfluorodecyl methacrylate (17FM) were kindly supplied by Osaka Chemicals. Methyl methacrylate (MMA), 2-methoxyethyl acrylate (MEA), poly(ethylene glycol) methyl ether methacrylate (PEGMA) ($M_n \approx 475$ g/mol) and 1,1,4,7,10,10-hexamethyltriethylenetetramine (HMTETA) were purchased from Sigma Aldrich. The monomers were passed through a column of activated neutral Al_2O_3 before use to remove inhibitor. Ethyl 2-bromoisobutyrate (EBB), chloroform and toluene (Sigma Aldrich) were used without further purification. Cu(I)Br was purified according to the method of Keller and Wycoff[25]. *N*-(*n*-Propyl)-2-pyridylmethanimine (**n-Pr-1**) was synthesized as previously described[26] and deoxygentated prior to use.

Instrumentation

Molecular weights were determined by size exclusion chromatography (SEC) performed on a Polymer Laboratories (PL) modular system with a PL gel 5 mm guard column (50 x 7.5 mm) and two PL gel 5 μm mixed D-columns (300 x 7.5 mm) (Polymer Laboratories) using tetrahydrofuran/triethylamine 95:5 as eluent using PMMA-standards (flow rate 1 ml min^{-1}, toluene as flow rate marker) unless otherwise stated. ^1H NMR was performed on a Bruker DPX400 spectrometer using $CDCl_3$ as solvent. The glass transition temperatures (T_g) were determined with a DSC Q1000 system (TA Instruments). Samples were heated to 150°C (10 °C/min) and cooled to -50°C (or -100°C) to remove any effects induced by prior treatment. The T_g was then determined by consecutive heating from -50°C (or -100°C) to 200°C at 10°C min^{-1}. Cooling to -100°C was only used for the polymers containing PMEA or PPEGMA, as these polymers have T_g's below ambient temperature. Thermogravimetric analysis (TGA) was performed on a TGA Q500 (TA Instruments) heating the polymer from ambient temperature to 600°C at a rate of 20 °C min^{-1} under nitrogen atmosphere. Samples for contact angle measurements were dissolved in dichloromethane (20 mg ml^{-1}) and spin coated (1000 rpm) onto glass slides. Measurements were performed on an OCA15plus contact angle system apparatus from Dataphysics with contact angles attained by the "needle-in" method. Contact angles were determined at minimum three different positions on the films.

Synthesis of P3FM – kinetic measurements

4.0 ml (28 mmol) of 3FM and 4.0 ml of toluene were charged to a Schlenk tube equipped with a magnetic stirrer and sealed with a rubber septum. 34 mg (0.24 mmol) of Cu(I)Br and 35 μl (0.24 mmol) of EBB were added, and 5 freeze-pump-thaw cycles were carried out to deoxygenate the reaction mixture. Reactants were thawed to ambient temperature, 75 μl (0.48 mmol) of **n-Pr-1** was added and the reaction carried out at the chosen temperature. Samples (~100 μl) were withdrawn by syringe under nitrogen at regular intervals for analysis by ^1H NMR and SEC. The polymer was dissolved in dichloromethane and precipitated in slightly acidic water (H_2SO_4). The product was recovered as a light green solid after removal of volatiles *in vacuo*. SEC of these polymers was performed using chloroform/triethylamine 95:5 as eluent, but otherwise similar to the previously mentioned system.

Synthesis of P3FM-*b*-PMMA (I & II, Table 2)

5.0 ml (35 mmol) of 3FM and 5.0 ml of toluene were charged to a Schlenk tube equipped with a magnetic stirrer and sealed with a rubber septum. 42 mg (0.29 mmol) of Cu(I)Br, and 45 µl (0.31 mmol) of EBB were added, and 5 freeze-pump-thaw cycles were performed. Reactants were thawed to ambient temperature, 90 µl (0.58 mmol) of **n-Pr-1** was added and reaction was allowed to proceed at 80°C. 4 ml (37 mmol) of deoxygenated MMA (50 % v/v solution in toluene) was added to the reaction after 2 hrs by either syringe (experiment I) or cannulation (experiment II). Samples were withdrawn by syringe under nitrogen at regular intervals for analysis by ^{1}H NMR and SEC. Catalyst was removed on a column of activated neutral Al_2O_3 and the product was recovered as a light green solid after removal of volatiles *in vacuo*.

Synthesis of P3FM-*b*-PMMA (III, Table 2)

5.0 ml (35 mmol) of 3FM and 5.0 ml of toluene were charged to a Schlenk tube equipped with a magnetic stirrer and sealed with a rubber septum. 44 mg (0.31 mmol) of Cu(I)Br, and 45 µl (0.31 mmol) of EBB were added and degassed via 5 freeze-pump-thaw cycles. Reactants were thawed to ambient temperature, 90 µl (0.58 mmol) of **n-Pr-1** was added and reaction allowed to proceed at 90°C. Deoxygenated MMA, 4 ml (37 mmol), of (50% v/v solution in toluene) was cannulated into the reaction after 2 hrs. Samples were withdrawn by syringe under nitrogen at regular intervals for analysis by ^{1}H NMR and SEC. The polymer was dissolved in THF and precipitated in slightly acidic water. The product was purified by precipitation in methanol/water (slightly acidic).

Synthesis of PMMA-*b*-P3FM (V, Table 2)

5.0 ml (47 mmol) of MMA and 5.0 ml of toluene were charged to a Schlenk tube equipped with a magnetic stirrer and sealed with a rubber septum. Cu(I)Br, 69 mg (0.48 mmol) and 70 µl (0.48 mmol) of EBB were added, and 3 freeze-pump-thaw cycles were performed. Reactants were thawed to ambient temperature, 145 µl (0.93 mmol) of **n-Pr-1** was added and reaction was carried out at 80°C. 4 ml (28 mmol) of deoxygenated 3FM (50 % v/v solution in toluene) was cannulated into the reaction after 3.5 hrs. Samples were withdrawn by syringe under nitrogen at regular intervals for analysis by ^{1}H NMR and SEC. Catalyst was removed on a column of activated neutral Al_2O_3 and the product was recovered as a light green solid after removal of volatiles *in vacuo*.

Synthesis of PMMA-macroinitiator

MMA, 5.0 ml (47 mmol), and 5.0 ml of toluene were charged to a Schlenk tube equipped with a magnetic stirrer and sealed with a rubber septum. Cu(I)Br, 68 mg (0.47 mmol) , and 70 µl (0.48 mmol) of EBB were added, and 3 freeze-pump-thaw cycles were carried out. The reactants mixture was thawed to ambient temperature prior to the addition of 145 µl (0.93 mmol) of **n-Pr-1** followed by polymerization at 90°C. Samples were withdrawn by syringe under nitrogen at regular intervals for analysis by ^{1}H NMR and SEC. Catalyst was removed on a column of activated basic Al_2O_3 and the product was recovered as a light green solid after removal of volatiles *in vacuo*. M_n = 4400 g mol^{-1}, PDI = 1.16.

Synthesis of PMMA-*b*-P3FM (IV, Table 2) from PMMA-macroinitiator

3FM, 2.9 ml (20 mmol) and 4.0 ml of toluene were charged to a Schlenk tube equipped with a magnetic stirrer and sealed with a rubber septum. Cu(I)Br, 26 mg (0.18 mmol) and 1.0 g (0.2 mmol) of PMMA-macroinitiator were added, and 5 freeze-pump-thaw cycles were carried out. Reactants were thawed to ambient temperature, 45 µl (0.29 mmol) of **n-Pr-1** was added and reaction was run at 80°C. Samples were withdrawn by syringe under nitrogen at regular intervals for analysis by ^{1}H NMR and SEC. The product was purified by precipitation in methanol/water (slightly acidic).

Synthesis of PMMA-*b*-P8FM (VI, Table 2)

MMA, 5.0 ml (47 mmol) and 5.0 ml of toluene were charged to a Schlenk tube equipped with a magnetic stirrer and sealed with a rubber septum. Cu(I)Br, 70 mg (0.49 mmol) and 70 µl (0.48 mmol) of EBB were added, and degassed via 3 freeze-pump-thaw cycles. Reactants were thawed to ambient temperature, 150 µl (0.96 mmol) of **n-Pr-1** was added and reaction proceeded at 80°C. A total of 4 ml (19 mmol) of degassed 8FM (50 % v/v solution in toluene) was cannulated into the reaction after 3.5 hrs. Samples were withdrawn by syringe under nitrogen at regular intervals for analysis by ^{1}H NMR and SEC. The product was purified by precipitation in methanol/water (slightly acidic).

Synthesis of PMMA-*b*-P17FM (VII, Table 2)

MMA, 5.0 ml (47 mmol), and 5.0 ml of toluene were charged to a Schlenk tube equipped with a magnetic stirrer and sealed with a rubber septum. Cu(I)Br,69 mg (0.48 mmol), and 70 µl (0.48 mmol) of EBB were added, and 3 freeze-pump-thaw cycles were carried out.

Reactants were thawed to ambient temperature, 145 µl (0.93 mmol) of **n-Pr-1** was added and reaction was allowed to proceed at 90°C. After 3.5 hrs 3.4 ml (10 mmol) of degassed 17FM (50 % V/V solution in toluene) was cannulated into the reaction. Samples were withdrawn by syringe under nitrogen at regular intervals for analysis by ^{1}H NMR and SEC. The product was purified by precipitation in petrol ether.

Synthesis of PPEGMA-*b*-P3FM (I, Table 3)

PEGMA, 5.0 ml (11 mmol), and 5.0 ml of toluene were charged to a Schlenk tube equipped with a magnetic stirrer and sealed with a rubber septum. Cu(I)Br, 40 mg (0.28 mmol) and 40 µl (0.26 mmol) of EBB were added, and 3 freeze-pump-thaw cycles were carried out. Reactants were thawed to ambient temperature, 85 µl (0.55 mmol) of **n-Pr-1** was added and reaction proceeded at 50°C. 4.8 ml (34 mmol) of degassed 3FM (50 % v/v solution in toluene) was cannulated into the reaction mixture after 9 hrs followed by an increase in temperature to 90 °C. Samples were withdrawn by syringe under nitrogen at regular intervals for analysis by ^{1}H NMR and SEC. Precipitation was not possible and the product was isolated by freeze drying.

Synthesis of P3FM-*b*-PPEGMA (II, Table 3)

3FM, 5.0 ml (35 mmol), and 5.0 ml of toluene were charged to a Schlenk tube equipped with a magnetic stirrer and sealed with a rubber septum. Cu(I)Br, 42 mg (0.29 mmol), and 45 µl (0.31 mmol) of EBB were added, and 5 freeze-pump-thaw cycles were carried out. 90 µl (0.58 mmol) of **n-Pr-1** was added after thawing the reaction mixture to ambient temperature. Polymerization was carried out at 90°C for 100 minutes, when the reaction mixture was cooled to 50 °C with liquid nitrogen followed by the cannulation of 5.0 ml (11 mmol) of degassed PEGMA (50 % v/v solution in toluene) into the Schlenk tube. ^{1}H NMR showed no reaction, and after 24 hours the temperature was increased to 90°C with the reaction proceeding 28 hours in total. Samples were withdrawn by syringe under nitrogen at regular intervals for analysis by NMR and SEC. Catalyst was removed on a column of activated basic Al_2O_3 and the product was recovered as a light brown solid after removal of solvent by freeze drying.

Synthesis of PMEA-*b*-P3FM (III, Table 3)

MEA, 5.0 ml (39 mmol), and 5.0 ml of toluene were charged to a Schlenk tube equipped with a magnetic stirrer and sealed with a rubber septum. Cu(I)Br, 38 mg (0.26 mmol), and 40 µl (0.26 mmol) of EBB were added, and 3 freeze-pump-thaw cycles were carried out. Reactants were thawed to ambient temperature, 70 µl (0.26 mmol) of HMTETA was added and reaction was performed at 90°C. 5.0 ml (35 mmol) of degassed 3FM (50 % V/V solution in toluene) was cannulated into the reaction mixture after 3.5 hrs. Samples were withdrawn by syringe under nitrogen at regular intervals for analysis by ^{1}H NMR and SEC. The polymer was dissolved in DCM and precipitated in methanol/water (slightly acidic).

Synthesis of P3FM-*b*-PMEA (IV & V, Table 3)

3FM, 5.0 ml (35 mmol), and 5.0 ml of toluene were charged to a Schlenk tube equipped with a magnetic stirrer and sealed with a rubber septum. Cu(I)Br, 42 mg (0.29 mmol), and 45 µl (0.31 mmol) of EBB were added, and 5 freeze-pump-thaw cycles were carried out. Reactants were thawed to ambient temperature, 80 µl (0.29 mmol) of HMTETA was added and reaction was carried out at 90 °C. 5.0 ml (39 mmol) of degassed MEA (50 % v/v solution in toluene) was cannulated into the reaction mixture after 1.5 hrs. Samples were withdrawn by syringe under nitrogen at regular intervals for analysis by ^{1}H NMR and SEC. The polymer was dissolved in DCM and precipitated in methanol/water (slightly acidic).

Results and discussion

Homopolymerization of 3FM

Homopolymerization of 3FM was undertaken at 4 different temperatures: 80, 90, 100 and 110 °C. Conversions were estimated from ^{1}H NMR analysis using the peak for C$\underline{H}_2$-CF_3 in the fluorinated methacrylate at δ_H 4.49 (q) (monomer) and δ_H 4.33 (polymer). The first-order kinetic plots for all the homopolymerizations are shown in Figure 1, while an example of molecular weight evolution is given in Figure 2. The results of all of the homopolymerizations are given in Table 1. The indicated molecular weights are, however, probably lower than the actual values due to the difference in molecular weight of the 3FM-unit and the PMMA-standards. Polymerization proceeded in a controlled fashion at all temperatures with linear first-order plots, molecular weights (M_n) increasing with conversion

and low polydispersities (PDI) throughout reaction. Molecular weights estimated by ^{1}H NMR were difficult to obtain due to peak overlap.

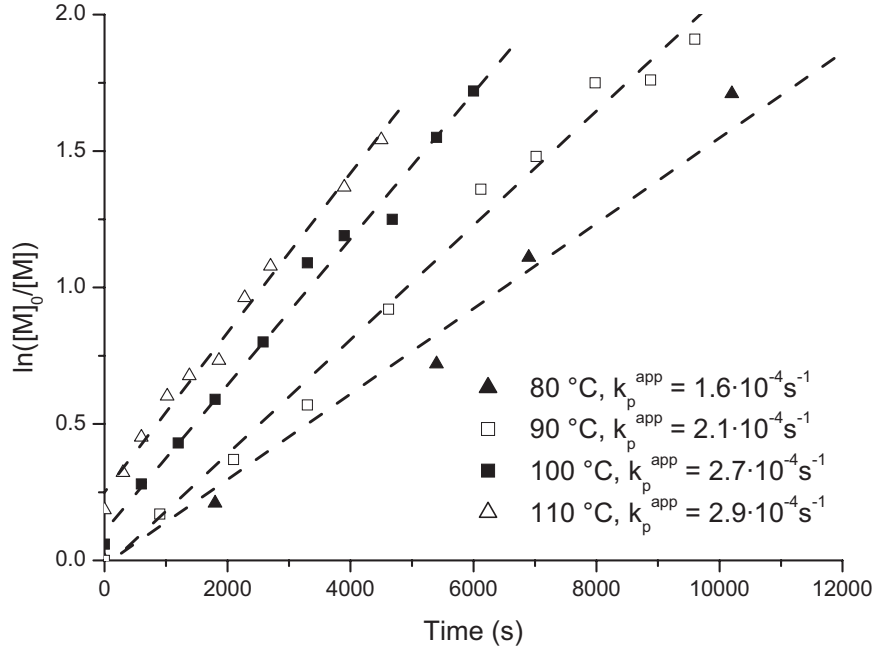

Figure 1. First-order plot for the homopolymerization of 3FM at 80°C (▲), 90°C (□) 100°C (■) and 110°C (△) in toluene solution. [M]:[I]:[Cu(I)Br]:[n-Pr-1] = 117:1:1:2. For the polymerization at 80 °C only data up to t = 12,000 s is shown.

Table 1. Homopolymerization of 3FM in toluene (50 v%).

	Polymer	Temperature (°C)	Time (min)	Conversion	$M_{n,\,SEC}$ (g mol^{-1})	PDI
I	P3FM	80 °C	320	0.94	9,900	1.35
II	P3FM	90°C	160	0.85	8,800	1.38
III	P3FM	100 °C	100	0.82	7,900	1.34
IV	P3FM	110 °C	75	0.79	6,200	1.28

[M]:[I]:[Cu(I)Br]:[n-Pr-1] = 117:1:1:2.

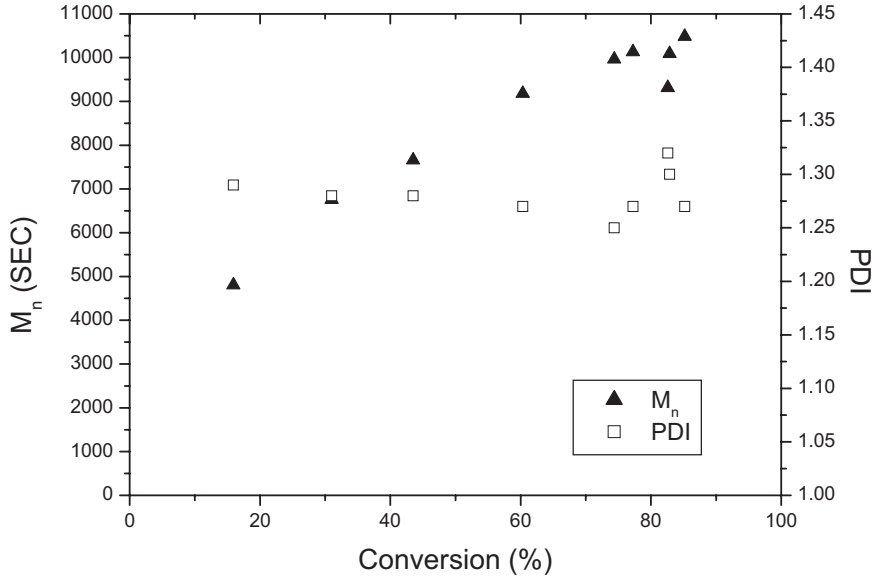

Figure 2. Evolution of M_n (▲) and PDI (□) for P3FM at 90 °C (entry II, Table 1). [M]:[I]:[Cu(I)Br]:[n-Pr-1] = 117:1:1:2. SEC was performed using chloroform as eluent.

The kinetic study exhibited a clear temperature dependency demonstrated by the acceleration of the polymerization reaction with increasing temperature. Apparent rate constants of reactivity, k_p^{app} ranging from $1.6 \cdot 10^{-4}$ s^{-1} to $2.9 \cdot 10^{-4}$ s^{-1} were found, which is in reasonably good agreement with the value of $1.2 \cdot 10^{-4}$ s^{-1} previously found for MMA at 90°C with a similar reaction system[26] ([M] : [I] = 100). The polymerization rate for 3FM was faster than for MMA, which has also been the observation for a number of fluoro-substituted styrenes compared to styrene in ATRP[27,28,29].

For all reactions t = 0 was defined as the time, when the temperature reached the required level, which at elevated temperatures was well after commencement of the polymerization, as reaction takes place above 80°C. Therefore the first-order plots do not start in origin for the higher temperatures. Polymerization proceeded in a controlled fashion at all temperatures with molecular weights increasing with conversion and relatively low PDI (<1.4). The activation energy of the reaction can be found from the Arrhenius plot, Figure 3, where the slope is equivalent to $-E_a/R$. Thus, E_a, the activation energy, of the polymerization is found to be 24 kJ mol^{-1}. This is a significantly lower than value of 61.3 kJ mol^{-1} found by Haddleton *et*

al. [30] for the homopolymerization of MMA in toluene (25 % solution). The difference can be attributed to the higher polymerization rate of 3FM resulting in a lower activation energy for this monomer, while the relative monomer concentration furthermore is elevated in this case.

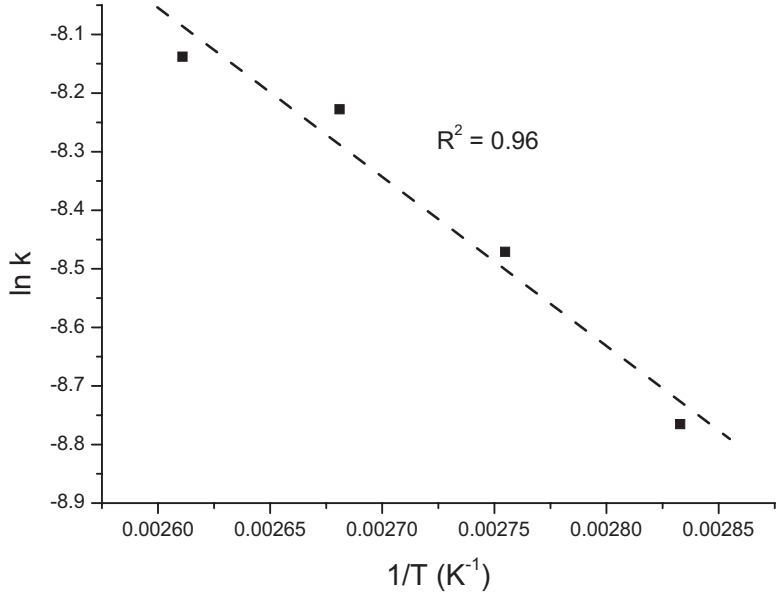

Figure 3. Arrhenius plot of the rate constants of reactivity, k_p^{app} for the homopolymerization of 3FM at 80, 90, 100 and 110°C in toluene solution. [M]:[I]:[Cu(I)Br]:[n-Pr-1] = 117:1:1:2.

Synthesis of copolymers of 3FM and MMA

The monomer with the lowest fluorine content, 3FM is the most soluble in conventional organic solvents and therefore studies were undertaken initially with polymers from this monomer in copolymerization with MMA. Conversions were estimated from ^{1}H NMR analysis using areas of the oxymethylene peaks at δ_H 4.49 (q) and δ_H 4.33 for 3FM and P3FM, respectively, Figure 4. Similarly the conversion of MMA was determined from the shift of the OCH_3-group from δ_H 3.72 (s) in the monomer to δ_H 3.59 in the polymer.

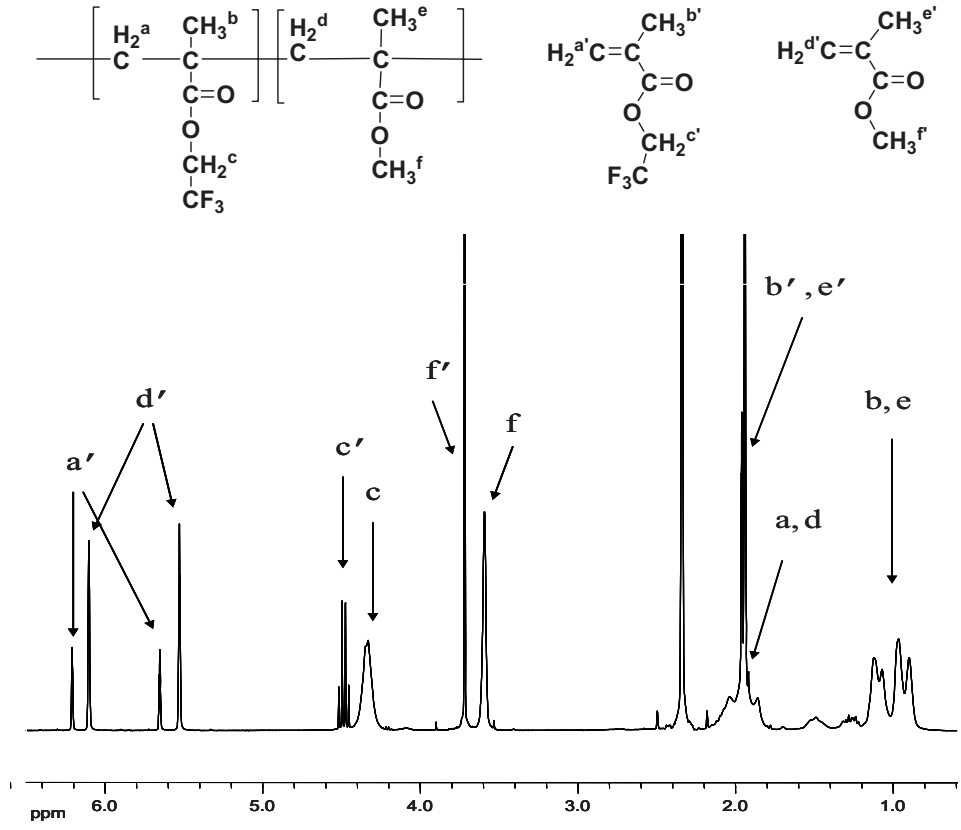

Figure 4. ^{1}H NMR-spectrum of a sample taken during the synthesis of P3FM-*b*-PMMA (entry I, Table 2) (t = 328 min) in toluene solution. The spectrum corresponds to 78 % conversion of 3FM and 45 % conversion of MMA. Assignments according to the structures above are indicated by the arrows (only φ-C<u>H</u>$_3$ δ 2.34 (s) from the solvent shown).

Sequential polymerizations

In the sequential polymerizations of the block copolymers, the second monomer was added at relatively high conversions of the first monomer, with both monomers continuing to polymerize after addition, as observed by ^{1}H NMR to give a gradient copolymer.

The first-order kinetic plot of the synthesis of PMMA-*b*-P3FM, Figure 5, was linear both before and after addition of 3FM indicating a low degree of termination. Evolution of M_n was linear with conversion, Figure 6 and PDI was low. For the polymerization of MMA from P3FM a small induction period was observed for the initiation of the second monomer, Figure 7. SEC-analysis showed a bimodal distribution for the P3FM-*b*-PMMA after the addition of MMA, Figure 8, indicating that some termination took place on addition of the second

monomer. This was, however, not the case for PMMA-*b*-P3FM, Figure 9, where a monomodal distribution was obtained. Furthermore, narrower molecular weight distributions were obtained for the polymerization of 3FM from PMMA than for the converse approach, Table 2. This may be due to the low solubility of P3FM in the solvent impeding further reaction. Increasing the reaction temperature from 80 to 90°C did not circumvent this, as the molecular weight distribution was broader at the elevated temperature. All the distributions obtained are, however, comparable with those found for the homopolymerization of 3FM, which indicates that these are the optimal results achievable with the given system. The values are also comparable with those found by Perrier *et al.*[10] in a similar system.

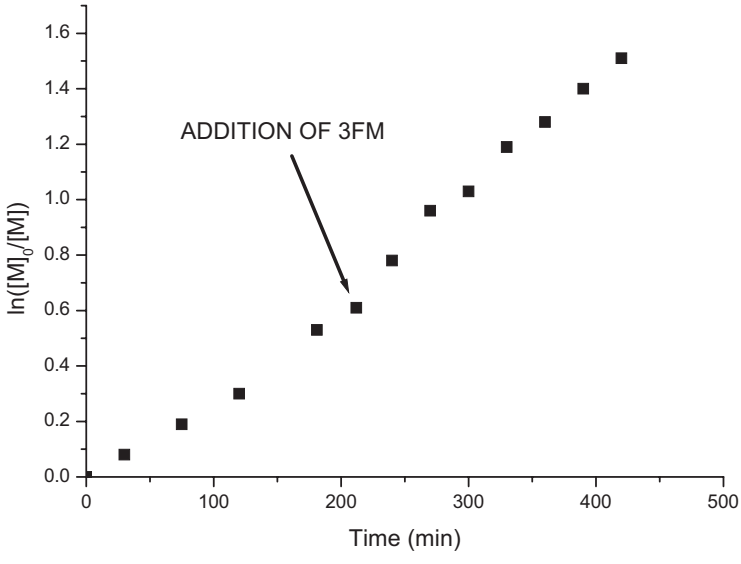

Figure 5. First-order kinetic plot for the synthesis of PMMA-b-P3FM (entry V, Table 2) in toluene solution at 80°C. [I]:[Cu(I)Br]:[n-Pr-1] = 1:1:2.

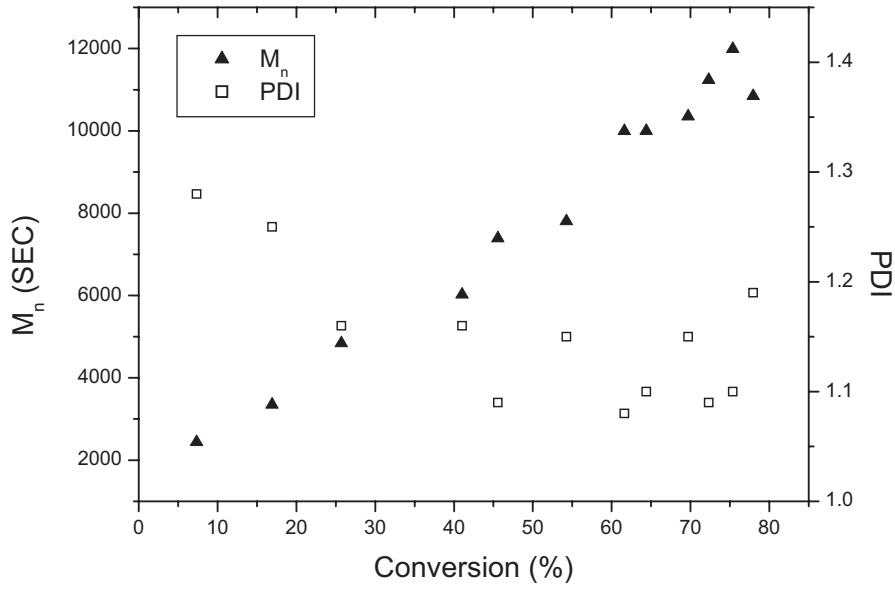

Figure 6. Evolution of M_n (▲) and PDI (□) for PMMA-*b*-P3FM (entry V, Table 2). [I]:[Cu(I)Br]:[n-Pr-1] = 1:1:2.

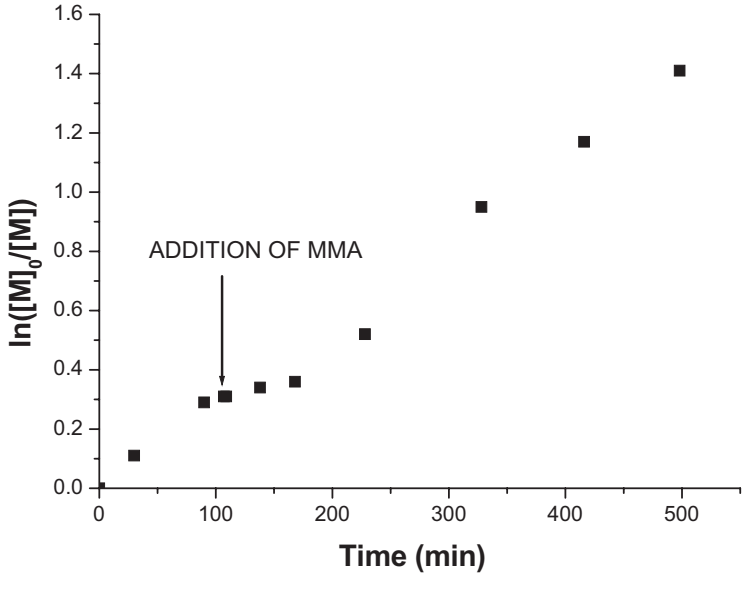

Figure 7. First-order kinetic plot for the synthesis of P3FM-*b*-PMMA (entry I, Table 2) in toluene solution at 80°C. [I]:[Cu(I)Br]:[n-Pr-1] = 1:1:2.

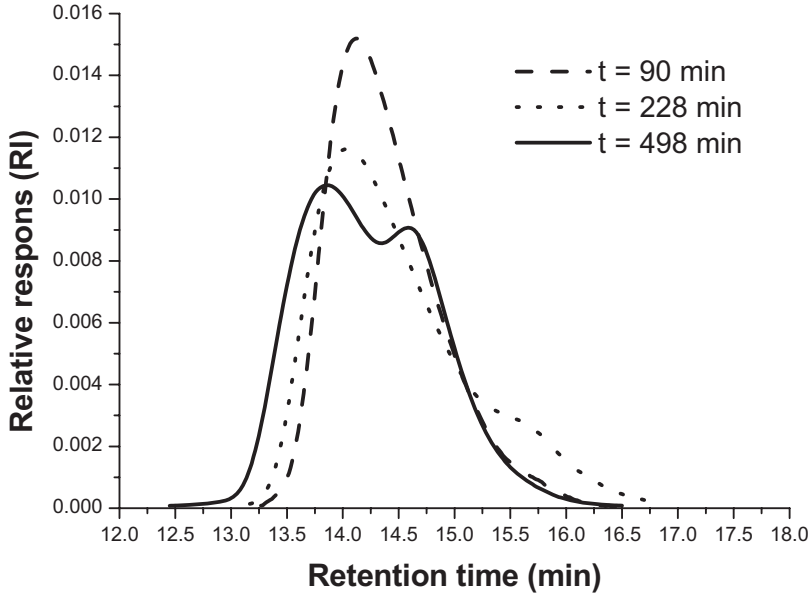

Figure 8. Development of the SEC traces during the synthesis of P3FM-*b*-PMMA (entry I, Table 2).

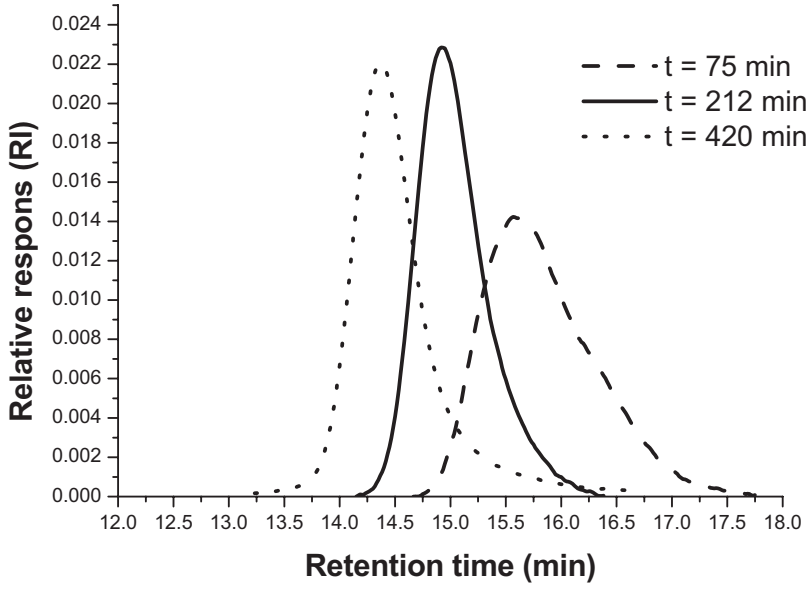

Figure 9. Development of the SEC traces for the synthesis of PMMA-*b*-P3FM (entry V, Table 2).

Table 2. Copolymers of MMA and fluorinated monomers, 3FM, 8FM and 17 FM.

[I]:[Cu(I)Br]:[n-Pr-1] = 1:1:2, Reaction at 80 °C in 50 v% toluene

	Copolymer	$[M_1]:[M_2]$	$[I]:[M_1]$	Reaction time (min)	$M_{n,\,theo}$ (g mol^{-1})	$m_1:m_2$[a] (%)	$M_{n,\,SEC}$ (g mol^{-1})	PDI
I	P3FM-*b*-PMMA	1 : 1	1 : 113	500	25,800	68 : 32	10,000	1.33
II	P3FM-*b*-PMMA	1 : 1	1 : 113	510	22,900	64 : 36	7,900	1.30
III	P3FM-*b*-PMMA[b]	1 : 1	1 : 113	455	23,600	64 : 36	9,200	1.50
IV	PMMA-*b*-P3FM[c]	--	1 : 100	240	27,800	16 : 84	25,300	1.12
V	PMMA-*b*-P3FM	1.7 : 1	1 : 98	420	15,000	44 : 56	9,200	1.08
VI	PMMA-*b*-P8FM	2.5 : 1	1 : 98	420	16,500	50 : 50	9,300	1.18
VII	PMMA-*b*-P17FM[b]	4.7 : 1	1 : 98	420	17,000	45 : 55	10,300	1.24

[a] *Incorporated weight fractions of the two monomers calculated from ^{1}H NMR*

[b] *Polymerized at 90 °C*

[c] *3FM polymerized from MMA-macroinitiator [I]:[M]=1 : 100*

Macroinitiator approach to block copolymers

Sequential polymerization is a fairly uncomplicated route to block copolymers with the only drawback being the lack of absolute control of the polymer structure due to the presence of two monomers during reaction resulting in gradient copolymers instead of true block copolymers. An attempt was made at synthesizing a true block copolymer using a PMMA-macroinitiator for the polymerization of 3FM. A well-defined low molecular weight PMMA was synthesized (M_n ~ 4400 g mol^{-1}) and subsequently used for further polymerization. The polymerization proceeded in a controlled fashion with a linear first-order kinetic plot, Figure 10. The molecular weight increased with conversion up to 57 % conversion after which some decrease is observed, whilst PDI was low throughout reaction, Figure 11. However, SEC-analysis showed residual macroinitiator, Figure 12, which is not the case with the sequential polymerization method. This is most probably due to exchange of the bromine of the end-groups during work-up resulting in non-initiating macroinitiator species[23]. The molecular weight of the PMMA-macroinitiator could be determined absolutely by SEC and the molecular weight of the copolymer could therefore be estimated by ^{1}H NMR. The molecular weight of 28,000 g mol^{-1} found by NMR corresponded well with the value of 25,000 g mol^{-1} found by SEC, although both values were somewhat higher than the theoretical value, which can be explained by macroinitiator efficiencies lower than 100 % consistent with the observations in SEC.

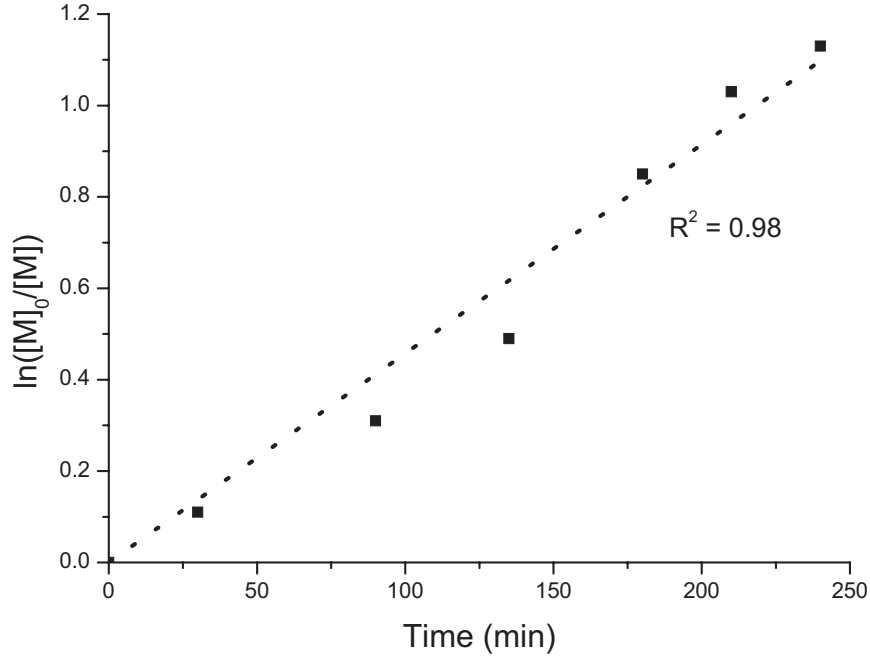

Figure 10. First-order kinetic plot for the polymerization of 3FM from a PMMA-macroinitiator (entry IV, Table 2) in toluene solution at 80 °C. [M]:[I]:[CuBr]:[n-Pr-1] = 100:1:1:2.

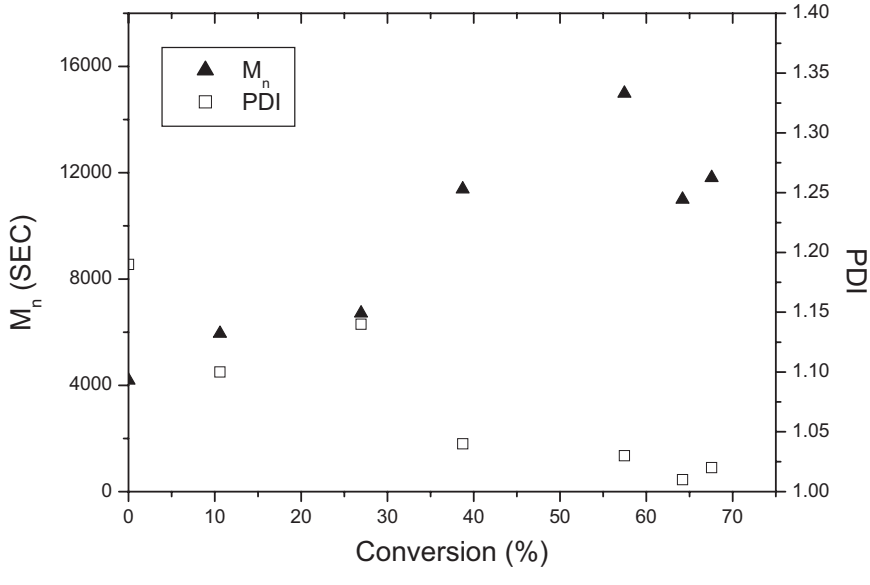

Figure 11. Evolution of molecular weight for the polymerization of 3FM from a PMMA-macroinitiator (M_n = 4400 g/mol) (entry IV, Table 2). SEC was performed using chloroform as eluent.

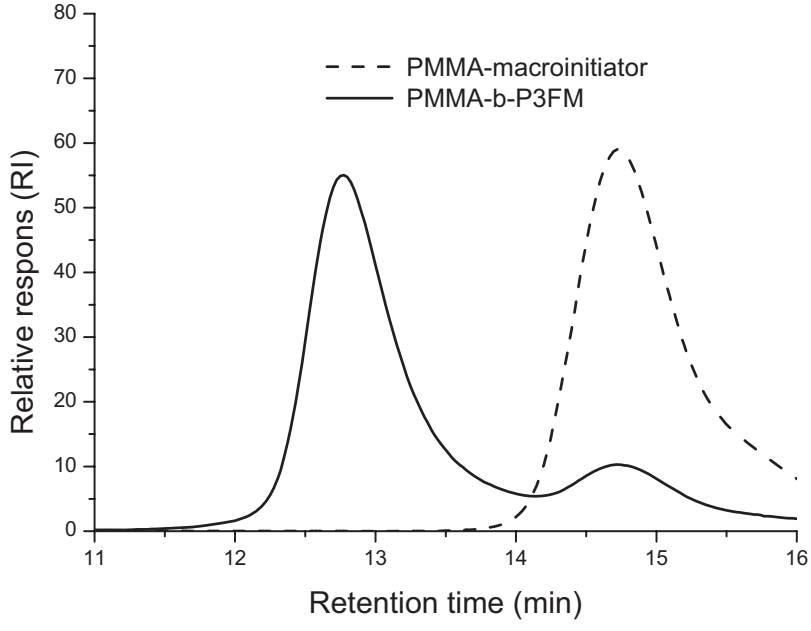

Figure 12. SEC-traces for the final product of the polymerization of 3FM from a PMMA-macroinitiator (entry IV, Table 2).

Comparison between the two polymerization methods deems the sequential to be faster and more efficient with the disadvantage of lower structure control, whereas the macroinitiator method has supreme control over structure, but is much more time-consuming due to the increased amount of work-up. The former polymerization method was therefore chosen for the remainder of the syntheses.

Synthesis of block copolymers with 8FM and 17FM

Whilst the homopolymerization of 3FM could be monitored by ^{1}H NMR (in $CDCl_3$), it was not possible to use this technique for the homopolymerization of 8FM and 17FM due to low solubility of the polymers in organic solvents. As products that could be solubilized in non-fluorinated solvents were targeted, the approach synthesizing the fluorinated segment first was abandoned for said monomers and only block copolymers generated from PMMA were synthesized i.e. PMMA-*b*-P8FM and PMMA-*b*-P17FM.

Monomer conversions were estimated from ^{1}H NMR-analysis using the peak for C$\underline{H}_2$-CF_2 in the fluorinated methacrylates. δ_H 4.60 (q) (monomer) and δ_H 4.44 (polymer) were used for estimating conversion of 8FM, while δ_H 4.39 (q) (monomer) and δ_H 4.24 (polymer) were compared for 17FM. The conversion of MMA was determined as previously described.

The first-order kinetic plots were similar to those acquired for the synthesis of PMMA-*b*-P3FM and were linear for both polymerizations, Figure 13, where the data for PMMA-*b*-P8FM is shown. Evolution of molecular weights of the copolymeric products was observed to be linear with conversion up to 70 % conversion, Figure 14 (data for PMMA-*b*-P17FM). SEC-analysis showed monomodal curves with low PDI's evidencing a controlled reaction mechanism, Table 2.

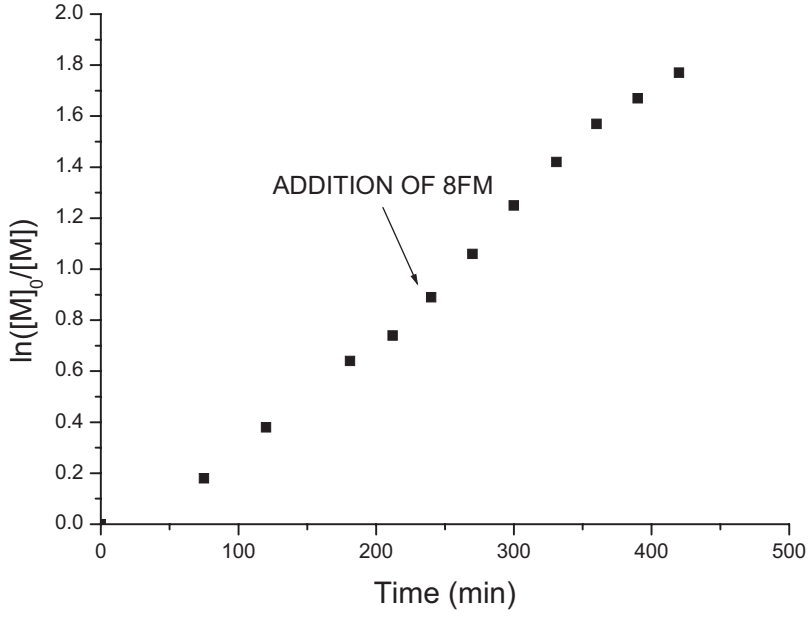

Figure 13. First-order kinetic plot for the synthesis of PMMA-*b*-P8FM (entry VI, Table 2) in toluene solution at 80 °C. [I]:[CuBr]:[n-Pr-1] = 1:1:2.

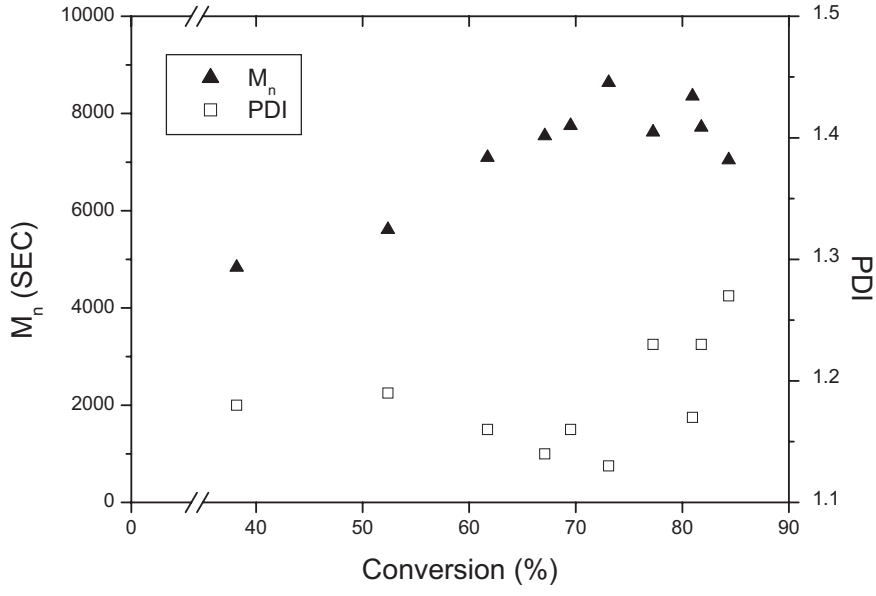

Figure 14. Evolution of Mn (▲) and PDI (□) for PMMA-b-P17FM (entry VII, Table 2). SEC was performed using chloroform as eluent.

Conversions of both MMA and fluorinated monomers in the synthesis of PMMA-*b*-PxFM copolymers are shown in Figure 15. Comparison of the kinetics of the three fluoromonomers indicates that the fluorinated pendant chain does not influence the rate of polymerization as long as the product is soluble at the given reaction conditions. There are no significant differences between the curves substantiating similar reactivity of the monomers, thereby proving the influence of the fluorinated segment only to be important in terms of solubility. It must, however, be stressed that in these three experiments the concentrations of the fluorinated monomers are not the same, since the same amount of fluorine in the final products was targeted. Furthermore the reaction temperature for 17FM was 10°C higher than for the other monomers.

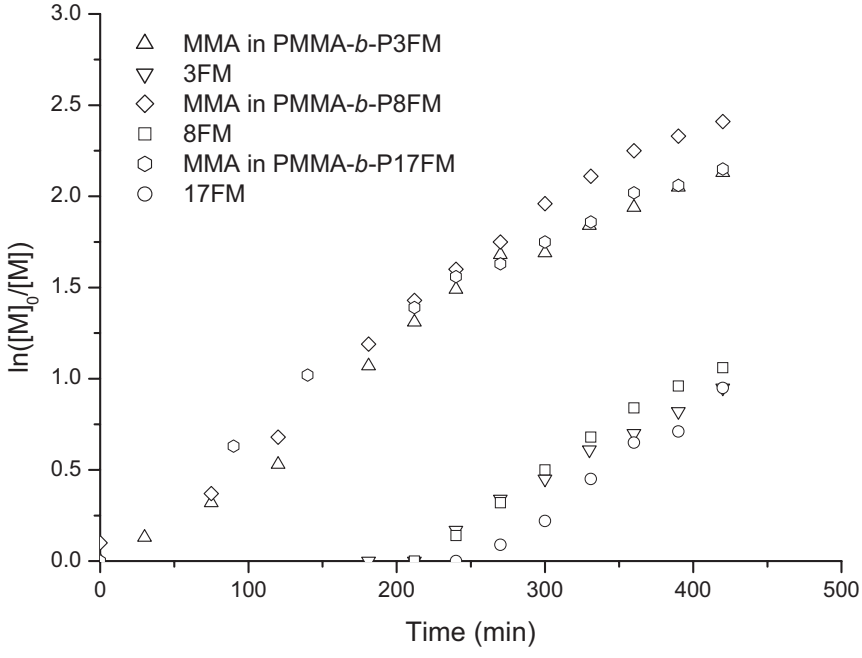

Figure 15. Individual conversions of MMA and fluorinated monomers in the synthesis of PMMA-b-PxFM copolymers in toluene solution. [I]:[CuBr]:[n-Pr-1] = 1:1:2.

Synthesis of copolymers of 3FM and PEGMA

Different reaction temperatures were chosen for the polymerizations of 3FM and PEGMA, as PEGMA cannot be polymerized successfully to high conversions (~60 %) at elevated temperatures[31]. For this reason a reaction temperature of 50°C was chosen for PEGMA, while 3FM was polymerized at 90°C. Conversions of 3FM were estimated as before, with conversions of PEGMA found by comparing the residual monomer peaks (δ_H 6.14 and δ_H 5.55) with the peak at δ_H 4.12 deriving from CO-O-C$\underline{H_2}$ in the polymer. The original peak at δ_H 4.28 (dd) in the monomer is hidden under the peak for P3FM during copolymerization introducing an element of uncertainty for the reported conversions.

The synthesis of PPEGMA-*b*-P3FM occured as anticipated with the propagation of 3FM from the PPEGMA-species, and also with an increased rate of polymerization of PEGMA at the elevated temperature, Figure 16. Molecular weights increased with conversion and PDI was relatively low (< 1.25) for the later stages of polymerization, Figure 17. For the converse approach polymerizing PEGMA from the P3FM-macroinitiator, no reaction was seen, when

the temperature was lowered to 50°C, the temperature utilized for the first successful copolymerization, but when the temperature was increased again, the reaction continued (data not shown). This indicates a thermal barrier for the transformation of the initiator from dormant to activated state rather than for the propagation of the second monomer. This is in good correspondence with previous observations in the homopolymerization of 3FM, where no polymerization took place at 70°C even at very long reaction times. It is concluded that if PEGMA is to be polymerized at 50°C with 3FM to form copolymers, this can only be undertaken starting from the former monomer. Results of the copolymerizations are shown in Table 3.

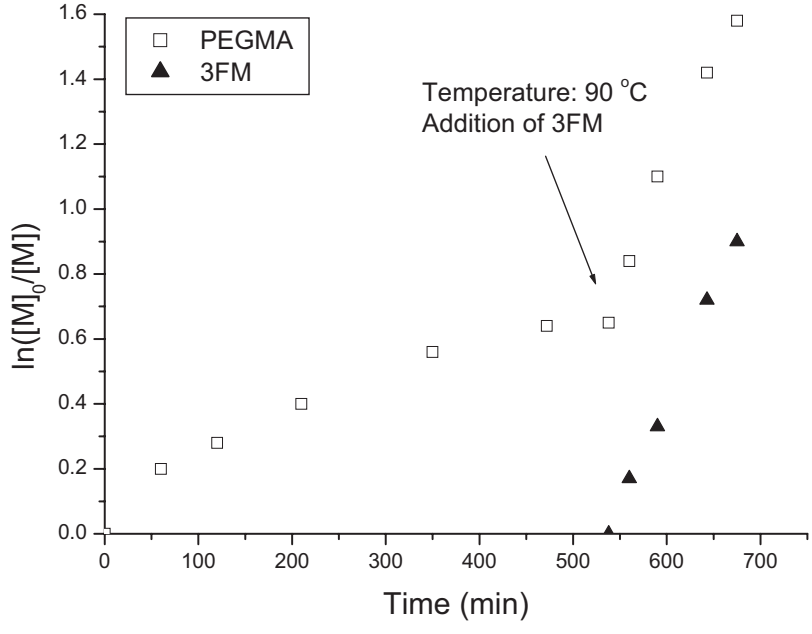

Figure 16. Individual conversions of the two monomers in the synthesis of PPEGMA-*b*-P3FM. Polymerization of PPEGMA proceeds at 50 °C until the addition of 3FM upon which the temperature is increased to 90 °C. [I]:[CuBr]:[n-Pr-1] = 1:1:2.

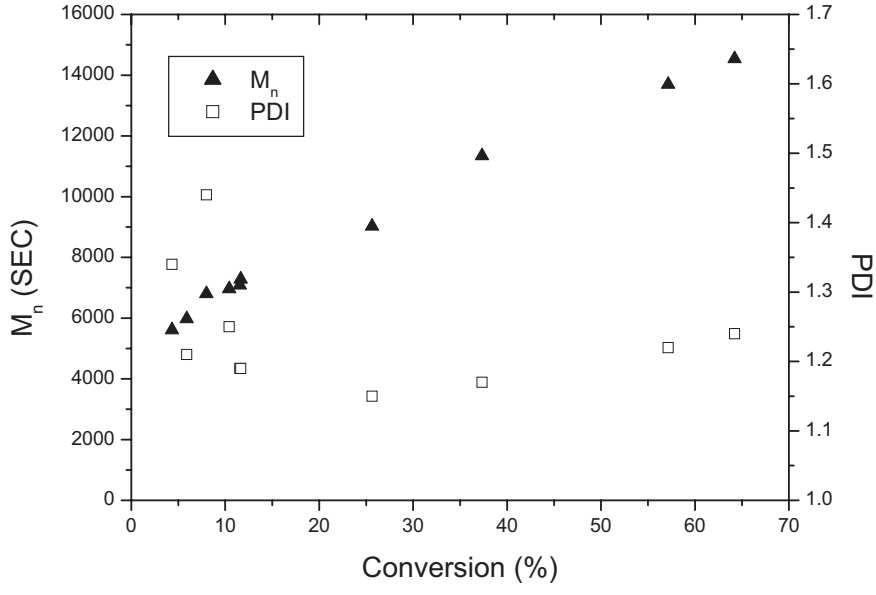

Figure 17. Evolution of M_n (▲) and PDI (□) for PPEGMA-*b*-P3FM. [I]:[CuBr]:[n-Pr-1] = 1:1:2.

Synthesis of copolymers of 3FM and MEA

Although the Cu(I)Br/**n-Pr-1** catalytic system was efficient in copolymerization of 3FM and MMA, preliminary experiments with homopolymerization of MEA indicated better control over kinetics with HMTETA as ligand. Conversions of 3FM were estimated as previously mentioned, while conversions of MEA were found by comparing the residual monomer peaks (δ_H 5.74 (dd), 6.15 (dd) and 6.43 (dd)) with the peak at δ_H 3.54, which derives from the signal of CO-O-C$\underline{H}_2$ in both monomer and polymer, as there is no significant shift in the signals during polymerization.

Polymerization starting from MEA had a linear first-order kinetic plot, Figure 18, with a linear evolution of molecular weight with global conversion, Figure 19. The PDI, however, increased drastically after the addition of 3FM, which could indicate the loss of control over the reaction, perhaps by incomplete initiation. This could be due to the difference in nature of the two monomers, as MEA is relatively hydrophilic, while 3FM is highly hydrophobic. The converse polymerization approach was also undertaken i.e. polymerization of MEA from P3FM. First-order kinetics indicated that the higher reactivity of 3FM made the polymerization of MEA difficult, when using sequential addition. PDI was high and evolution

of molecular weight was not linear with conversion. Furthermore, repeating the experiment indicated a lack of reproducibility of the polymerization results (entries IV and V, Table 3) illustrated by the considerable difference in monomer ratios in the final products.

It must be concluded that the two monomers 3FM and MEA are not compatible and cannot be copolymerized in a controlled fashion at the chosen reaction conditions.

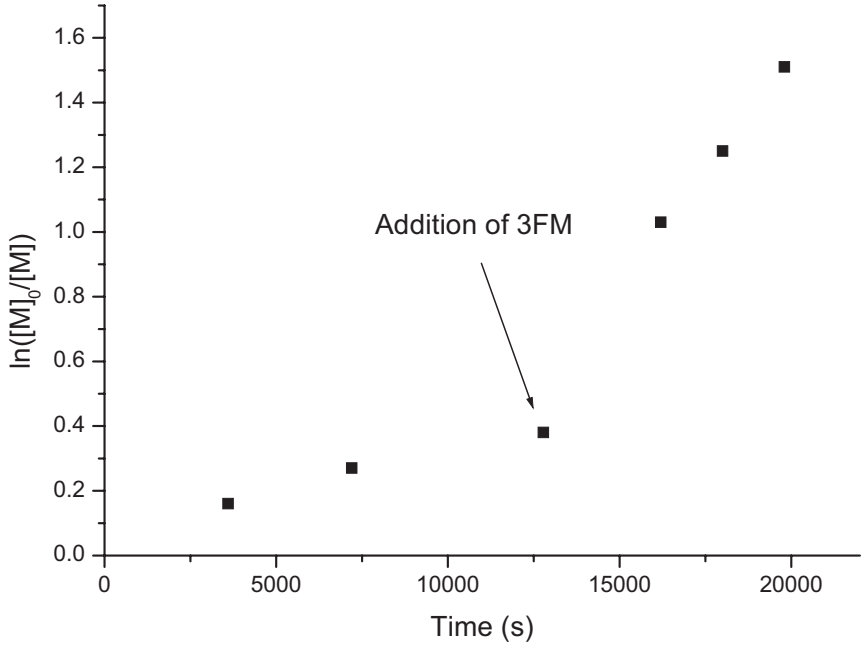

Figure 18. First-order kinetic plot of the synthesis of PMEA-*b*-P3FM (entry III, Table 3) in toluene at 90 °C. [I]:[CuBr]:[HMTETA] = 1:1:1.

Table 3 Results for the synthesis of amphiphilic block copolymers of 3FM and the hydrophilic monomers MEA and PEGMA.

[I]:[Cu(I)Br] = 1:1, Reaction temperature: 90 °C

	Copolymer	$[M_1]:[M_2]$	Ligand	Catalyst:ligand	$[I]:[M_1]$	Reaction time (min)	$m_1;m_2$[a]	$M_{n,\,theo}$ (g mol^{-1})	$M_{n,\,SEC}$ (g mol^{-1})	PDI
I	PPEGMA-*b*-P3FM[b]	1 : 3	n-Pr-1	1 : 2	1 : 42	675	45 : 55	29,900	16,500	1.18
II	P3FM- *b* -PPEGMA	3 : 1	n-Pr-1	1 : 2	1 : 113	1675	63 : 37	26,200	17,500	1.22
III	PMEA- *b* -P3FM	1 : 1	HMTETA	1 : 1	1 : 150	330	47 : 53	33,200	10,400	1.57
IV	P3FM- *b* –PMEA	1 : 1	HMTETA	1 : 1	1 : 113	600	68 : 32	20,800	10,300	1.42
V	P3FM- *b* –PMEA	1 : 1	HMTETA	1 : 1	1 : 113	560	91 : 9	31,100	27,400	1.56

[a] *Wt fractions of the two monomers*

[b] *PEGMA polymerized at 50 °C*

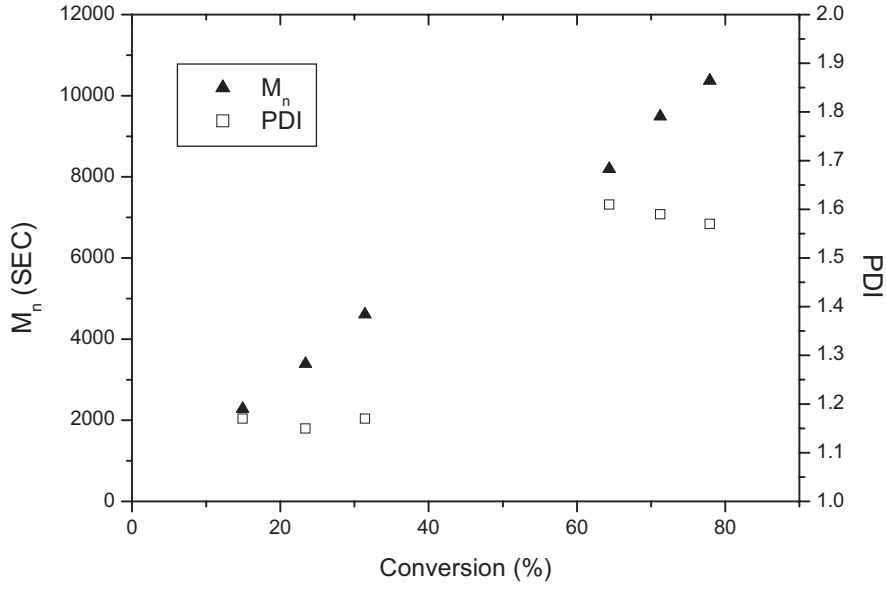

Figure 19. Evolution of M_n (▲) and PDI (□) for the synthesis of PMEA-*b*-P3FM (entry III, Table 3).

Thermal properties

The glass transition temperature (T_g) of each synthesized copolymer was determined by DSC, Table 4. In most cases a single T_g was seen with an intermediate value compared to the T_gs found for the two homopolymers.

T_g's between 66 and 83°C were determined for the copolymers of MMA and 3FM, which coincides with the T_g value of 59°C found for P3FM (M_n = 8600 g mol^{-1}) and 101°C for PMMA (M_n = 18,600 g mol^{-1}). Only one T_g was detectable for the "true" block copolymer PMMA-*b*-P3FM (entry IV), although two values were anticipated. This could be explained by the proximity of the T_g-values of the two homopolymers due to the size of the PMMA block, as T_g for the PMMA-macroinitiator was found to be 69°C. The T_g of 83°C is fairly high, however, it is reasonable to expect a T_g higher than 59 °C for the large P3FM block with M_n > 20,000.

PMMA-*b*-P8FM exhibited a T_g of 66°C, which is an average value between 101 and 27°C, respectively found for the homopolymers. The T_g of PMMA-*b*-P17FM was determined to be 95°C, which is close to the value for PMMA. A homopolymer of 17FM did not show any glass transition, but displayed a crystalline melting temperature (T_m) of 88°C, which was not observed in the copolymer. A single transition was found for the two copolymers of 3FM and

PEGMA. Due to the nature of the polymers, microphase separation was expected, but as these copolymers are gradient block copolymers, the pure blocks are apparently to short for this to take place. For both PPEGMA-*b*-P3FM and P3FM-*b*-PPEGMA T_g values close to that for PPEGMA were found: -51 and -62°C, respectively.

Table 4. Glass transition temperatures and thermal stabilities of the synthesized copolymers.

Previous entry	(Co)polymer	$M_{n,\,SEC}$ (g mol^{-1})	T_g (°C)	Residual weight (%)		
				200 °C	300 °C	400 °C
Table 2, I	P3FM-*b*-PMMA	10,300	67	90	75	10
Table 2, II	P3FM-*b*-PMMA	7,900	80	97	84	13
Table 2, III	P3FM-*b*-PMMA	9,200	77	90	83	35
Table 2, IV	PMMA-*b*-P3FM	25,300	83	98	50	8
Table 2, V	PMMA-*b*-P3FM	9,600	66	75	56	22
Table 2, VI	PMMA-*b*-P8FM	9,300	66	99	72	28
Table 2, VII	PMMA-*b*-P17FM	10,300	95	95	85	26
Table 3, I	PPEGMA-*b*-P3FM	16,500	-51	95	81	12
Table 3, II	P3FM-*b*-PPEGMA	17,500	-62	96	82	10
Table3, III	PMEA-*b*-P3FM	11,100	-31 & 13	100	87	26
Table 3, IV	P3FM-*b*-PMEA	10,300	-6	99	86	12
Table 3, V	P3FM-*b*-PMEA	27,400	68	96	64	4
	P3FM	8,600	59	97	45	4
	P8FM	-[a]	27	98	36	11
	P17FM	-[a]	-	79	62	12
	PMMA[b]	4,400	69	94	87	61
	PMMA	18,600	101	96	92	35
	PMEA	18,200	-37	99	98	42
	PPEGMA	7,600	-65	96	88	27

[a]M_n could not be determined. [b]PMMA-macroinitiator.

The copolymer PMEA-*b*-P3FM exhibited block copolymer behavior with two distinct T_g's of -31 and 13°C, respectively. The first T_g is close to T_g for PMEA, while the second is intermediary compared to the values for the two homopolymers. The consequence of the faster reaction kinetics of 3FM was the polymerization of mainly this monomer after addition during the copolymerization resulting in formation of a block copolymer with two distinct blocks with two thermal transitions. The relatively low value of 13°C found for the second T_g is probably due to two factors: the presence of PMEA in the P3FM block and the relatively short length of this block. For one P3FM-*b*-PMEA copolymer (entry IV) a single T_g of -6°C was found, while a value of 68°C was found for the other (entry V). This apparent inconsistency derives from the difference in composition, as the latter copolymer consists of mainly P3FM.

Thermal stability

Fluorine content in polymers often increases thermal stability as observed in the case of fluorinated polystyrenes[28,29]. In order to compare the thermal stabilities of the polymers we report the residual wt% at temperatures of 200, 300 and 400°C, Table 4. Non-fluorinated homopolymers synthesized for DSC were also used for comparison in TGA. Homopolymers of the fluorinated monomers 3FM and 8FM exhibited similar degradation behavior with two distinct degradation peaks. The first was deduced to derive from the cleavage of part of the fluorinated alkyl chain from the backbone. For P3FM the scission can take place either in the ester group (between the carbonyl and oxygen), between the ester group and the fluorinated ethyl, or in the ethyl pendant chain. Weight losses in reasonable agreement with these possible routes were observed with weight losses of 36 % (loss of CF_3) at 185 - 250°C and weight loss of 56 % (loss of O-CH_2-CF_3) at 250 - 305°C. For P8FM scission seems to take place between the oxygen and the fluorinated chain (loss of 64 wt% at 190 - 320°C) possibly by the formation of a 5-membered ring, while the degradation mechanism of P17FM is uncertain. Similar behavior was observed by Zuev et al.[32] in the thermal degradation of equivalent fluorinated acrylates, where scission of the fluorinated alkyl chains by various routes were seen as well as unzipping of the backbone to yield monomeric species. The observed degradation patterns were also seen in the TGA analysis of the copolymers of 3FM and MMA, Figure 20, as well as the copolymers PMMA-*b*-P8FM and PMMA-*b*-P17FM. The fluorinated homopolymers P3FM, P8FM and P17FM were less stable than PMMA, as they exhibited excessive degradation between 200 and 300°C, while PMMA showed a minor weight loss in this temperature interval (loss of 13 wt%). The fluorinated block copolymers with PMMA had intermediate thermal stabilities compared to the two equivalent homopolymers.

The thermal behavior of copolymers of 3FM and PEGMA was closer to that exhibited by PPEGMA, indicating that the thermal stability was not significantly decreased by the less thermally stable fluoropolymer. The same tendency was observed for the three copolymers of MEA and 3FM, where the latter polymer only to a lesser extent reduced the thermal stability compared to PMEA. The most fluorinated copolymer P3FM-*b*-PMEA (entry V) was the least thermally stable with a degradation of 36 wt% at 300°C, while PMEA is almost intact at this temperature (residual 98 wt%).

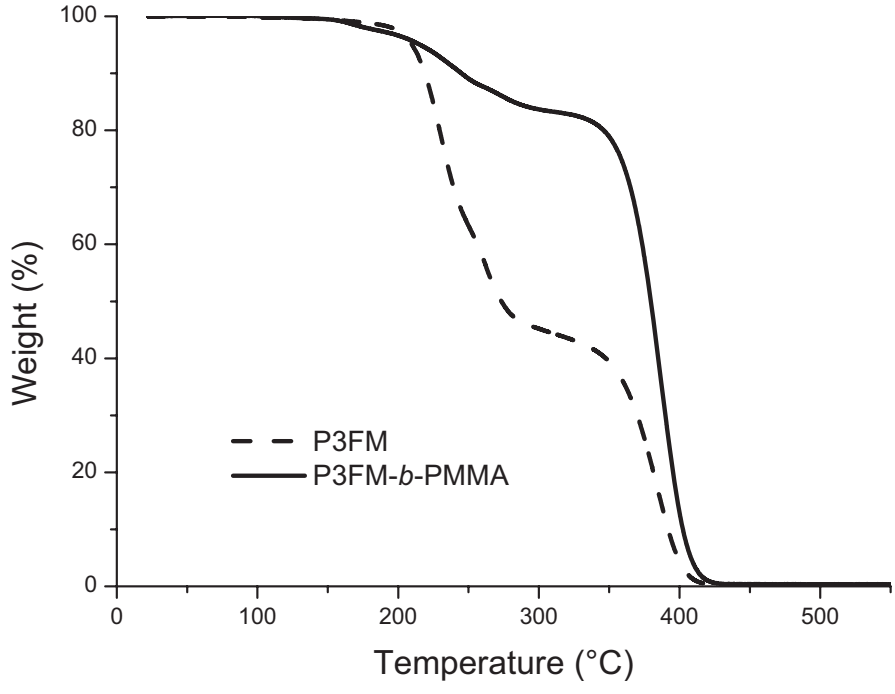

Figure 20. TGA-curves for P3FM and P3FM-*b*-PMMA (entry II, Table 2).

Surface Activity

Dynamic contact angles of water were measured on films that had been spin coated on glass slides followed by annealing, Table 5.

The advancing (Θ_{adv}) and receding (Θ_{rec}) contact angles of water on a film of pure P3FM were 95° and 81°, respectively. It was not possible to form coherent films of P8FM or P17FM under the same conditions as used for the other films and no contact angle data are therefore given for these films. Θ_{adv} found for the copolymers of 3FM and MMA, 92° to 94°, were very close to the value for P3FM, while Θ_{rec} differed to a greater extent. The PMMA block is responsible for the reduction in Θ_{rec} and since PMMA is a relatively hydrophobic polymer, this reduction is small. The distribution of the two monomers in the copolymer did not influence the surface activity, as there was no significant difference between the copolymers I, IV and V. The high surface activity is ascribed to migration of the fluorinated chains to the surface resulting in a fluorine enriched film surface[33,34]. The film of PMMA-*b*-P8FM appeared not to be coherent, but the contact angles, Θ_{adv} = 92° and receding Θ_{rec} = 77°,

obtained for this copolymer were comparable to results for the P3FM/PMMA copolymers. The highest Θ_{adv} was found for PMMA-*b*-P17FM: 118°, reflecting the large increase in hydrophobic properties relative to the PMMA homopolymer. The longer fluorinated alkyl chain yields the most hydrophobic film, while Θ_{rec} for this polymer film was 76°, which is comparable to the values found for the other copolymeric films.

Table 5. Water contact angles of fluorinated copolymers.

Entry	Polymer	$M_{n, SEC}$ (g mol^{-1})	$\Theta_{advancing}$	$\Theta_{receding}$
	PMMA	18,600	73 (± 1)	58 (± 2)
	PMEA	7,500	55 (± 9)	11 (± 3)
	PPEGMA	7,600	42 (± 6)	19 (± 3)
	P3FM	8,600	95 (± 4)	81 (± 8)
Table 2, I	P3FM-*b*-PMMA	10,300	96 (± 4)	84 (± 2)
Table 2, IV	PMMA-*b*-P3FM	25,300	94 (± 6)	73 (± 9)
Table 2, V	PMMA-*b*-P3FM	9,600	93 (± 6)	75 (± 2)
Table 2, VI	PMMA-*b*-P8FM	9,300	92 (± 4)	77 (± 5)
Table 2, VII	PMMA-*b*-P17FM	10,300	118 (± 3)	76 (± 2)
Table 3, I	PPEGMA-*b*-P3FM	16,500	99 (± 2)	52 (± 4)
Table 3, II	P3FM-*b*-PPEGMA	17,500	95 (± 1)	80 (± 2)
Table 3, III	PMEA-*b*-P3FM	11,100	96 (± 1)	44 (± 5)
Table 3, IV	P3FM-*b*-PMEA	10,300	96 (± 2)	81 (± 2)

For the copolymers PPEGMA-*b*-P3FM and P3FM-*b*-PPEGMA Θ_{adv} was almost the same, 99° and 95°, respectively, while the Θ_{rec} was markedly lower for the former copolymer (52° vs. 80°). This is most probably due to the fact that this copolymer has a pure PPEGMA block, which can form hydrophilic domains resulting in a low Θ_{rec}. The same tendency was seen for copolymers of MEA and 3FM, where both PMEA-*b*-P3FM and P3FM-*b*-PMEA had a Θ_{adv} of 96°, while Θ_{rec} had values of 44° and 81°, respectively. For both hydrophilic monomers the copolymerization with 3FM lead to a significant increase in both Θ_{adv} and Θ_{rec}.

Conclusions

The apparent rate constants of polymerization (k_p^{app}) of 3FM were assessed at temperatures from 80 to 110 °C to have values between $1.6 \cdot 10^{-4}$ s^{-1} and $2.9 \cdot 10^{-4}$ s^{-1}. The obtained k_p^{app} values were used to approximate an activation energy of 24 kJ mol^{-1} by the Arrhenius equation. Block copolymers of MMA and fluorinated methacrylates were polymerized by controlled radical polymerization (ATRP). It was possible to synthesize block copolymers

starting from 3FM, although the converse approach yielded better results. Well-defined block copolymers of MMA and 8FM and 17FM, respectively were synthesized. Kinetic experiments indicated that the length of the fluorinated pendant chain does not influence the reactivity in ATRP. Novel copolymers of 3FM and hydrophilic monomers PEGMA were synthesized by ATRP in toluene. Copolymerizations of 3FM and MEA yielded the targeted product although control over polymerization was insufficient.

The introduction of the fluorinated monomers 3FM, 8FM and 17FM reduced the thermal properties of copolymers with MMA compared to the latter homopolymer. Copolymers of 3FM and PEGMA exhibited thermal properties equivalent to those of PPEGMA. The thermal properties of P3FM/PMEA copolymers were slightly reduced compared to the homopolymer of MEA. All of the synthesized copolymers exhibited hydrophobic properties evidenced by dynamic contact angle measurements of water on spin coated film surfaces. In most cases advancing contact angles of water were above 90° and for PMMA-*b*-P17FM values up to 120° were found.

Acknowledgements

N. Hansen would like to thank Novo Nordisk A/S for supporting her project as well as the following funds for supporting her stay at the University of Warwick: Ingeniørvidenskabelig Fond og G.A. Hagemanns Mindefond; Berg, Nielsens Legat; Knud Højgaards Fond & Otto Mønsteds Fond.

References

(1) Hansen, N. M. L, Jankova, K., and Hvilsted, S. *Eur. Polym. J.* **2007,** *43*(*2)*, 255-293

(2) Roche, V., Vacandio, F., Bertin, D., and Massiani, Y. *J. Electroceram.* **2006,** *16*(*1)*, 41-47

(3) Jankova, K., Jannasch, P., and Hvilsted, S. *J. Mater. Chem.* **2004,** *14*(*19)*, 2902-2908

(4) Fu, G. D., Kang, E. T., Neoh, K. G., Lin, C. C., and Liaw, D. J. *Macromolecules* **2005,** *38*(*18)*, 7593-7600

(5) Eberhardt, M. and Theato, P. *Macromol. Rapid Commun.* **2005,** *26*(*18)*, 1488-1493

(6) Inoue, Y., Watanabe, J., Takai, M., Yusa, S., and Ishihara, K. *J. Polym. Sci. Part A:Polym. Chem.* **2005,** *43*(*23)*, 6073-6083

(7) (a) Kato, M., Kamigaito, M., Sawamoto, M., and Higashimura, T. *Macromolecules* **1995,** *28*(*5)*, 1721-1723 (b) Wang, J.S., Matyjaszewski, K. J. Am. Chem. Soc. **1995**, *117(20)*, 5614-5615

(8) Betts, D., Johnson, T., LeRoux, D., and DeSimone, J. M. *ACS Symposion Series* **1998,** *685*, 418-432

(9) Li, K., Wu, P. P., and Han, Z. W. *Polymer* **2002,** *43*(*14)*, 4079-4086

(10) Perrier, S., Jackson, S. G., Haddleton, D. M., Ameduri, B., and Boutevin, B. *Macromolecules* **2003,** *36*(*24)*, 9042-9049

(11) Zhang, Z. B., Ying, S. K., Hu, Q. H., and Xu, X. D. *J. Appl. Polym. Sci.* **2002,** *83*(*12)*, 2625-2633

(12) Xia, J. H., Johnson, T., Gaynor, S. G., Matyjaszewski, K., and DeSimone, J. *Macromolecules* **1999,** *32*(*15)*, 4802-4805

(13) Li, H., Zhang, Z. B., Hu, C. P., Ying, S. K., Wu, S. S., and Xu, X. D. *React. Func. Polym.* **2003,** *56*(*3)*, 189-197

(14) Shemper, B. S. and Mathias, L. J. *Eur. Polym. J.* **2004,** *40*(*4)*, 651-665

(15) Lim, K. T., Lee, M. Y., Moon, M. J., Lee, G. D., Hong, S. S., Dickson, J. L., and Johnston, K. P. *Polymer* **2002,** *43*(*25)*, 7043-7049

(16) Hussain, H., Budde, H., Horing, S., and Kressler, J. *Macromol. Chem. Phys.* **2002,** *203*(*14)*, 2103-2112

(17) Villarroya, S., Zhou, J. X., Duxbury, C. J., Heise, A., and Howdle, S. M. *Macromolecules* **2006,** *39*(*2)*, 633-640

(18) Granville, A. M. and Brittain, W. J. *Macromol. Rapid Commun.* **2004,** *25*(*14)*, 1298-1302

(19) Chen, R. X., Feng, C., Zhu, S. P., Botton, G., Ong, B., and Wu, Y. L. *J. Polym. Sci. Part A:Polym. Chem.* **2006,** *44*(*3)*, 1252-1262

(20) Tanaka, M. *Bio-Med. Mater. Eng.* **2004,** *14*(*4)*, 427-438

(21) Tanaka, M. and Mochizuki, A. *J Biomed. Mater. Res. Part A* **2004,** *68A*(*4)*, 684-695

(22) Li, G. F., Shen, Y., Morita, S., Nishida, T., and Osawa, M. *J. Am. Chem. Soc.* **2004,** *126*(*39)*, 12198-12199

(23) Bednarek, M., Jankova, K., and Hvilsted, S. *J. Polym. Sci. Part A:Polym. Chem.* **2007,** *45*(*3)*, 333-340

(24) Hansen, N. M. L, Haddleton, D. M., and Hvilsted, S. *J. Polym. Sci. Part A:Polym. Chem.* **2007,** *45*(*24)*, 5770-5780

(25) Keller, R. N. and Wycoff, H. D. *Inorg.Synth.* **1946,** *2*, 1-4

(26) Haddleton, D. M., Crossman, M. C., Dana, B. H., Duncalf, D. J., Heming, A. M., Kukulj, D., and Shooter, A. J. *Macromolecules* **1999,** *32*(*7)*, 2110-2119

(27) Qiu, J. and Matyjaszewski, K. *Macromolecules* **1997,** *30*(*19)*, 5643-5648

(28) Jankova, K. and Hvilsted, S. *Macromolecules* **2003,** *36*(*5)*, 1753-1758

(29) Hvilsted, S., Borkar, S., Siesler, H. W., and Jankova, K. *Advances in Controlled/Living Radical Polymerization;* Matyjaszewski, K. Ed.; ACS Symposion Series Vol 854; American Chemical Society: Washington, DC, 2003; Chapter 17, pp 236-249

(30) Haddleton, D. M., Kukulj, D., Duncalf, D. J., Heming, A. M., and Shooter, A. J. *Macromolecules* **1998,** *31*(*16)*, 5201-5205

(31) Lecolley, F *Ph.D. Thesis: New Polymers from Living Radical Polymerisation for Biological Applications* Chapter 3: Synthesis and Characterization of N-succinimidyl ester functionalized Poly(mPEGMA), **2004,** *University of Warwick, UK*

(32) Zuev, V. V., Bertini, F., and Audisio, G. **2006,** *91*(*3)*, 512-516

(33) Borkar, S., Jankova, K., Siesler, H. W., and Hvilsted, S. *Macromolecules* **2004,** *37*(*3)*, 788-794

(34) Wang, J. G. and Ober, C. K. *Macromolecules* **1997,** *30*(*24)*, 7560-7567

Natanya Majbritt Louie Hansen

Synthesis of Amphiphilic Copolymers by Atom Transfer Radical Polymerization

ISBN: 978-87-91435-61-7